

Design, Characterization and Evaluation of Polymeric and Solid Lipid Nanoparticulate Systems of Olanzapine for Enhanced Efficacy

THESIS

Submitted in partial fulfilment
of the requirements for the degree of
DOCTOR OF PHILOSOPHY

by

EMIL JOSEPH

Under the Supervision of
PROF. R. N. SAHA



BITS Pilani
Pilani | Dubai | Goa | Hyderabad

BIRLA INSTITUTE OF TECHNOLOGY AND SCIENCE, PILANI

2015

BIRLA INSTITUTE OF TECHNOLOGY & SCIENCE, PILANI

CERTIFICATE

This is to certify that the thesis entitled “**Design, Characterization and Evaluation of Polymeric and Solid Lipid Nanoparticulate Systems of Olanzapine for Enhanced Efficacy**” and submitted by **Emil Joseph**, ID. No. **2009PHXF001P** for award of Ph.D. Degree of the Institute, embodies original work done by him under my supervision.

Prof. RANENDRA N. SAHA

Shri B. K. Birla & Smt. Sarala Birla Chair Professor
Director
Birla Institute of Technology & Science, Pilani, Dubai Campus
Dubai, UAE.

Date:

Acknowledgements

I would like to express my most sincere gratitude and deepest feelings to my research supervisor Prof. Ranendra N. Saha, Director, BITS, Pilani, Dubai campus for his guidance, timely advice, constructive criticism and encouragement throughout my research work and professional development. It is my honor to work under him, whose competent mentorship, new ideas, never give-up approach and co-operative nature; imbued the enthusiasm in me throughout this endeavor. I would not be able to find apt words to express my gratitude for the parental love of him and his family to me throughout the period of my research. I am and will always remain profoundly grateful to him all my life.

I convey my gratitude to Prof. V.S. Rao, acting Vice-Chancellor, BITS Pilani, Prof. B. N. Jain, former Vice-Chancellor, BITS Pilani, Prof. A. K. Sarkar, Director, BITS Pilani, Pilani campus and Prof. G. Raghurama, former director, BITS Pilani, Pilani campus for allowing me to carry out my doctoral research work in the institute.

I express my special gratitude and thanks to Prof. Hemant R. Jadhav, Associate Dean, ARD, BITS, Pilani, Prof. S.K. Verma, Dean, ARD , BITS, Pilani and Prof. R. Mahesh, Dean, Faculty affairs BITS, Pilani, for their motivating words, administrative support and guidance at different point of time during my doctoral research.

I am indebted to Dr. S. Murugesan, Head, Department of Pharmacy, BITS Pilani, Pilani campus for his constant support. I am highly thankful to Prof. Shrikant Charde, former Head, Department of Pharmacy BITS Pilani, Pilani campus/present Head, Department of Pharmacy BITS Pilani, Hyderabad Campus, who is also my DAC member for the timely suggestions and immense support during various stages of my research work.

I would like to express my sincere thanks to Dr. Atish Paul, Convener, Departmental Research Committee, Dr. Anil Jindal and Dr. Sunil Dubey Doctoral Advisory Committee members for their valuable comments and intellectual guidance while compiling this thesis.

My heartfelt thanks to my lab mates Satish Reddi, Vibhu and Garima Balwani for their motivation, companionship and unequivocal support during my research studies. They made this journey immensely enjoyable and interesting. I express my heartiest thanks to Prashant Raut for always being my good friend at BITS and supported me endlessly

both professionally and personally. I sincerely thank Yashwant Kurhe for sharing his valuable friendship with me and helping me in executing animal studies of this research.

My special thanks to Dr. Gautam Singhvi, Mrs. Archana Kakkar, Dr. Jaipal A, Mr. M.M Pandey, Dr. Shvetank Bhatt and Mr. Mahaveer Singh for sharing their precious friendship and philosophical thoughts with me. They have made my life very alive and meaningful in Pilani. I am highly thankful to Dr. Pallavi Singh, Dr.Muthu Sudali, Dr. Ashok Penta and Dr. Vadiraj Kurdekar whom made my life very interesting during my doctoral research. I would like to thank Zarna, Department of Biological Sciences for her understanding, scholastic company and also for the immense help provided while using equipment of their lab. Words are not enough to thank my intimate research scholar friends, Goru Santosh, Almesh Kadakal, Vajir Malik, Pankaj Wadhwa, Anuradha P, Sruthi R, Arghya Dhar, Sourabh Sharma, Deepali Gupta, Subhash Chander, SNC Sridhar, Saurabh Mundra, and Nisha for offering their treasured friendship. I would like to specially thank Dr. Sushil Yadav, in-charge, central animal house facility, for supporting me during the experimentation in central animal facility and also for his treasured friendship with me.

I would like to extend by sincere gratitude to the faculty members Dr. Anil Gaikwad, Dr. Rajiv Taliyan, Mrs. Priti Jain, Dr. Deepak Chitkara and Dr. Anupama Mittal, who have supported me in numerous ways during my research.

I wish to thank to whole non-teaching staff Mr. Rampratap Suthar, Mr. Lakshman, Mr. Puran, Mr. Navin, Mr. Sajjan, Mr. Tarachand, Mr. Vishal and Mr. Mahendar for their support. I am also very thankful to my childhood friends, Mr. Feby Mathew and Mr. Bobby George who have supported me personally in several times during my research.

I acknowledge University Grants Commission for providing me financial assistance for my doctoral research and Department of Science and Technology for the international travel grant for young scientist for attending AAPS conference at Chicago, USA.

Specially, I am grateful to my beloved parents and my siblings for their constant inspiration, endless love and countless blessings. I can hardly find enough words to express my heartily gratitude to my beloved wife Antu, for her unconditional love, immense sacrifice and infinite moral support for the completion of the thesis.

Date:

Emil Joseph

Abstract

The effectiveness of a drug delivery system is highly dependent on its ability to deliver the therapeutic agent selectively/preferentially to the target site with no/minimum adverse effects. Targeting the therapeutic agent to the brain is always a challenging task for the formulation scientists because of the presence of blood brain barrier, with tight junctions in the brain endothelial cells. The application of nanotechnology for the drug delivery to the brain opens the doors of new opportunities for the formulation scientists for the better brain delivery. In the current research, studies were carried out to design and characterize polymeric/solid lipid nanoparticulate delivery systems to enhance the therapeutic efficacy of Olanzapine (OLN) with preferential brain distribution and minimized adverse effects.

As analytical methods are highly essential for the successful development of any kind of drug delivery systems, new UV-spectrophotometric and liquid chromatographic (analytical and bio analytical) methods, suitable for the current project, were developed in-house and successfully validated. These validated analytical methods were applied successfully for the analysis of drug during various preformulation and formulation studies. The bioanalytical methods developed were found to be highly sensitive and selective for the estimation of OLN in biological samples such as rat plasma and various organs. These bioanalytical methods were successfully applied for the estimation of OLN during in-vivo pharmacokinetic and biodistribution studies of the pure drug and nanoparticulate formulations in rats.

Preformulation studies demonstrated that OLN exhibited a pH dependent solubility in different buffers with high solubility in acidic pH buffers and low solubility in basic pH buffers. Distribution coefficients in various buffers and dissociation constant were determined successfully. Solution state stability studies suggested that OLN was found to be more stable in acidic pH as compared to alkaline pH, and degradation kinetics was found to be of first order. The solid admixtures of OLN with various excipients showed good stability with high drug content values during solid state stability studies. Results obtained for the drug-excipient compatibility studies by DSC, demonstrated no significant interaction with various excipients selected for the formulation development.

OLN-loaded nanoparticles were prepared successfully using nanoprecipitation and emulsification-ultrasonication techniques. These methods were easy, reproducible, and

they produced nanoparticles with narrow size distribution and good entrapment efficiency. The influence of different formulation variables such as polymer/solid lipid concentration, surfactant concentration and drug proportions on studied responses such as size, encapsulation efficiency and drug content were studied in detail. OLN-loaded nanoparticles prepared from selected biodegradable polymer/solid lipids sustained the release of drug for prolonged period of time as found by the in-vitro release studies. Morphological studies by SEM have shown that both polymeric and solid lipid nanoparticles were spherical in shape with smooth surface. The formulations also exhibited high redispersibility after freeze drying and stability study results demonstrated good stability, with no significant change in the drug content, average particle size and release characters for the formulations stored at frozen conditions for a period of 6 months.

In-vivo pharmacokinetic and biodistribution studies in rat indicated that as compared to OLN solution, nanoparticulate formulations demonstrated higher AUC values along with prolonged residence time of OLN in the rat blood circulation. More importantly, the distribution of OLN to the brain was significantly enhanced with increased residence times for coated nanoparticulate formulations, followed by un-coated nanoparticulate formulations as compared with OLN solution. Biodistribution study showed low uptake of studied nanoparticulate systems by kidney and heart, thereby decreasing the nephrotoxicity and adverse cardiovascular effects. Moreover, good compatibility of developed nanoformulations in rats was observed without any undesirable effects, during the entire course of study. The results of pharmacokinetic and biodistribution study indicate that OLN-loaded nanoparticulate systems may be highly promising for preferential distribution of OLN with effective OLN concentrations in brain for prolonged period of time.

In-vivo evaluation and adverse effects studies of OLN-loaded nanoparticulate systems in animal model have demonstrated an improved therapeutic efficacy than pure OLN. The antipsychotic effect of OLN-loaded nanoparticulate systems was maintained for a prolonged period of time. The adverse effects studies demonstrated a decreased extra pyramidal side effects and inhibition in weight gain as compared to the pure OLN. From these preliminary data it can be concluded that the OLN-loaded nanoformulations could be effective in the treatment of psychotic disorders with minimum adverse effects.

Table of contents

Chapter	Content	Page No.
	Acknowledgement	i-ii
	Abstract	iii-iv
	List of tables	v-vi
	List of figures	vii-xii
	List of abbreviations	xiii-xvi
1	Introduction	1-32
2	Drug profile	33-43
3	Analytical and bioanalytical methods	44-72
4	Preformulation studies	73-88
5	Formulation design and development	89-141
6	Pharmacokinetic and biodistribution studies	142-162
7	In-vivo evaluation and adverse effects studies	163-180
8	Summary and conclusions	181-183
	Appendix	
	List of publications and presentations	A
	Biography of candidate and supervisor	B

List of Tables

Table No.	Caption	Page No.
1.1	List of nanoformulations investigated for brain distribution	10
2.1	Pharmacokinetic parameters of OLN	37
2.2	List of marketed formulations of OLN	40
3.1	Optical characteristics, summary of statistical data, and validation parameters of UV-spectroscopic method of OLN	50
3.2	Data of accuracy studies by standard addition method	51
3.3	Repeatability and intermediate precision data of UV-spectroscopic method in 100mM HCl and phosphate buffer saline	52
3.4	Results of forced degradation study of OLN using RP-HPLC method	60
3.5	Results of repeatability and intermediate precision study of RP-HPLC method	61
3.6	Results of recovery studies of RP-HPLC method by placebo spiking and standard addition technique	62
3.7	Intra-day and inter-day precision study data of OLN in rat plasma	68
3.8	Accuracy study data of OLN in rat plasma	68
3.9	Recovery data of OLN in rat plasma	69
3.10	Stability data of OLN in rat plasma	69
4.1	Physical and bulk characteristics of OLN	77
4.2	Wavelength attribution of IR spectrum of OLN	78
5.1	Composition and characterization of nanoparticles prepared with PCL by nanoprecipitation technique	110
5.2	Composition and characterization of nanoparticles prepared with stearic acid by nanoprecipitation technique	111
5.3	Composition and characterization of nanoparticles prepared with glyceryl monostearate by nanoprecipitation technique	112
5.4	Composition and characterization of nanoparticles prepared with stearic acid by emulsification-ultrasonication technique	113

Table No.	Caption	Page No.
5.5	Composition and characterization of nanoparticles prepared with glyceryl monostearate by emulsification-ultrasonication technique	114
5.6	Best fitting of in-vitro release data using mathematical modeling	130
5.7	Stability study results for the selected OLN nanoparticle formulations stored at various conditions (3 & 6 months)	137
6.1	Pharmacokinetic parameters of OLN and OLN loaded NP in plasma after i.v administration (n=3)	148
6.2	Pharmacokinetic parameters of OLN and OLN loaded NP in brain after i.v administration (n=3)	150
6.3	Pharmacokinetic parameters of OLN and OLN loaded NP in liver after i.v administration (n=3)	151
6.4	Pharmacokinetic parameters of OLN and OLN loaded NP in lungs after i.v administration (n=3)	153
6.5	Pharmacokinetic parameters of OLN and OLN loaded NP in kidney after i.v administration (n=3)	154
6.6	Pharmacokinetic parameters of OLN and OLN loaded NP in spleen after i.v administration (n=3)	156
6.7	Pharmacokinetic parameters of OLN and OLN loaded NP in heart after i.v administration (n=3)	158

List of Figures

Figure No.	Caption	Page No.
1.1	Schematic representation of blood-brain barrier	6
1.2	General transport mechanisms across blood-brain barrier	7
3.1	Overlaid spectrum of pure OLN at LQC, MQC & HQC levels in 100mM HCl buffer (a) and phosphate buffer saline (b)	49
3.2	Overlaid spectrum of pure OLN with marketed commercial sample in 100mM HCl buffer with pH 1.2 (a) and phosphate buffer saline (b)	51
3.3	Representative chromatogram of OLN (800ng.mL ⁻¹) with RT 5.8 min	59
3.4	Representative chromatograms of forced degradation study of OLN: Acid hydrolysis (a); Base hydrolysis (b); Oxidation (c)	60
3.5	Three-dimensional surface plots of responses such as tailing factor (a), peak height (b) retention time (c) and peak area (d)	63
3.6	Overlaid chromatograms of blank rat plasma and plasma spiked with OLN (4.8min) and IS, Risperidone (9.9min)	67
4.1	FTIR spectra of OLN	78
4.2	Preformulation study profile: solubility determination	79
4.3	Preformulation study profile: Log D determination	79
4.4	Preformulation study profile: pKa determination	80
4.5	Solution state stability analysis of OLN in buffer solutions	81
4.6	Solid state stability analysis of OLN	82
4.7	DSC thermograms of OLN, stearic acid and mixture of both	83
4.8	DSC thermograms of OLN, poly caprolactone and mixture of both	84
4.9	DSC thermograms of OLN, glyceryl monostearate and mixture of both	84
4.10	DSC thermograms of OLN, pluronic F68 and mixture of both	85
4.11	DSC thermograms of OLN, Poly vinyl alcohol and mixture of both	85
4.12	Overlaid FTIR spectra of OLN with excipients	86

Figure No.	Caption	Page No.
5.1	Response surface for particle size of PCL NP: effect of polymer (A) and surfactant concentration (B)	97
5.2	Response surface for particle size of ST NP: effect of polymer (A) and surfactant concentration (B)	97
5.3	Response surface for particle size of GLY NP: effect of polymer (A) and surfactant concentration (B)	98
5.4	Response surface for encapsulation efficiency of PCL NP: effect of polymer (A) and surfactant concentration (B)	100
5.5	Response surface for encapsulation efficiency of ST NP: effect of polymer (A) and surfactant concentration (B)	100
5.6	Response surface for encapsulation efficiency of GLY NP: effect of polymer (A) and surfactant concentration (B)	101
5.7	Response surface for particle size of ST NP: effect of solid lipid (A), surfactant concentration (B) and drug:lipid ratio (C)	102
5.8	Response surface for particle size of GLY NP: effect of solid lipid (A), surfactant concentration (B) and drug:lipid ratio (C)	103
5.9	Response surface for encapsulation efficiency of ST NP: effect of solid lipid (A), surfactant concentration (B) and drug:lipid ratio (C)	105
5.10	Response surface for encapsulation efficiency of GLY NP: effect of solid lipid (A), surfactant concentration (B) and drug:lipid ratio (C)	105
5.11	Response surface for drug content of ST NP: effect of solid lipid (A), surfactant concentration (B) and drug:lipid ratio (C)	107
5.12	Response surface for drug content of GLY NP: effect of solid lipid (A), surfactant concentration (B) and drug:lipid ratio (C)	107
5.13	Representative size distribution by intensity profile and SEM image of PCL NP (a, b), C PCL NP (c, d), GLY NP (e, f) & C GLY NP (g, h)	115
5.14	Representative zeta potential distribution profile of PCL NP (a), C PCL NP (b), GLY NP (c) & C GLY NP (d)	116
5.15	In-vitro release profiles of nanoparticulate systems prepared with various polymer/solid lipids with PF68 as stabilizer prepared using nanoprecipitation method	117

Figure No.	Caption	Page No.
5.16	In-vitro release profiles of nanoparticulate systems prepared with various polymer/solid lipids with PVA as stabilizer prepared using nanoprecipitation method	117
5.17	Effect of polymer amount on in-vitro release profiles of OLN loaded PCL NP prepared by nanoprecipitation method	118
5.18	Effect of lipid amount on in-vitro release profiles of OLN loaded ST NP prepared by nanoprecipitation method	119
5.19	Effect of lipid amount on in-vitro release profiles of OLN loaded GLY NP prepared by nanoprecipitation method	119
5.20	Effect of lipid amount on in-vitro release profiles of OLN loaded ST NP prepared by emulsification sonication technique	120
5.21	Effect of lipid amount on in-vitro release profiles of OLN loaded GLY NP prepared by emulsification sonication technique	120
5.22	Effect of various stabilisers on in-vitro release profiles of nanoparticulate systems prepared with PCL prepared by nanoprecipitation method	121
5.23	Effect of various stabilisers on in-vitro release profiles of nanoparticulate systems prepared with Stearic acid using nanoprecipitation method	122
5.24	Effect of various stabilisers on in-vitro release profiles of nanoparticulate systems prepared with Glyceryl monostearate using nanoprecipitation method	122
5.25	Effect of surfactant concentration on in-vitro release profiles of OLN loaded PCL NP prepared by nanoprecipitation method	123
5.26	Effect of surfactant concentration on in-vitro release profiles of OLN loaded ST NP prepared by nanoprecipitation method	123
5.27	Effect of surfactant concentration on in-vitro release profiles of OLN loaded GLY NP prepared by nanoprecipitation method	124
5.28	Effect of surfactant concentration on in-vitro release profiles of OLN loaded ST NP prepared by emulsification sonication technique	124
5.29	Effect of surfactant concentration on in-vitro release profiles of OLN loaded ST NP prepared by emulsification sonication technique	125

Figure No.	Caption	Page No.
5.30	Comparative in-vitro release profiles of OLN from coated and un coated PCL NP prepared by nanoprecipitation method	126
5.31	Comparative in-vitro release profiles of OLN from coated and un coated ST NP prepared by nanoprecipitation method	126
5.32	Comparative in-vitro release profiles of OLN from coated and un coated GLY NP prepared by nanoprecipitation method	127
5.33	Comparative in-vitro release profiles of OLN from coated and un coated ST NP prepared by emulsification sonication technique	127
5.34	Comparative in-vitro release profiles of OLN from coated and un coated GLY NP prepared by emulsification sonication technique	128
5.35	Effect of D: L ratio on in-vitro release profile of OLN loaded ST NP prepared by emulsification sonication method	129
5.36	Effect of D: L ratio on in-vitro dissolution profile of OLN loaded GLY NP prepared by emulsification sonication method	129
5.37	In-vitro release profiles of OLN from optimized nanoparticulate formulations of PCL NP	133
5.38	In-vitro release profiles of OLN from optimized nanoparticulate formulations of GLY NP	133
5.39	In-vitro release profiles of OLN from optimized nanoparticulate formulations of C PCL NP	134
5.40	In-vitro release profiles of OLN from optimized nanoparticulate formulations of C GLY NP	134
5.41	DSC thermograms of pure OLN and OLN loaded PCL nanoparticles	135
5.42	DSC thermograms of pure OLN and OLN loaded GLY nanoparticles	135
6.1	OLN concentration in plasma versus time profile following i.v. administration of the pure OLN and OLN loaded nanoparticles in rats	147
6.2	OLN concentration in brain versus time profile following i.v. administration of the pure OLN and OLN loaded nanoparticles in rats	149

Figure No.	Caption	Page No.
6.3	OLN concentration in liver versus time profile following i.v. administration of the pure OLN and OLN loaded nanoparticles in rats	151
6.4	OLN concentration in lungs versus time profile following i.v. administration of the pure OLN and OLN loaded nanoparticles in rats	153
6.5	OLN concentration in kidney versus time profile following i.v. administration of the pure OLN and OLN loaded nanoparticles in rats	154
6.6	OLN concentration in spleen versus time profile following i.v. administration of the pure OLN and OLN loaded nanoparticles in rats	156
6.7	OLN concentration in heart versus time profile following i.v. administration of the pure OLN and OLN loaded nanoparticles in rats	158
7.1	Effect of pure olanzapine and nanoparticulate formulations of olanzapine on apomorphine induced sniffing behavior at 30 min	165
7.2	Effect of pure olanzapine and nanoparticulate formulations of olanzapine on apomorphine induced sniffing behavior at 1 h	166
7.3	Effect of pure olanzapine and nanoparticulate formulations of olanzapine on apomorphine induced sniffing behavior at 4 h	166
7.4	Effect of pure olanzapine and nanoparticulate formulations of olanzapine on apomorphine induced sniffing behavior at 8 h	167
7.5	Effect of pure olanzapine and nanoparticulate formulations of olanzapine on apomorphine induced sniffing behavior at 12 h	167
7.6	Effect of pure olanzapine and nanoparticulate formulations of olanzapine on apomorphine induced sniffing behavior at 24 h	168
7.7	Effect of pure olanzapine and nanoparticulate formulations of olanzapine on apomorphine induced sniffing behavior at 48 h	168
7.8	Effect of pure olanzapine and nanoparticulate formulations of olanzapine on apomorphine induced climbing behavior at 30 min	169
7.9	Effect of pure olanzapine and nanoparticulate formulations of olanzapine on apomorphine induced climbing behavior at 1 h	169

Figure No.	Caption	Page No.
7.10	Effect of pure olanzapine and nanoparticulate formulations of olanzapine on apomorphine induced climbing behavior at 4 h	170
7.11	Effect of pure olanzapine and nanoparticulate formulations of olanzapine on apomorphine induced climbing behavior at 8 h	170
7.12	Effect of pure olanzapine and nanoparticulate formulations of olanzapine on apomorphine induced climbing behavior at 12 h	171
7.13	Effect of pure olanzapine and nanoparticulate formulations of olanzapine on apomorphine induced climbing behavior at 24 h	171
7.14	Effect of pure olanzapine and nanoparticulate formulations of olanzapine on apomorphine induced climbing behavior at 48 h	172
7.15	Effect of OLN and nanoformulations of OLN on catalepsy score (s) at 0 min	173
7.16	Effect of OLN and nanoformulations of OLN on catalepsy score (s) at 30 min	174
7.17	Effect of OLN and nanoformulations of OLN on catalepsy score (s) at 60 min	174
7.18	Effect of OLN and nanoformulations of OLN on catalepsy score (s) at 120 min	175
7.19	Effect of OLN and nanoformulations of OLN on catalepsy score (s) at 180 min	175
7.20	Effect of OLN and nanoformulations of OLN on catalepsy score (s) at 240 min	176
7.21	Effect of OLN and nanoformulations of OLN on body weight (g)	177

List of Abbreviations and Symbols

%	Percentage
% CDR	Percentage cumulative drug released
% RSD	Percentage relative standard deviation
% RTD	Percentage remaining to be degraded
λ_{\max}	Wavelength of maximum absorbance
<	Less than
=	Equal to
\approx	Approximately equal to
°C	Degree centigrade
°C.min ⁻¹	Degree centigrade per minute
5-HT	5- Hydroxy tryptamine
ACN	Acetonitrile
ANOVA	Analysis of variance
AT	Accelerated temperature
AUC	Area under curve
AUMC	Area under the first moment curve
BCS	Biopharmaceutical classifications system
cm	Centimeter
C _{max}	Maximum concentration
CNS	Central nervous system
Conc.	Concentration
cPs	Centipoises
CR	Controlled release
CYP	Cytochrome P450 enzyme system
CRT	Controlled room temperature
DC	Drug content
DCM	Dichloro methane
DMSO	Dimethyl sulfoxide
DSC	Differential scanning calorimetry
EDTA	Ethylene di amine tetra acetic acid
EE	Entrapment/Encapsulation efficiency
EPS	Extra pyramidal symptoms
et al.,	Co-workers

f_2	Similarity factor
FDA	Food and drug administration
F_r	Relative bioavailability
FTIR	Fourier transform infra red
g	Gram
$g.L^{-1}$	Gram per litre
HETP	Height equivalent to theoretical plates
h	Hour
HQC	Higher quality control
ICH	International conference on harmonization
IP	Indian Pharmacopoeia
IR	Immediate release
IS	Internal standard
i.v	Intravenous
J/g	Joule per gram
K	Release rate constant for 'Korsmeyer-Peppas' empirical equation
K_0	Zero order release rate constant
K_1	First order release rate constant
K_{deg}	Degradation rate constant
Kg	Kilogram
$Kg.cm^{-2}$	Kilogram per square centimeter
K_H	Release rate constant representative of square root kinetics
L	Litre
LC	Liquid chromatography
LCMS	Liquid chromatography coupled with mass spectrophotometer
$L.h^{-1}.kg^{-1}$	Litre per hour per kilogram
$L.kg^{-1}$	Litre per kilogram
LLE	Liquid-liquid extraction
LLOQ	Lower limit of quantification
LOD	Limit of detection
LOQ	Limit of quantification
LQC	Lower quality control
MDT	Mean dissolution time
mg	Milligram

mg.mL ⁻¹	Milligram per millilitre
min	Minute
mL.min ⁻¹	Millilitre per minute
MPS	Mononuclear phagocyte system
MQC	Medium quality control
MRT	Mean residence time
M_t/M_∞	Fraction of drug released at time t
n	Diffusional exponent indicative of release mechanism in krosmeier-peppas model
NDDS	Novel drug delivery systems
NP	Nanoparticles
NE	Norephinephrine
ng.mL ⁻¹	Nanogram per millilitre
OLN	Olanzapine
PDDS	Particulate drug delivery systems
PBS	Phosphate buffer saline
PDI	Polydispersity index
PEG	Poly ethylene glycol
PF 68	Pluronic F68/Poloxamer 188
P-gp	P-glycoprotein
pH	Negative log to the base 10 of hydrogen ion concentration
PNP	Polymeric NP
PVA	Poly vinyl alcohol
p-value	Significance level in statistical tests (probability of a type I error)
$P_{o/w}$	Equilibrium partition coefficient
QC	Quality control
r^2	Regression coefficient
R_f	Retention factor
RH	Relative humidity
RP-HPLC	Reverse phase-High performance liquid chromatography
Rpm	Revolutions per minute
RT	Retention time
S	Slope of the least square regression line
SD	Standard deviation
SEM	Scanning electron microscopy

SLN	Solid lipid nanoparticles
SNRI	Serotonin and norepinephrine reuptake inhibitors
SPE	Solid phase extraction
SSRIs	Selective serotonin reuptake inhibitors
$t_{1/2}$	Half-life
$t_{50\%}$	Time to reach 50% of initial concentration
$t_{90\%}$	Time to reach 90% of initial concentration
T50%	Time taken for 50% of drug release from formulations
T80%	Time taken for 80% of drug release from formulations
TCA's	Tricyclic antidepressants
TDW	Triple distilled water
TEM	Transmission electron microscopy
T_g	Glass transition temperature
TLC	Thin layer chromatography
T_{max}	Time taken to reach maximum concentration
USP	United States Pharmacopoeia
UV	Ultra Violet
V_d	Apparent volume of distribution
Vis	Visible
V_{ss}	Apparent volume of distribution at steady-state
XRD	X-ray powder diffraction patterns
w/w	Weight by weight
ZP	Zeta potential
$\mu\text{g.mL}^{-1}$	Micro gram per millilitre

Chapter 1

Introduction

1.1 Introduction

Antipsychotics, an important category of central nervous system (CNS) acting drugs, are widely used for the treatment of severe mental disorders such as schizophrenia and bipolar disorder [1, 2]. These two psychiatric disorders tremendously affect world population and have significant socioeconomic impact, morbidity and mortality. The most common manifestations of schizophrenia include auditory hallucinations, disorganized speech or bizarre delusions and thoughts with significant social and occupational dysfunctions [3, 4]. Positive symptoms such as auditory hallucinations, delusions, thinking disorder etc. and negative symptoms such as anhedonia, lack of desire to form relationship (asociality), lack of motivation etc. are observed in schizophrenic patients. In first-degree relatives, there is a high risk of acquiring schizophrenia and about 10% probability is expected. Hypertension and maternal viral infection during the course of pregnancy are also found to be associated with the etiology of schizophrenia. Studies of postmortem schizophrenic brains have shown evidence of misplaced cortical neurons with abnormal morphology. It has also been postulated that stress may also be involved in acute attacks of schizophrenia, mostly in the age group of 15 to 35 years [5-9].

Significant facts and figures about schizophrenia include a) It affects about 24 million people worldwide; b) According to the World Health Organization, schizophrenia is the eighth leading cause of disability worldwide among 15-44 year old population; c) Approximately 10% of people with schizophrenia commit suicide and 20% to 40% of people with schizophrenia make at least one suicide attempt in their lifetime; d) People living with severe and persistent mental illness are more likely than the general population to suffer from heart disease, hypertension, diabetes, obesity, asthma, gastrointestinal disorders, skin infections and acute respiratory disorders; e) More than 50% of people with schizophrenia are not receiving appropriate care; f) 90% of people with untreated schizophrenia are in developing countries such as India [10-12].

The recovery stages of schizophrenia are classified mainly into three stages namely acute phase, stabilization phase and maintenance phase. Medication is the primary treatment in acute phase and if given the right drug and dose, schizophrenia medication can greatly minimize the psychotic symptoms within 5 to 7 weeks and

hospitalization is required in this stage. The most important aim of treatment in the stabilization phase is to prevent relapse, reduce symptoms even more, thereby, help the patient to move forward into a more stable recovery phase. During maintenance phase of recovery, the important goal is to sustain symptom remission or control, minimize the risk of hospitalization and relapse as well as to teach common skills necessary for day-to-day life [13-15].

Bipolar disorder or manic-depressive illness is another major psychiatric disorder that can be treated with anti-psychotics [16]. This psychiatric disorder causes unusual shifts in energy, mood and activity levels. In this disorder, because of chemical imbalance in the brain, person would be in either a manic state or depressive state and there are rare times only when the state of individual is between the two states. This disorder can cause the person to behave in a very risky manner. Bipolar disorder patients are often seen as self-destructive and they often have highly troubled relationships, careers etc. Moreover, bipolar disorder can lead to suicide if not treated on time [17, 18].

1.2 Antipsychotic medication and its limitations

Antipsychotics which are used for the treatment of schizophrenia and bipolar disorder, can be classified broadly into three categories based on the underlying mechanism of action. These are typical anti-psychotics, atypical anti-psychotics and a newer category of drugs called dopamine partial agonists [19]. Several antipsychotic drugs act by blocking the dopamine D₂ receptors present in the brain. These receptors are vital in dopamine pathway and are responsible for increasing or decreasing dopamine, a catecholamine neurotransmitter in the brain [20]. Dopamine has been shown to be essential for the normal activity of the CNS; its reduced concentration within the brain has been associated with parkinson's disease, while an excess may cause such conditions as schizophrenia. Typical antipsychotics like Chlorpromazine, Fluphenazine, Perphenazine and Prochlorperazine block the D₂ receptor, but are relatively non-specific and block receptors in other biochemical pathways such as nigrostriatal, tuberoinfundibular and mesocortical pathways [21].

Atypical antipsychotics such as Clozapine, Olanzapine (OLN), Quetiapine and Ziprasidone appear to be slightly more discriminating than the typical antipsychotics.

In addition to the D₂ receptors, the atypical antipsychotics have been shown to block serotonin receptors, such as 5HT_{2A}, 5HT_C and 5HT_{1A} receptors. The dopamine partial agonist such as Aripiprazole is sometimes referred to as atypical antipsychotics. They are quite similar to the atypical antipsychotics in that they also act on both dopamine and serotonin receptors and appear to mediate its antipsychotic effects mainly by partial agonism of the dopamine D₂ receptor [22, 23]. Conventional treatment of antipsychotics is done by delivering medications in the form of tablets, capsules, solutions for injections etc.

1.2.1 Limitations of conventional antipsychotic formulations

a. Non selective distribution: Non selective distribution of many antipsychotics like OLN, Risperidone etc. produce a high level of adverse cardiovascular effects resulting in hypotension, prolonging ECG QT-corrected interval, chest pain, tachycardia, peripheral edema, ventricular tachycardia/fibrillation, ventricular arrhythmias and even sudden death [24, 25].

b. Adverse effects: Conventional formulations of antipsychotic drugs are always associated with numerous undesirable adverse effects. Many patients suffer from drug-induced extra pyramidal symptoms (EPS) such as drug-induced Parkinsonism, acute dystonia reactions, akathisia, tardive dyskinesia and tardive dystonia. Most of drugs available for treatment of CNS disorders such as schizophrenia and bipolar disorder are prone to produce these extra pyramidal side effects when used at therapeutic doses [26].

Furthermore, as compared to typical antipsychotics, atypical antipsychotics such as OLN is highly capable of causing dose dependent weight gain, or in worse case even obesity. These are also associated with metabolic disturbances, sexual dysfunction, hyper salivation, hyperprolactinemia and constipation [27, 28].

c. Lack of response and resistance: Many patients do not respond or only partially respond to the currently available drug treatments, and it is estimated that 40% and 80% of those treated with antipsychotics accounts for this. The severity of adverse effects and the lack of efficacy in large number of patients often results in poor patient compliance thus results in diminished therapeutic effect [29, 30].

d. Discontinuation of antipsychotic medication: Non-adherence to antipsychotic medication occurs, which is mainly due to forgetfulness and potential adverse effects of antipsychotic drugs [31, 32].

Most of these adverse effects (EPS, weight gain, metabolic disturbances etc.) are dose and concentration dependent. Positron-emission tomography (PET) can be used to estimate D₂-like receptor occupancy in the brain needed for an antipsychotic effect and the level above which EPS develops. For the atypical antipsychotic Risperidone or OLN, the antipsychotic effect starts at approximately 60% occupancy, with occupancy above 80% leading to EPS [33, 34]. Accordingly, there is a need for antipsychotic drug formulations that control or eliminate psychotic symptoms with fewer or negligible side effects, and which can be formulated to increase patient compliance. These can be achieved by controlled release of the drug from dosage forms and selective distribution (V_d of OLN is 1000 L) of the drug to brain using novel drug delivery approaches, which will decrease dose, dose dependent side effects, frequency of administration and consequently increased patient compliance.

1.3 Novel drug delivery approaches for CNS active drugs

Drug delivery to the brain is always a challenging task for the formulation scientists because of the presence of blood brain barrier (BBB) with tight junctions in the brain endothelial cells. It has been estimated that more than 98% of CNS active drugs coming out of synthetic pipelines are not able to cross the BBB to achieve a sufficient therapeutic drug concentration [35]. Also, majority of the small molecule drugs (>98%) and almost all of the large molecule drugs including biotechnology based products fail to cross blood brain barrier. If pharmaceutical scientists could deliver these molecules across the blood brain barrier, numerous diseases affecting CNS could have been treated in a more efficient way. Numerous traditional approaches have been investigated for this purpose such as prodrugs, disruption of blood brain barrier, intra-cerebral injection/use of implants etc. Prodrugs are generally bioreversible derivatives of drug molecules that undergo a chemical/enzymatic biotransformation to convert to active drugs to produce pharmacological action in the body [36]. Prodrug approach has been explored to convert the drug to a more lipophilic compound, thereby improving the passage across blood brain barrier. Prodrugs based on chemical derivatives such as, lipophilic esters and other

hydrophobic compounds have been studied. More sophisticated prodrug approaches comprises of macromolecular delivery mechanisms (e.g. receptor-mediated prodrug transport), endogenous transporters (e.g. carrier-mediated prodrug transport) as well as gene-mediated enzyme prodrug therapy [36, 37]. Prodrug approach is often limited due to the premature conversion of prodrug to the drug in plasma itself by the plasma-enzymes.

Disruption of the BBB is another traditional approach, which makes the tight junctions of the endothelial cells leaky and provides access for the blood components to the brain [38]. Various techniques have been investigated for the disruption such as osmotic disruption, ultrasound disruption and disruption by bradykinin-analogue. In the case of osmotic disruption, the osmotic shock causes endothelial cells to shrink, thus disrupting the tight junctions. A classic example for this is the administration of a hypertonic mannitol solution with subsequent administration of drugs through intra-carotid artery increased the drug concentration in brain and tumor tissue as compared to the administration of drug alone [38]. Magnetic Resonance Imaging (MRI)-guided focused ultrasound technique is another useful approach for BBB disruption. In a study performed by Feng et al, it has been demonstrated that, Evans Blue (EB) extravasation can be enhanced by the application of repeated sonication [39]. Sonication was applied at an ultrasound frequency of 1 MHz and a repetition frequency of 1 Hz. There was nearly two-fold increase in EB extravasation in groups with a second sonication compared with the single sonication group. The selective B₂ bradykinin receptor agonist, Cereport (also called RMP-7), also has been shown to increase permeability transiently of the blood brain barrier. There are evidences of enhanced CNS delivery of carboplatin, loperamide, and cyclosporin-A, when administered along with RMP-7 [40]. The major limitation associated with BBB disruption technique is the increased brain uptake of plasma albumin and other protein components of blood, which are toxic to brain cells [41].

Intra-cerebral injection/use of implants is another useful traditional approach. The bolus injection of therapeutic agents and the placement of a biodegradable drug-impregnated wafer rely on the principle of diffusion to drive the drug into the infiltrated brain. Various types of paclitaxel-loaded, lipidic implants and PLGA-based microparticles with controlled release kinetics during several weeks have been prepared and characterized in-vitro by K. Elkharraz et al [42]. These devices can

directly be injected into the brain tissue (intracranial administration) overcoming the restriction that paclitaxel is unable cross the blood-brain barrier to a significant extent upon systemic administration. They have found that this type of controlled drug delivery system is helpful to improve the local treatment of operable and inoperable brain tumors.

These traditional approaches are less successful to cross the BBB for better brain delivery and most of them are associated with numerous adverse effects. Moreover, some of these approaches are highly destructive in nature, which is extremely harmful to the body in long term. Thus, it is a challenge to enhance drug permeability to brain for effective therapeutic efficacy with no or limited side effects and with better patient compliance.

1.3.1 Structure of blood brain barrier and transport mechanisms

The BBB is considered to be a dynamic and complex barrier separating blood and the CNS that strictly controls the exchanges between the compartments of blood and brain. BBB is a natural biological barrier that plays a crucial role in the protection of the brain by restricting the entry of untoward substances such as toxic molecules, pathogens, and numerous other external molecules thereby maintaining the brain homeostasis. An illustration of BBB is shown in Figure 1.1

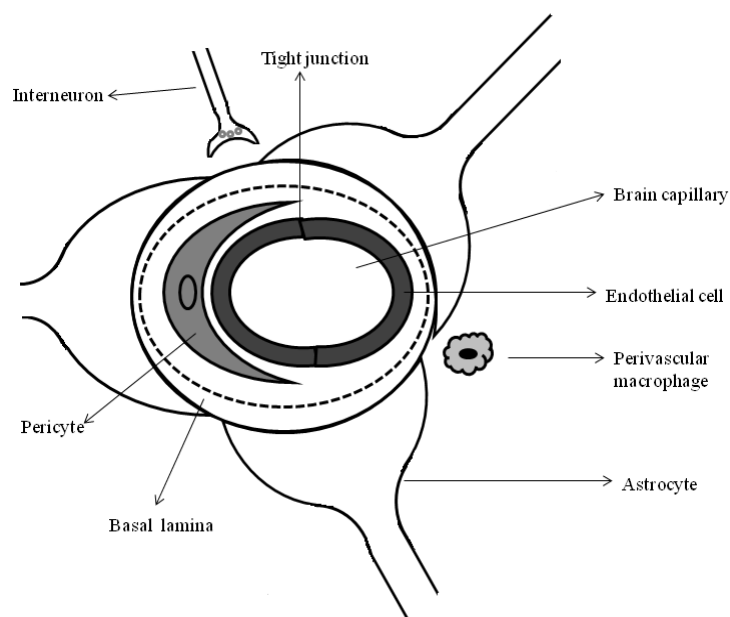


Figure 1.1: Schematic representation of blood-brain barrier

Endothelial cells present in the brain and other parts of the body vary significantly due to the presence of intracellular tight junctions, less extent paracellular diffusion of hydrophilic molecules, relatively high number of mitochondrial cells thereby high metabolic activity, and a relatively higher number of active transporters (for transport/efflux of nutrients/toxic compounds) [43]. The basal lamina composed mainly of collagen, glycoproteins, and proteoglycans, is involved in the dynamic regulation of BBB with the aid of multiple basal lamina proteins, matrix metalloproteases, their inhibitors, and the tissue inhibitor of metalloproteases. The astrocytes and glial cells present in the BBB also contribute largely for the barrier integrity through glial-derived neurotrophic factor, angiopoietin-1 and angiotensin II. Brain micro vessels have numerous pericytes and ratio of pericytes to endothelial cells was linked with the barrier capacity. Endothelium, pericytes, perivascular astrocytes are in very close contact with neuronal projections.

1.3.2 General transport mechanisms across blood brain barrier

The major transport mechanisms to the BBB are depicted in Figure 1.2. These include paracellular aqueous pathway, transcellular lipophilic pathway, transport protein pathway, receptor mediated transcytosis, and adsorptive transcytosis.

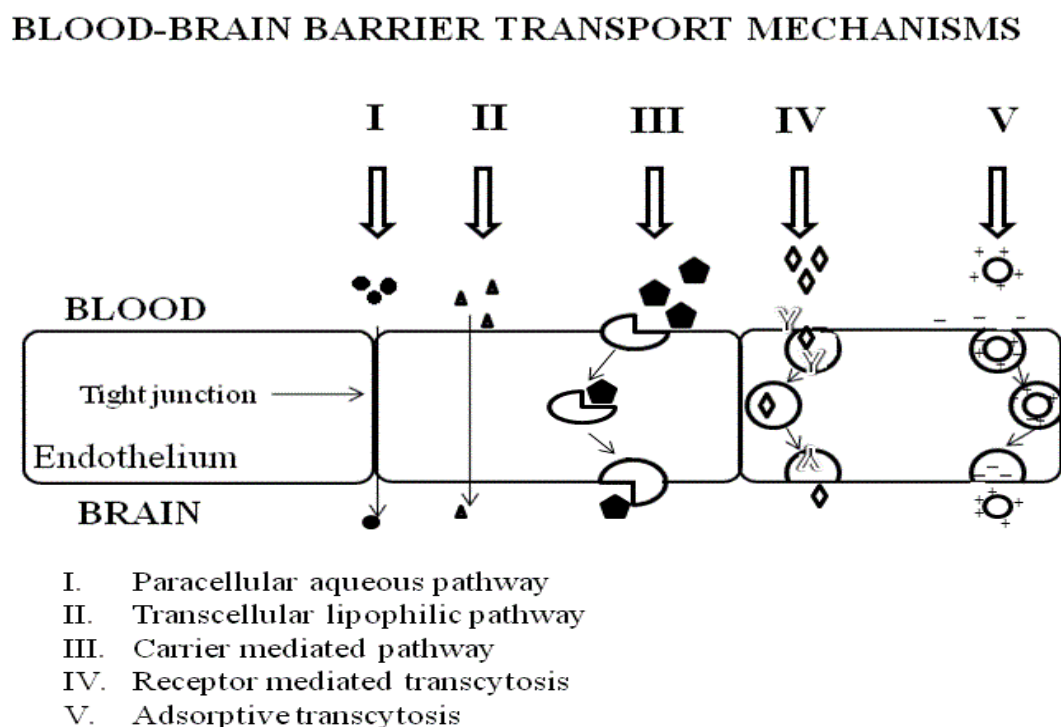


Figure 1.2: General transport mechanisms across blood-brain barrier

Paracellular aqueous pathway is a rare pathway across BBB through which small water-soluble molecules diffuse into the brain. Lipophilic molecules such as alcohol, steroid hormones etc. penetrate transcellularly by dissolving in their lipid plasma membrane. In transport proteins/carrier-mediated transport, a protein transporter binds to glucose or amino acids, which triggers a conformational change in the protein and helps in the transport of the molecule to the other side. The receptor-mediated transcytosis type of transport mechanism is for the selective uptake of macromolecules. These systems include receptors for transferrin, insulin, lipoprotein etc. that are also explored for the ligand based nanoformulations. Another kind of transport mechanism, called adsorptive-mediated transcytosis is triggered by an electrostatic interaction between a positively charged substance such as charged moiety of a peptide, and the negatively charged plasma membrane surface such as heparin sulphate proteoglycans [44].

The aforementioned components of BBB and specific transport mechanisms make BBB highly dynamic and complex, thereby restricting the entry of various drug molecules. Since traditional approaches could not solve these problems, pharmaceutical scientists looked forward and found out newer approaches such as nanotechnology in order to deliver drugs across BBB successfully.

1.3.3 Nanotechnology for delivery of CNS active drugs

The application of nanotechnology for drug delivery to the brain opens the doors of opportunities for the formulation scientists for better brain delivery of existing and newer potential molecules with CNS activity. It has been assumed that the majority of the potential CNS drugs, which have inability to cross BBB, could be modified by nanotechnology in order to achieve better therapeutic action. It would bring about rebirth to many drugs, which have been discontinued due to their failure to gain therapeutic concentration in the brain.

1.3.4 Mechanisms of nanoformulations facilitating brain delivery

Kreuter J. et al., described number of possibilities that could explain the mechanisms of the delivery of nanoformulations across the BBB, which are discussed below: [45, 46].

- a. As compared to the pure drugs, there is an increased retention of the nanoformulations in the brain blood capillaries combined with more adsorption to the capillary walls. These retention and adsorption create a higher concentration gradient that would enhance the transport across the endothelial cell layer and result in better delivery to the brain.
- b. The nanoformulations could lead to an opening of the tight junctions between the brain endothelial cells. The drug could then permeate through the tight junctions in either free form or together with the nanoparticles in bound form.
- c. There is a general surfactant effect of nanoformulations characterized by solubilization of the endothelial cell membrane lipids that would further lead to membrane fluidization and thereby enhanced drug permeability through BBB.
- d. The nanoformulations may be endocytosed by the endothelial cells of the brain capillaries that would result in the release of the drugs within these cells and delivery to the brain. Drug bound nanoformulations could be transcytosed through the endothelial cell layer.
- e. Surfactant, which is used as the coating agent, could inhibit the efflux system, especially P-glycoprotein (Pgp). Endocytosis via the low density lipoprotein (LDL) receptor, mediated by the adsorption of apolipoprotein B and/or E from the blood is also a suggested mechanism for the nanoformulations coated with polysorbate-Tween 20, 40, 60 and 80, and poloxamers such as Pluronic F68 [46, 47].

1.3.5 Nanoformulations investigated

Numerous nanoformulations have been investigated successfully for better brain delivery, which include nanoparticulate systems (polymeric/solid lipid), liposomes, dendrimers, nanoemulsions, nanosuspensions, and ligand-mediated nanosystems out of which polymeric and solid lipid NP have been discussed in detail below. Summary of these systems investigated with examples is listed in Table.1.1.

1.3.5.1 Nanoparticulate systems

Nanoparticles (NP) are colloidal particles, less than 1000 nm that can be used for better drug delivery and prepared either by encapsulating the drug within a vesicle and/or by dispersing the drug molecules within a matrix [62].

Table 1.1: List of nanoformulations investigated for brain distribution

Formulation	Material used	API	Advantages
Polymeric NP	PLGA and PCL	Etoposide	Selective distribution with higher brain permeability [48]
	Chitosan	Venlafaxine	Better brain uptake, higher direct transport percentage [49]
	PLA-PEG-tween 80	Amphotericin B	Drug concentration in mice brain greatly enhanced, reduced the toxicity of AmB to liver, kidney etc. [17]
	PBCA-tween 80	Doxorubicin	Augmented accumulation of NP in the tumor site and in the contra lateral hemisphere [50]
Solid lipid nanoparticles/ Nanostructured lipid carriers	Cetyl palmitate, dynasan and witepsol	Camptothecin	Higher affinity to the porcine brain capillary endothelial cells as compared to macrophages [51]
	Trimyristin, tripalmitin and tristearin	Clozapine	The AUC and MRT of clozapine SLN were significantly higher in brain [52]
	Stearic acid	Idarubicin	Drug and its metabolite were detected in the brain only after IDA - SLN administration [53]
Liposomes	Tripalmitin, gelucire and vitamin E	Baicalein	Brain-targeting efficiency of baicalein was greatly improved by NLC [54]
	DPPC, DC, Chol, DOPE, DHPE DSPC, cholesterol, DSPE	Oregon Green Citicoline	Liposomes were strongly internalized in cultured cell lines within 6 h [55] Considerable increase (10-fold) in the bioavailability of the drug in the brain parenchyma [56]
Dendrimers	Polyamidoamine	Paclitaxel	12-fold greater permeability across porcine brain endothelial cells [57]
	Poly propyleneimine	Docetaxel	Higher targeting efficiency and biodistribution to the brain [58]
Miscelles	Block copolymers of ethylene oxide/propylene oxide	Olanzapine	Demonstrated higher drug targeting index (5.20), drug targeting efficiency (520.26%) and direct transport percentage (80.76%) [59]
Nanoemulsion	Glyceryl monocaprylate	Risperidone	Higher drug transport efficiency (DTE%) and increased direct nose to brain drug transport (direct transport percentage, DTP%) [60]
	Flax-seed and safflower oil	Saquinavir	Improved brain uptake [61]

Nanoparticulate drug delivery systems have been extensively studied in recent years for spatial and temporal delivery, especially in tumour and brain targeting. NP have great promise for better drug delivery as found in both pharmaceutical and clinical research. As a drug carrier, NP have significant advantages like better bioavailability, systemic stability, high drug loading, long blood circulation time and selective distribution in the organs/tissues with longer half-life. These systems have been increasingly used in order to improve brain delivery of the therapeutic agents. Majorly investigated nanoparticulate systems for aforementioned applications are polymeric nanoparticles and solid lipid nanoparticles, whose preparation methods, characterization and in vivo fate are discussed in detail in following sections.

1.3.5.2 Polymeric nanoparticles

NP, prepared from a wide variety of biodegradable/biocompatible polymers such as poly (D, L-lactide-co-glycolide) (PLGA), poly (D, L-lactide) (PLA), polybutyl cyanoacrylates (PBCA), polycaprolactone (PCL) etc. are extensively used for the delivery of drugs to the CNS. They pose numerous advantages, which include protecting the drug from degradation, releasing a therapeutic load in the optimal dosage range and enabling the delivery of the therapeutic agent to the preferential site [63].

Numerous investigations have been done in order to deliver the drug across BBB by incorporating in polymeric nanoparticulate drug delivery systems. In a study by our group, etoposide loaded PLGA and PCL NP were prepared and biodistribution and pharmacokinetics of radio labeled etoposide and etoposide loaded PLGA and PCL NP were studied. Etoposide and etoposide-loaded NP labeled with Tc-99m were administered intravenously and their respective biodistribution and pharmacokinetic parameters were determined. The results showed an overall high residence of NP compared to etoposide and demonstrated the advantage of PLGA and PCL NP as drug carrier for etoposide in enhancing the bioavailability with selective distribution with higher brain permeability and possibility of reducing the etoposide-associated toxicity. In another study, Imatinib mesylate loaded PLGA NP were prepared and biodistribution and pharmacokinetics were studied in rat model. The results showed that nanoparticulate formulations increased the extent of drug permeation to brain with nearly 100% increase in Mean Residence Time (MRT) and threefold increase in

Area Under the Curve (AUC^{∞}) as compared to pure drug [48].

There are numerous evidences for the existence of a direct nose-to-brain delivery route for nanoparticulate systems administered to the nasal cavity and transported via the olfactory epithelium and/or via the trigeminal nerves directly to the CNS. Haque S et al studied this approach where they prepared venlafaxine (VLF) loaded chitosan NP to enhance the uptake of VLF to brain via intranasal (i.n.) delivery. The higher drug transport efficiency (508.59) and direct transport percentage (80.34) of VLF Chitosan NP as compared to other formulations suggested its better efficacy in treatment of depression [49].

Coating of the NP with surfactants is another useful approach since it can induce increased brain uptake and its mechanism have been described in the earlier section. Numerous studies have been performed in this direction and it has been found that coating with surfactant systems resulted in enhanced brain concentration of drug/dye as compared with uncoated systems [17, 50].

1.3.5.2.1 General methods of polymeric nanoparticles preparation

Various methods have been reported for the preparation of polymeric NP and can be classified into two main categories based on the criteria, whether preparation involves polymerization reaction or directly obtained from preformed polymer [64].

1.3.5.2.1.1 Nanoparticles obtained by polymerization of monomer

a. Emulsion polymerization

Emulsion polymerization is one of the low time consuming methods for NP preparation [65]. Continuous phase used in this method can be either organic or aqueous. The monomer is dispersed into an emulsion or inverse microemulsion or into a non-solvent. Surfactants were also used during the preparation in order to prevent the aggregation during polymerization process. This method is less preferred for NP preparation recently because of the requirement of large amounts of organic solvents, which are highly toxic to the body. In addition, there is a requirement of surfactants and initiators, which have to be eliminated from the final NP. Furthermore, the polymers formed from these kinds of monomers are non-biodegradable in nature, which also resulted in low acceptability of this preparation

method. As a further improvement of this method, scientists have used poly methyl methacrylate (PMMA), poly ethyl cyano acrylate (PECA) and poly butyl cyanoacrylate (PBCA) polymers to prepare NP using less toxic organic solvents such as cyclohexane (ICH class 2) and n-pentane (ICH class 3) [64].

b. Interfacial polymerization

In this method, monomer and drug are dissolved in a mixture, containing an oil and alcohol, which then extruded through a small needle into an aqueous solution under continuous stirring with or without organic solvents like acetone or ethyl alcohol. Spontaneous formation of NP occurs by the polymerization of monomer with the help of initiating ions in the aqueous phase. The concentration of the resultant colloidal suspension can be performed by evaporation under reduced pressure. Cyanoacrylate monomers are mainly used in this method and examples of drugs incorporated during NP preparation by this method include insulin, indomethacin, calcitonin etc. [66].

c. Interfacial polycondensation

Interfacial polycondensation is another method for preparing polymeric NP using monomers, where lipophilic monomer such as phthaloyldichloride and hydrophilic monomer such as diethylenetriamine are used, with or without surfactants. In recent methods, polyether urethane was used for NP preparation by this method [67].

1.3.5.2.1.2 Nanoparticles obtained from preformed polymers

a. Emulsification / solvent evaporation

In this method, as a first step, polymer solution containing drug to be incorporated is emulsified into an aqueous phase and as a second step, the emulsion formed is evaporated thereby precipitating into nanospheres. High energy homogenization techniques are utilized in order to disperse drugs containing polymeric organic solution into aqueous phase or non solvent organic phase such as ethyl acetate or chloroform. The evaporation of the solvent can be performed by increasing the temperature under vacuum or by continuous stirring. Polymers such as PLGA, poly caprolactone, poly hydroxybutyrate, ethyl cellulose etc. have been used in this method for NP preparation and drugs such as testosterone, cyclosporin a, indomethacin, albumin etc. were incorporated into these systems [68].

b. Solvent displacement and interfacial deposition

Both these methods are based on spontaneous emulsification of an internal organic phase containing polymer into an external water phase. Solvent displacement method produces either nanospheres or nanocapsules; interfacial deposition produces only nanocapsules [69].

In solvent displacement method, preformed polymer in organic solvent is precipitated and the solvent is diffused into aqueous phase in either the presence or absence of surfactants. The polymer deposited on the interface between the aqueous and organic phase is precipitated instantaneously due to the speedy diffusion of organic solvent. In order to achieve this, a completely miscible solvent is used and it should be non-solvent to the polymer for maximum result. In this technique, if a small quantity of non toxic oil is added in the organic phase, nanocapsules also can be prepared, where high drug loading efficiency have been reported for hydrophobic drugs. Only water miscible organic solvents such as acetone or dichloromethane are used in this method and as per the diffusion rate, spontaneous emulsification occurs. This method is useful for the encapsulation of hydrophobic drugs and less suitable for hydrophilic drugs. Mechanism of NP must be similar to the diffusion process found in spontaneous emulsification. Various polymers such as PCL, PLA, PLGA etc. are widely used for preparation of NP by this method. Drug such as Cyclosporin was used for entrapping in NP by this method with very high entrapment efficiency (97%) [64]. Interfacial deposition, which is majority an emulsification/solidification technique, produces nanocapsules. In this method, an extra component of oily nature, which is immiscible with mixture, but highly miscible with the solvent of polymer, is incorporated in the preparation. Nanocapsules were obtained by the deposition of polymer on the interface of fine oil droplets and aqueous phase.

c. Emulsification/solvent diffusion

In this technique, the polymer is solubilized in a partially water soluble solvent like propylene carbonate, which is saturated with aqueous phase for thermodynamic equilibration of both liquids. As a next step, this saturated system is emulsified in an aqueous phase with stabilizer, thereby diffusing the solvent to the external phase and producing nanocapsules or nanospheres based on oil/polymer ratio. The solvent is then removed by evaporation or filtration. This technique exhibited high

encapsulation efficiencies and good batch-to-batch uniformity with narrow size distribution. In case of incorporation of hydrophilic drugs, there is a chance of oozing out of drug into the external aqueous phase. A large number of polymers have been used for NP preparation by this method and these include PLA, PLGA, gelatin etc. Drugs such as doxorubicin, coumarin, cyclosporin etc. have been incorporated by this method [70].

d. Salting out with synthetic polymers

In this method of NP preparation, salting out technique is used to separate water miscible solvent from aqueous solution. In a way, it can be considered as a modified procedure of emulsification/solvent diffusion technique. In this technique, polymer and drug are made to dissolve in an organic solvent such as acetone. This solution is further emulsified into an aqueous system containing electrolytes such as magnesium chloride, magnesium acetate, calcium chloride etc. Sometimes, non-electrolytes like sucrose also were used as salting out agent. Stabilizers such as polyvinyl pyrolidone were also used in the preparation as stabilizing agent. The oil/water emulsion is further diluted with sufficient aqueous phase in order to ease the diffusion of acetone into the aqueous external phase resulting in the formation of nanospheres. The solvent and salting out agent are removed further by techniques such as cross flow filtration. Nanospheres with high encapsulation efficiencies are prepared by this technique using polymers such as PLA, ethyl cellulose etc. [71].

e. Desolvation of macromolecules

This is another technique of NP preparation where desolvation is done by charge and pH changes or adding desolvating agents such as alcohol or concentrated solutions of inorganic salts. No heat process is involved during the preparation and therefore it is suitable for thermo liable drugs. Macromolecular materials used for this method include gelatin, casein, serum albumin (human and bovine) etc. [72].

f. Supercritical fluid technology

This is a comparatively recent method of NP preparation where a combination of drug and polymer are made to solubilize in a supercritical or compressed fluid (supercritical CO₂) and subsequently passed through a nozzle where the solution is expanded. The supercritical fluid gets evaporated in this process and eventually solute

particles get precipitated in nano size. This technique produces particles free of solvent residues because of the complete evaporation of supercritical fluid during the expansion process. Numerous drugs have been incorporated by this technique including protein drug such as insulin and obtained highly promising results. Polymers such as PEG/PLA are used for NP preparation using this method. However, the capital investment required for initial set up is very high. In addition, the solubility of polar substances in supercritical fluid is very less extent only, therefore this method is comparatively less suitable for hydrophilic drugs [73, 74].

1.3.5.3 Solid lipid nanoparticles (SLN)

SLN are colloidal particles composed of biocompatible/biodegradable lipid matrix that is solid at body temperature and exhibit size in a range of 100 to 400 nm. SLN offer several advantages such as controlled drug release, targeted delivery, increased drug stability, high drug payload, least biotoxicity, large-scale production and ease of sterilization [75]. General ingredients used in the preparation of SLN are solid lipid(s), emulsifier(s) and water. The term “lipid” has a broader sense here and includes triglycerides (e.g. tristearin), fatty acids (e.g. stearic acid), partial glycerides (e.g. Inwitor), steroids (e.g. cholesterol) and waxes (e.g. cetyl palmitate).

SLN are widely used for the delivery of active pharmaceutical ingredients to the brain because of the above-mentioned advantages and its enhanced ability to cross BBB. For instance, camptothecin-loaded SLN were prepared using cetyl palmitate, Dynasan 114 and Witipsol E85 by hot high-pressure homogenization by Martins et al [51]. A higher affinity of the SLN to the porcine brain capillary endothelial cells (BCEC) was shown in comparison to macrophages. In-vivo studies in rats showed that fluorescently labeled SLN were detected highly in the brain after i.v. administration.

A newer version of SLN called nanostructured lipid carriers (NLC), with increased drug loading are also becoming popular recently for brain targeting which are composed of a solid lipid and a certain amount of liquid lipid (oil), maintaining the solid state at both room and body temperature [76, 77].

1.3.5.3.1 Preparation techniques of solid lipid nanoparticles

SLN are prepared from lipid, emulsifier, and water/solvent by various production techniques [75, 78].

a. High pressure homogenization (HPH)

High-pressure homogenization technique is one of the most powerful and reliable methods of SLN preparation [79]. In this method, liquid is pushed through a very narrow gap of very small size with high pressure upto 2000 bar, thereby accelerating the fluid to a very high velocity of more than 1000km/h. Because of very high shear stress and cavitation forces, particles disrupt down to a range of sub-micron size. There are two basic approaches generally used in high-pressure homogenization technique, namely hot homogenization and cold homogenization.

i. Hot homogenization

In this technique, the drug is initially solubilized in lipid melt. A pre-emulsion is prepared by dispersing this lipid melt into a surfactant aqueous solution, which is kept under stirring and heated, to a temperature above the melting point of the lipid. The resultant pre-emulsion is then subjected to high-pressure homogenization using a high shear mixing device for many cycles (2-5) applying pressure in a range upto 1500 bar. The prepared nano sized emulsion is then allowed to cool down to room temperature or sometimes even to lower temperature [79]. In this cooling down process, the nano droplets are solidified and produce an aqueous dispersion of SLN. Care should be taken while selecting the number of cycles in the homogenization process since large number of cycles may result in contamination of SLN with homogenizer metal and may increase the particle size due to particle coalescence, which happens due to high surface free energy of particles. More number of cycles may also increase the production cost of SLN prepared by this technique. This method is mainly suitable for SLN preparation of hydrophobic drugs and temperature resistant drugs [79, 80].

ii. Cold homogenization technique

In order to overcome the problems associated with hot homogenization technique, such as, temperature induced degradation of active ingredient, distribution of active ingredient into aqueous phase during homogenization process, complexity of

crystallization step etc., and cold homogenization technique has been introduced [75]. In this method, initially the active ingredient is made to dissolve/disperse in lipid melt, similar to that of hot homogenization process. Subsequently, the lipid melt with the active ingredient in it is rapidly cooled down with the help of liquid nitrogen/dry ice. This rapid cooling result in the homogeneous distribution of active ingredient within the lipid matrix. The solidified lipid mixture is then subjected to milling process by using a ball/mortar mill to obtain particles in a size range of 50-100 microns. These microparticles are then dispersed in chilled surfactant solution and subjected to high pressure homogenization at or below room temperature in order to produce SLN [75, 78]. This technique generally produces particles with higher size and broader distribution as compared to hot homogenization technique. Even though this technique was emerged as an alternative for hot homogenization to avoid high temperature, in initial steps, there is an involvement of heat, therefore makes this method unfavourable for very temperature sensitive drugs, which are unstable at a temperature of melting point of lipid. However, as compared to hot homogenization technique, this technique minimizes the exposure of active ingredient to a very high temperature.

b. Solvent emulsification-evaporation technique

In this method, the solid lipid is solubilized in water immiscible organic solvent such as chloroform, cyclohexane, ethyl acetate etc. and the active ingredient is either dissolved or dispersed in it [81]. This organic phase obtained is added into an aqueous system containing surfactant and emulsified by stirring/homogenization. The organic solvent present is subsequently removed by evaporation under reduced pressure or by mechanical stirring. SLN are obtained by the precipitation of lipid phase in the aqueous phase upon removal of organic solvent. This technique is suitable for hydrophobic drugs; however, hydrophilic drugs also can be incorporated by this method by preparing w/o/w emulsion and solubilizing hydrophilic drug in internal aqueous phase. This method is highly suitable for thermo liable drugs since there is no involvement of heat during the preparation. However, the toxicity from residual organic solvent present in the final formulation must be carefully addressed.

c. Solvent emulsification diffusion technique

The lipid is initially dissolved in a partially aqueous miscible solvent such as isobutyric acid, benzyl alcohol, tetrahydro furan etc. and consequently emulsified in an aqueous solution containing surfactant by mechanical stirring. This emulsion is further diluted into an excess aqueous phase at a controlled temperature, which results in the diffusion of solvent into external aqueous phase, thereby precipitating the SLN. Various techniques such as distillation or ultra filtration are used for the removal of solvent. The lipid concentration, nature, surfactant, rate of stirring, processing temperature etc. are critical for optimizing the formation of SLN [82].

d. Solvent displacement/nanoprecipitation technique

This method is used widely in the preparation of polymeric NP, and later on, this technique has been modified and used for SLN preparation [83]. In this technique, solid lipid and active ingredient are solubilized in water miscible organic solvents such as acetone, methanol, ethanol, isopropanol etc., and subsequently injected/dispersed into an aqueous dispersion containing surfactant with stirring, thereby producing suspension of SLN [84]. The solvent present is removed by different techniques such as distillation, ultracentrifugation, evaporation under reduced pressure, lyophilization etc. This method is suitable for hydrophobic drugs, which are incorporated with high loading efficiencies. In addition, the heat involved is very less during the process, thereby suitable for temperature sensitive active ingredients [81].

e. Microemulsion based technique

This method is based on the dilution of microemulsions, which is a thermodynamically stable isotropic mixture made of oil/lipid, emulsifier and water. In this technique, both lipid and aqueous phase with emulsifier are made to mix at a temperature above melting point of lipid, in suitable ratios under stirring [78]. The hot microemulsion obtained is diluted into chilled aqueous phase, which is kept at constant stirring. Large quantity of aqueous phase is used for dilution, which sometimes may go upto 50 times of microemulsion. By dilution with cold aqueous phase, lipid droplets are solidified and produce SLN. One of the major disadvantage of this technique is its proneness to phase transitions with minor changes in composition

or thermodynamic variables. Further, large quantities of solvents have to be removed from final formulation, which is a tedious process.

f. Supercritical fluid method

In this method, drug and solid lipid are made to solubilize in a supercritical or compressed fluid such as supercritical CO₂ and subsequently passed through a nozzle where the solution is expanded. The supercritical fluid is evaporated in this process and eventually solute particles are precipitated in nano size. This technique produces particles free of solvent residues because of the complete evaporation of supercritical fluid during the expansion process [85, 86].

1.3.5.3.2 Secondary production steps and characterization of polymeric/solid lipid nanoparticles

a. Lyophilization

Lyophilization or freeze-drying is one of the most significant secondary production steps in NP preparation, which enhances the physical and chemical stability of the formulation obtained [87]. Lyophilization aids to increase the long-term stability for a NP preparation with hydrolyzable drugs. When the nanoparticulate systems are lyophilized into solid preparation, it prevents ostwald ripening as well as hydrolytic degradation, thereby increasing the stability. After lyophilization, NP can be more easily incorporated into different dosage forms such as tablets, capsules, parental dispersions, pellets etc. In lyophilization, the NP dispersion is freeze-dried which is then subjected to evaporation under vacuum. Cryoprotectant such as sorbitol, mannitol, glucose, trehalose etc. are added to the dispersion in order to prevent or minimize particle aggregation and to redisperse the lyophilizates in a more efficient way. These cryoprotectants aid in NP stability by minimizing osmotic activity of water. They act as placeholders and prevent the contact between discrete NP. They also interact with polar head groups of surfactants present, and act as a pseudo hydration shell [88].

b. Spray drying

Spray drying is a less frequently used method for transforming aqueous NP dispersion into a dry product. Spray dryers make use of hot gases and atomizers/nozzles to disperse effectively the NP dispersion and therefore sometimes result in aggregation

and partial melting of NP. In case of solid lipid NP, melting can be minimized by incorporating ethanol in dispersion medium [89].

c. Sterilization

Sterilization is another secondary production step which is highly desirable for NP meant for parenteral administration. Aseptic production of NP, filtration, gamma irradiation, heating etc. are the general methods used for sterilizing nanoparticulate systems [90]. In the case of heat resistant drugs and nanoparticle material, autoclaving is a good method of choice. It was also found that sterilizing of nanoparticulate systems by this method could slightly increase the particle size. Sterilization by filtration requires high pressure and should not cause any change in the nanoparticulate system with respect to stability and drug release characteristics. In the case of gamma irradiation, free radicals are obtained and may undergo secondary reactions leading to chemical modifications. High molecular mobility and presence of oxygen enhances degradation reactions induced by gamma radiations [91].

1.3.5.3.3. Characterization of nanoparticles

In order to find out whether the obtained nanoparticles meet the required criteria and objectives, several characterization methods are used. Most widely applied methods for characterization include particle size (techniques- dynamic light scattering, static light scattering, acoustic methods etc.), zeta potential, electron microscopy (scanning, transmission etc.), atomic force microscopy, differential scanning calorimetry, x-ray diffraction, entrapment efficiency, drug content, in-vitro drug release (including study of release kinetics and mechanisms) etc. These methods are discussed in detail in ‘chapter 5 - Formulation design and development’ of the thesis.

1.3.5.3.4 In-vivo fate and toxicity aspects of nanoparticles

Nanoparticulate systems administered through oral or transdermal route exhibit negligible/very few problems in biological systems. In addition, NP administered via intra muscular or subcutaneous route do not cause much problems if appropriate surfactants are used. The particle size is not that significant for these routes as compared to administration by parenteral route. Particle size distribution is the major issue associated with intravenous injection of nanoparticulate systems. There is a potential danger of capillary blockage because of bigger particles or aggregation of

particles, which may even lead to death due to embolism. The diameter of fine capillaries present in human is about 9 microns in diameter. Therefore, the NP must be in submicron size, if designed for parenteral administration [92].

The interaction of NP with phagocytizing cells has been studied extensively by many groups. The macrophages of mononuclear phagocyte system immediately removes/clears the the NP present in the blood circulation, considering them as foreign bodies. This occurs more for NP with more than 200 nm and of hydrophobic nature. In order to overcome this, PEGylation has been done to obtain stealth particles with hydrophilic surface, and therefore exhibited long half-life in blood circulation. Various other polymers or surfactants such as tweens, PVA, polyacrylamides etc. have also been used to overcome phagocytosis, thereby increasing circulation time and better targeting efficiency [92, 93].

The in-vivo fate of administered NP is dependent on diverse factors including administration route, interaction with biological surroundings such as adsorption of biological material, enzymatic process etc. When nanoparticulate systems were administered intravenously, numerous pharmacokinetics and biodistribution studies suggested the prolonged presence of drug in blood circulation with NP than pure drug solution. NP also exhibited higher drug concentrations in lung, spleen and brain, while pure drug solution distributed more into liver and kidneys [45, 94]. However, diverse reports are available in the literature regarding the pharmacokinetics and biodistribution profiles of administered NP depending on the drug, polymer or solid lipid, surfactants, particle size, charge, route of administration and many other factors [95-101].

1.4 Objectives of the current research work

The problems associated with OLN antipsychotic therapy, as discussed earlier, indicated that there is a need for novel delivery systems, preferably a targeted and controlled release formulation of OLN. This would reduce the dose, the frequency of administration while maintaining effective concentration and lower the occurrence and intensity of adverse effects to have better patient compliance with improved therapeutic level for the treatment of schizophrenia and bipolar disorder. The nanoencapsulation of OLN, which is extensively distributed from conventional dosage forms throughout the body, with very high value of volume of distribution

(about 1000 L), would alter the distribution characteristics of the drug, and preferentially distribute into brain, thereby reducing the required dose and dose dependent associated adverse effects. Thus it is planned to design nanoparticulate delivery system of OLN with an objective of selective distribution and extended release for better efficacy.

Therefore, present research work was aimed at:

- Design and development of novel polymeric and solid lipid nanoparticulate drug delivery systems of OLN for preferential brain distribution and better efficacy
- Evaluation of the developed nanoparticulate drug delivery systems of OLN and optimization of various design parameters
- Comparison of biodistribution, pharmacokinetics and in-vivo efficacy as well as adverse effects of the developed delivery systems with pure drug administration in suitable animal model

In order to achieve these objectives, it was also planned for in-house development and validation of simple and sensitive analytical (UV & HPLC) and bioanalytical (HPLC) methods to estimate OLN in different samples like bulk powder, formulations, in-vitro dissolution samples, stability samples and biosamples.

References

- [1] S. Leucht, C. Corves, D. Arbter, R.R. Engel, C. Li, J.M. Davis, Second-generation versus first-generation antipsychotic drugs for schizophrenia: a meta-analysis, *Lancet*, 373 (2009) 31-41.
- [2] M. Sajatovic, M. Valenstein, F.C. Blow, D. Ganoczy, R.V. Ignacio, Treatment adherence with antipsychotic medications in bipolar disorder, *Bipolar Disord*, 8 (2006) 232-241.
- [3] S.H. Schultz, S.W. North, C.G. Shields, Schizophrenia: a review, *Am Fam Physician*, 75 (2007) 1821-1829.
- [4] L.F. Reddy, W.P. Horan, M.F. Green, Revisions and Refinements of the Diagnosis of Schizophrenia in DSM-5, *Clinic Psychol Sci Prac*, 21 (2014) 236-244.
- [5] M.J. Millan, K. Fone, T. Steckler, W.P. Horan, Negative symptoms of schizophrenia: clinical characteristics, pathophysiological substrates, experimental models and prospects for improved treatment, *Eur Neuropsychopharmacol*, 24 (2014) 645-692.
- [6] F.H. Duffy, E. D Angelo, A. Rotenberg, J. G Heydrich, Neurophysiological differences between patients clinically at high risk for schizophrenia and neurotypical controls - first steps in development of a biomarker, *BMC Med*, 13 (2015) 15-516.
- [7] H.J. Sorensen, E.L. Mortensen, J.M. Reinisch, S.A. Mednick, Association between prenatal exposure to bacterial infection and risk of schizophrenia, *Schizophr Bull*, 35 (2009) 631-637.
- [8] B.C. Ho, P. Nopoulos, M. Flaum, S. Arndt, N.C. Andreasen, Two-year outcome in first-episode schizophrenia: predictive value of symptoms for quality of life, *Am J Psychiatry*, 9 (1998) 1196-1201.
- [9] R. Tandon, H.A. Nasrallah, M.S. Keshavan, Schizophrenia, "just the facts" 4. Clinical features and conceptualization, *Schizophr Res*, 110 (2009) 1-23.
- [10] S.W Chan, Global perspective of burden of family caregivers for persons with schizophrenia, *Arch Psychiatry Nurs*, 25 (2011) 339-349.
- [11] S.G. Siris, Suicide and schizophrenia, *J psychopharmacol*, 15 (2001) 127-135.
- [12] N.N. Wig, S.R. Murthy, The birth of national mental health program for India, *Indian J Psychiatry*, 57 (2015) 315-319.
- [13] S.L. Giraldez, O.V. Fernandez, P.F. Iglesias, E.F. Pedrero, M.M.P. Pineiro, New trends in treatment for psychosis, *Psychol Spain*, (2011) 33-47.

- [14] H. Takeuchi, T. Suzuki, H. Uchida, K. Watanabe, M. Mimura, Antipsychotic treatment for schizophrenia in the maintenance phase: a systematic review of the guidelines and algorithms, *Schizophr Res*, 134 (2012) 219-225.
- [15] S. Miyamoto, N. Miyake, L. Jarskog, W. Fleischhacker, J. Lieberman, Pharmacological treatment of schizophrenia: a critical review of the pharmacology and clinical effects of current and future therapeutic agents, *Mol Psychiatry*, 17 (2012) 1206-1227
- [16] R.S. McIntyre, J.Z. Konarski, Tolerability profiles of atypical antipsychotics in the treatment of bipolar disorder, *J Clin Psychiatry*, 66 (2005) 28-36.
- [17] J.F. Goldberg, R.H. Perlis, C.L. Bowden, M.E. Thase, D.J. Miklowitz, L.B. Marangell, J.R. Calabrese, A.A. Nierenberg, G.S. Sachs, Manic symptoms during depressive episodes in 1,380 patients with bipolar disorder: findings from the STEP-BD, *Am J Psychiatry*, 166 (2009) 127-130.
- [18] J. Angst, J.M. Azorin, C.L. Bowden, G. Perugi, E. Vieta, A. Gamma, A.H. Young, B.S. Group, Prevalence and characteristics of undiagnosed bipolar disorders in patients with a major depressive episode: the BRIDGE study, *Arch Gen Psychiatry*, 68 (2011) 791-799.
- [19] H.Y. Meltzer, Update on typical and atypical antipsychotic drugs, *Annu Rev Med*, 64 (2013) 393-406.
- [20] O.D. Howes, S. Kapur, The dopamine hypothesis of schizophrenia: version III—the final common pathway, *Schizophr Bull*, 35 (2009) 549-562.
- [21] P. Seeman, Targeting the dopamine D2 receptor in schizophrenia, *Expert Opin Ther Targets*, 10 (2006) 515-531.
- [22] S. Cuisiat, N. Bourdiol, V. Lacharme, A.N Tancredi, F. Colpaert, B. Vacher, Towards a new generation of potential antipsychotic agents combining D2 and 5-HT1A receptor activities, *J Med Chem*, 50 (2007) 865-876.
- [23] H. Meltzer, B. Massey, The role of serotonin receptors in the action of atypical antipsychotic drugs, *Curr Opin Pharmacol*, 11 (2011) 59-67.
- [24] W.A. Ray, S. Meredith, P.B. Thapa, K.G. Meador, K. Hall, K.T. Murray, Antipsychotics and the risk of sudden cardiac death, *Archiv Gen Psychiatry*, 58 (2001) 1161-1167.
- [25] P. Pacher, V. Kecskemeti, Cardiovascular side effects of new antidepressants and antipsychotics: new drugs, old concerns?, *Curr Pharm Des*, 10 (2004) 2463-2475.

- [26] H. Lublin, J. Eberhard, S. Levander, Current therapy issues and unmet clinical needs in the treatment of schizophrenia: a review of the new generation antipsychotics, *Int Clin Psychopharmacol*, 20 (2005) 183-198.
- [27] D.M. Gardner, R.J. Baldessarini, P. Waraich, Modern antipsychotic drugs: a critical overview, *Can Med Assoc J*, 172 (2005) 1703-1711.
- [28] S. Gentile, Long-term treatment with atypical antipsychotics and the risk of weight gain, *Drug Saf*, 29 (2006) 303-319.
- [29] R.R. Conley, C.A. Tamminga, J.J. Bartko, C. Richardson, M. Peszke, J. Lingle, J. Hegerty, R. Love, C. Gounaris, S. Zaremba, Olanzapine compared with chlorpromazine in treatment-resistant schizophrenia, *Am J Psychiatry*, 155 (1998) 914-920.
- [30] H.L. Seifert, D.H. Adams, B.J. Kinon, Discontinuation of treatment of schizophrenic patients is driven by poor symptom response: a pooled post-hoc analysis of four atypical antipsychotic drugs, *BMC Med*, 3 (2005) 3-21.
- [31] A. Staring, M.V. Gaag, G. Koopmans, J. Selten, J.V. Beveren, M. Hengeveld, A. Loonen, C. Mulder, Treatment adherence therapy in people with psychotic disorders: randomised controlled trial, *Br J Psychiatry*, 197 (2010) 448-455.
- [32] D. Novick, J.M. Haro, D. Suarez, V. Perez, R.W. Dittmann, P.M. Haddad, Predictors and clinical consequences of non-adherence with antipsychotic medication in the outpatient treatment of schizophrenia, *Psychiatry Res*, 176 (2010) 109-113.
- [33] S. Grimwood, P.R. Hartig, Target site occupancy: emerging generalizations from clinical and preclinical studies, *Pharmacol Ther*, 122 (2009) 281-301.
- [34] R. Medori, E. Mannaert, G. Grunder, Plasma antipsychotic concentration and receptor occupancy, with special focus on risperidone long-acting injectable, *Eur Neuropsychopharmacol*, 16 (2006) 233-240.
- [35] W.M. Pardridge, Alzheimer's disease drug development and the problem of the blood-brain barrier, *Alzheimers Dement*, 5 (2009) 427-432.
- [36] J. Rautio, K. Laine, M. Gynther, J. Savolainen, Prodrug approaches for CNS delivery, *Aaps J*, 10 (2008) 92-102.
- [37] B. Pavan, A. Dalpiaz, N. Ciliberti, C. Biondi, S. Manfredini, S. Vertuani, Progress in drug delivery to the central nervous system by the prodrug approach, *Molecules*, 13 (2008) 1035-1065.
- [38] R. Gabathuler, Approaches to transport therapeutic drugs across the blood-brain barrier to treat brain diseases, *Neurobiol Dis*, 37 (2010) 48-57.

- [39] F.Y. Yang, Y.S. Lin, K.H. Kang, T.K. Chao, Reversible blood–brain barrier disruption by repeated transcranial focused ultrasound allows enhanced extravasation, *J Control Release*, 150 (2011) 111-116.
- [40] C.V. Borlongan, D.F. Emerich, Facilitation of drug entry into the CNS via transient permeation of blood brain barrier: laboratory and preliminary clinical evidence from bradykinin receptor agonist, *Cereport, Brain Res Bull*, 60 (2003) 297-306.
- [41] N. Vykhodtseva, N.M. Dannold, K. Hynynen, Progress and problems in the application of focused ultrasound for blood–brain barrier disruption, *Ultrasonics*, 48 (2008) 279-296.
- [42] K. Elkharraz, N. Faisant, C. Guse, F. Siepmann, B.A Yegin, J.M. Oger, R. Gust, A. Goepferich, J.P. Benoit, J. Siepmann, Paclitaxel-loaded microparticles and implants for the treatment of brain cancer: preparation and physicochemical characterization, *Int J Pharm*, 314 (2006) 127-136.
- [43] N. Weiss, F. Miller, S. Cazaubon, P.O. Couraud, The blood-brain barrier in brain homeostasis and neurological diseases, *Biochim Biophys Acta - Biomembr*, 1788 (2009) 842-857.
- [44] Y. Chen, L. Liu, Modern methods for delivery of drugs across the blood–brain barrier, *Adv Drug Deliv Rev*, 64 (2012) 640-665.
- [45] J. Kreuter, Nanoparticulate systems for brain delivery of drugs, *Adv Drug Deliv Rev*, 47 (2001) 65-81.
- [46] J. Kreuter, Nanoparticulate systems for brain delivery of drugs, *Adv Drug Deliv Rev*, 64, Supplement (2012) 213-222.
- [47] J. Kreuter, Influence of the surface properties on nanoparticle-mediated transport of drugs to the brain, *J Nanosci Nanotechnol*, 4 (2004) 484-488.
- [48] M. Snehalatha, K. Venugopal, R.N. Saha, A.K. Babbar, R.K. Sharma, Etoposide loaded PLGA and PCL nanoparticles II: biodistribution and pharmacokinetics after radiolabeling with Tc-99m, *Drug Deliv*, 15 (2008) 277-287.
- [49] S. Haque, S. Md, M. Fazil, M. Kumar, J.K. Sahni, J. Ali, S. Baboota, Venlafaxine loaded chitosan NPs for brain targeting: Pharmacokinetic and pharmacodynamic evaluation, *Carbohydr Polym*, 89 (2012) 72-79.
- [50] A. Ambruosi, A.S. Khalansky, H. Yamamoto, S.E. Gelperina, D.J. Begley, J. Kreuter, Biodistribution of polysorbate 80-coated doxorubicin-loaded [14C]-poly

(butyl cyanoacrylate) nanoparticles after intravenous administration to glioblastoma-bearing rats, *J Drug Target*, 14 (2006) 97-105.

[51] S. Martins, I. Tho, I. Reimold, G. Fricker, E. Souto, D. Ferreira, M. Brandl, Brain delivery of camptothecin by means of solid lipid nanoparticles: formulation design, in vitro and in vivo studies, *Int J Pharm*, 439 (2012) 49-62.

[52] K. Manjunath, V. Venkateswarlu, Pharmacokinetics, tissue distribution and bioavailability of clozapine solid lipid nanoparticles after intravenous and intraduodenal administration, *J Control Release*, 107 (2005) 215-228.

[53] G.P. Zara, A. Bargoni, R. Cavalli, A. Fundaro, D. Vighetto, M.R. Gasco, Pharmacokinetics and tissue distribution of idarubicin-loaded solid lipid nanoparticles after duodenal administration to rats, *J Pharm Sci*, 91 (2002) 1324-1333.

[54] M.J. Tsai, P.C. Wu, Y.B. Huang, J.S. Chang, C.L. Lin, Y.H. Tsai, J.Y. Fang, Baicalein loaded in tocol nanostructured lipid carriers (tocol NLCs) for enhanced stability and brain targeting, *Int J Pharm*, 423 (2012) 461-470.

[55] M. A. Bellavance, M. B. Poirier, D. Fortin, Uptake and intracellular release kinetics of liposome formulations in glioma cells, *Int J Pharm*, 395 (2010) 251-259.

[56] P. R. Cabrer, J. Agulla, B. Argibay, M. P. Mato, J. Castillo, Serial MRI study of the enhanced therapeutic effects of liposome-encapsulated citicoline in cerebral ischemia, *Int J Pharm*, 405 (2011) 228-233.

[57] H.M. Teow, Z. Zhou, M. Najlah, S.R. Yusof, N.J. Abbott, A.D. Emanuele, Delivery of paclitaxel across cellular barriers using a dendrimer-based nanocarrier, *Int J Pharm*, 441 (2013) 701-711.

[58] V. Gajbhiye, N.K. Jain, The treatment of Glioblastoma Xenografts by surfactant conjugated dendritic nanoconjugates, *Biomater*, 32 (2011) 6213-6225.

[59] G.A. Abdelbary, M.I. Tadros, Brain targeting of olanzapine via intranasal delivery of core-shell difunctional block copolymer mixed nanomicellar carriers: In vitro characterization, ex vivo estimation of nasal toxicity and in vivo biodistribution studies, *Int J Pharm*, 452 (2013) 300-310.

[60] M. Kumar, A. Misra, A.K. Babbar, A.K. Mishra, P. Mishra, K. Pathak, Intranasal nanoemulsion based brain targeting drug delivery system of risperidone, *Int J Pharm*, 358 (2008) 285-291.


[61] T.K. Vyas, A. Shahiwala, M.M. Amiji, Improved oral bioavailability and brain transport of Saquinavir upon administration in novel nanoemulsion formulations, *Int J Pharm*, 347 (2008) 93-101.

- [62] R.N. Saha, S. Vasanthakumar, G. Bende, M. Snehalatha, Nanoparticulate drug delivery systems for cancer chemotherapy, *Mol Membr Biol*, 27 (2010) 215-231.
- [63] L. Costantino, D. Boraschi, Is there a clinical future for polymeric nanoparticles as brain-targeting drug delivery agents?, *Drug Discov Today*, 17 (2012) 367-378.
- [64] C.P. Reis, R.J. Neufeld, A.J. Ribeiro, F. Veiga, Nanoencapsulation I. Methods for preparation of drug-loaded polymeric nanoparticles, *Nanomedicine*, 2 (2006) 8-21.
- [65] E.B. Mock, H. De Bruyn, B.S. Hawkett, R.G. Gilbert, C.F. Zukoski, Synthesis of anisotropic nanoparticles by seeded emulsion polymerization, *Langmuir*, 22 (2006) 4037-4043.
- [66] K. Krauel, N. Davies, S. Hook, T. Rades, Using different structure types of microemulsions for the preparation of poly (alkylcyanoacrylate) nanoparticles by interfacial polymerization, *J Control Release*, 106 (2005) 76-87.
- [67] K. Bouchemal, S. Briançon, E. Perrier, H. Fessi, I. Bonnet, N. Zydowicz, Synthesis and characterization of polyurethane and poly (ether urethane) nanocapsules using a new technique of interfacial polycondensation combined to spontaneous emulsification, *Int J Pharm*, 269 (2004) 89-100.
- [68] J. Jaiswal, S.K. Gupta, J. Kreuter, Preparation of biodegradable cyclosporine nanoparticles by high-pressure emulsification-solvent evaporation process, *J Control Rel*, 96 (2004) 169-178.
- [69] H.S. Ribeiro, B.S. Chu, S. Ichikawa, M. Nakajima, Preparation of nanodispersions containing β -carotene by solvent displacement method, *Food Hydrocoll*, 22 (2008) 12-17.
- [70] H. Murakami, M. Kobayashi, H. Takeuchi, Y. Kawashima, Preparation of poly (DL-lactide-co-glycolide) nanoparticles by modified spontaneous emulsification solvent diffusion method, *Int J Pharm*, 187 (1999) 143-152.
- [71] M.R. Kumar, U. Bakowsky, C. Lehr, Preparation and characterization of cationic PLGA nanospheres as DNA carriers, *Biomater*, 25 (2004) 1771-1777.
- [72] C. Coester, K. Langer, H.V. Briesen, J. Kreuter, Gelatin nanoparticles by two step desolvation a new preparation method, surface modifications and cell uptake, *J Microencapsul*, 17 (2000) 187-193.
- [73] K. Byrappa, S. Ohara, T. Adschiri, Nanoparticles synthesis using supercritical fluid technology—towards biomedical applications, *Adv Drug Deliv Rev*, 60 (2008) 299-327.

- [74] M.S. Kim, S.J. Jin, J.S. Kim, H.J. Park, H.S. Song, R.H. Neubert, S.J. Hwang, Preparation, characterization and in vivo evaluation of amorphous atorvastatin calcium nanoparticles using supercritical antisolvent (SAS) process, *Eur J Pharm Biopharm*, 69 (2008) 454-465.
- [75] W. Mehnert, K. Mader, Solid lipid nanoparticles: Production, characterization and applications, *Adv Drug Deliv Rev*, 47 (2001) 165-196.
- [76] R.H. Muller, R.D. Petersen, A. Hommoss, J. Pardeike, Nanostructured lipid carriers (NLC) in cosmetic dermal products, *Adv Drug Deliv Rev*, 59 (2007) 522-530.
- [77] Y.M. Tsai, C.F. Chien, L.C. Lin, T.H. Tsai, Curcumin and its nano-formulation: The kinetics of tissue distribution and blood–brain barrier penetration, *Int J Pharm*, 416 (2011) 331-338.
- [78] R.H. Mueller, K. Maeder, S. Gohla, Solid lipid nanoparticles (SLN) for controlled drug delivery—a review of the state of the art, *Eur J Pharm Biopharm*, 50 (2000) 161-177.
- [79] V. Jennings, A. Lippacher, S. Gohla, Medium scale production of solid lipid nanoparticles (SLN) by high pressure homogenization, *J microencapsul*, 19 (2002) 1-10.
- [80] N.A. Alhaj, R. Abdullah, S. Ibrahim, A. Bustamam, Tamoxifen drug loading solid lipid nanoparticles prepared by hot high pressure homogenization techniques, *Am J Pharmacol Toxicol*, 3 (2008) 219-224.
- [81] W. Mehnert, K. Mäder, Solid lipid nanoparticles: Production, characterization and applications, *Adv Drug Deliv Rev*, 64, Supplement (2012) 83-101.
- [82] M. Trotta, F. Debernardi, O. Caputo, Preparation of solid lipid nanoparticles by a solvent emulsification–diffusion technique, *Int J Pharm*, 257 (2003) 153-160.
- [83] C. Fonseca, S. Simoes, R. Gaspar, Paclitaxel-loaded PLGA nanoparticles: preparation, physicochemical characterization and in vitro anti-tumoral activity, *J Control Rel*, 83 (2002) 273-286.
- [84] E.K.N. Pelaez, N.M. Munoz, A.G. Quintanar, D.Q. Guerrero, Optimization of the emulsification and solvent displacement method for the preparation of solid lipid nanoparticles, *Drug Dev Ind Pharm*, 37 (2011) 160-166.
- [85] P. Chattopadhyay, B.Y. Shekunov, D. Yim, D. Cipolla, B. Boyd, S. Farr, Production of solid lipid nanoparticle suspensions using supercritical fluid extraction of emulsions (SFEE) for pulmonary delivery using the AERx system, *Adv Drug Deliv Rev*, 59 (2007) 444-453.

- [86] Y. Chen, R. Jin, Y. Zhou, J. Zeng, H. Zhang, Q. Feng, Preparation of solid lipid nanoparticles loaded with Xionggui powder-supercritical carbon dioxide fluid extraction and their evaluation in vitro release, *Chinese mater medic*, 31 (2006) 376-379.
- [87] E. Zimmermann, R. Muller, K. Mader, Influence of different parameters on reconstitution of lyophilized SLN, *Int J Pharm*, 196 (2000) 211-213.
- [88] W. Abdelwahed, G. Degobert, S. Stainmesse, H. Fessi, Freeze-drying of nanoparticles: formulation, process and storage considerations, *Adv Drug Deliv Rev*, 58 (2006) 1688-1713.
- [89] C. Freitas, R.H. Muller, Spray-drying of solid lipid nanoparticles (SLN TM), *Eur J Pharm Biopharm*, 46 (1998) 145-151.
- [90] R. Cavalli, O. Caputo, M.E. Carlotti, M. Trotta, C. Scarnecchia, M.R. Gasco, Sterilization and freeze-drying of drug-free and drug-loaded solid lipid nanoparticles, *Int Journal Pharm*, 148 (1997) 47-54.
- [91] Y.N. Konan, R. Gurny, E. Allémann, Preparation and characterization of sterile and freeze-dried sub-200 nm nanoparticles, *Int J Pharma*, 233 (2002) 239-252.
- [92] J. Wong, A. Brugger, A. Khare, M. Chaubal, P. Papadopoulos, B. Rabinow, J. Kipp, J. Ning, Suspensions for intravenous (IV) injection: a review of development, preclinical and clinical aspects, *Adv Drug Deliv Rev*, 60 (2008) 939-954.
- [93] Y. Sheng, C. Liu, Y. Yuan, X. Tao, F. Yang, X. Shan, H. Zhou, F. Xu, Long-circulating polymeric nanoparticles bearing a combinatorial coating of PEG and water-soluble chitosan, *Biomater*, 30 (2009) 2340-2348.
- [94] S.C. Yang, L.F. Lu, Y. Cai, J.B. Zhu, B.W. Liang, C.Z. Yang, Body distribution in mice of intravenously injected camptothecin solid lipid nanoparticles and targeting effect on brain, *J Control Rel*, 59 (1999) 299-307.
- [95] D.E. Owens, N.A. Peppas, Opsonization, biodistribution, and pharmacokinetics of polymeric nanoparticles, *Int J Pharm*, 307 (2006) 93-102.
- [96] K. Manjunath, V. Venkateswarlu, Pharmacokinetics, tissue distribution and bioavailability of clozapine solid lipid nanoparticles after intravenous and intraduodenal administration, *J Control Rel*, 107 (2005) 215-228.
- [97] S.D. Li, L. Huang, Pharmacokinetics and biodistribution of nanoparticles, *Mol Pharm*, 5 (2008) 496-504.

- [98] W.T.A. Jamal, K.T.A. Jamal, A. Cakebread, J.M. Halket, K. Kostarelos, Blood circulation and tissue biodistribution of lipid--quantum dot (L-QD) hybrid vesicles intravenously administered in mice, *Bioconjug Chem*, 20 (2009) 1696-1702.
- [99] T. Banerjee, S. Mitra, A.K. Singh, R.K. Sharma, A. Maitra, Preparation, characterization and biodistribution of ultrafine chitosan nanoparticles, *Int J Pharm*, 243 (2002) 93-105.
- [100] M.D. Lobato, I.M. Rubio, M.A. Holgado, J.A. Fuentes, M.F. Arevalo, L.M. Banderas, Enhanced cellular uptake and biodistribution of a synthetic cannabinoid loaded in surface-modified poly(lactic-co-glycolic acid) nanoparticles, *J Biomed Nanotechnol*, 10 (2014) 1068-1079.
- [101] A. Li, H.P. Luehmann, G. Sun, S. Samarajeewa, J. Zou, S. Zhang, F. Zhang, M.J. Welch, Y. Liu, K.L. Wooley, Synthesis and in vivo pharmacokinetic evaluation of degradable shell cross-linked polymer nanoparticles with poly(carboxybetaine) versus poly(ethylene glycol) surface-grafted coatings, *ACS Nano*, 6 (2012) 8970-8982.



Chapter 2

Drug profile

2.1 Introduction

Since its approval by FDA in 1996, OLN, an atypical antipsychotic, is one of the most significant drugs for schizophrenia treatment. It is widely prescribed by physicians as an integral part of psychiatric treatment, due to its efficiency in controlling both positive and negative symptoms of schizophrenia with fewer side effects, which is a general quality observed with most of the atypical antipsychotics as compared to typical ones such as Haloperidol. Chemically, OLN is a thienobenzodiazepine derivative which closely resembles another well known atypical antipsychotic-Clozapine [1, 2].

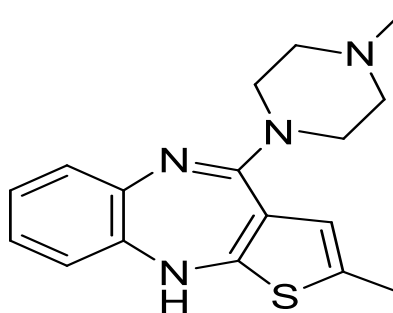
The mechanism of antipsychotic action of OLN is still unclear, but it has been postulated that 5HT receptor antagonistic action is primarily responsible for its antipsychotic effect [3]. It is also believed that fewer extrapyramidal adverse effects of atypical antipsychotics such as OLN are due to its higher affinity towards 5HT receptors than to dopaminergic receptors. Because of its significant use in psychiatry, numerous formulations are available in market and numbers are increasing day by day. The formulations of OLN are manufactured and marketed by Eli Lilly and company worldwide under the brand name Zyprexa. The patent on OLN by Eli Lilly and company expired in 2011 and since then it became generic and numerous pharmaceutical companies such as G.L Pharma, Mylan, Sanitas, LKM etc have introduced various formulations of OLN to the market [4].

Some of the important drug information and properties of OLN are listed below:

2.2 Physical and chemical properties [5-7]

Chemical name OLN is chemically designated as 2-methyl-4-(4-methyl-1-piperazinyl)-10H-thieno [2, 3-b] [1, 5] benzodiazepine

Chemical structure



Synonym	Olanzapin, Olanzapina, Olanzapinum, Zyprexa
Empirical formula	$C_{17}H_{20}N_4S$
Molecular weight	312.432
CAS No	132539-06-1
Melting point	195 °C
Physical description	OLN is a light yellow coloured, odourless powder.
Dissociation constant (pKa)	pKa1 = 4.01; pKa2 = 7.24
Permeability coefficient (Log P)	2.0
Solubility	OLN exhibits a very low solubility of 39.88 mg.L ⁻¹ in water, at 25 °C. It is soluble in organic solvents such as methanol, ethanol, chloroform and acetonitrile; highly soluble in dichloromethane and acetone.
BCS class	Class II, poorly soluble and highly permeable drug.

2.3 Pharmacodynamics

2.3.1 Mechanism of action

There is not sufficient knowledge about mechanism of antipsychotic activity of OLN. It is believed that it involves the antagonism of serotonin receptors and dopamine receptors. The binding profile indicates that OLN has low affinity for β -adrenergic receptors, moderate affinity for dopamine-D₂ and acetylcholine muscarinic receptors, and high affinity for 5-HT_{2A}, 5-HT_{2B}, 5-HT_{2C} and 5-HT₆ and histamine (H₁) receptors. OLN is also known to interact non-selectively with other dopamine receptors and 5-HT₁, 5-HT₃, 5-HT₄ and 5-HT₇ [8, 9].

2.3.2 Therapeutic indications

For patients who have shown a response to the initial treatment of schizophrenia, OLN is used for their treatment as it is effective in maintaining the clinical improvement during continuation therapy [10, 11].

OLN is used by the patients whose manic episode has shown a positive response to OLN treatment. OLN is used for the treatment varying from moderate to severe manic episode for the inhibition of re-appearance in patients with bipolar disease [12].

Oral OLN is used in addition with lithium or valproate for the treatment of manic or mixed episodes associated with bipolar I disorders. After two 6 week clinical trials in human volunteers its efficacy was established. Safety and efficacy for longer term has not been systematically evaluated in clinical studies. Oral fluoxetine and OLN in combination is indicated for the treatment of resistant depression which is associated with bipolar I disorder, based on clinical studies [13, 14].

2.3.3 Tolerability

In different studies conducted, it was observed that the OLN is safe in therapeutic doses [15]. Also it was observed by Perry et al., that the clinical response to OLN among schizophrenic patients was directly dependent on its blood concentration and a minimum effective concentration of 9 ng.mL⁻¹ plasma was suggested [16]. The drug concentrations of OLN in the serum showed a tendency to increase with respect to the daily oral dose. This was proved by testing samples of plasma from many patients receiving 10-20 mg OLN daily – the drug in serum indicated 8-31 ng.mL⁻¹ of drug. 1655 serum samples of OLN were analyzed and the mean concentrations of 36 ng.mL⁻¹ were found. OLN's toxicity were observed at blood concentrations above 70 ng.mL⁻¹ [17].

2.3.4 Adverse Effects

2.3.4.1 Extrapyramidal side effects

In many cases people may develop adverse effects of OLN like extrapyramidal effects which is characterized by restlessness, tremor, stiffness and it's rarely cause tardive dyskinesia where one's movements becomes slow or jerky or involuntary. In some cases, this condition may be permanent. Extrapyramidal symptoms (EPS) are reported to be dose dependent (15-32%) [18, 19].

2.3.4.2 Weight Gain

As compared to typical antipsychotics, atypical antipsychotics are capable of causing weight gain, or in worse case even obesity. Like these atypical antipsychotics, OLN may also cause obesity and weight gain which in return are well known risk factors for hypertension, increase in blood cholesterol levels especially in teenagers, type II diabetes, coronary heart disease, heart stroke, gallbladder disease, respiratory problems and even some types of cancer in general population [20]. Amongst the above disorders - type-II diabetes and cardiovascular diseases are more likely to be developed. Due to above mentioned disorders and weight gain in patients lead to discontinuing their treatment [21].

2.3.4.3 Cardiovascular adverse effects

OLN produces a high level of adverse cardiovascular effects resulting in hypotension, prolonging ECG QT-corrected interval, chest pain, tachycardia, peripheral edema, ventricular tachycardia/fibrillation, ventricular arrhythmias and even sudden death [22, 23].

2.3.4.4 Others

Few other side-effects include drowsiness, dizziness, lightheadedness, stomach upset, dry mouth, constipation, increased appetite, difficulty swallowing, shaking or tremors, signs of infection (such as fever, persistent sore throat), slow heartbeat, fainting, mental/mood changes (such as confusion, restlessness), numbness/tingling of arms/legs, yellowing eyes/skin, trouble urinating, rise in blood sugar level. This medication may increase a certain natural substance (prolactin) made by the body. For females, this increase in prolactin may result in unwanted breast milk, missed/stopped periods, or difficulty in conceiving. For males, it may result in decreased sexual ability, inability to produce sperm, or enlarged breasts [24].

This medication may rarely cause a very serious condition called neuroleptic malignant syndrome (NMS) which is characterized by the following symptoms: fever, muscle stiffness/pain/tenderness/weakness, severe tiredness, severe confusion, sweating, fast/irregular heartbeat, dark urine, changes in the amount of urine [25].

2.4 Pharmacokinetics

The pharmacokinetic profile of OLN is as summarized in Table 2.1

Table 2.1: Pharmacokinetic parameters of OLN

Parameter	Value
Bioavailability	87%
Volume of distribution (V_d)	1000 L
T_{max}	4.9 ± 1.8 h
Plasma protein binding	93%
Elimination	Urine (57%; 7% as unchanged drug), faeces (30%)
Elimination half- life ($t_{1/2}$)	33.1 ± 10.3 h

2.4.1 Absorption

After oral administration, there is almost complete absorption of OLN (87%). When six healthy male subjects were administered a single dose of 12 mg, then the maximum concentration (C_{max}) and the time required to reach (t_{max}) were found to be 11 ± 1 ng.mL⁻¹ and 4.9 ± 1.8 h, respectively. Couple of studies were performed on healthy volunteers using ¹⁴C OLN. Few related events occurring post the administration of OLN like dry mouth, dizziness, taste perversion, asthenia, nausea, arrhythmia, elevated heart rate, orthostatic hypotension, transient ALT elevation (in all subjects) were reported. For a single dose of 12-12.5 mg the average C_{max} was 10.5 ± 1.0 ng.mL⁻¹ (HPLC). Only 28% of radioactivity was accounted for OLN at t_{max} (4.9 h), which represented considerable first pass metabolism. It was indicated that there was no considerable distribution into the red blood cells, since radioactivity in plasma exceeded that in blood. For the total radioactivity, i.e., due to the OLN and the metabolites, the mean plasma half-life was 58.7 ± 7.1 h and for OLN was 25.5 ± 1.6 h. Following a daily dosage of 10 mg, within seven days, steady state levels were reached with up to a 3-fold accumulation (C_{max} and AUC). The rate and extent of OLN absorption were unaffected by the intake of food [26, 27].

2.4.2 Distribution

The plasma protein binding was approximately 93% over the therapeutic concentration range. In the alpha-1 glycoprotein and albumin, OLN is easily liable to bound them.

There is a widespread distribution throughout the body with a volume of distribution of 1000 L [26, 27].

2.4.3 Metabolism

It is metabolised considerably in humans via allylic hydroxylation, N-oxidation, N-dealkylation, glucuronidation, and a combination of these. This is the most prominent pathway both in terms of excretory product in the species and in terms of contribution to drug related circulating species. 10-N-glucuronide and 4-desmethylolanzapine are the chief metabolites found in humans. In-vitro evaluations conducted on the human cytochrome P450 isoenzymes - which are utilized in the formation of the three major metabolites of OLN - CYP_{1A2}, CYP_{2D6}, and the flavin (which contains mono-oxygenase system) indicated that they play a major role in the oxidation of OLN. In-depth studies have been carried out to explore the interaction of OLN with human cytochromes, further metabolism of OLN has also been investigated in-vitro and in human liver slices. It has been found that OLN is very well metabolized that it probably undergoes first pass metabolism in humans. The metabolic pathways of paramount importance for OLN are via glucuronidation and P450 CYP_{1A2} (N desmethyl and 7-hydroxy metabolites), while CYP_{2D6} (2-hydroxymethyl metabolite) and flavin containing monooxygenase (FMO₃) (N-oxide) pathways are minor with regard to circulating metabolites in humans. These isoenzymes also metabolize Caffeine, Imipramine, Theophylline, and Fluvoxamine. Metabolites derived via CYP_{3A} have not been identified in humans [26-28].

2.4.4 Elimination

The major route of elimination of OLN seems to be the first pass metabolism i.e., via urine. This is because most of the parent drug undergoes metabolism in the liver. Urinary excretion of unchanged OLN is a minor elimination pathway. Yet unchanged OLN and N-10 glucuronide conjugate have been found in human faeces, representing 2% and 8% of an oral dose respectively. Over the clinical dosage range it displays linear kinetics. Approximately 26.1 ± 12.1 h are taken for the systemic clearance of OLN. Approximately 33.1 ± 10.3 h is the plasma elimination half-life ($t_{1/2}$). Young women and the elderly have shown a decreased clearance as compared to that shown by young men and young patients respectively. In the case of healthy subjects the median $t_{1/2}$ was 31 h, ranging from 14.5 to 79.5 h. The amount of variance is large i.e., 4-5 fold

but within the same subject the variance is smaller than that between different subjects [26-28].

2.5 Dosage and administration

2.5.1 For Schizophrenia [23, 24]

Oral

For oral route, an initial dose of 5 to 10 mg orally once a day is recommended. The maintenance dose and the maximum dose are 10 and 20 mg respectively.

Injection

Short-acting injection

Initial dose of OLN short acting injection is 10 mg. A low dose of 5 or 7.5 mg may be considered when clinical factors warrant. The safety of total daily dose of OLN higher than 30 mg has not been evaluated in clinical trials.

Extended release injectable formulation

The extended release injectable suspension of OLN is intended for deep intramuscular injection. The efficacy of OLN extended release injectable suspension is demonstrated within the range of 150 to 300 mg administered every 2 weeks and with 405 mg administered every 4 weeks.

2.5.2 For bipolar disorder [23, 24]

Oral

Monotherapy of OLN for oral delivery, 10-15 mg once a day is recommended for the initial dose. The maintenance dose and the maximum dose are 5-20 mg and 20 mg orally once a day respectively.

For oral delivery of OLN in a combination therapy with lithium or valproate, 10 mg once a day was recommended for the initial dose. However the maintenance dose as well maximum dose were same as the monotherapy of OLN i.e., 5-20 mg and 20 mg orally once a day respectively.

Injection

For intra-muscular route, 10 mg once as an initial dose was recommended which is also a recommended dose for the therapy of bipolar disorder. However lower dose of 5 mg

or 7.5 mg may also be considered in the case of clinical factor warrant. The subsequent doses up to 10 mg may also be given if agitation warranting additional intramuscular doses persists following with the initial dose. In the controlled clinical trials, the efficacy of repeated doses of intra muscular-OLN in agitated patients has not been systematically evaluated. In the clinical trials, the safety of total daily dose greater than 30 mg (or 10 mg injections given more frequently than 2 hours after the initial dose and four hours after the second dose) has not been evaluated.

2.6 Marketed formulations

Several brands of OLN are commercially available with wide range of strength i.e., 2.5, 5, 7.5, 10, 15 and 20 mg along with different formulations such as tablet, powder and solvent for solution for injection with oral and intramuscular route and powder for solution for injection. List of marketed formulation of OLN as shown in Table 2.2.

Table 2.2: List of marketed formulations of OLN


Brand name	Formulation	Company name
Olace	Tablet	La Pharma
Meltolan	Tablet	Alkem
Manza	Tablet	Orchid
Joyzol	Tablet	Wockhardt
Joylon MD	Tablet	Lupin
Olandus	Tablet	Zydus
Olanex	Tablet	Ranbaxy
Olapex	Tablet	Reliance Life Science
Olexar	Tablet	Cipla
Olima	Tablet	Mankind
Oleanz Tab	Tablet	Sun Pharma
Ozapin MD	Tablet	Ipca
Psychozap	Tablet	Cadila
Zyprexa	Powder for injection	Eli Lilly

References

- [1] C. Tamminga, The promise of new drugs for schizophrenia treatment, *Can J Psychiatry*, 42 (1997) 265-273.
- [2] R.W. Buchanan, J. Kreyenbuhl, D.L. Kelly, J.M. Noel, D.L. Boggs, B.A. Fischer, S. Himelhoch, B. Fang, E. Peterson, P.R. Aquino, The 2009 schizophrenia PORT psychopharmacological treatment recommendations and summary statements, *Schizophr Bulletin*, 36 (2010) 71-93.
- [3] H.Y. Meltzer, Z. Li, Y. Kaneda, J. Ichikawa, Serotonin receptors: their key role in drugs to treat schizophrenia, *Prog Neuropsychopharmacol Biol Psychiatry*, 27 (2003) 1159-1172.
- [4] M. Bartholow, Top 200 drugs of 2011, *Pharm Tim*, July, 10 (2012).
- [5] <http://www.chemspider.com/Chemical-Structure.10442212.html> accessed on 10th June 2014.
- [6] <http://pubchem.ncbi.nlm.nih.gov/compound/olanzapine#section=Chemical-Vendors> accessed on 10th June 2014.
- [7] <http://www.chemicaland21.com/lifescience/phar/OLANZAPINE.htm> accessed on 10th June 2014.
- [8] M.A. Raggi, R. Mandrioli, C. Sabbioni, V. Pucci, Atypical antipsychotics: pharmacokinetics, therapeutic drug monitoring and pharmacological interactions, *Curr Med Chem*, 11 (2004) 279-296.
- [9] P. Seeman, Atypical antipsychotics: mechanism of action, *Can J Psychiatry*, 47 (2002) 27-38.
- [10] M. Sungur, H. Soygur, P. Güner, B. Üstün, I. Çetin, I.R. Falloon, Identifying an optimal treatment for schizophrenia: A 2-year randomized controlled trial comparing integrated care to a high-quality routine treatment, *Int J Psychiatry Clinic Prac*, 15 (2011) 118-127.
- [11] R. Tandon, Antipsychotic treatment of schizophrenia, *J Clin Psychiat*, 72 (2011).
- [12] M. Tohen, S. Kanba, R.S. McIntyre, S. Fujikoshi, H. Katagiri, Efficacy of olanzapine monotherapy in the treatment of bipolar depression with mixed features, *J Affect Disord*, 164 (2014) 57-62.
- [13] P.E. Keck, S.L.M. Elroy, J.M. Hawkins, Bipolar Disorder: An Update on Recent therapeutic trials, *Psychopharm Rev*, 46 (2011) 25-30.

- [14] A. Cipriani, C. Barbui, G. Salanti, J. Rendell, R. Brown, S. Stockton, M. Purgato, L.M. Spineli, G.M. Goodwin, J.R. Geddes, Comparative efficacy and acceptability of antimanic drugs in acute mania: a multiple-treatments meta-analysis, *Lancet*, 378 (2011) 1306-1315.
- [15] M. Rao, C. Hiemke, K. Grasmader, P. Baumann, Olanzapine: pharmacology, pharmacokinetics and therapeutic drug monitoring, *Fortsc Der Neurol Psychiatrie*, 69 (2001) 510-517.
- [16] P.J. Perry, T. Sanger, C. Beasley, Olanzapine plasma concentrations and clinical response in acutely ill schizophrenic patients, *J Clinic Psychopharmacol*, 17 (1997) 472-477.
- [17] M. Bogusz, K. Kruger, R. Maier, R. Erkwoh, F. Tuchtenhagen, Monitoring of olanzapine in serum by liquid chromatography–atmospheric pressure chemical ionization mass spectrometry, *J Chromatogr B Biomed Sci Appl.*, 732 (1999) 257-269.
- [18] S. Leucht, G.P. Walz, D. Abraham, W. Kissling, Efficacy and extrapyramidal side-effects of the new antipsychotics olanzapine, quetiapine, risperidone, and sertindole compared to conventional antipsychotics and placebo. A meta-analysis of randomized controlled trials, *Schizophr Res*, 35 (1999) 51-68.
- [19] K. Gao, D.E. Kemp, S.J. Ganocy, P. Gajwani, G. Xia, J.R. Calabrese, Antipsychotic-induced extrapyramidal side effects in bipolar disorder and schizophrenia: a systematic review, *J Clinic Psychopharmacol*, 28 (2008) 203.
- [20] S. Gupta, T. Droney, S. A. Samarra, P. Keller, B. Frank, Olanzapine: weight gain and therapeutic efficacy, *J Clinic Psychopharmacol*, 19 (1999) 273-275.
- [21] U. Eder, B. Mangweth, C. Ebenbichler, E. Weiss, A. Hofer, M. Hummer, G. Kemmler, M. Lechleitner, W.W. Fleischhacker, Association of olanzapine-induced weight gain with an increase in body fat, *Am. J psychiatry*, 10 (2014) 1719-1722.
- [22] P. Pacher, V. Kecskemeti, Cardiovascular side effects of new antidepressants and antipsychotics: new drugs, old concerns?, *Curr Pharm Des*, 10 (2004) 2463-2475.
- [23] W.A. Ray, S. Meredith, P.B. Thapa, K.G. Meador, K. Hall, K.T. Murray, Antipsychotics and the risk of sudden cardiac death, *Archiv Gen Psychiatry*, 58 (2001) 1161-1167.
- [24] <http://www.rxlist.com/zyprexa-drug.htm> accessed on 16th September 2014.

- [25] J. Ananth, S. Parameswaran, S. Gunatilake, K. Burgoyne, T. Sidhom, Neuroleptic malignant syndrome and atypical antipsychotic drugs, *J Clin Psychiatry*, 65 (2004) 464-470.
- [26] K. Kassahun, E. Mattiuz, E. Nyhart, B. Obermeyer, T. Gillespie, A. Murphy, R.M. Goodwin, D. Tupper, J.T. Callaghan, L. Lemberger, Disposition and biotransformation of the antipsychotic agent olanzapine in humans, *Drug Metabol Dispos*, 25 (1997) 81-93.
- [27] J.T. Callaghan, R.F. Bergstrom, L.R. Ptak, C.M. Beasley, Olanzapine, *Clinic pharmacokinet*, 37 (1999) 177-193.
- [28] J. Sheehan, J. Sliwa, J. Amatniek, A. Grinspan, C. Canuso, Atypical antipsychotic metabolism and excretion, *Curr Drug Metabol*, 11 (2010) 516-525.



Chapter 3

Analytical and bioanalytical methods

3.1 Introduction

Accurate and precise analytical methods are integral part in the development of formulations. The design attributes of the developed formulations can be measured accurately by validated analytical methods. Development and validation of simple, sensitive, precise and inexpensive analytical methods suitable for routine use, are highly essential for the determination of drug in bulk, preformulation studies, formulations, in-vitro drug release samples, stability study, and in-vivo pharmacokinetic studies. Therefore, suitable analytical methods are required during drug design and formulation development process for the optimum development and characterization of formulations.

UV spectrophotometric method is among the top most cost effective analytical methods and extensive literature survey revealed only a few spectrophotometric methods for the estimation of OLN [1, 2]. Firdous et al [1] developed a method in 100% organic solvent (methanol) and is therefore a highly expensive method for day to day analysis. Also, volatile nature of organic solvent would result in loss of medium, thereby change in concentration of the drug, thus affecting the accuracy of the method. Another method reported by Pradhan et al [2] provided more importance to the degradation study than validation and assay, even though degradation results obtained by UV spectrophotometric methods are less acceptable since identification of degradation products are highly difficult by these methods. Studies of significant importance for formulation scientists such as preformulation studies are not considered during the applicability of any of the reported methods.

Further, only few HPLC methods have been reported for the estimation of OLN in bulk drug and pharmaceutical dosage form either as single drug or in combination with fluoxetine [3]. Many of these reported methods are not validated [3, 4] and no method has been found in the literature for the estimation of OLN in novel drug delivery systems such as nanoparticles even though the demand for such a method is very high due to numerous ongoing research of encapsulating OLN in these delivery systems. Various HPLC methods in biomatrices have been reported elsewhere in literature for the estimation of OLN alone or in combination with other antipsychotics [5-13]. These methods are very time consuming with long run times, use expensive organic solvents and require complicated treatment techniques for the analysis. Further, the usage of sophisticated instruments with highly expensive detectors and requirement of highly skilled persons, limit their applications.

This is of significant importance in research since it is always preferable to obtain successful findings in animal models before extending the studies to human. Therefore, the availability of simple analytical methods in rat plasma for OLN estimation is always advantageous for the scientists actively involved in pharmacokinetic and biodistribution studies of OLN and its novel formulations.

Therefore, the present study describes two simple, cost effective, reliable and less time consuming UV spectrophotometric methods for the estimation of OLN in bulk, formulation and preformulation studies. In addition, a simple, sensitive and accurate liquid chromatographic method was developed and validated as per ICH guidelines for the routine analysis of OLN in bulk and novel drug delivery systems such as polymeric or solid lipid nanoparticles. Liquid chromatographic method was also optimised for estimation of drug in biomatrix samples. All developed methods were validated according to the standard guidelines [14]. Suitable statistical tests were performed to check validity of the developed methods [15]. These validated methods were used for the estimation of OLN in bulk, formulations, in-vitro release samples, stability samples and plasma samples collected during pharmacokinetic studies.

3.2. Method I: Spectroscopic method

3.2.1 Experimental

a. Materials and methods

UV-NIR spectrophotometer (Jasco, Japan, model V-570) connected to computer, loaded with software (Spectra Manager) was used. The wavelength accuracy was 0.1nm and for the analysis, matched quartz cuvettes of 10 mm were used. For carrying out robustness study, a double-beam ultra violet - visible - spectrophotometer (Perkin Elmer, USA, model LAMBDA EZ210) connected to computer loaded with software (PESSW, Version 1.2 and Revision E) was used. OLN was gifted by IPCA Labs Pvt. Ltd., Mumbai, India. Potassium dihydrogen phosphate, disodium hydrogen phosphate and sodium chloride were purchased from S.D. Fine Chemicals, India. Methanol and hydrochloric acid were purchased from Merck, India. High quality pure water was obtained using Millipore purification assembly (Millipore, Molsheim, France, model Elix SA 67120).

b. Analytical method development

In order to develop a meaningful and sensitive analytical method for the estimation of OLN, numerous media consisting of different buffers and organic solvents: either alone or in combinations at different proportions were investigated. Absorbance of OLN in various media at respective wavelengths was determined and apparent molar absorptivity and Sandell's sensitivity were calculated and was also considered while selecting the optimized solvent system. Furthermore, the cost effectiveness and reproducibility of the solvent system was also considered during the selection procedure.

c. Calibration standards

Stock solutions of $100 \mu\text{g.mL}^{-1}$ of OLN were prepared by dissolving 5mg of the drug in 50 mL of 100 mM HCl and 100 mM phosphate buffer saline (PBS) in separate volumetric flasks. From these solutions, different aliquots were withdrawn and transferred to a series of 10 mL volumetric flasks. The volume was made up with respective medium to obtain six different concentrations in a range of $3\text{-}18 \mu\text{g.mL}^{-1}$ for hydrochloric acid medium (pH 1.2) and $4\text{-}24 \mu\text{g.mL}^{-1}$ for phosphate buffer saline medium (pH 7.4) respectively. The spectrum was recorded from 400 nm to 200 nm with scanning speed of 400 nm per min and optimum wavelengths were selected. These selected wavelengths were further set in fixed wavelength measurement mode of the spectrophotometer and absorbance was measured in order to obtain calibration curve data.

d. Analytical method validation

i. Specificity

In order to determine the specificity of the developed methods, OLN solutions ($10 \mu\text{g.mL}^{-1}$) were prepared along with various pharmaceutical excipients such as lactose, poly caprolactone, poloxomer 188, poly vinyl alcohol, glyceryl monostearate, stearic acid, micro crystalline cellulose, starch, hydroxy propyl methyl cellulose, methyl cellulose, dextrose, magnesium stearate, talc etc. and spectrum was recorded from 400 nm to 200 nm at a scanning speed of 400 nm per min. The spectrum of fresh OLN solution with same concentration was also recorded and any change in the absorbance in the whole wavelength range was studied. The spectrum of fresh OLN solution ($10 \mu\text{g.mL}^{-1}$) was overlaid with spectrum obtained from the same concentration of commercial dosage form (Tablet) of OLN.

ii. Accuracy

The accuracy of the proposed methods was determined by standard addition method. Different concentrations of pure drug (2, 5 and 10 $\mu\text{g.mL}^{-1}$) were added to previously analyzed formulation samples of equal concentration (5 $\mu\text{g.mL}^{-1}$). The concentration of drug added was calculated after analyzing the final solution obtained using respective analytical method. The % analytical recovery was studied in each case using the formula: $R = [(C_t - C_f)/C_a] \times 100$, where R is % analytical recovery; C_t is the total drug concentration measured after standard addition; C_f is the initial drug concentration taken from formulation; and C_a is the drug concentration added to pre-analyzed formulation.

iii. Precision

In order to study the precision of developed analytical methods, three different quality control standards: low quality control, medium quality control and high quality control (LQC, MQC and HQC) covering the whole calibration range were selected. For the method with 100 mM HCl medium, LQC, MQC and HQC selected were 3, 9 and 18 $\mu\text{g.mL}^{-1}$ respectively whereas for PBS medium, these were 4, 12 and 24 $\mu\text{g.mL}^{-1}$ respectively. With these selected QC standards, precision of the developed methods were studied at two levels: intra-day repeatability studies and inter-day intermediate precision studies. In intra-day repeatability studies, quality control standards in triplicates were analyzed at three different times in the same day and percent relative standard deviation (% RSD) was calculated to study the repeatability of developed methods. Inter-day precision studies were performed in a similar way, on three consecutive days (n=27) instead of a single day and % RSD was determined.

iv. Linearity

The linearity of the proposed methods were determined by analyzing six different concentrations (n=9) prepared from the stock solution and applying least square regression analysis on the obtained data. The concentration range selected for linearity study was 3 to 18 $\mu\text{g.mL}^{-1}$ for HCl medium and 4 to 24 $\mu\text{g.mL}^{-1}$ for PBS medium. One way ANOVA test was applied to the obtained absorbance data of the each concentration of the selected calibration range in replicates.

v. Limit of detection and limit of quantitation (LOD and LOQ)

LOD and LOQ were calculated as per standard formula, $3.3\sigma/S$ and $10\sigma/S$, respectively, where the terms S and σ are slope of the standard calibration curve and standard deviation of the y-intercept of calibration equation respectively [10].

vi. Robustness

Robustness of the proposed methods were studied by minutely changing an internal parameter such as pH (± 0.1 units) of the selected medium and measuring the absorbance in order to study the effect of these minor changes on the results obtained. Robustness was expressed as mean absolute recovery.

vii. Ruggedness

Ruggedness of these proposed methods were studied with the help of another double-beam ultra violet - visible - spectrophotometer (Perkin Elmer, USA, model LAMBDA EZ210) connected to computer loaded with software (PESSW, Version 1.2 and Revision E). The concentrations determined for same solutions by both the instruments were compared during the ruggedness study.

viii. Bench top stability study

The stock solution of OLN was kept at room temperature for 24 h. The concentration of drug was estimated after suitable dilutions and compared with fresh OLN solutions of same concentration. Percentage analytical recovery was calculated and stability of the drug in proposed medium was determined.

ix. Estimation from formulations

The developed and validated spectrophotometric methods were applied for the estimation of OLN from conventional, well established dosage form such as tablets of varying strengths.

Twenty OLN tablets of reputed brand were purchased from local market and pulverized with the help of a mortar and pestle into fine powder. From this, powder equivalent to 10 mg of OLN was transferred to 100 mL volumetric flask and extracted for 30 min with respective solvent systems along with methanol as co-solvent. This was filtered using whatman filter paper (No. - 40) and the filtrate obtained was diluted suitably to get a concentration of $10 \mu\text{g}\cdot\text{mL}^{-1}$ before analyzing by developed methods.

3.2.2. Results and discussion

a. Analytical method development

Numerous media consisting of different aqueous systems such as 100 mM HCl, 100 mM NaOH, phosphate buffers of pH 5.8-8.0 and acetate buffers of pH 3.6-5.8 were investigated alone or in combination with organic solvents at different proportions. Presence of organic solvents such as methanol or acetonitrile did not show any significant change in sensitivity of the methods investigated and therefore it was decided to minimize the use of organic solvents and limit them as co-solvents with

minimum usage, since it would result in reduction of analysis cost. Also, OLN showed pH dependent absorbance and hence pH of the solvent is of important concern in the selection and preparation of media. Final selection of the optimized solvent systems, 100 mM HCl and PBS pH 7.4 were based on various criteria such as applicability of the method, sensitivity, ease of sample preparation, cost effectiveness, stability of drug in investigating medium, reproducibility and ability to cope with minute changes in the medium (e.g. pH) without affecting the results. The spectra of OLN in the HCl medium and PBS medium are shown in Figure 3.1.

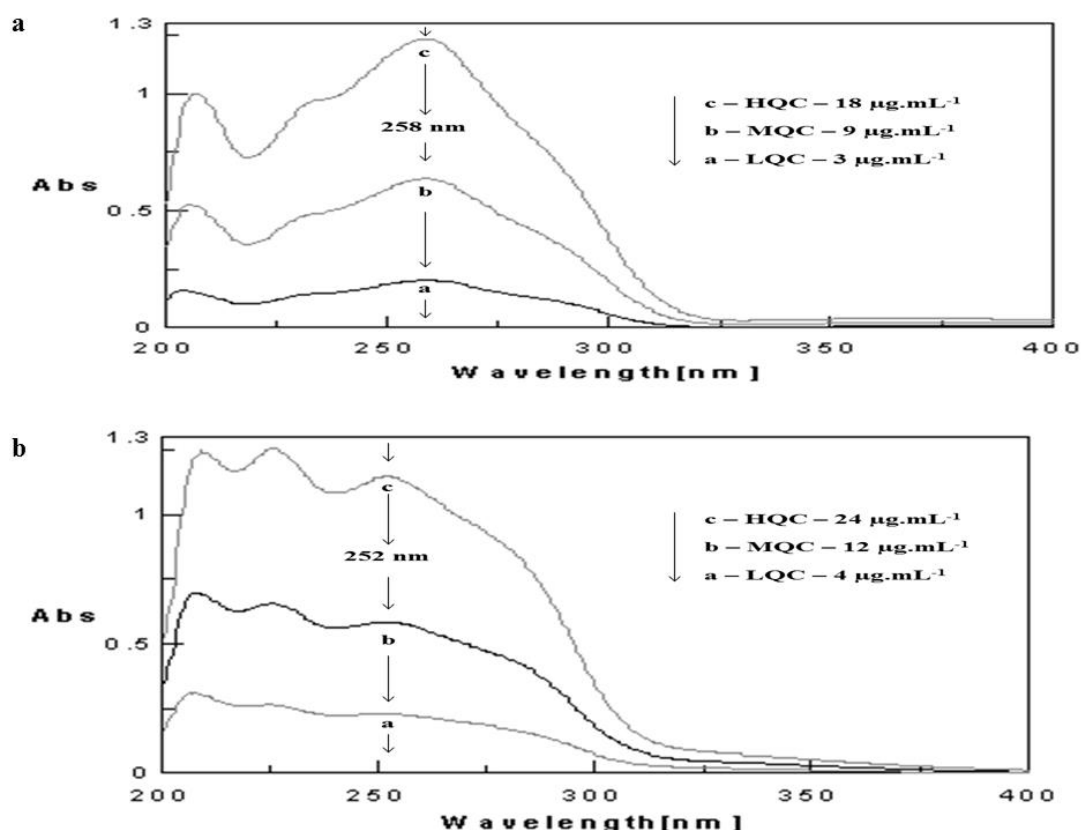


Figure 3.1: Overlaid spectrum of pure OLN at LQC, MQC & HQC levels in 100 mM HCl buffer (a) and phosphate buffer saline (b)

From the spectrum analysis, the λ_{\max} of OLN in 100 mM hydrochloric acid medium and phosphate buffer saline were found to be 258 and 252nm, respectively. Sandell's sensitivity of OLN in HCl medium and PBS medium were found to be 0.0144 and 0.0175 $\mu\text{g}\cdot\text{cm}^{-2}/0.001\text{A}$ respectively. It was also found that absorption spectrums of OLN solutions after 24 h were overlaying with fresh solutions in both the media without any significant change. Further, apparent molar absorptivity of the drug was calculated to be $2.17 \times 10^4 \text{ mol}^{-1}\text{cm}^{-1}$ in 100 mM HCl medium and $1.78 \times 10^4 \text{ mol}^{-1}\text{cm}^{-1}$ in the PBS medium [Table 3.1].

Table 3.1: Optical characteristics, summary of statistical data, and validation parameters of UV-spectroscopic method of OLN

Parameter	Hydrochloric acid medium (pH 1.2)	Phosphate buffer saline medium (pH 7.4)
Apparent molar absorptivity ($l\ mol^{-1}cm^{-1}$)	2.17×10^4	1.78×10^4
Sandell's sensitivity ($\mu g.cm^{-2}/0.001A$)	0.0144	0.0175
Calibration range	3-18 $\mu g.mL^{-1}$	4-24 $\mu g.mL^{-1}$
Slope (S.E. ^a)	0.0697 (1.6×10^{-4})	0.0571 (1.3×10^{-4})
95% confidence limits of slope	0.0693 to 0.0700	0.0568 to 0.0574
Intercept (S.E. ^a)	0.0080 (8.04×10^{-3})	-0.0052 (2.01×10^{-3})
95% confidence limits of intercept	0.0044 to 0.0116	-0.0092 to -0.0011
Regression coefficient (r^2)	0.9999	0.9998
Detection Limit ($\mu g.mL^{-1}$)	0.1680	0.2018
Quantitation Limit ($\mu g.mL^{-1}$)	0.5091	0.6115

^aStandard error of mean.

b. Calibration curve

The linear regression equations obtained by applying least square regression analysis for OLN were found to be: absorbance = $0.0697 \times$ concentration in $\mu g.mL^{-1}$ + 0.008; ($r^2 = 0.9999$) in 100 mM HCl medium; absorbance = $0.0571 \times$ concentration in $\mu g.mL^{-1}$ - 0.0052; ($r^2 = 0.9998$) in PBS medium.

c. Analytical method validation

i. Specificity and selectivity

The presence of commonly used excipients did not show any interference with the absorbance of OLN. There was no change in the UV-spectra of drug in the presence of commonly used excipients in both the media investigated. Absorption spectrum obtained for pure OLN was almost identical with the spectra of marketed formulation in both the media under investigation [Figure 3.2]. All these results indicate that developed methods are highly specific and selective for OLN in the presence of various commonly used excipients, therefore can be applied for different dosage forms with wide range of excipients.

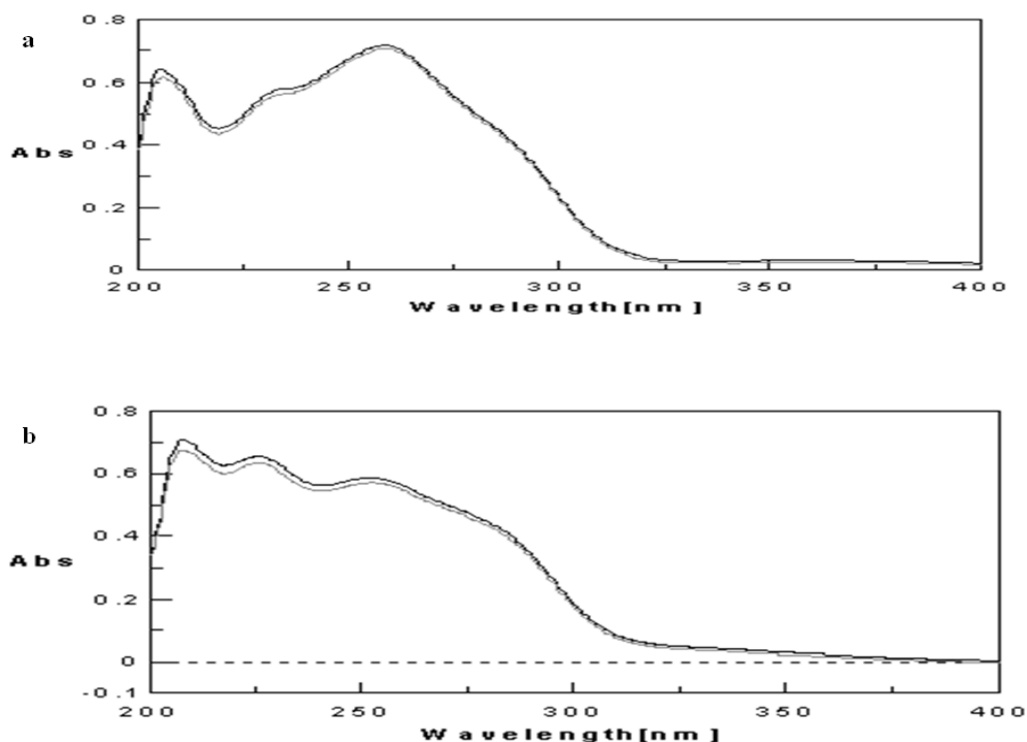


Figure 3.2: Overlaid spectrum of pure OLN with marketed commercial sample in 100 mM HCl buffer with pH 1.2 (a) and phosphate buffer saline (b)

ii. Accuracy

The accuracy of the proposed methods was studied by standard addition method by evaluating the recovery of the spiked pure drug samples [Table 3.2].

Table 3.2: Data of accuracy studies by standard addition method

Medium	Con of drug in formulations ($\mu\text{g.mL}^{-1}$)	Con of pure drug added ($\mu\text{g.mL}^{-1}$)	Con of drug recovered ($\mu\text{g.mL}^{-1}$)	% Analytical recovery \pm SD
HCl	5.02	2	2.01	100.5 \pm 1.18
	5.02	5	4.99	99.86 \pm 0.78
	5.02	10	10.12	101.21 \pm 0.54
PBS	5.03	2	2.02	100.9 \pm 1.68
	5.03	5	5.07	101.51 \pm 0.83
	5.03	10	10.02	100.26 \pm 1.07

Each result represents the average of six separate determinations

The mean percentage recoveries (% RSD) obtained in the HCl medium after spiking three different levels of pure drug were found to be between 99.86 \pm 0.78 and 101.21 \pm 0.54%. The mean percentage recoveries (% RSD.) in PBS medium were found to be between 100.26 \pm 1.07 and 101.51 \pm 0.83%.

These results reveal that any minute addition in the drug concentration in the prepared solution can be determined accurately by both the developed methods and therefore both these methods are found to be highly accurate as per ICH guidelines.

iii. Precision

Intra-day and inter-day repeatability were studied to investigate the precision of the developed methods.

Table 3.3: Repeatability and intermediate precision data of UV-spectroscopic method in 100 mM HCl and phosphate buffer saline

Medium	QC Levels	Repeatability (Intra-day) (n=9)						Intermediate Precision (Inter-day) (n=27)	
		Day (1)		Day (2)		Day (3)		Mean	%RSD
		Mean	%RSD	Mean	%RSD	Mean	%RSD		
HCl	LQC	2.97	0.98	3.02	0.87	2.99	1.04	2.96	1.14
	MQC	9.09	0.39	9.04	0.76	9.08	0.61	9.08	0.78
	HQC	17.91	0.49	18.16	0.88	18.08	0.96	18.04	0.68
PBS	LQC	4.03	2.40	3.98	1.60	4.04	0.98	4.08	1.49
	MQC	12.43	0.69	12.09	0.96	12.18	1.11	12.49	0.68
	HQC	24.33	1.60	24.16	1.21	24.23	0.92	24.28	1.51

Mean values represented are in $\mu\text{g.mL}^{-1}$

Percentage RSD of intraday repeatability studies ranged from 0.69 to 2.4% in the HCl medium and 0.39 to 1.04% in PBS medium, at all the levels of LQC, MQC, and HQC [Table 3.3].

These results demonstrate inter-assay precision and precision under identical operating conditions over small time intervals. The RSD values of intermediate precision study were found to be less than 3% in both the selected media. Inter-day precision study evaluates precision mainly within laboratory variations in three consecutive days. The RSD values obtained for both the methods at all the three different levels were well within the acceptable range demonstrating excellent precision of the selected methods.

iv. Linearity

The linearity range of OLN in HCl medium was found to be 3–18 $\mu\text{g.mL}^{-1}$ at 258 nm. In PBS medium, the linearity range observed was 4–24 $\mu\text{g.mL}^{-1}$ at 252 nm. The proposed methods demonstrated very low standard error of slope and intercept which

indicated very high precision of both the developed methods. The values of mean slope and intercept are well within the 95% confidence interval which indicated good linearity. Also, there were high levels of goodness of fit of regression equations demonstrated by both the methods. Furthermore, regression coefficient values obtained were high, near to unity indicating the linearity of the proposed methods.

v. Limit of detection and limit of quantitation

The limit of detection and limit of quantitation in HCl medium, calculated as per standard formulae were 0.1680 and 0.5091 $\mu\text{g.mL}^{-1}$, respectively, and in PBS medium these were found to be 0.2018 and 0.6115 $\mu\text{g.mL}^{-1}$, respectively. The values of both these limits in both the media show that developed methods were sufficiently sensitive for the estimation of OLN in very low concentrations. Also LOD and LOQ obtained theoretically for both the methods were cross checked practically and found to be similar with negligible changes.

vi. Robustness

The results obtained for robustness study demonstrated that minor changes of internal parameters such as pH of the investigating medium (± 0.1) did not show any significant change on absorbance of OLN. The mean percentage recovery with SD were calculated and found to be 99.97 ± 1.07 and $100.76 \pm 1.34\%$ in the HCl medium and PBS medium respectively. Therefore both the methods are sufficiently robust enough to estimate OLN even with minor pH changes in both the media.

vii. Ruggedness

The concentrations determined for the same solution by both UV - visible - spectrophotometers (Jasco, Japan, Model V-570 and Perkin Elmer, USA, model LAMBDA EZ210) were similar and percentage recovery obtained was well within the limits; $100.95 \pm 0.592\%$ for HCl medium and $100.58 \pm 1.230\%$ for PBS medium, indicating the ruggedness of both the methods. These findings allow analysts to perform the estimation of OLN in both media in a different instrument under identical conditions.

viii. Bench top stability study

The OLN solution in selected medium did not show any significant changes in concentration after 24 h when stored at room temperature. The percentage recoveries of $99.12 \pm 0.43\%$ and $99.36 \pm 0.51\%$ were obtained for HCl and PBS medium respectively, were well within the limits, indicating the stability of OLN in both the media for 24 h.

ix. Estimation from formulations

The applicability of the developed methods is of major concern while deciding the success of any analytical method. Therefore, these proposed methods were applied for the estimation of OLN in commercial tablets of various strengths, procured from the drug market. In HCl medium, % assay for Oleanz® 2.5, 5 & 10 were found to be 101.12 ± 0.98 , 100.76 ± 0.84 and $101.69 \pm 0.46\%$ respectively; in PBS medium, % assay for Oleanz® 2.5, 5 & 10 were found to be 99.52 ± 1.04 , 101.15 ± 0.59 and $100.54 \pm 0.63\%$ respectively. Both the methods estimated OLN in marketed formulations successfully (within the assay limits), proving the utility of the proposed methods. These results further prove that both the methods are unaffected by the presence of numerous excipients used during the formulation of these commercial dosage form. Furthermore, the amount of drug estimated with very low standard deviation demonstrated the precision of these proposed methods.

3.3 Method II: Chromatographic analytical method

3.3.1 Experimental

a. Chemicals and reagents

Analytically pure OLN (99.95% w/w) was obtained as a gift sample from IPCA Lab Pvt. Ltd., India. HPLC grade acetonitrile and triethylamine were purchased from Merck, India. HPLC grade water was obtained from Milli-Q assembly (USA) and was further filtered through a 0.22 μm membrane using ultra-filtration system (Millipore, France) before use. Potassium acetate, acetic acid, concentrated HCl, sodium hydroxide, hydrogen peroxide (S.D Fine chemicals, Mumbai) used were of analytical grade.

b. Instrumentation

The chromatographic analysis were carried out on a LC 10A (Shimadzu, Japan) system which consisted of two pumps (LC-10AT VP), auto sampler (SIL-10HT A) and a UV-visible detector (SPD 10A VP). Chromatographic peaks were integrated using LC work station® (Shimadzu, Japan) loaded on a computer system (IBM,USA). A five digit analytical balance Mettler Toledo (AG 135, Mettler, GMBH, Greifensee, Switzerland) was used for all weighing. A digital pH meter (pH tutor, Eutech Instruments, Singapore) was used for the adjustment of pH of mobile phase and ultra sonicator (1201, Systronics Instruments, India) was used for degassing mobile phase. All other instruments used for the experiment, including those used for nanoparticulate preparation were of reputed brands and functioning as

well as reproducibility were regularly checked.

c. Analytical method development

A variety of buffers and pH media were investigated in the development of LC method for the analysis of OLN in bulk and formulations. The effects of various organic modifiers and their combinations on peak area and peak symmetry were studied. Various ion pairing agents were investigated for improving peak properties. Various responses such as retention time, peak area, peak height and tailing factor were studied.

d. Optimized chromatographic conditions

The chromatographic separations were performed on a reverse phase C₁₈ column (Phenomenex, 250×4.6mm i.d which was packed with a particle size of 5 μm) using acetate buffer pH 4 with TEA (0.09% v/v)-acetonitrile (75:25, %v/v) at a flow rate of 1 mL min⁻¹. The quantitation was carried out at 258 nm with an injection volume of 30μL. Analysis was performed at ambient temperature of 25 °C after baseline stabilization for 1 h.

e. Preparation of stock and standard solutions

A stock solution of OLN (1 mg.mL⁻¹) was prepared by dissolving appropriate quantity of drug in solvent media consisting of acetonitrile: milli-Q water (25:75 v/v). Seven calibration standards (n=9) comprising 25, 50, 100, 200, 400, 800 and 1600 ng.mL⁻¹ were freshly prepared by serial dilution in mobile phase.

f. Preparation of sample solutions

Nanoparticulate preparation equivalent to 10 mg of OLN was weighed and transferred to a 100 mL calibrated flask and nanoparticles were digested with 10 mL of acetonitrile by ultra-sonication (20 min, 25 °C). The volume was made up with solvent media, centrifuged at 10,000 rpm for 20 min and supernatant was collected. Aliquot of supernatant was transferred to a 100 mL of calibrated flask and volume was made up with mobile phase.

g. System suitability

System suitability parameters were determined in order to study the system performance. Various system suitability factors such as retention time of the analyte, tailing factor, repeatability, resolution and number of theoretical plates were studied as per specifications. In order to check the system suitability, six replicates of OLN standard

solutions were injected into the HPLC systems and various suitability parameters were studied.

h. Method validation

The optimized chromatographic conditions were validated by evaluating linearity, range, specificity, precision, accuracy, sensitivity, and robustness [15, 16].

i. Linearity and range

The standard stock solution was diluted with mobile phase to prepare seven concentration levels ranging from 25 to 1,600 ng.mL⁻¹. These calibration standards were injected in triplicates into the HPLC column, keeping the injection volume constant at 30 µL and analyzed. Average peak area at each concentration level was subjected to linear regression analysis with the least square method. One-way analysis of variance (ANOVA) was performed as each response obtained at seven concentration levels.

ii. Specificity

Specificity is the ability of the method to accurately measure the analyte response in the presence of all potential sample components. The specificity of the developed method for OLN was carried out by placebo and spiked placebo analysis technique. On three consecutive days, placebo and formulation standards (in-house prepared NP) were prepared and analyzed by developed method. Chromatograms obtained were compared with freshly prepared calibration standards.

Besides, forced degradation studies were also performed to evaluate the specificity of the developed method in distinguishing the drug from its degradation products. Stock solutions of OLN in the mobile phase were exposed to hydrolytic, oxidative, thermal and photolytic stresses to carry out forced degradation studies. The hydrolytic study was done by using 1 N HCl (acidic hydrolysis) and 1 N NaOH (basic hydrolysis) at 80 °C for 6 h; and oxidation study was carried out using 3% H₂O₂ at 40 °C for 6 h. For thermal and photolytic studies, the solutions were exposed to 50 °C and UV light in UV-chamber respectively for about 24 h. The solutions were diluted appropriately with the mobile phase and injected into the HPLC system for analysis. All solutions injected were analyzed against a control solution stored at room temperature.

iii. Precision

Precision of the method was evaluated through repeatability (intra-day) and intermediate (inter-day) precision. Different quality control (QC) standards prepared

at lower (LQC = 25 ng.mL⁻¹, medium (MQC = 400 ng.mL⁻¹) and higher (HQC =1,600 ng.mL⁻¹) concentration levels were used for the study. For repeatability (intra-day), six series of three QC standards were prepared freshly and analyzed. For intermediate precision study (inter-day), standards were prepared and analyzed on three consecutive days. The RSD results were used to assess precision of the method.

iv. Accuracy

To determine the accuracy of the developed method, recovery study was conducted by placebo spiking and standard addition techniques. In the placebo spiking method, a known amount of standard solution was added to placebo blank at five concentration levels 50, 75, 100, 125, and 150% of the labeled claim. In the standard addition technique, known amounts of pure drug was added in sample solution of previously analyzed formulation sample of polymeric NP at three different levels. Each concentration levels were processed in six replicates on three different days and the results are expressed as mean absolute recovery.

v. LOD and LOQ

The limit of detection is the lowest concentration of the analyte that can be detected by the selected method of analysis and limit of quantitation is the lowest concentration of the analyte under investigation that can be determined with acceptable precision and accuracy under stated operational conditions of the developed method. LOD and LOQ were determined using formulae $3.3\sigma S^{-1}$ and $10\sigma S^{-1}$ respectively, where σ was the standard deviation of the response (y-intercept) and S was the slope of the calibration curve.

vi. Robustness

The percentage of organic phase-acetonitrile (20, 25 and 30%), buffer strength (10, 25 & 50 mM) and pH (3.5, 4.0 & 4.5) of aqueous phase were selected as the significant factors and studied. Various responses such as retention time, peak area, peak height and tailing factor were studied. Surface plots were obtained using design-expert® software (version 8.0.7.1) and effect of each variable or combination of variables on responses were carefully investigated.

vii. Solution stability

Stability of drug in mobile phase was determined by injecting calibration standards and formulation standards at 0, 6, 12, 24 and 48 h in triplicates.

viii. Estimation from formulations

The developed and validated chromatographic method is applied for the estimation of OLN from conventional dosage form such as tablets of varying strengths. Twenty OLN tablets of a reputed brand were purchased from local market and pulverized with the help of a mortar and pestle into fine powder. From this, powder equivalent to 10 mg of OLN was transferred to 100 mL volumetric flask and extracted for 30 min with mobile phase along with methanol as co-solvent. This was filtered using whatman filter paper (No. - 40) and the filtrate obtained was diluted suitably to get a concentration of 1000 ng.mL⁻¹ before analyzing by developed method. For the estimation of OLN from in-house developed NP, sample solution of freeze dried NP (10 mg) for analysis was prepared by digesting in acetonitrile (30 mL, 30 min, 25 °C) by ultra-sonication and diluting suitably using mobile phase before analysis.

3.3.2 Results and discussion

a. Analytical method development

Numerous buffers and pH media were investigated in the development of LC method for the analysis of OLN in bulk and formulations. The effects of various organic modifiers such as acetonitrile, methanol and their combinations on peak area and peak symmetry were studied. Among the organic modifiers, acetonitrile has been found to have more sensitivity for peak area and symmetry for OLN. Various ion pairing agents such as trifluoroacetic acid, triethylamine and sodium dodecylsulfate were investigated for improving peak properties and triethyl amine was selected. In the present method, various responses such as retention time, peak area, peak height and tailing factor were studied in detail during the method development process. Flow rate (1 mL.min⁻¹) and volume injected (30 µL) were kept constant after initial investigations. A significant importance is given for optimizing the retention time also since an appropriately low run time would result in better saving of resources and time. Therefore while selecting the optimised method, more importance was given to % acetonitrile which was optimized as 25% for optimum run time and selected for the analysis.

b. System suitability

System suitability was performed by injecting six replicates of quality control samples and the resolution of peaks was found to be 3.04. The tailing factor of the analyte peak was 1.18 and retention time was found to be 5.8 min. Further, the theoretical plate numbers for OLN was found to be 7929.99, which should be >5000 as per USP.

c. Method validation

i. Linearity and range

Calibration curve obtained by the least square regression analysis between average peak area and the concentration demonstrated linear relationship with a regression coefficient of 0.9998. The best-fit linear equation obtained was, average peak area (mVs) = $130.49 \times \text{concentration (ng.mL}^{-1}) - 127.26$. At all concentrations, standard deviation of peak area was significantly low and % RSD was below 3%. The representative chromatogram of OLN with RT 5.8 min is depicted in Figure 3.3.

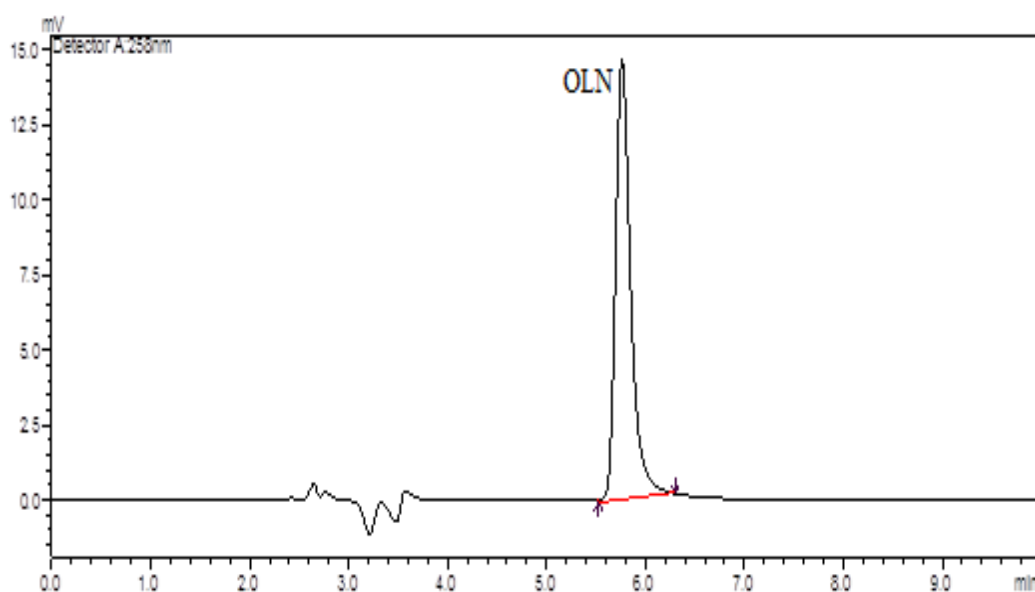


Figure 3.3: Representative chromatogram of OLN (800 ng.mL⁻¹) with RT 5.8 min

ii. Specificity

Placebo samples showed no interference with the drug peak, which indicated selectivity of the proposed method for OLN in the presence of potential formulation excipients. Also when compared with calibration standards, drug spiked placebo samples showed no significant changes in peak area and retention time. The results obtained from forced degradation studies are depicted in Figure 3.4 and summarized in Table 3.4. OLN was highly stable when subjected to thermal or photolytic stress conditions. OLN was prone to acid hydrolysis and the degradation products (D₁, D₂ and D₃) were detected at 4.0, 4.8 and 7.7 min. Alkaline hydrolysis also degraded OLN to obtain two degradation products same as that of acid hydrolysis (D₁ and D₂), along with an additional degradation product, which was eluted at 9.2 min (D₄).

Furthermore, OLN was also degraded when subjected to oxidation and obtained D₁ and D₂, which were same as that of acid and base hydrolysis. Additionally, a third prominent degradation product (D₅) was found and eluted at 5.3 min. These results were in accordance to the degradation behavior of OLN reported in the literature. [16, 17]. These results indicated that degradation products obtained by the forced degradation study of OLN could be successfully detected and differentiated from the OLN peak by the proposed RP-HPLC method.

Table 3.4: Results of forced degradation study of OLN using RP-HPLC method

Stress condition	Degradation (%)	Retention times of degraded products (min)
Acid hydrolysis (1 N HCl at 80 °C)	8.2	4.0, 4.8 and 7.7
Base hydrolysis (1 N NaOH at 80 °C)	9.5	4.0, 4.8 and 9.2
Oxidation (3% H ₂ O ₂ at 40 °C)	10.34	4.0, 4.8 and 5.3
Thermal stress (50 °C)	Not observed	Not observed
Photo-degradation (UV chamber)	Not observed	Not observed

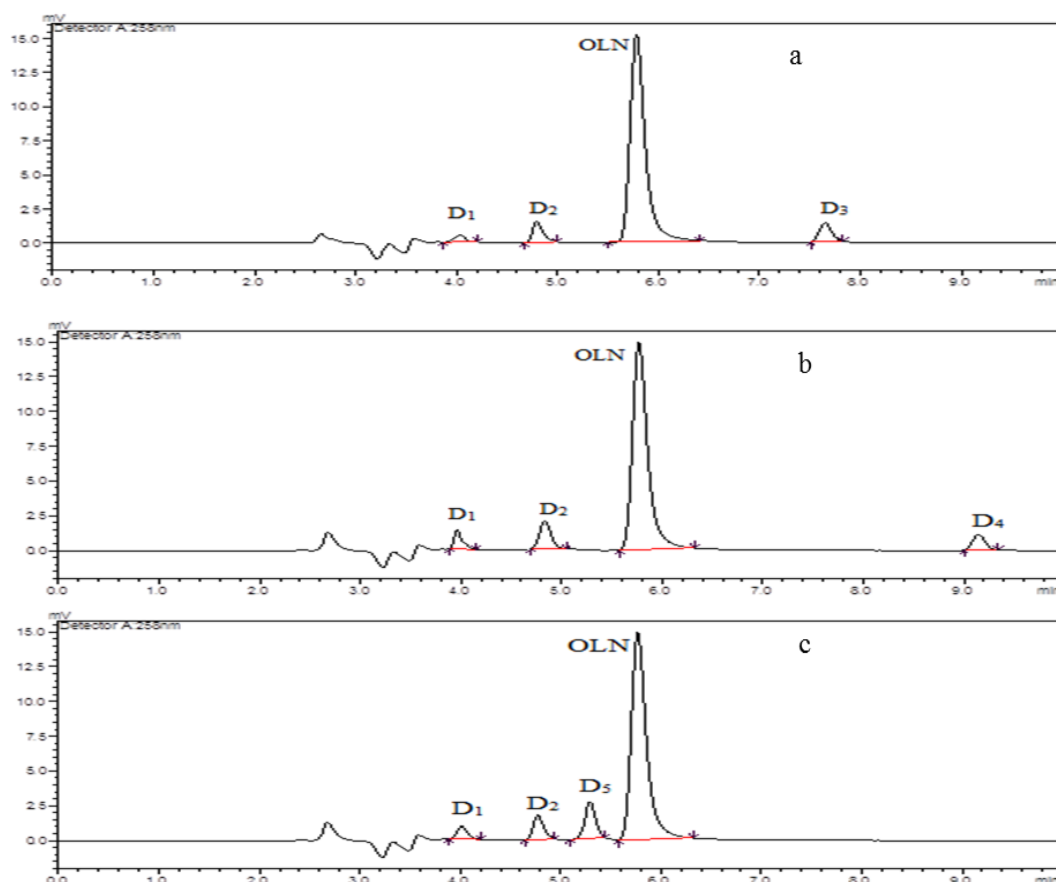


Figure 3.4: Representative chromatograms of forced degradation study of OLN: Acid hydrolysis (a); Base hydrolysis (b); Oxidation (c)

iii. Precision

In the intra-day repeatability study, QC standards showed insignificant variation in measured response, which indicated that the method was repeatable with % RSD below 3%. Similarly, inter-day % RSD was significantly low ($\leq 2.06\%$) for intermediate precision. % RSD values for repeatability and intermediate precision were within the acceptable range indicating the excellent repeatability and intermediate precision [Table 3.5].

Table 3.5: Results of repeatability and intermediate precision study of RP-HPLC method

QC Levels	Repeatability (Intra-day) (n=6)						Intermediate Precision (Inter-day) (n=18)	
	Day (1)		Day(2)		Day(3)		Mean	%RSD
	Mean	%RSD	Mean	%RSD	Mean	%RSD		
LQC (25)	25.24	2.63	25.06	2.12	25.19	1.98	25.16	2.06
MQC (400)	398.61	1.74	401.38	2.59	399.84	1.48	399.94	1.88
HQC (1600)	1602.68	0.98	1601.89	1.32	1598.54	1.28	1601.03	1.64

Mean values represented are in ng.mL^{-1}

iv. Accuracy

As shown in the data from Table 3.6, the method showed high absolute recoveries at all five concentration levels in placebo spiking method. Moreover, the absolute recoveries obtained from standard addition method were in good agreement with placebo spiking method. The results of the accuracy study indicated that the method was suitable for determination of OLN from novel drug delivery systems such as NP.

Table 3.6: Results of recovery studies of RP-HPLC method by placebo spiking and standard addition technique

Product	Technique	Concentration of drug in formulation (ng.mL ⁻¹)	Concentration of pure drug added (ng.mL ⁻¹)	Mean % recovery	% RSD
Polycaprolactone nanoparticles	Placebo spiking	0	200	100.23	0.47
		0	400	100.47	0.20
		0	600	100.45	0.12
		0	800	99.76	0.02
		0	1200	99.81	0.01
	Standard addition	400.03	200	100.28	0.17
		400.03	400	99.84	0.05
		400.03	600	100.22	0.03

Each level was processed independently and injected in six replicates

v. LOD and LOQ

The LOD and LOQ values were found to be 4.41 and 13.38 ng.mL⁻¹, respectively. Upon repeated injection at quantitation limit, retention time and peak area were not affected and mean absolute recovery was high with low % RSD and percentage bias.

vi. Robustness

Three-dimensional surface plots of obtained responses were made by applying design-expert software and are presented in Figure 3.5. Also the parabolic interactions between the selected variables are investigated by carefully analyzing the results obtained. A total of 17 experiments were carried out and values obtained were studied. The % acetonitrile showed significant effect on retention time as depicted in surface plots indicating the sensitivity of % acetonitrile amongst all the selected factors. Only retention time was significantly affected by the studied factors. Other responses such as peak area, peak height and tailing factor were not affected significantly by any of the studied variables.

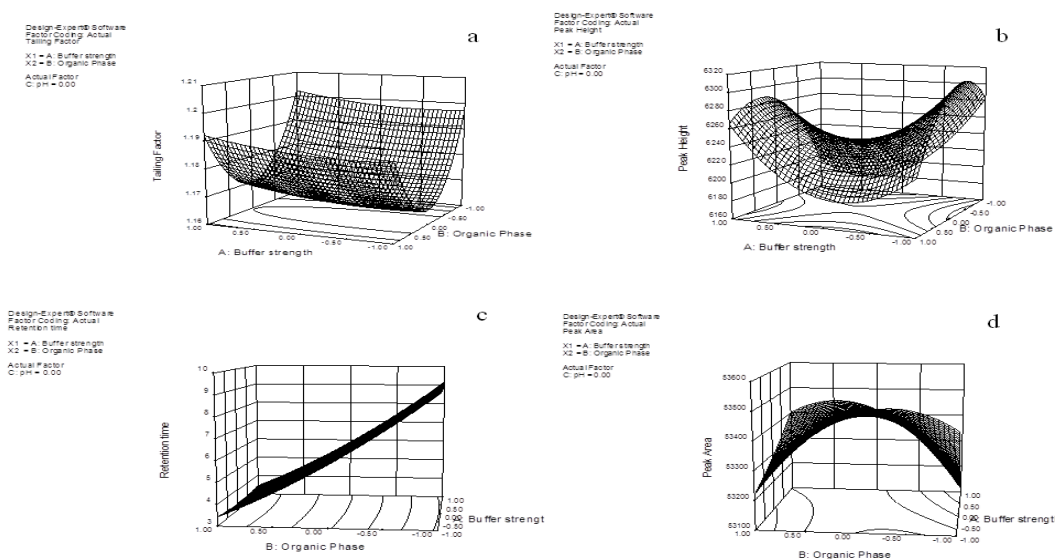


Figure 3.5: Three-dimensional surface plots of responses such as tailing factor (a), peak height (b) retention time (c) and peak area (d)

vii. Solution stability

The % RSD of the assay of OLN during solution stability experiments were $\leq 0.82\%$. The results indicated that the drug was stable in mobile phase for 48 h.

viii. Estimation from formulations

The developed HPLC method was applied for the estimation of OLN in commercial dosage forms such as tablets of various strengths, procured from the drug market. The percentage assay for Oleanz® 2.5, 5 & 10 were found to be 101.88 ± 1.82 , 101.36 ± 1.63 and 100.82 ± 0.94 % respectively, indicating that the developed method is unaffected by the presence of numerous excipients present in tablet. The drug content of in-house developed polymeric and solid lipid nanoparticulate systems were also successfully determined by the proposed method. The results are presented in detail in chapter 5.

3.4 Method III: Chromatographic bioanalytical method

3.4.1 Experimental

a. Chemicals and reagents

HPLC grade methanol, acetonitrile, isopropyl alcohol, hexane, petroleum ether, dichloro butane, acetic acid and tri ethyl amine were purchased from Merck India Pvt. Ltd., Mumbai, India. HPLC grade water was produced using milli-Q assembly (USA) and was filtered further through a $0.22 \mu\text{m}$ membrane filter with the help of Millipore ultra-filtration system (Millipore, France) before using in HPLC system.

All other chemicals and reagents used during the experiment were of analytical grade.

b. Instrumentation

The chromatographic analysis for the estimation of OLN in rat plasma were carried out on a LC 10A (Shimadzu, Japan) system fitted with two pumps (LC-10AT VP), auto sampler (SIL-10HT A) and a sensitive UV-visible detector (SPD 10A VP).

Integration of chromatographic peaks were performed using LC work station® (Shimadzu, Japan) loaded on a computer system (IBM,USA). Vortex mixer (Spinix) was used for the uniform mixing of plasma and extraction solvent. In order to remove organic extraction solvent, vacuum concentrator (Labconco, USA) was used.

c. Chromatographic conditions

The chromatographic separations were carried out on a reverse phase C₁₈ column (Phenomenex, 250×4.6mm i.d; 5 µm particle size) using acetate buffer of pH 4 consisting tri ethyl amine (0.09% v/v) in combination of acetonitrile (72:28, %v/v) at 1 mL min⁻¹ flow rate. The optimum detection wave length selected was 258 nm with an injection volume of 70 µL. Analysis was performed at ambient temperature (25 °C) after performing baseline stabilization for about 1 h.

d. Preparation of standard solutions and plasma samples

Accurately weighed OLN and Risperidone (RIS) were dissolved in methanol:milli Q water mixture (25:75) to obtain stock solutions of 1 mg.mL⁻¹ concentration and kept for storage at -20 °C before use. The working standard solutions of OLN were prepared by serially diluting OLN stock solution to get varying concentrations of 0.4, 1, 2, 4, 8, 16, 32 and 64 µg.mL⁻¹. Similarly, RIS working standard solution was also prepared at a concentration of 3 µg.mL⁻¹ by accurately diluting RIS stock solution with diluents (methanol: milli Q water mixture). Blood from rats was collected by retro-orbital route and plasma was separated by processing with anticoagulant EDTA (ethylenediamine tetra acetic acid).

Different calibration standards of OLN in plasma (10, 25, 50, 100, 200, 400, 800 and 1600 ng.mL⁻¹) were prepared by adding 5µL of working standard solutions of OLN and IS into 200 µL blank rat plasma. Different quality control (QC) samples were selected as 10, 25, 400 and 1600 ng.mL⁻¹ for LLOQ, low, medium, and high quality control samples respectively and each of these concentrations were prepared separately in plasma in the same way as that of concentrations of calibration samples prepared.

e. Liquid-liquid extraction technique

Liquid liquid extraction technique was also used for sample preparation. 5 μL each of working drug solution and IS was spiked into 200 μL of blank plasma which was maintained with suitable pH. Then suitable volume of organic solvent system (hexane, dichloro methane and di ethyl ether) either alone or in combination at different ratio was added and vortex mixed. It was then centrifuged at 5000 rpm at 4 $^{\circ}\text{C}$ for 15 min and organic layer was collected into another eppendorf. The extraction was performed for a second time in a similar way and both the extracts. were collectively kept in vacuum centrifuge for 4 h for the complete evaporation of organic solvent. The residue was reconstituted to 200 μL with diluent by vortex mixing for 5 min. It was centrifuged again at 12000 rpm and 4 $^{\circ}\text{C}$ for 15 min and clear supernatant was collected and transferred to HPLC vials and analyzed.

f. Method validation

i. Specificity

The specificity of the developed method was ensured by analysing blank plasma collected from six different rats and comparing the peaks obtained with plasma spiked with drug and internal standard as well as plasma collected after intravenous injection. The specificity of the method was evaluated by judicious study of the chromatograms for the presence of any interference peaks of plasma components at the retention times of drug and internal standard.

ii. Calibration curve and linearity

Linearity of the method was studied by preparing different concentrations of the OLN from working standard solutions to obtain a range of calibration concentrations from 10 to 1600 $\text{ng}\cdot\text{mL}^{-1}$. Each concentration selected in calibration range was prepared six times along with internal standard (IS) and analyzed by proposed method. The ratio of average peak areas of OLN to IS-Risperidone was calculated and a graph was plotted between these ratio and respective concentrations of OLN to obtain the calibration curve equation.

iii. Precision and accuracy

Intra-day and inter-day precision and accuracy of the developed method was investigated by preparing the four OLN QC samples at LLOQ, low, medium and high concentrations (n=6) and analyzing them by developed method. The precision of the method was studied from the calculated values of relative standard deviation at each concentration level. The inter-day precision was determined by analyzing QC samples

on three consecutive days and studying the % RSD of the obtained concentration values. Accuracy of the proposed method was determined by the comparison of average measurements of concentrations obtained by the proposed method with the nominal concentration values and was expressed as percent accuracy.

iv. Recovery

The recoveries of OLN and internal standard were determined by analyzing OLN QC samples including LLOQ which were treated as per the optimized sample preparation method as described previously. The peak area of OLN was then compared with that of OLN solution of same concentrations prepared in aqueous diluent and analyzed by the proposed method. Also, the extraction recovery of risperidone, the internal standard was calculated by analyzing plasma samples spiked with RIS at a medium level of concentration ($3 \mu\text{g.mL}^{-1}$) using the same method under similar conditions. The experiments were performed repeatedly for sufficient number of times ($n=6$) to establish the recoveries.

v. Stability

The stability study of OLN in plasma was performed by analyzing six replicates of QC samples at lower (25 ng.mL^{-1}) and higher (1600 ng.mL^{-1}) concentration levels. The stability was determined at three different levels such as freeze/thaw, bench top and long term. In freeze/thaw stability study, three cycles of freezing/thawing (-80°C to room temperature) were performed before determining the stability. Bench top stability of OLN in rat plasma was determined at room temperature for a period of 24 h. Furthermore, long term stability of OLN in plasma was assessed at -80°C for a period of 30 days. After the specified period of stability study, the samples were analyzed and concentration of OLN present in the plasma was determined in each case. The stability was then established by comparison of concentration calculated for the test samples kept for stability with the nominal concentration of OLN.

3.4.2 Results and discussion

a. HPLC method validation

i. Specificity

Specificity of an analytical method is of prime importance especially when biological matrix is involved, since there is a great chance of the presence of interfering components in those matrices which have similar physico-chemical properties as that of drug under investigation or IS. Therefore, chromatograms obtained after analyzing blank plasma and plasma spiked with OLN and IS were overlaid (Figure 3.6) the

average retention time of OLN and RIS was found to be 4.8 min and 9.8 min, respectively. From the overlaid chromatograms, it was clearly observed that there were no interfering peaks found at the retention times of OLN or IS - Risperidone. These results indicate that the developed method is highly specific to the drug under investigation-OLN and IS without any interference of the biological matrix.

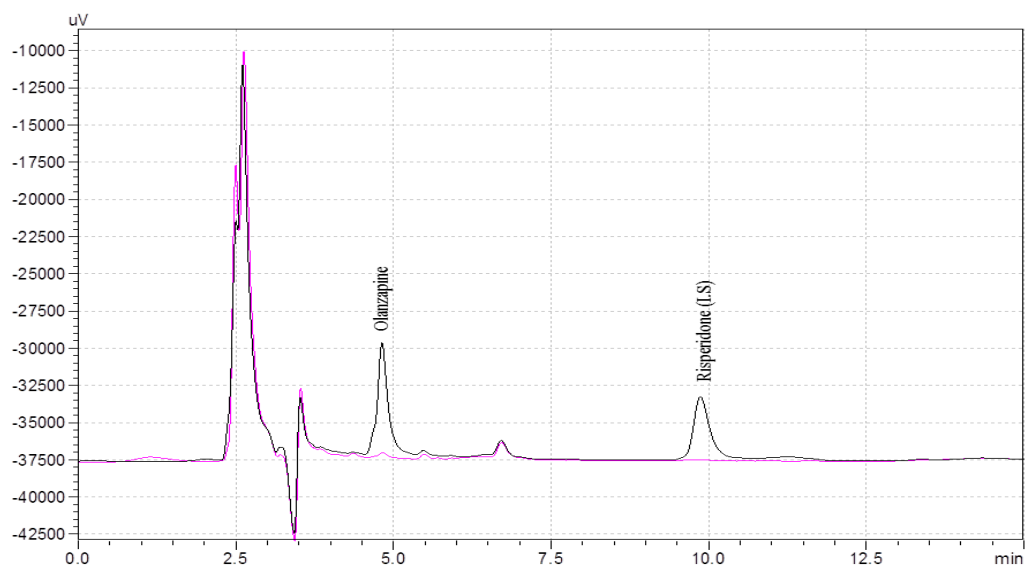


Figure 3.6: Overlaid chromatograms of blank rat plasma and plasma spiked with OLN (4.8 min) and IS, Risperidone (9.9 min)

ii. Linearity of calibration curve

The method was found to be highly linear by least square regression analysis for OLN in rat plasma over a concentration range of 10–1600 ng.mL⁻¹. The average correlation coefficient found was 0.9998 and typical regression equation was $Y=0.004X+0.001$, where Y represents the ratio of peak area of OLN to RIS and X represents the concentration of OLN in present in rat plasma.

iii. Precision and accuracy

The % RSD for intra-day precision results obtained after studying four quality control samples including LLOQ, was < 7% (Table 3.7). Similar studies for inter-day precision on three consecutive days resulted in % RSD < 10%.

Accuracy studies, as determined by the comparison of average measurements of concentrations obtained for the quality control samples with the nominal concentration values was found to be 98.19 to 105.21% (Table 3.8).

Table 3.7: Intra-day and inter-day precision study data of OLN in rat plasma

Q.C level (ng.mL ⁻¹)	%RSD-Intra day (n=6)	% RSD-Inter day (n=18)
LLOQ (10)	5.01	9.49
LQC (25)	6.16	5.46
MQC (400)	5.77	3.91
HQC (1600)	4.17	2.45

Table 3.8: Accuracy study data of OLN in rat plasma

Q.C level (ng.mL ⁻¹)	Avg. Conc. Recovered (ng.mL ⁻¹)	% RSD	% Recovery
LLOQ (10)	10.52	8.10	105.21
LQC (25)	25.91	6.92	103.65
MQC (400)	392.77	5.02	98.19
HQC (1600)	1610.05	3.86	100.63

Each result represents the average of six independent determinations

Both accuracy and precision values obtained by the proposed method were well within the limits as per FDA guidelines which instruct that % RSD should be less than 15% at all quality control levels other than LLOQ where % RSD could be up to 20%.

iv. Recovery

OLN and internal standard showed a very high level percentage recovery of 90.12 ± 5.69 to 93.82 ± 2.82 and $94.45 \pm 2.55\%$ respectively by the proposed method (Table 3.9). The high recovery percentages of OLN and IS indicate the high efficiency of extraction by liquid-liquid extraction technique, using hexane: dichloro methane (30:70). High recovery percentages and consistency in the ratio obtained for the peak area of drug under investigation and IS are of significant importance in a procedure such as liquid liquid extraction since several critical steps and process are involved during the sample preparation.

Table 3.9: Recovery data of OLN in rat plasma

QC level	Mean absolute recovery (%)	% RSD
	± S.D	
LLOQ	90.12 ± 5.69	6.31
LQC	93.10 ± 2.94	3.16
MQC	91.21 ± 4.89	5.36
HQC	93.82 ± 2.82	3.02

Each result represents the average of six independent determinations

v. Stability

The stability experiments were performed by analyzing lower and higher quality control samples after subjecting those to all possible extreme conditions which they might come across from the point of blood collection to final analysis by HPLC. The results of these stability studies are represented in Table 3.10.

The results of freeze-thaw stability study indicates that OLN is very stable in rat plasma for three freeze - thaw cycles when these samples were stored at a temperature of -80°C and then thawed to room temperature. The stability of these samples was calculated by comparing with the normal concentration and the % recovery was calculated and found to be in the range of 94.15 to 98.48 %.

Table 3.10: Stability data of OLN in rat plasma

Stability Type	Con. at Zero time	Conc. after stability period	% recovery	% bias
Bench top/short term stability (room temp for 24 h)	24.69	23.80	96.42	-3.58
	1633.26	1602.90	98.14	-1.86
Long term stability (at -80°C for 30 days)	24.58	23.97	97.50	-2.50
	1616.98	1547.77	95.72	-4.28
Freeze thaw stability (3 cycles)	24.63	23.18	94.15	-5.85
	1595.89	1571.60	98.48	-1.52

Each result represents the average of six independent determinations

The freeze-thaw stability of investigating drug is very important since plasma would be stored at -80°C when not in use and many times after thawing to room temperature, plasma had to be stored again until further usage where it would be again

brought back to very extreme storage condition such as -80°C . The stability of the drug sample after three freeze-thaw cycles ensure the easy handling of plasma during the developmental as well as applicability studies such as pharmacokinetic studies which would bring about optimum results. During the bench top stability studies, which are significant during post-treatment of the samples, it was found that OLN is highly stable at room temperature for 24 h because the post-treatment of the samples was carried out under this condition. It was also found out from long term stability studies that OLN was very much stable at -80°C for a period of one month. These findings would provide a thorough understanding about stability of the drug under these specified conditions and give sufficient flexibility during pharmacokinetic study for storage of collected plasma samples for sufficient time duration as well as during analysis of very large number of samples by HPLC. It was also found out during the analytical method development study in aqueous systems, which was carried out prior to that of bioanalytical method development that stock solutions of OLN and IS were sufficiently stable (OLN $\geq 95.72\%$; IS $\geq 96.18\%$) for one month when stored in a freezer which was maintained below -80°C , which further indicates aqueous stability of the drug under investigation and IS selected.


Conclusions

The proposed UV methods are highly accurate, precise, robust, less time consuming and rugged. Both the methods have produced very good linearity and can be routinely used for the estimation of OLN in bulk and various pharmaceutical dosage forms. The recovery values were very high and the presence of excipients did not interfere with the absorbance of OLN. Furthermore, a new and sensitive RP-HPLC method also has been developed for the determination of OLN. The simple isocratic method developed was found to be highly specific, linear, precise, accurate and robust. Further, the limit of detection and limit of quantification determined were very low indicating the high sensitivity of the proposed method. The recovery values obtained were very high and the presence of excipients did not interfere with the analysis of OLN. Furthermore, in assay studies, actual estimations of OLN from formulations were in good agreement with their respective label claims with selective detection of OLN. In addition, the HPLC bioanalytical method developed was found to be highly sensitive and selective for the estimation of OLN in rat plasma and can be used for in-vivo pharmacokinetic studies of various controlled release formulations in rodent model.

References

- [1] S. Firdous, T. Aman, A. Nisa, Determination of olanzapine by UV spectrophotometry and non-aqueous titration, *J Chem Soc Pak*, 27 (2005) 163-167.
- [2] K. Kumar Pradhan, S. Kumari, R. Samanta, Development and validation of a stability indicating uv spectroscopic method for olanzapine in bulk and pharmaceutical dosage forms, *Int J Pharm & Pharm Sci*, 6 (2014) 353-358.
- [3] B.V. Reddy, K.S. Reddy, J. Sreeramulu, G. Kanumula, Simultaneous determination of olanzapine and fluoxetine by HPLC, *Chromatographia*, 66 (2007) 111-114.
- [4] L.A.E.A. Hussien, M.F.A. Ghani, A.M.A.E. Alamein, E.H. Mohamed, Stability-indicating methods for the determination of olanzapine in presence of its degradation products, *Eur J Chem*, 5 (2014) 311-320.
- [5] E. Choong, S. Rudaz, A. Kottelat, D. Guillarme, J.L. Veuthey, C.B. Eap, Therapeutic drug monitoring of seven psychotropic drugs and four metabolites in human plasma by HPLC-MS, *J Pharm Biomed Anal*, 50 (2009) 1000-1008.
- [6] L.J. Dusci, L. Peter Hackett, L.M. Fellows, K.F. Ilett, Determination of olanzapine in plasma by high-performance liquid chromatography using ultraviolet absorbance detection, *J Chromatogr B Analyt Technol Biomed Life Sci*, 773 (2002) 191-197.
- [7] S. Gopinath, R.S. Kumar, S. Alexander, P. Danabal, Development of a rapid and sensitive SPE-LC-MS/MS method for the simultaneous estimation of fluoxetine and olanzapine in human plasma, *Biomed Chromatogr*, 26 (2012) 1077-1082.
- [8] M. Josefsson, M. Roman, E. Skogh, M.L. Dahl, Liquid chromatography/tandem mass spectrometry method for determination of olanzapine and N-desmethylOLN in human serum and cerebrospinal fluid, *J Pharm Biomed Anal*, 53 (2010) 576-582.
- [9] K. Kobylinska, K.M. Bus, M. Bukowska-Kiliszek, A high-performance liquid chromatography with electrochemical detection for the determination of olanzapine in human plasma, *Acta Pol Pharm*, 65 (2008) 759-762.
- [10] M.L. Lu, C.H. Lin, Y.C. Chen, H.C. Yang, T.H. Wu, Determination of olanzapine and N-desmethyl-OLN in plasma using a reversed-phase HPLC coupled with coulochemical detection: correlation of olanzapine or N-desmethyl-OLN concentration with metabolic parameters, *PLoS One*, 8 (2013) 135-139.

- [11] R.V. Nirogi, V.N. Kandikere, M. Shukla, K. Mudigonda, S. Maurya, R. Boosi, A. Yerramilli, Development and validation of a sensitive liquid chromatography/electrospray tandem mass spectrometry assay for the quantification of olanzapine in human plasma, *J Pharm Biomed Anal*, 41 (2006) 935-942.
- [12] M.A. Saracino, A. Koukopoulos, G. Sani, M. Amore, M.A. Raggi, Simultaneous high-performance liquid chromatographic determination of olanzapine and lamotrigine in plasma of bipolar patients, *Ther Drug Monit*, 29 (2007) 773-780.
- [13] G. Zhang, A.V. Terry, M.G. Bartlett, Liquid chromatography/tandem mass spectrometry method for the simultaneous determination of olanzapine, risperidone, 9-hydroxyrisperidone, clozapine, haloperidol and ziprasidone in rat plasma, *Rapid Commun Mass Spectrom*, 21 (2007) 920-928.
- [14] International Conference on Harmonization, ICH, Q2A validation of analytical procedure: Methodology. Geneva., (1994).
- [15] S. Bolton, C. Bon, *Pharmaceutical statistics: practical and clinical applications*, CRC Press, 2009.
- [16] S. Hiriyanna, K. Basavaiah, P.S. Goud, V. Dhayanithi, K. Raju, H. Pati, Identification and characterization of olanzapine degradation products under oxidative stress conditions, *Acta Chromat*, 20 (2008) 81-93.
- [17] A. Pathak, S.J. Rajput, Development of a stability-indicating HPLC method for simultaneous determination of olanzapine and fluoxetine in combined dosage forms, *J Chromatogr Sci*, 47 (2009) 605-611.



Chapter 4

Preformulation studies

4.1 Introduction

Preformulation studies are considered to be the one of the most significant preliminary steps in pharmaceutical development of a drug substance into various dosage forms [1, 2]. The physical and chemical properties of the drug substance (s) alone and in combination with excipients are investigated and critical properties are identified in this study. Preformulation studies help in several decisions making in formulation development of the drug product and provide a strong foundation for development of a dosage form that is highly robust during processing and storage conditions [3]. OLN is a well-established and widely prescribed anti-psychotic drug and therefore, numerous information about physico-chemical characteristics are available in literature. Since our aim was to formulate polymeric and solid lipid nanoparticulate delivery systems for OLN using selected preformed polymers and solid lipid, some preformulation studies were still required for successful formulation development. Based on these requirements, various preformulation experiments such as bulk characterization, solubility, partition coefficient, the drug-excipient compatibility and stability studies were designed and executed.

4.2 Materials

OLN was gifted by IPCA Lab Pvt. Ltd., Mumbai, India. Potassium dihydrogen phosphate, disodium hydrogen phosphate, glycine, sodium hydroxide and sodium chloride were purchased from S.D. Fine Chemicals, India. Methanol, octanol and hydrochloric acid were purchased from Merck, India. Poly (ϵ -caprolactone) (PCL) with M.W of 40,000, Stearic acid (M.W 284.4), Glyceryl monostearate (M.W 358.6), polyvinyl alcohol (PVA) with a molecular weight of 13,000-23,000 (98% hydrolyzed), polysorbate 80 (Tween 80) were procured from Sigma Aldrich, USA. Poloxamer 188 (Pluronic® F-68) (PF-68) was gifted by BASF, Germany. Excipients were purchased from Sigma Aldrich Chemicals, USA. High quality pure water was obtained using Millipore purification assembly (Millipore, Molsheim, France, Model Elix SA 67120) was used for the preparation of various aqueous phases used in the different studies. All other chemicals used were of analytical grade and purchased from Qualigens, Mumbai or S.D. Fine Chemicals, India.

4.3 Equipment/Instruments

A sensitive analytical balance (five digit-Mettler Toledo, Switzerland) was used for all weighing purposes. The pH were determined with pH meter (Eutech pH meter, Mumbai, India) equipped with a combined glass electrode. Rotary flask shaker (REMI Instruments, India) and vortex mixer (Spinix, India) were used for solubility analysis. Stability studies were carried out in humidity and temperature control cabinet (Thermolab, India and Wadegati, India). Bulk density and tapped density were determined with Thermonic (Campbell, India) densitometer. Thermal analysis was performed using heat flux type differential scanning calorimeter - DSC-60 (Shimadzu, Japan) with TA-60WS thermal analyzer (integrating software: TA-60WS collection monitor, version 1.51; analysis software: TA-60; temperature range: -150 to 600 °C; heat flow range: ± 40 mW; temperature program rate: 0 to 99° C.min⁻¹; atmosphere: nitrogen at 40 mL.min⁻¹). Drug-excipient compatibility study was also carried out using Fourier Transform Infrared (FTIR) spectrophotometer (Shimadzu, Japan; model: IR Prestige 21; model software: IR Solutions, version 1.0). Analytical instruments mentioned in chapter 3 were used for analysis of all samples.

4.4 Experimental

4.4.1 Physical characterization

Physical appearance and melting point were performed for physical characterization of pure OLN. Color of OLN was determined with visual observation. Melting point of OLN was determined by capillary method using digital auto melting point apparatus (Labtronics, India).

4.4.2 Bulk characteristics

The UV-spectrum of OLN was recorded by preparing, a fresh solution of 10 $\mu\text{g.mL}^{-1}$ in 90:10 % v/v milli Q water-methanol system. IR spectrum of OLN was recorded by using fourier transform infrared spectroscopy (FTIR; IR Prestige-21, Shimadzu, Kyoto, Japan).

4.4.3 Determination of solubility

The solubility studies of OLN were carried out using modified shake flask method [4, 5]. Buffered and unbuffered solutions of varying pH ranging from 1 to 12 were prepared and 2 mL of these solutions were transferred to micro centrifuge tubes in

which excess of drug was added and kept for shaking in an orbital mechanical shaker for 24 h at 37 ± 0.5 °C. The micro centrifuge tubes were checked in between and excess of drug in each tube was always maintained. After the completion of 24 h, micro centrifuge tubes containing drug samples were kept for centrifugation for 10 min at 10,000 rpm and supernatant was collected which was further diluted suitably and analyzed by the proposed method.

4.4.4 Determination of distribution coefficients

The distribution coefficients (D) were determined using traditional shake flask method with minor modifications [6-8]. Octanol was selected as organic phase and different buffers with pH ranging from 2 to 12 were used as aqueous phase. Before commencing the experiment, organic phase and aqueous phase were presaturated with each other by mixing and shaking together for 24 h for the complete saturation and then these two phases were separated by centrifugation at 2000 rpm for 5 min. An accurate quantity (5 mL) of presaturated aqueous phase was withdrawn to a conical flask and OLN was dissolved in this to obtain a suitable concentration ($40 \mu\text{g.mL}^{-1}$). To this, equal quantity of presaturated organic phase was added and kept for shaking for 24 h on an orbital shaker at 37 °C. After specified time, both the phases were separated by centrifugation and aqueous phase was subjected for UV analysis with the validated method and concentration at time t (C_t) was calculated. The concentration of OLN in aqueous phase at time zero (C_0) was already determined in the initial phase of experiment-before mixing the organic phase. The distribution coefficient of OLN was calculated using the standard formula,

$$D = [C_0 (\text{Aqueous}) - C_t (\text{Aqueous})] / C_t (\text{Aqueous})$$

4.4.5 Determination of dissociation constant (pK_a)

The dissociation constant (pK_a) was determined spectrophotometrically by the house developed UV method [9, 10]. Various buffers of different pH in the range of 1-12 were prepared using 0.2 M solutions of sodium dihydrogen phosphate, potassium dihydrogen phosphate and sodium chloride in order to obtain final buffer molarity and ionic strength of 0.01 M and 0.02 M respectively. The final pH of the resultant solutions was adjusted with 0.1 N NaOH/HCl as per the requirements. OLN primary stock solution of $100 \mu\text{g.mL}^{-1}$ was prepared. From this stock solution, an accurate volume was transferred into separate calibrated volumetric flasks and further

made up the volume with media of varying pH to obtain concentration of $10 \mu\text{g.mL}^{-1}$ which is in the calibration range of the proposed method. The spectrums of the obtained solutions were recorded for the UV wavelength range of 200-400 nm at a scanning speed of 200 nm.sec^{-1} . Spectrums recorded were further overlaid and the wavelength at which a largest change in absorbance in spectrums of OLN at different pH was selected. The absorbance values obtained at this selected wavelength were plotted against pH of the prepared solutions. The pK_a was determined by plotting a first derivative absorbance spectrum with $\Delta\text{Abs}/\Delta\text{pH}$ vs. pH and the point of inflection in the curve was identified.

4.4.6 Stability studies

a) Solution state stability studies

In order to study the solution state stability of OLN, different buffered solutions of pH 1.2, 3.0, 4.5, 6.8, 7.4, 10 and 12 were prepared. A stock solution of 1 mg.mL^{-1} OLN was prepared in methanol and from that $1 \mu\text{g.mL}^{-1}$ of OLN solutions were prepared in different pH solutions for the stability analysis. The prepared samples were stored at $25 \pm 3 \text{ }^\circ\text{C}$ and at different time points (12, 24, 48, 72, 96 and 120 h), samples were withdrawn for drug analysis using in-house developed HPLC method. The results were analyzed in order to determine the order of degradation and rate constants. The $t_{90\%}$, time taken to degrade 10 % of the drug to reach 90% of initial concentration was determined to find the shelf life of OLN [11, 12].

b) Solid state stability

In this study, the solid admixtures of the drug with each excipient (1:1) were prepared by geometric mixing and the resulting mix was then passed through sieve #100 in order to ensure a uniform mixing. Excipients selected include PCL, glyceryl mono-stearate, stearic acid, poloxomer 188, PVA and mannitol. The resultant admixtures were transferred to glass vials, and labeled. These samples were stored at different storage conditions such as long term stability condition or controlled room temperature (CRT: $25 \pm 2 \text{ }^\circ\text{C}/ 60 \pm 5\% \text{ RH}$), accelerated condition (AT: $40 \pm 2 \text{ }^\circ\text{C}/75 \pm 5\% \text{ RH}$) and refrigerated condition (FT: $5 \pm 2 \text{ }^\circ\text{C}$) as per ICH stability guidelines. At predetermined time intervals (1, 2, 3, 4, 5 and 6 months), samples (in triplicates) were withdrawn and characterized for physical observations and drug content [12, 13]. Drug content was analyzed by validated HPLC method (Chapter 3).

4.4.7 Compatibility study

a) Differential scanning calorimetry (DSC) Analysis

Compatibility of drug and excipients was carried out using differential scanning calorimetric study by recording DSC thermograms of both pure drug and individual excipients and for the combination of drug and excipients [14, 15]. After suitably processing the samples, about 4 mg of the sample was accurately weighed and was sealed in standard aluminium pans with lid by crimping. Thermograms were recorded from 30 to 300 °C at a temperature increase rate of 10 °C per min. Exothermic peaks were directed towards upward. The sample heating environment was kept under nitrogen gas at a flow rate of 50 mL.min⁻¹. The thermograms of pure drug and pure excipient were overlaid with the thermograms of drug-excipient mixture in order to determine the presence of any incompatibility in the mixture. Any incompatibility present, could be clearly observed by a shift or masking of drug melting peak at the melting point region of the drug.

b) FTIR spectroscopy

FTIR spectroscopy study was also carried out in order to find out the compatibility of OLN with the selected excipients [16, 17]. The physical mixture of drug (OLN) and the selected excipients (PCL, stearic acid, glyceryl monostearate, PVA and PF 68) were prepared in equal proportion and kept at room temperature (25 ± 3 °C). FTIR spectrum was recorded after 6 months and any incompatibility between the drug and excipients were studied.

4.5 Results and discussion

4.5.1 Physical characterization

OLN appeared as a light yellow coloured, odourless powder. Melting point of pure OLN was found to be 192 ± 0.5 °C which was in accordance with the literature as represented in Table 4.1 [18].

Table 4.1: Physical and bulk characteristics of OLN

Parameters	Characterization
Physical appearance	Light yellow coloured, odourless powder
Melting point	192 ± 0.5 °C

4.5.2 Bulk characteristics

The UV-spectrum of OLN was determined and λ_{max} was found to be at 252 nm. The FTIR spectra of pure OLN demonstrated all the characteristic bands of OLN (Figure 4.1; Table 4.2.).

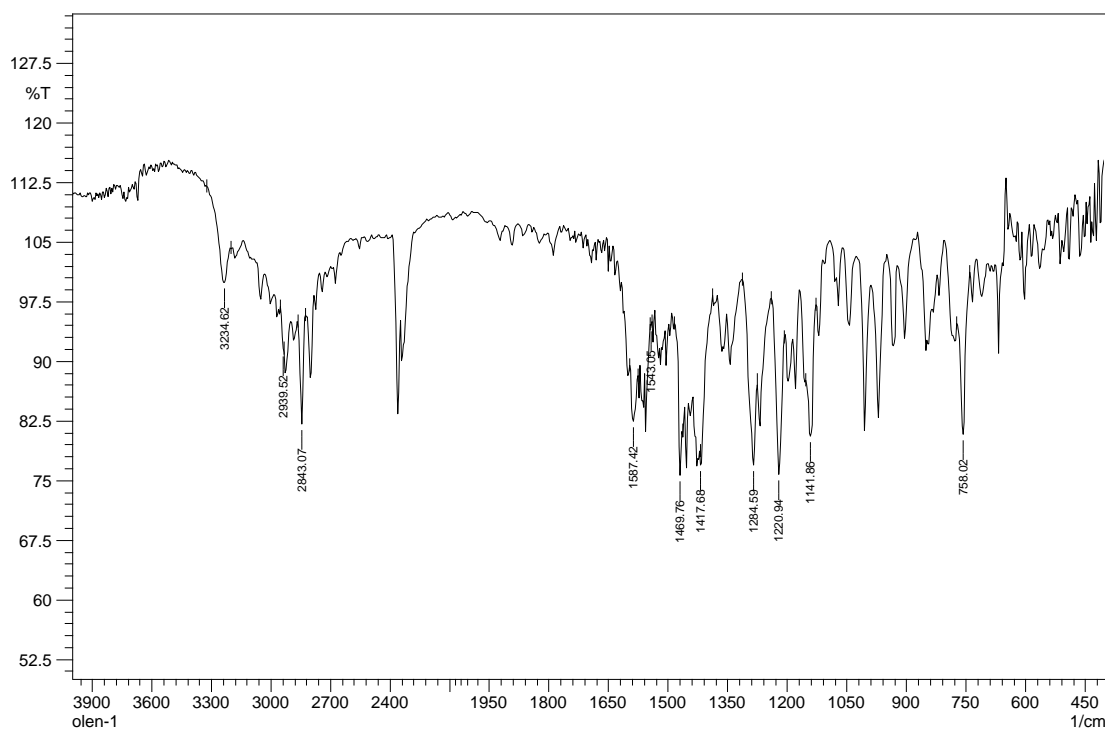


Figure 4.1: FTIR spectra of OLN

Table 4.2. : Wavelength attribution of IR spectrum of OLN

Wavelength (cm ⁻¹)	Attribution
3234	NH and OH stretching
2939	C-H stretching
1587	C=C stretching
1417	C=N stretching
1284	C-N stretching

4.5.3 Determination of solubility

OLN showed pH dependent solubility in different buffers with high solubility in acidic buffers and low solubility in basic buffers [Figure 4.2], owing to the fact that OLN exists more in ionized form in acidic media and unionized form in basic media. Therefore, being a basic drug, ionized species of OLN is more in acidic buffers which

is majorly responsible for the higher solubility in acidic buffers. In basic buffers, unionized species of OLN is comparatively more than ionized species thereby, resulting in decreased solubility.

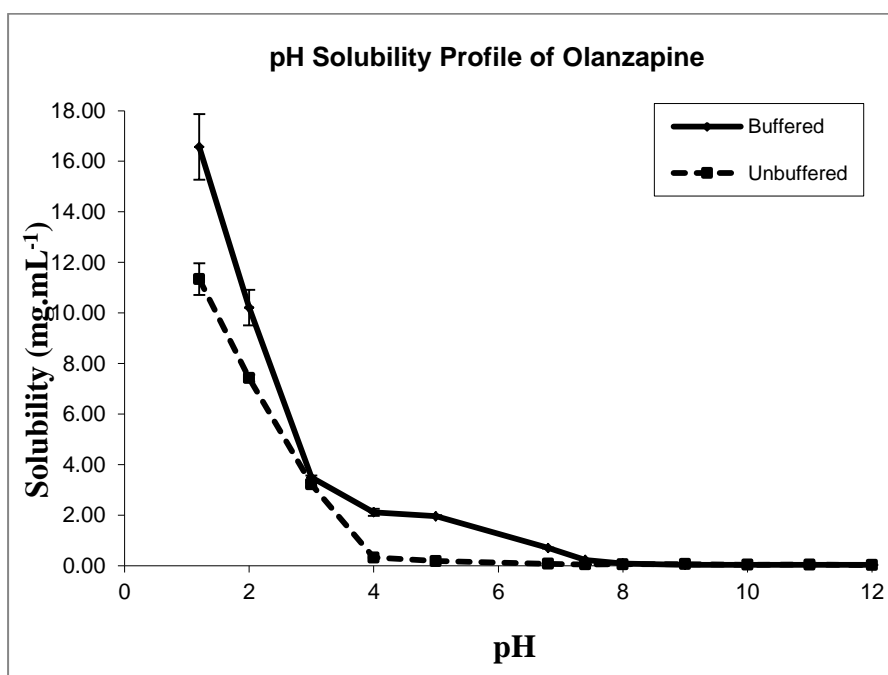


Figure 4.2: Preformulation study profile: solubility determination

4.5.4 Determination of distribution coefficient

The distribution coefficient of OLN also followed pH dependency during the estimation in various buffers of acidic and alkaline pH. This behavior is clearly visible in graph [Figure 4.3] which shows a trend of higher log D in alkaline buffers and lower values in acidic buffers.

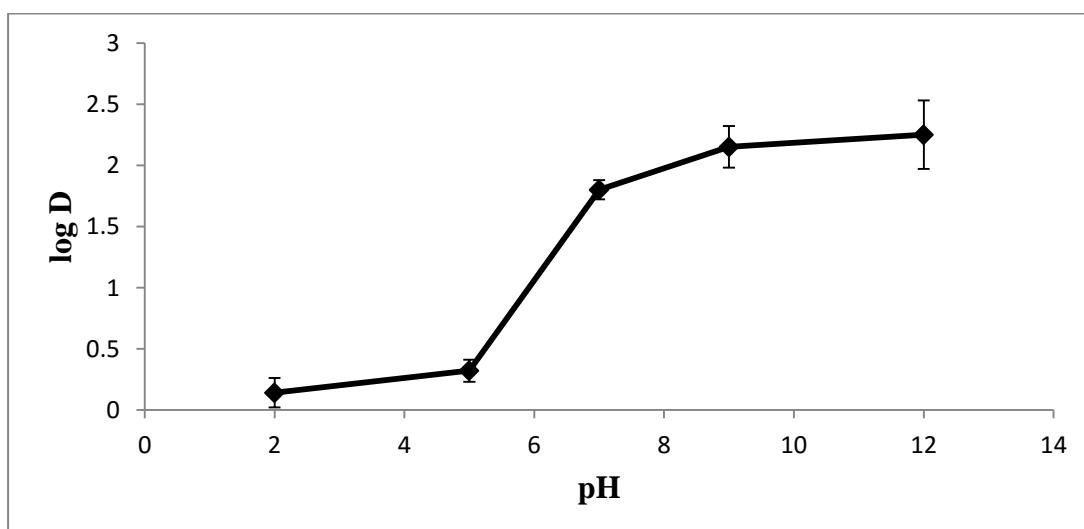


Figure 4.3: Preformulation study profile: Log D determination

High percentage of unionized species at alkaline pH is responsible for these higher values and low percentage of unionized species at acidic pH is represented by low log D values at lower pH buffers. The percentages of ionized and unionized species are very significant at biological pH since this can affect passage of drug molecules through biological membranes in the body as unionized species pass preferably, than ionized ones.

4.5.5 Determination of dissociation constant

The dissociation constant of OLN by spectrophotometric method was found to be 4.4. The wavelength for studying pK_a was selected based on the distinguishable absorbance values at each pH solutions. The first derivative graph was carefully studied to find out the point of inflection which corresponds to the largest change in the absorbance [Figure 4.4].

pK_a is the pH at which drug molecules exist as ionized and unionized in equal proportions. Ionized species have a separate behavior of absorbance as compared to unionized species and at different pH buffers drug exists in both the forms at different proportions based on the ionization of the drug molecules at that particular pH. When pH is value of pK_a , where both the forms are equally present, the trend of absorbance changes to the maximum which is evident by the inflection point in first derivative graph; a graph between minor changes in absorbance with pH vs. pH.

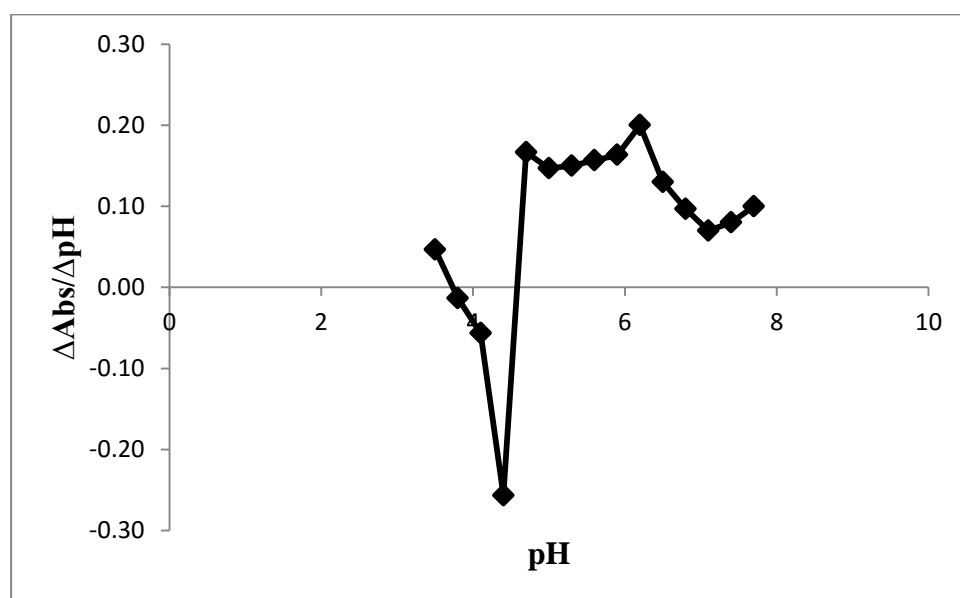


Figure 4.4: Preformulation study profile: pK_a determination

4.5.6 Stability studies

a) Solution state stability studies

It was observed that OLN followed first order reaction kinetics [Figure 4.5]. The degradation rate constant (K_{deg}) for all the solutions of pH; 6.8, 7.4, 4.5, 3.0, 1.2, 10.0, & 12.0 were found to be 9.6×10^{-3} , 13.58×10^{-2} , 2.3×10^{-2} , 3.17×10^{-2} , 3.73×10^{-2} , 4.58×10^{-2} and 5.75×10^{-2} respectively. The $t_{90\%}$ (days) of OLN in different pH solution were, 10.8, 7.75, 4.57, 3.31, 2.82, 2.29 and 1.83 days respectively. The rate profile demonstrated that the degradation of OLN is acid and base catalyzed. The degradation rate constant was found to be high at extreme pH (both at extreme acidic and extreme alkaline), and was less in neutral pH (6-8) for all the three levels of drug concentrations investigated. OLN was found to be more stable in acidic pH as compared to alkaline pH. It has been suggested that, acid catalyzed degradation is mediated by protonation of the sulphur atom of the thieno moiety, resulting in the rupture of the C-S bond adjacent to diazepine ring. For base catalyzed degradation, the mechanism suggested involve proton transfer from the secondary amine in the benzodiazepine ring to the sulfur atom, resulting in electron delocalization and subsequent cleavage of the C-S bond [19].

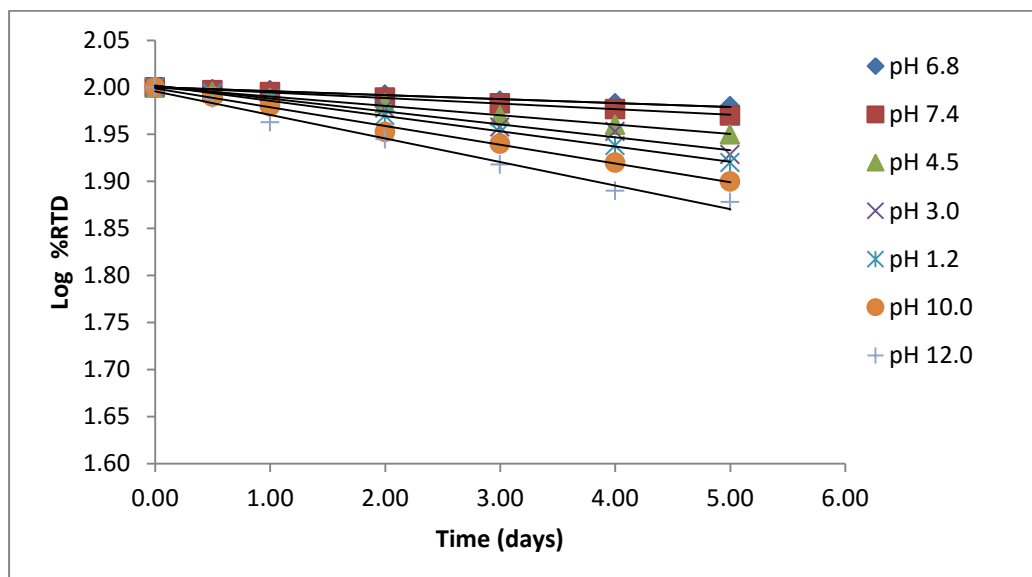


Figure 4.5: Solution state stability analysis of OLN in buffer solutions.

b) Solid state stability

The solid admixtures of OLN with various excipients showed good stability with drug content values ranging from 99.29 to 100.01% during the storage period. At refrigerated condition (FT: 5 ± 2 °C), pure OLN and the solid admixtures of OLN

with various excipients were found to be highly stable for the entire period of study (06 months). The log % RTD versus time plots for pure OLN and the solid admixtures were linear indicating first order kinetics with high regression coefficient ($r^2 = 0.9829$) [Figure 4.6]. In refrigerated condition, room condition and accelerated condition, the degradation rate constants for pure OLN were found to be 6.91×10^{-4} , 9.21×10^{-4} and $9.44 \times 10^{-4} \text{ month}^{-1}$ respectively. The $t_{90\%}$ values for pure OLN at refrigerated condition, room condition and accelerated condition were found to be 152.55, 114.41 and 111.62 months respectively.

The degradation rate constant (K_{deg}) values for the solid admixtures stored at refrigerated conditions were ranging from 6.98×10^{-4} to $7.17 \times 10^{-4} \text{ month}^{-1}$. The $t_{90\%}$ values were ranging from 147.01 to 151.21 months. The K_{deg} values for the solid admixtures stored at CRT conditions were ranging from 9.31×10^{-4} to $9.78 \times 10^{-4} \text{ month}^{-1}$. The $t_{90\%}$ values were ranging from 113.21 to 107.77 months. The K_{deg} values for admixtures stored at AT conditions were ranging from 9.98×10^{-4} to $12.42 \times 10^{-4} \text{ month}^{-1}$. The $t_{90\%}$ values were ranging from 84.86 to 105.61 months. These results suggested good solid state stability of OLN alone and in combination with excipients.

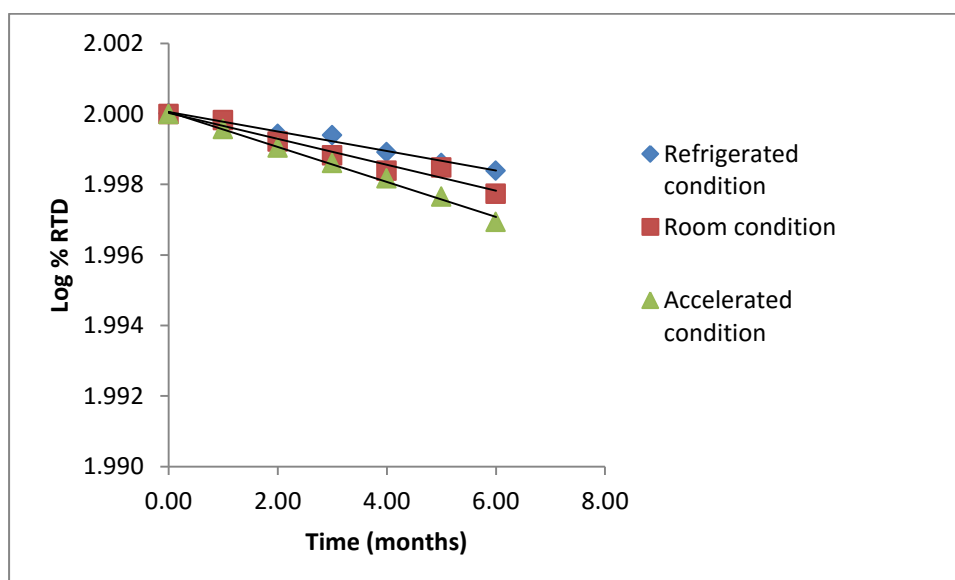


Figure 4.6: Solid state stability analysis of OLN

4.5.7 Compatibility studies

The differential scanning calorimetric study was used in order to detect any incompatibilities due to drug-excipient interaction. Any abrupt or drastic change in the thermal behavior of either the drug or excipient differential scanning calorimetric study may indicate a possible drug-excipient interaction. The thermograms obtained for pure drug, pure excipients, physical mixture of drug and excipients are shown in Figure 4.7 to 4.11. The melting endotherms of OLN were well preserved in all the cases. OLN showed a melting peak endotherm at 198 °C. As shown in the Figure 4.7, in the case of OLN: stearic acid physical admixture, the melting peak of drug was distinctly seen and the enthalpy remained unchanged (-37.36 mcal). Similarly in cases of stearic acid, glyceryl mono stearate, polyvinyl alcohol, PF-68 etc. also, the endothermic peak of OLN was retained with no change in the shape of the endotherm and enthalpy. The observations clearly suggested the absence of incompatibility between selected excipients and OLN.

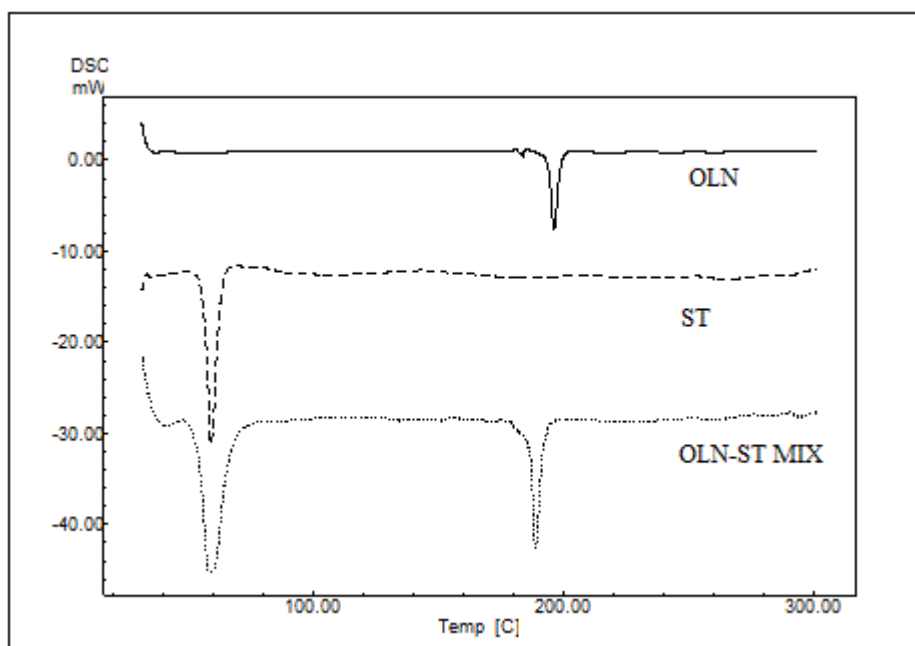


Figure 4.7: DSC thermograms of OLN, stearic acid and mixture of both.

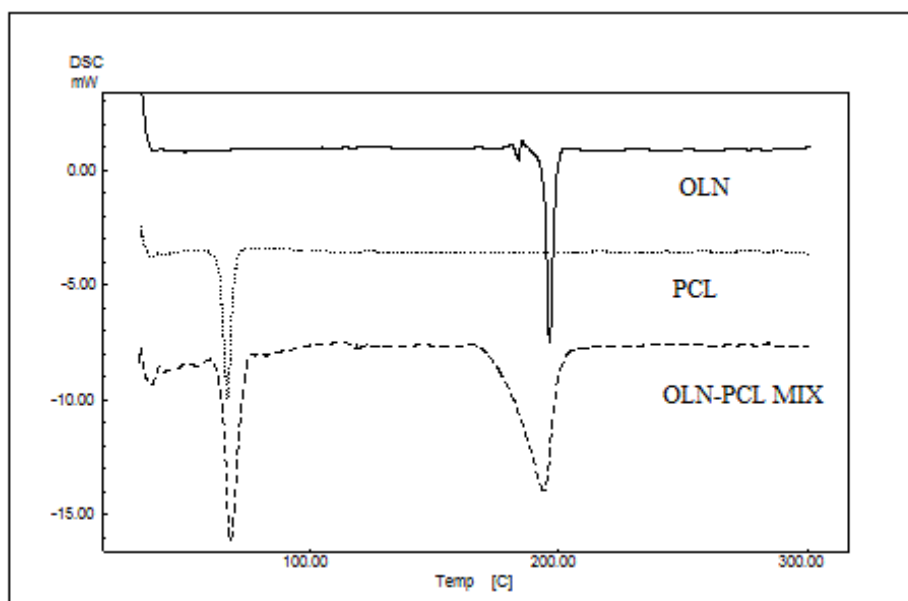


Figure 4.8: DSC thermograms of OLN, poly caprolactone and mixture of both.

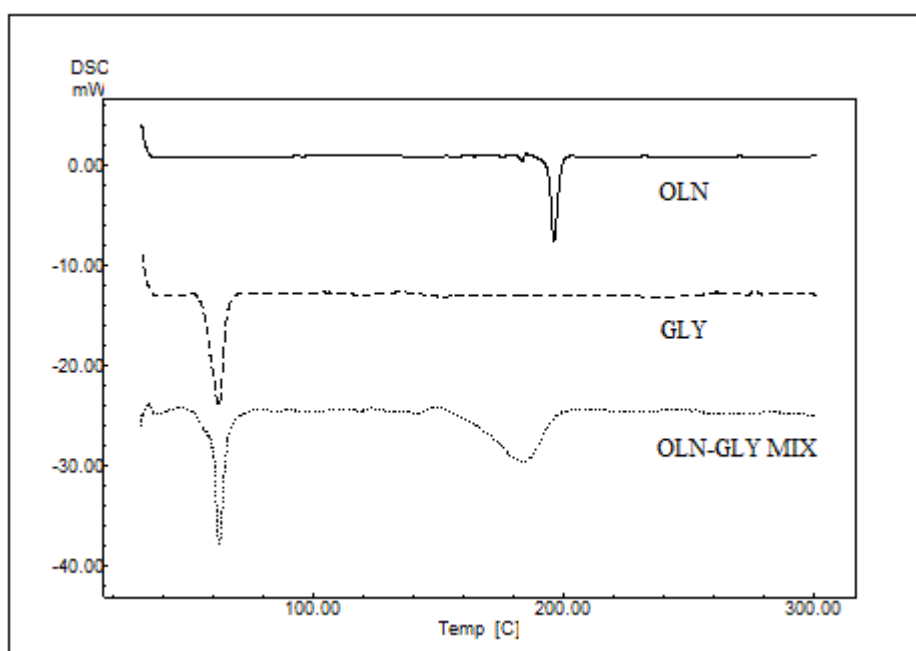


Figure 4.9: DSC thermograms of OLN, glyceryl monostearate and mixture of both.

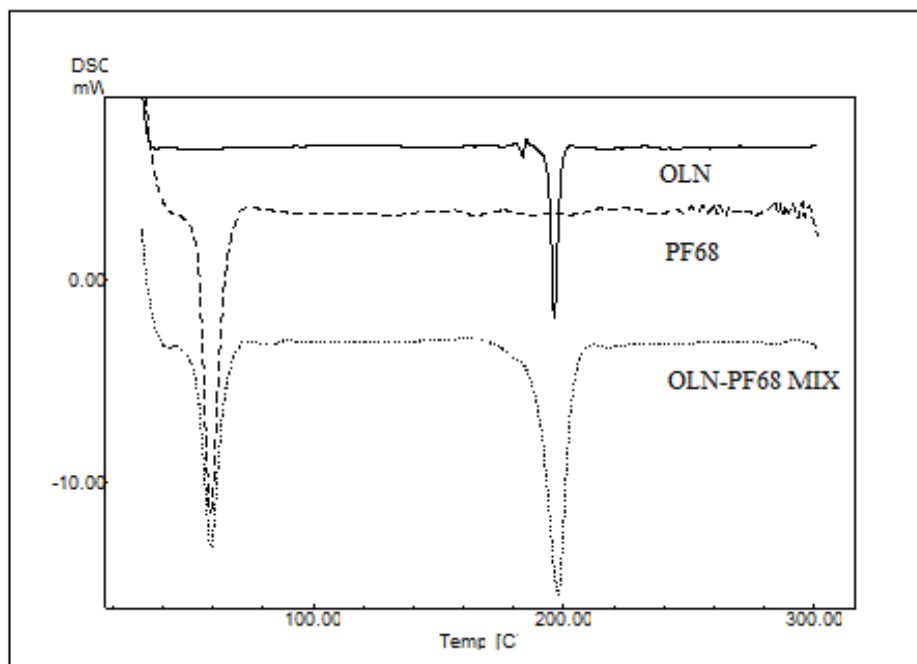


Figure 4.10: DSC thermograms of OLN, pluronic F68 and mixture of both.

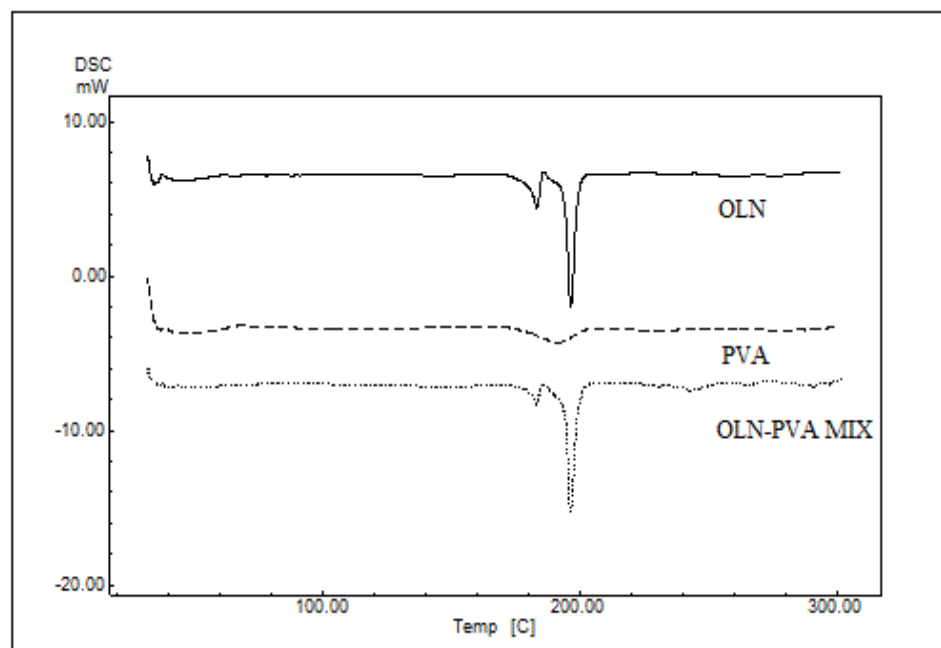


Figure 4.11: DSC thermograms of OLN, Poly vinyl alcohol and mixture of both.

The data obtained from the compatibility studies of OLN with various selected excipients by DSC was further supported by results of FTIR studies (Figure 4.12).

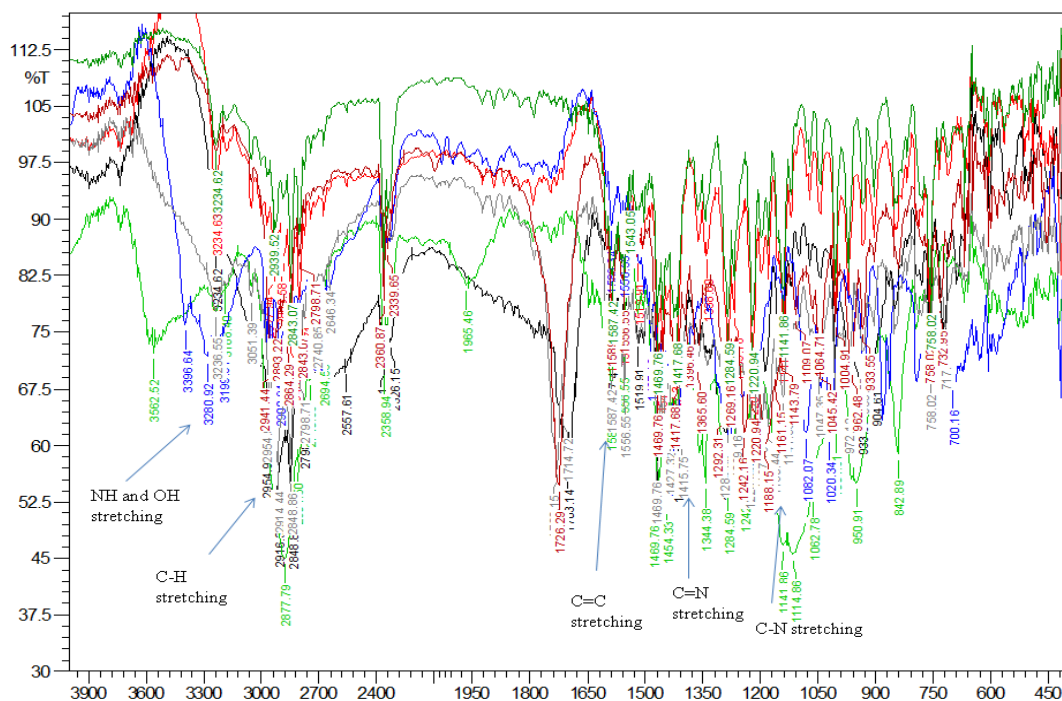


Figure 4.12 : Overlaid FTIR spectra of OLN with excipients

The FTIR spectrum of pure OLN and solid admixtures of OLN with various selected excipients are shown in Figure 4.12, which was characterized after 6 months of storage. The characteristic peaks found include peaks at 3234 cm^{-1} (NH and OH stretching), 2939 cm^{-1} (C-H stretching), 1587 cm^{-1} (C=C stretching), 1419 cm^{-1} (C=N stretching) and 1284 cm^{-1} (C-N stretching) which were present in all the spectrum, same as that of control sample, indicated the stable nature of OLN in all the solid admixtures studied.

Conclusions

Preformulation studies demonstrated that OLN exhibited a pH dependent solubility in different buffers with high solubility in acidic pH buffers and low solubility in basic pH buffers. Distribution coefficients in various buffers and dissociation constant were determined successfully. Solution state stability studies suggested that OLN was found to be more stable in acidic pH as compared to alkaline pH, and degradation kinetics was found to be of first order. The solid admixtures of OLN with various excipients showed good stability with high drug content values during solid state stability studies. Results obtained for the drug-excipient compatibility studies by DSC, demonstrated no significant interaction with various excipients selected for the formulation development.

References

- [1] H. Nyqvist, Preformulation studies of drug substances for solid dosage forms, *Drug Dev Ind Pharm*, 12 (1986) 953-968.
- [2] D.B. Volkin, G. Sanyal, C.J. Burke, C.R. Middaugh, Preformulation studies as an essential guide to formulation development and manufacture of protein pharmaceuticals, in: *Development and Manufacture of Protein Pharmaceuticals*, Springer, (2002) 1-46.
- [3] G. Banker, N. Anderson, The theory and practice of industrial pharmacy; Lachman, L, 3rd, (1991) 297-300.
- [4] K.J. Box, G. Volgyi, E. Baka, M. Stuart, K.T. Novak, J.E. Comer, Equilibrium versus kinetic measurements of aqueous solubility, and the ability of compounds to supersaturate in solution—a validation study, *J Pharm Sci*, 95 (2006) 1298-1307.
- [5] E. Baka, J.E. Comer, K.T. Novak, Study of equilibrium solubility measurement by saturation shake-flask method using hydrochlorothiazide as model compound, *J Pharm Biomed Anal*, 46 (2008) 335-341.
- [6] J.C. Dearden, G.M. Bresnen, The measurement of partition coefficients, *Mol Inform*, 7 (1988) 133-144.
- [7] S.K. Poole, C.F. Poole, Separation methods for estimating octanol–water partition coefficients, *J Chromatogr B*, 797 (2003) 3-19.
- [8] A. Berthod, S. Carda-Broch, Determination of liquid–liquid partition coefficients by separation methods, *J Chromatogr A*, 1037 (2004) 3-14.
- [9] M. Pandey, A. Jaipal, A. Kumar, R. Malik, S. Charde, Determination of pK_a of felodipine using UV–Visible spectroscopy, *Spectrochim Acta A Mol Biomol Spectrosc*, 115 (2013) 887-890.
- [10] A.J. Cessna, R. Grover, Spectrophotometric determination of dissociation constants of selected acidic herbicides, *J Agric Food Chem*, 26 (1978) 289-292.
- [11] P. Jin, S. Madieh, L.L. Augsburger, The solution and solid state stability and excipient compatibility of parthenolide in feverfew, *AAPS PharmSciTech*, 8 (2007) 200-205.
- [12] E.R. Oberholtzer, G.S. Brenner, Cefoxitin sodium: Solution and solid-state chemical stability studies, *J Pharm Sci*, 68 (1979) 863-866.
- [13] M. Lai, E. Topp, Solid-state chemical stability of proteins and peptides, *J Pharm Sci*, 88 (1999) 489-500.

- [14] P. Mura, M. Faucci, A. Manderioli, G. Bramanti, L. Ceccarelli, Compatibility study between ibuprofen and pharmaceutical excipients using differential scanning calorimetry, hot-stage microscopy and scanning electron microscopy, *J Pharm Biomed Anal*, 18 (1998) 151-163.
- [15] L. Bernardi, P. Oliveira, F. Murakami, M.A. Silva, S.H. Borgmann, S. Cardoso, Characterization of venlafaxine hydrochloride and compatibility studies with pharmaceutical excipients, *J Therm Anal Calorim*, 97 (2009) 729-733.
- [16] A.A. Araujo, L.P. Mercuri, F.M. Carvalho, M. dos Santos Filho, J.R. Matos, Thermal analysis of the antiretroviral zidovudine (AZT) and evaluation of the compatibility with excipients used in solid dosage forms, *Int J Pharm*, 260 (2003) 303-314.
- [17] R.K. Verma, S. Garg, Selection of excipients for extended release formulations of glipizide through drug–excipient compatibility testing, *J Pharm Biomed Anal*, 38 (2005) 633-644.
- [18] G.I. Polla, D.R. Vega, H. Lanza, D.G. Tombari, R. Baggio, A.P. Ayala, J. Mendes Filho, D. Fernández, G. Leyva, G. Dartayet, Thermal behaviour and stability in Olanzapine, *Int J Pharm*, 301 (2005) 33-40.
- [19] C. Mbah, Olanzapine degradation kinetics in aqueous solution, *Pharmazie*, 66 (2011) 168-170.

Chapter 5

Formulation design and development

5.1 Introduction

The prospective of NP as potential drug delivery systems is progressively being realized as these offer numerous applications. The diverse properties and advantages of nanoparticulate drug delivery systems such as selective biodistribution, in-vitro and in-vivo drug stability, better bioavailability, controlled drug release, etc. make these systems potential candidate to carry therapeutic agents into targeted organ or tissue or even to cells [1]. However, it is very challenging for formulation scientists to prepare optimised nanoparticulate drug delivery system since various factors and processing variables would significantly affect on the performance of the drug delivery system [2, 3]. In the present study, different nanoparticulate systems for OLN have been planned using biodegradable and biocompatible polymer such as poly (ϵ -caprolactone) (PCL) and solid lipids such as stearic acid and glyceryl monostearate, with clear objectives of selective distribution, better efficacy and no or less side effects. Extensive literature survey and studies were carried out for the selection and further optimization of suitable method as well as process by identifying critical variables involved. The characteristics such as low average particle size, narrow particle size distribution with less polydispersibility index, high drug content, good encapsulation efficiency, controlled release characteristics were aimed by the study which would be capable for selective biodistribution in-vivo.

5.2 Experimental

5.2.1 Materials

OLN was received as a gift sample from IPCA Labs Pvt. Ltd. (Mumbai, India). Poly (ϵ -aprolactone) (M.W of 40,000), Stearic acid (M.W 284.4) and Glyceryl mono stearate (M.W 358.6) were procured from Sigma Aldrich, USA. Poloxamer 188 (Pluronic® F-68) (PF-68) was gifted by BASF, Germany. Excipients such as polyvinyl alcohol (PVA) with a molecular weight of 13,000-23,000 (98% hydrolyzed), Polysorbate 80 (Tween 80) were purchased from Sigma Aldrich Chemicals, USA. HPLC grade solvents such as Acetone, Methylene chloride, Methanol, Acetonitrile etc. were purchased from Merck, India. All other chemicals and solvents procured were of the highest purity available and used as received without any additional treatments. Purified water was prepared by filtering the freshly collected Milli-Q® water (Millipore®, France) through 0.22 μ m membrane filter.

5.2.2 Apparatus / Equipment / Instruments

Magnetic stirrer with temperature control (Remi, India, Tarsons India); temperature controlled centrifuge (Remi, India); Homogenizer (Kinematica®, USA); and Sonicator (Bath type: Toshiba, India; Probe type: Microson, USA) were used for NP preparation. Vacuum evaporator (Rotavapor, Büchi, Switzerland) was used for evaporation of organic solvents. Refrigerator (Vest-Frost, India) was used to freeze the samples at $-20\text{ }^{\circ}\text{C}$. Lyophilizers (Heto-Maxi Dry-Lyo, Germany; Labconco, USA) were used for freeze-drying of prepared NP. Zetasizer nano ZS, Malvern Instruments, UK, was used for particle size and zeta potential analysis. A Scanning electron microscope (SEM) (Morgagni, Philips, USA) equipped with a CCD camera (Megaview-III, Soft Imaging Systems) available at the DST-Analytical facility, Cochin University, Cochin was employed for acquisition of the images.

5.2.3 Preparation of nanoparticles

Nanoparticles were prepared by two different techniques.

I. Nanoprecipitation technique

i. Preparation of polymeric and solid lipid nanoparticles

Polymeric and solid lipid NP were prepared by nanoprecipitation method using biocompatible polymer such as poly (ϵ -caprolactone) and solid lipids such as stearic acid and glyceryl monostearate [4-6]. The methods adopted were slightly modified according to present requirements for the preparation of NP. Briefly, polymer/solid lipid and drug were dissolved in suitable organic solvent (acetone) by magnetic stirring with slight heating. This solution was further injected into distilled water containing surfactant (PF68/PVA) under moderate stirring. This mixture was bath sonicated (30 min for polymeric systems; 1 h for solid lipid systems). Stirring was continued for 6-8 h, further processed (vacuum concentrated using rotavapour, centrifuged at 14,000 rpm at $25\text{ }^{\circ}\text{C}$ for 20 min, re-dispersed in milli Q water) and lyophilized. For lyophilization, prefreezing of samples was performed at $-20\text{ }^{\circ}\text{C}$ for 24 h, and then the flasks were connected to freeze-drier under vacuum (1 mbar, $-110\text{ }^{\circ}\text{C}$). Cryoprotectant such as mannitol was used during process. The process was continued to obtain free-flowing dried powder of NP.

ii. Experimental Design

A QbD based 3^2 full factorial design was used for the optimization of formulations. The effect of amount of polymer/solid lipid concentration (A) and surfactant (B) on particle size (Y_1) and encapsulation efficiency (Y_2) were investigated. Effect of independent variables were studied at three levels viz. high (+1), medium (0) and low (-1) level.

The levels selected were:

- a. Polymer/solid lipid: 50 mg (-1), 150 mg (0) & 300 mg (+1) (volume selected, 25 mL);
- b. Surfactant: 0.2% (-1), 0.6% (0) & 1.5% (volume selected, 50 mL);

Design-expert® software (version 8.0.7.1, Stat-Ease Inc., MN) was used to design and study the experimental parameters and obtained responses.

II. Emulsification-ultra sonication technique

i. Preparation of solid lipid nanoparticles

SLN using glyceryl mono stearate and stearic acid were also prepared using homogenization-ultra sonication technique. The procedure followed was in accordance with previously reported methods of SLN preparation with minor modifications [7-9]. In brief, initially, solid lipid was heated 5-10 °C above the melting point of the lipid and OLN was made to dissolve in it. An aqueous phase was prepared by dissolving surfactant (poloxomer 188) in Milli-Q water and heated to same temperature of oil phase. Hot oil phase was further added to the hot aqueous phase and subjected to high-speed homogenization at 18,000 rpm (homogenizer: Kinematica®, USA) for 3 min, thereby producing a hot oil-in-water (o/w) emulsion. This was further subjected to probe ultrasonication (Probe type: Microson, USA) for 10 min (700W) with 6 sec on and 3sec off cycles. The hot nanoemulsion was then cooled down to room temperature, thereby producing SLN. This was further processed (centrifuged at 14,000 rpm at 25 °C for 20 min, re-dispersed in milli Q water) and lyophilized.

ii. Experimental Design

In the method of preparation of SLN using emulsification-ultra sonication technique, three factors such as solid lipid content, concentration of surfactant and drug:solid lipid ratio were selected at three levels in order to study their influence on responses

such as particle size, EE and DC. A Box Behnken design was employed for the study with 17 runs based on 3 factors and 3 levels. This design was highly suitable for the investigation of quadratic response surface and for generating a second order polynomial model. The independent variables studied in this design such as amount of solid lipid (A), concentration of surfactant-poloxamer 188 (B) and the ratio of drug to solid lipid (C) were investigated at three different levels (low, middle, and high) and were represented by (-1), (0) and (+1).

The levels selected were:

- a. Solid lipid: 500 mg (-1), 1000 mg (0) & 2500 mg (+1);
- b. Surfactant: 0.5 (-1), 1 (0) & 2% (volume selected, 50 mL);
- c. Drug: lipid ratio: 1:20 (-1), 1:10 (0) & 1:5 (+1)

Other factors of significance, such as homogenization time, sonication time and freeze drying were also investigated in order to study the influence on responses selected.

Tween 80 coating of prepared nanoparticles

Coating of the optimized nanoparticulate systems with tween 80 was carried out in order to improve brain targeting efficiency of the formulations. Different arguments have been put forth in literature regarding the tween 80 coating and brain targeting. These include inhibition of the efflux system especially P-glycoprotein (Pgp), endocytosis via the low density lipoprotein (LDL) receptor mediated by the adsorption of apolipoprotein B and/or E from the blood [10, 11]. Briefly, freeze-dried nanoparticles were dispersed in PBS containing 1% of tween 80 (20 mg NP.mL⁻¹). This dispersion was further sonicated for 10 min for complete dispersion of NP and then incubated at room temperature for 30 min. The dispersion was kept at -20⁰ C for 12 h and consequently lyophilized and stored [12].

5.2.4 Characterization of nanoparticles

In order to find out whether the obtained NP meet the required criteria and objectives several characterization methods were used as discussed below.

a. Particle size distribution and zeta potential

The average particle size distribution and zeta potential of individual formulation were analysed using a Zetasizer (nano ZS®, Malvern, UK). Freeze-dried nanoparticulate formulations were suitably dispersed in Milli-Q water, which was

previously ultra-sonicated for 30 min and filtered through 0.22 μm membrane using Millipore® filtration system. The dispersion of NP was kept into size/zeta capillary cell and analyzed. A laser beam is directed toward the sample present in capillary cell and the fluctuation intensity of the scattered light is detected. The electrophoretic mobility is proportional to the variation observed and can thus be determined. The average particle size, zeta potential, and polydispersity index (PI) were determined. An average of three measurements (12 trials in each measurement) was performed during the analysis after the stabilization time of 120 seconds.

b. Particle shape and morphology

Scanning electron microscopy (SEM) was performed for morphological characterization of the obtained NP. The prepared nanoparticulate formulations were dispersed in pure Milli-Q water, which was previously ultrasonicated for 30 min. Scanning electron microscopy is performed in order to get a better understanding of the particle size and to study the topography of a sample. Briefly, the samples for SEM were prepared by lightly sprinkling the NP on a double adhesive tape which was struck to an aluminium stub. The stubs were then coated with gold. The samples were then randomly scanned and photomicrographs were taken at defined magnifications. In this technique, a beam of high-energy electrons is made to focus on the sample and when it penetrates the surface, it results in an interaction between electrons and surface atoms. Secondary, back scattered, auger electrons are produced and these in turn create signals, and detected by energy dispersive x-ray analysis. The secondary electrons produced during scanning of beam on the surface of particles are detected, which can reveal information regarding texture, chemical composition, as well as crystalline structure of the sample's surface.

c. Drug estimation

The drug analysis was performed in order to determine the EE and drug content of the individual nanoparticulate formulations. For this, accurately weighed lyophilized NP were transferred to a cleaned calibrated flask and digested by dissolving the polymeric/solid lipid matrix in a suitable organic solvent system (acetonitrile). The system was kept under ultra-sonication for 30 min, at 25 °C for the complete release of drug from the nanoparticulate systems. The amount of drug present was determined using in-house developed analytical method (discussed in Chapter 3). Estimations

were performed in triplicates and results obtained were represented as average with standard deviations (SD). The EE of the drug in NP was expressed as the percentage of the amount of drug entrapped in the nanoparticulate formulation relative to the initial amount of the drug added to the formulation. The EE was calculated using the following formula.

$$EE (\%) = \frac{\text{Amount of drug in NP (mg)}}{\text{Amount of drug added (mg)}} \times 100$$

The DC of the nanoparticulate formulations was expressed as the percentage of the amount of drug present in the unit weight. The DC was calculated from the amount of the drug present per unit weight of the final product using following formula.

$$DC (\%) = \frac{\text{Amount of drug in nanoparticles (mg)}}{\text{Amount of nanoparticles (mg)}} \times 100$$

d) In-vitro drug release studies

The release of OLN from in-house developed polymeric and solid lipid nanoparticulate systems has been studied using dialysis bag technique [13]. In brief, 2 mL of the nanoparticulate dispersions (equivalent to 1mg of OLN) was placed in dialysis bag (Spectrapor, cut off 12,500 kDa), tied suitably on both the sides, and placed into 100 mL of dissolution media. The media consisted of PBS of pH 7.4 with 2% tween 80 in order to achieve sink condition. Pure OLN (1mg) was dissolved in PBS with surfactant (PF 68; 1% w/v) and studied for drug release for comparison with nanoparticulate formulations. The entire system was kept on magnetic stirrer with a continuous stirring speed of 100 rpm. At specified time intervals (0.5, 1, 2, 4, 8, 12, 18, 24, 30, 36, 48 and 60 h), 1 mL of sample was collected and replaced with fresh buffer. The amount of drug present has been determined by using in-house developed and validated high profile liquid chromatographic method (Chapter 3).

The obtained drug release data were fitted to various kinetic equations such as Zero order, First order, Higuchi, Korsmeyer-Peppas, Hixson-Crowell and Baker-Lonsdate model to find the order and mechanism of OLN release from the nanoparticulate systems.

Zero order: $X = K_0t$; First order: $\text{Log } X = \text{Log } X_0 - K_1t / 2.303$;

Higuchi model: $Q = K_H t^{1/2}$; Korsmeyer peppas model: $M_t/M_\infty = K t^n$;

Hixson-Crowell equation: $F = 100[1 - (1 - k_{hc}t)^3]$; Baker-Lonsdate (BK) equation:
 $BL = 3/2[1 - (1 - F/100)^{2/3}] - F/100 = k_{BL}t, k_{BL} = [3 \times D \times C_s / (r_0^2 \times C_0)]$

Where, X_0 is initial amount of drug, X is amount of drug released at time t , M_t/M_∞ is the fraction of drug released at any time t ; and K_0 , K_1 , K_H , k_{hc} , k_{BL} and K are release rate constants. The diffusional exponent, n is indicative of mechanism of drug release: a value of $n = 0.45$ indicates fickian or case I release; $0.45 < n < 0.89$ indicates non-fickian or anomalous release; $n = 0.89$ indicates case II release; and $n > 0.89$ indicates super case II release. F is the percentage drug released in time t . D is the diffusion coefficient, C_s is the saturation solubility, r_0 is the initial radius for a sphere or cylinder or the half-thickness for a slab, C_0 is the initial drug loading in the matrix.

5.2.5 Thermal study

DSC study was performed for optimized batches (PCL NP, C PCL NP, GLY NP, GLY NP). Sample preparation was same as mentioned in chapter 4. These studies were carried out in order to study the physical state of the polymer/solid lipid and drug in formulation and to investigate any possible interaction between drug and polymer/solid lipid within the matrix.

5.2.6 Stability studies

Stability studies of nanoparticulate formulations were carried out at three different storage conditions: ambient (25 ± 2 °C); refrigerated (5 ± 3 °C); and frozen (-20 ± 5 °C) in hermetically sealed glass vials. The stability studies were performed for 3 and 6 months. Once the stability period is completed, samples were collected and analyzed in terms of degree of aggregation, drug content, particle size, release profiles and ease of redispersibility. Besides, effect of freeze-drying on the average particle size and particle size distribution was studied by assessing redispersibility for optimized formulations. In this study, the freeze-dried formulations were reconstituted by dispersing it into Milli-Q water and the obtained dispersions were then compared with respective fresh formulations.

5.3 Results and discussions

5.3.1 Formulation considerations

a. Nanoprecipitation technique

The nanoprecipitation method is generally employed in order to incorporate hydrophobic drugs into the nanoparticulate systems. Polymeric/solid lipid nanoparticulate systems were prepared by this technique, which, mainly relies on the rapid diffusion of the solvent across interface between the solvent-polymer/ solid lipid and the aqueous phase. The independent factors selected were thought to influence significantly on selected responses such as mean particle size and EE. The results obtained are represented in Table 5.1-5.3.

Design-Expert software was used in order to obtain polynomial equations involving the main response and interaction factors based on various parameters like predicted residual sum of squares, multiple correlation coefficients and adjusted multiple correlation coefficient. The validation of these polynomial equations obtained was performed statistically by using ANOVA. Response surface plots were made to study the effects of the predetermined factors on the responses such as EE, and particle size. The careful study of equations and surface plots would result in understanding the effects of each variable independently and in combination with other variables on each response parameter.

i. Effects on particle size

The full polynomial model equations for particle size obtained by the response surface regression procedure by using Design-Expert software was found to be:

$$\text{PCL NP: Particle size} = +74.95231 + 23.45667 A - 1.6650 B \dots \dots \dots \text{Eq (1)}$$

$$\text{ST NP: Particle size} = +162.66 + 36.04 A - 22.84 B - 8.74 AB + 9.31 A^2 + 6.87 B^2 \dots \dots \text{Eq (2)}$$

$$\text{GLY NP: Particle size} = +221.31 + 73.59 A - 27.47 B \dots \dots \dots \text{Eq (3)}$$

Where, A is polymer concentration and B is surfactant concentration.

Response surface plots for particle size were obtained as shown in Figure 5.1-5.3.

Design-Expert® Software
Factor Coding: Actual
Particle size
X1 = A: Polymer concentration
X2 = B: Surfactant concentration

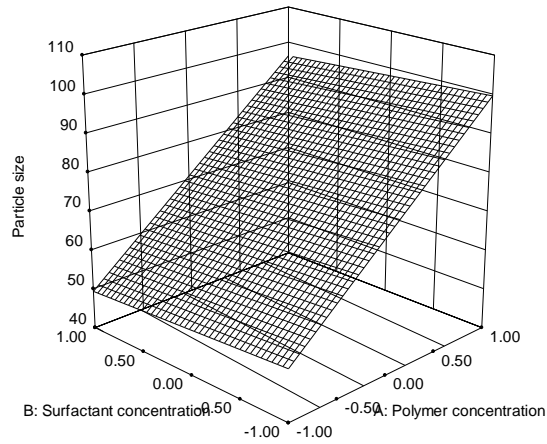


Figure 5.1: Response surface for particle size of PCL NP: effect of polymer (A) and surfactant concentration (B)

Design-Expert® Software
Factor Coding: Actual
Particle size
X1 = A: Polymer concentration
X2 = B: Surfactant concentration

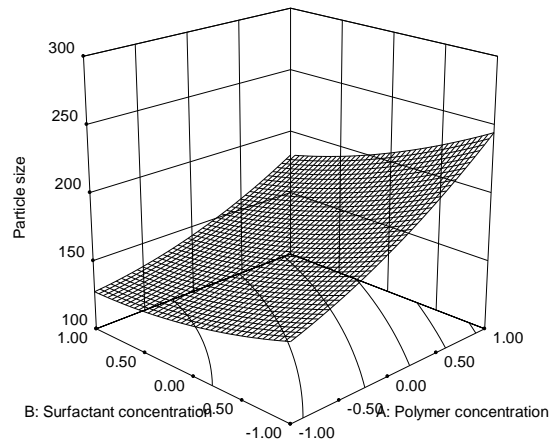


Figure 5.2: Response surface for particle size of ST NP: effect of polymer (A) and surfactant concentration (B)

Design-Expert® Software
 Factor Coding: Actual
 Particle size
 X1 = A: Polymer concentration
 X2 = B: Surfactant concentration

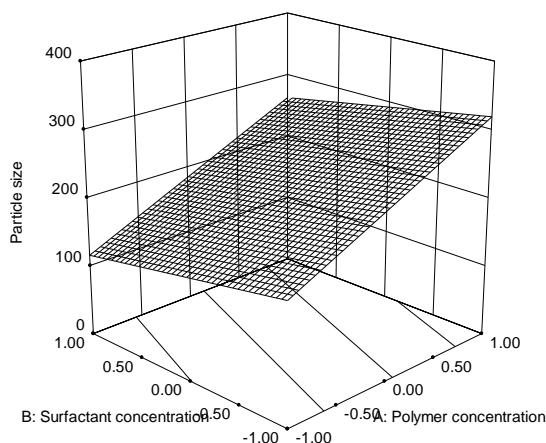


Figure 5.3: Response surface for particle size of GLY NP: effect of polymer (A) and surfactant concentration (B)

By analyzing the coefficients of the equation (Eq 1-3) and surface plots (Figure 5.1-5.3), it could be evident that particle size was highly influenced by both the selected independent factors. The positive and negative value of a factor in the regression equation indicates the increase and decrease in response respectively with the factor. All the formulations were found to be highly influenced positively for particle size as evident by the respective equations and surface plots. An increased amount of polymer/solid lipid resulted in an increased particle size. The coefficients of A for PCL NP (23.45), ST NP (36.04), and GLY NP (73.59) were found to be very high as compared to coefficients of other studied factors, thereby demonstrating its grand significance among the studied factors. Comparing the three formulations, GLY NP had much higher impact as compared with ST NP and PCL NP as observed by the magnitude of their respective coefficients.

This kind of behavior might be due to the increased viscosity of organic phase, because of high concentration of polymer/solid lipid, which in turn results in reduction in the diffusion rate of the solute molecules of organic phase into external aqueous phase and consequently results in formation of bigger particles [14]. This effect can also be explained using Stoke's law by studying the density difference between internal and external phase [15]. Moreover, in case of SLN, there is a higher tendency of lipid to coalesce at high lipid concentration.

An increase in the concentration of surfactant (poloxomer 188), the particle size was found to be decreased. The analysis of surface plots and negative coefficients of B in equations 1-3, for PCL NP (-1.66), ST NP (-22.84), and GLY NP (-27.47) indicated a negative relation between surfactant concentration and particle size is present. A less extent relationship was observed as compared with the effect of polymer/solid lipid concentration and in reverse manner, as indicated by value of coefficients. Numerous reasons have been suggested for this behavior. Increased amount of surfactant would result in decreased surface tension between organic phase and external aqueous phase. Furthermore, surfactant would help in stabilization of the obtained particles, thereby preventing particle aggregation [14].

The cross-interaction of polymer/solid lipid and surfactant on the size was also found to be significant for ST NP because the coefficient of AB (-8.74) obtained was high and have a negative impact on studied response, i.e. particle size of prepared ST NP are negatively influenced by the combination of both the studied factors. These effects were not significantly observed in the cases of PCL NP and GLY NP, which were evident by the absence of coefficients of AB in equations represented for them.

ii. Effects on encapsulation efficiency

The effect of the studied independent variables on encapsulation efficiency could be explained by the following polynomial equations (Eq 4-6) and Figures 5.4-5.6:

PCL NP: Encapsulation efficiency = +82.13+7.34 A-2.34 B-0.46 AB-10.73 A²-0.74 B².....Eq (4)

ST NP: Encapsulation efficiency = +71.43+14.78 A-2.76 B+2.36 AB-4.54 A²+0.16 B².....Eq (5)

GLY NP: Encapsulation efficiency = +86.28+6.69 A-2.16 B-1.00 AB-5.19 A²+0.42 B².....Eq (6)

Where, A is polymer concentration and B is surfactant concentration

Design-Expert® Software
Factor Coding: Actual
Encapsulation efficiency
X1 = A: Polymer concentration
X2 = B: Surfactant concentration

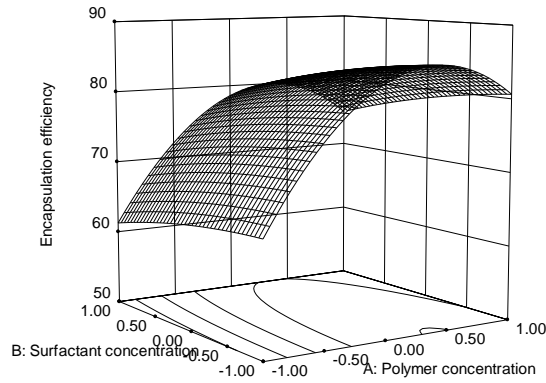


Figure 5.4: Response surface for encapsulation efficiency of PCL NP: effect of polymer (A) and surfactant concentration (B)

Design-Expert® Software
Factor Coding: Actual
Encapsulation efficiency
X1 = A: Polymer concentration
X2 = B: Surfactant concentration

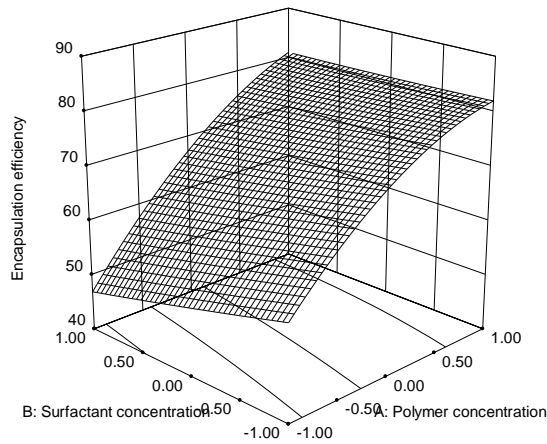


Figure 5.5: Response surface for encapsulation efficiency of ST NP: effect of polymer (A) and surfactant concentration (B)

Design-Expert® Software
 Factor Coding: Actual
 Encapsulation efficiency
 X1 = A: Polymer concentration
 X2 = B: Surfactant concentration

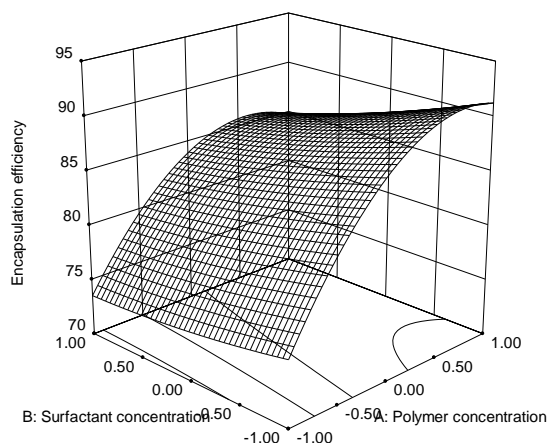


Figure 5.6: Response surface for encapsulation efficiency of GLY NP: effect of polymer (A) and surfactant concentration (B)

The equations and surface plots suggest that all the formulations have been found to be influenced positively by polymer/solid lipid, for encapsulation efficiency, similar to that of particle size, but to a lesser extent. An increased amount of polymer/solid lipid resulted in an increased encapsulation efficiency. The coefficients of A for PCL NP (7.34), ST NP (14.78), and GLY NP (6.69) were found to be high and surface plots clearly show a distinct positive variation for high polymer/solid lipid concentration. This was an expected result, since with an increased hydrophobic polymer/surface lipid; more space for the encapsulation of lipophilic drug such as OLN would be available. Moreover, in case of glyceryl monostearate, an increased concentration of glycerides would act as solubilizing agents for highly hydrophobic drug like OLN [16].

EE was also affected by the amount of surfactant present. The analysis of surface plots and negative coefficients of B in equations 4-6, for PCL NP (-2.34), ST NP (-2.76), and GLY NP (-2.16) found that a negative relation between surfactant concentration and EE is present. There was a decrease in EE observed with an increased concentration of surfactant. This effect can be explained by the increased aqueous solubility of OLN with an increased concentration of surfactant in external aqueous phase [17, 18]. The combination of both factors also found to have influence on EE, which is evident by the equation and surface plots. The coefficients of AB for

PCL NP, ST NP, and GLY NP were found to be less compared to individual factors studied, and therefore less significantly affected.

b. Emulsification-ultra sonication technique

The results obtained for NP prepared by emulsification-ultra sonication technique are represented in Table 5.4-5.5. All the selected independent variables such as the amount of solid lipid, concentration of surfactant and drug: solid lipid ratio were found to have significant influence on the selected responses. These effects were highly evident from the quadratic equations and response surfaces obtained from design-expert software.

i. Effects on particle size

The full second-order polynomial model for particle size obtained by the response surface regression is given by:

ST NP: Particle size = +135.00+78.13 A-29.63 B+4.75 C +2.25 AB+9.50 AC+3.50 BC+53.37 A²+1.88 B²+4.63C².....Eq (7)

GLY NP: Particle size = +170.80+79.75 A-29.12 B-1.63 C-5.50 AB+5.00 AC+4.25 BC+52.98A²+9.73B²+0.22C².....Eq(8)

Where, A is solid lipid concentration, B is of surfactant concentration and C is drug: solid lipid ratio

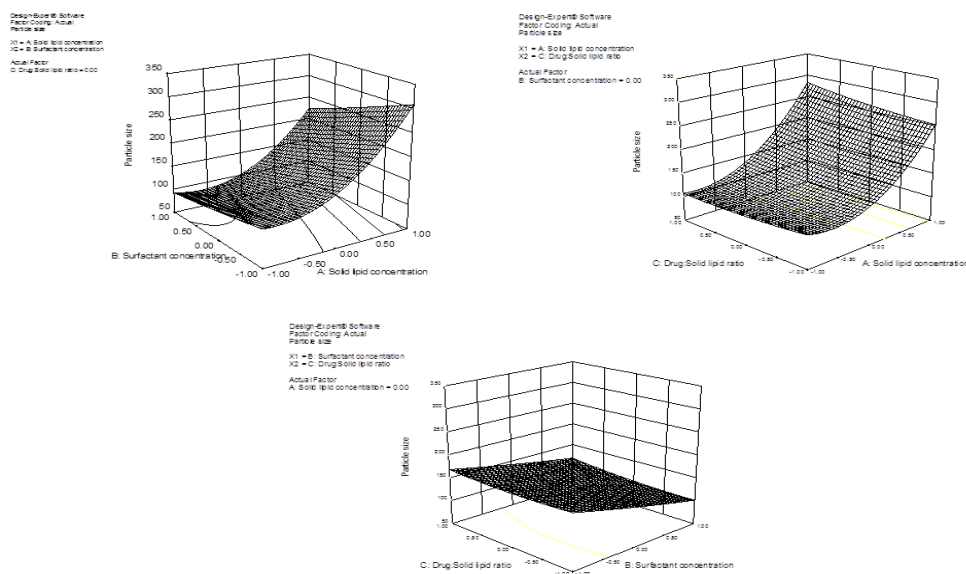


Figure 5.7: Response surface for particle size of ST NP: effect of solid lipid (A), surfactant concentration (B) and drug:lipid ratio (C)

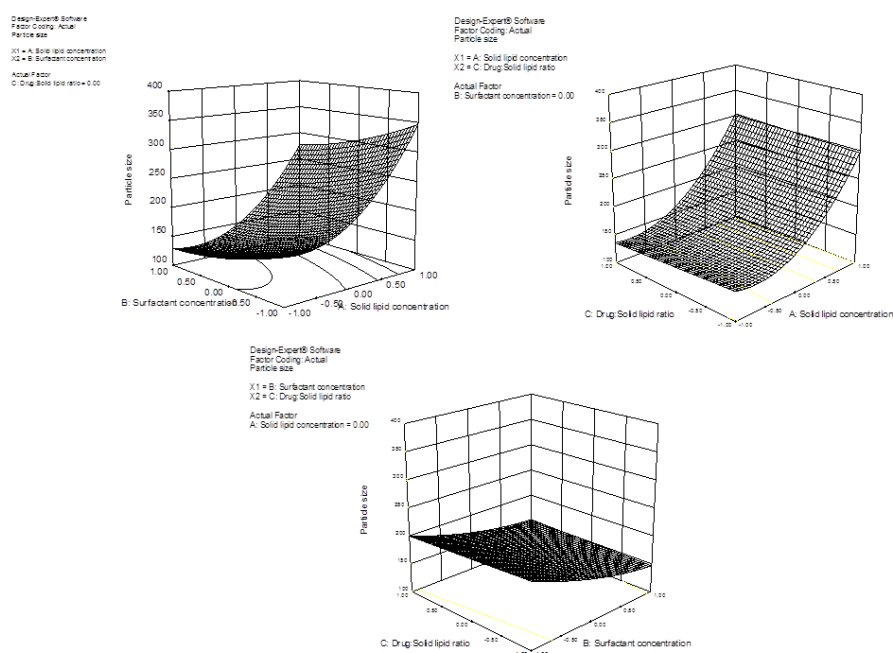


Figure 5.8: Response surface for particle size of GLY NP: effect of solid lipid (A), surfactant concentration (B) and drug:lipid ratio (C)

By studying the coefficients in the given second order polynomial equation and surface plots, it is apparent that particle size is highly influenced by the selected factors. Both ST NP and GLY NP have been found to be positively influenced by solid lipid concentration for particle size, as evident by their respective equations and surface plots. An increased amount of solid lipid resulted in an increased particle size in both the cases. Similar to the nanoprecipitation method, in the current method also have coefficients of A for ST NP (78.13), and GLY NP (79.75) which were very high as compared to coefficients of all other studied factors, and hence demonstrating very high significance among other factors. By increasing the solid lipid concentration, the exerted shear and sonication energy would not be sufficient for size reduction of nanoemulsion, which would result in bigger sized particles [19, 20]. Another reason for increased particle size could be the less availability of sufficient surfactant for covering the surface of the obtained particles, thereby they tend to increase in size. Besides, it is a widely accepted fact that there is a higher tendency of lipid to coalesce at high lipid concentration.

On the contrary, an increase in the concentration of surfactant (poloxomer 188), resulted in a decrease in particle size for both the formulations. The analysis of

surface plots and negative coefficients of B in equations 4-6, for ST NP (-29.63), and GLY NP (-29.12) found that there exists a negative relation between surfactant concentration and particle size. Similar to nanoprecipitation technique, a less extent relationship is observed as compared with the effect of solid lipid concentration on particle size. The reasons for decreasing the particle size could be explained in different ways, most importantly, an increased amount of surfactant would result in decreased surface tension between internal and external phases, resulting in the formation of smaller particles [21, 22]. In addition, surfactant would help in stabilization of the obtained particles, thereby preventing particle aggregation [23].

As compared to the lipid concentration and surfactant concentration, the studied third factor, drug:lipid ratio, had a very low impact on particle size as can be evident by very less magnitude of coefficients for C in both the formulations. However, in the case of ST NP, the amount of drug used, demonstrated a positive impact on particle size, coefficient which might be due to the incorporation of drug into the particles and thereby resulting incremental size of the particles.

As can be seen in Eq 7-8 and Figure 5.7, the combination of all the three factors affected the particle size. For instance, an increase in the lipid amount and surfactant concentration, resulted in increased particle size, that might be because of the reasons discussed for solid lipid concentration which was responsible for higher particle size and not having enough surfactant in the dispersion in order to cover the surfaces of particles obtained. Similarly, the combination of other factors demonstrated a positive impact on particle size, which is marked by the coefficients in equations and surface plots.

ii. Effects on encapsulation efficiency

The quadratic equation obtained from the study is given by:

$$\text{ST NP: Encapsulation efficiency} = +80.64 + 7.54 A - 0.54 B - 13.06 C - 1.82 AB + 2.89 AC - 0.60 BC - 10.18 A^2 - 11.68 B^2 - 3.18 C^2 \dots \dots \dots \text{Eq(9)}$$

$$\text{GLY NP: Encapsulation efficiency} = +83.94 + 8.62 A - 0.099 B - 12.49 C - 1.34 AB + 2.04 AC - 0.75 BC - 10.70 A^2 - 8.17 B^2 - 1.52 C^2 \dots \dots \dots \text{Eq(10)}$$

Where, A is solid lipid concentration, B is of surfactant concentration and C is drug:solid lipid ratio

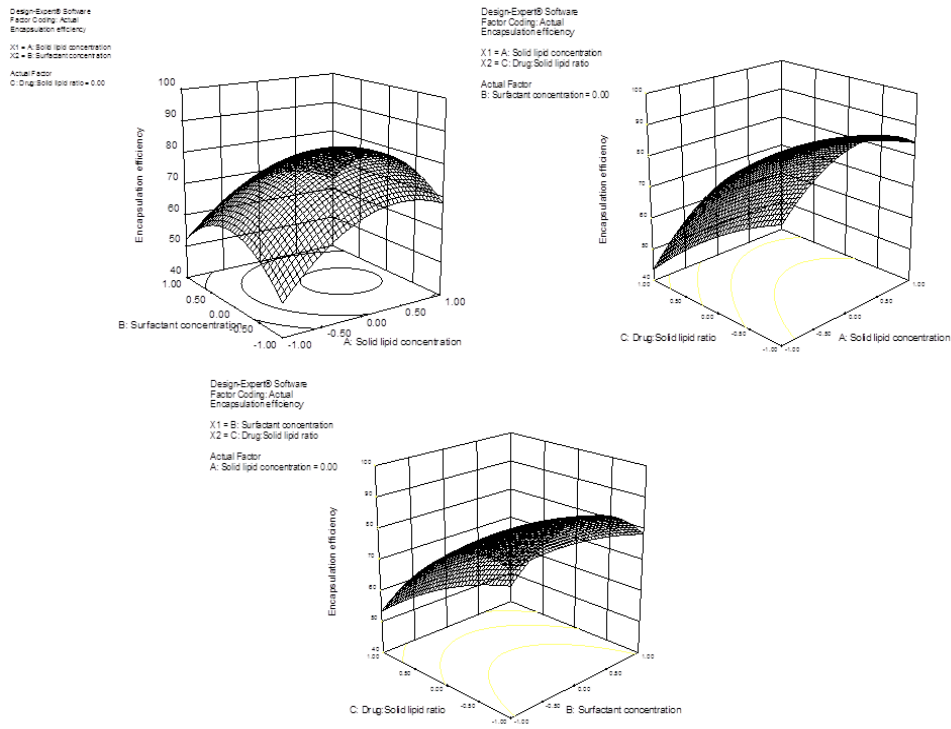


Figure 5.9: Response surface for encapsulation efficiency of ST NP: effect of solid lipid (A), surfactant concentration (B) and drug:lipid ratio (C)

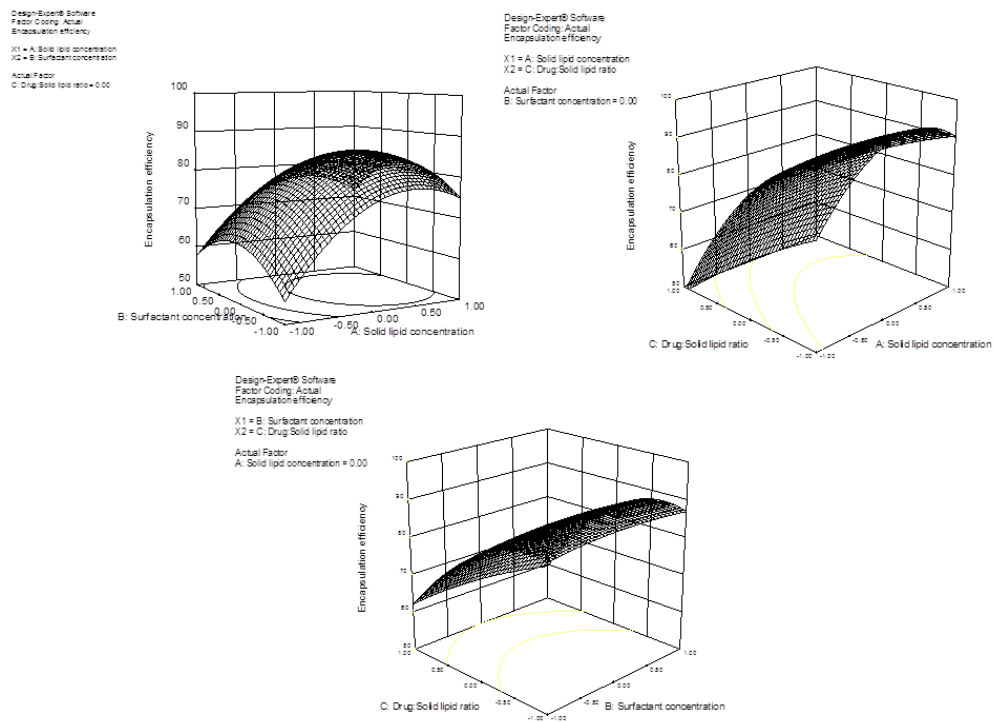


Figure 5.10: Response surface for encapsulation efficiency of GLY NP: effect of solid lipid (A), surfactant concentration (B) and drug:lipid ratio (C)

The equations (Eq 9-10) and surface plots (Figures 5.9-5.10) suggest that both the formulations have been found to be influenced positively by solid lipid concentration, for encapsulation efficiency. An increased amount of solid lipid resulted in an increased encapsulation efficiency. Similar to nanoprecipitation method, in the current method also, the coefficients of A for ST NP (7.54) and GLY NP (8.62) were found to be high and surface plots clearly show a distinct positive variation for high solid lipid concentration. This phenomenon, as discussed earlier are mainly due to the availability of more space for the encapsulation of lipophilic drug such as OLN in hydrophobic lipid and acting of lipids such as GMS, as solubilizing agents for highly hydrophobic drug like OLN.

EE was less affected by the amount of surfactant present. The analysis of surface plots and negative coefficients of B in equations, for ST NP (-0.54), and GLY NP (-0.09) suggest a negative relation between surfactant concentration and EE, but to a less/negligible extent only.

The EE is highly influenced by the factor C (drug: lipid ratio).The coefficients of C for ST NP (-13.06), and GLY NP (-12.49) were found to be very high thereby demonstrating its significance among the studied factors. Even though drug concentration has been increased, an increase in EE was not observed. This might be due to the fact that the lipid present might not be able to accommodate the increased amount of drug present, which would result in a decreased EE [24].

The combination of factors also found to influence EE, as demonstrated by the equation and surface plots. The coefficients of AB for ST NP and GLY NP were found to be -1.82 and -1.34 respectively, thereby showing a negative impact on EE. The coefficients of AC for ST NP and GLY NP were found to be comparatively high with values, 2.89 and 2.04 respectively, showing a positive impact on EE, whereas coefficients of BC for ST NP and GLY NP were found to be negligible with values 0.60 and 0.75 respectively.

iii. Effects on drug content

The full second-order polynomial equation for drug content obtained by the response surface regression is given by:

$$\text{ST NP: Drug content} = +6.66 + 0.75 A + 0.38 B + 1.87 C - 0.15 AB + 0.65 AC + 0.76 BC - 0.26 A^2 - 1.55 B^2 - 0.44 C^2 \dots \dots \dots \text{Eq(11)}$$

$$\text{GLY NP: Drug content} = +6.94 + 0.82 A + 0.50 B + 2.20 C - 0.11 AB + 0.61 AC + 0.97 BC - 0.32 A^2 - 1.24 B^2 - 0.26 C^2 \dots \dots \dots \text{Eq(12)}$$

Where, A is solid lipid concentration, B is of surfactant concentration and C is drug:solid lipid ratio

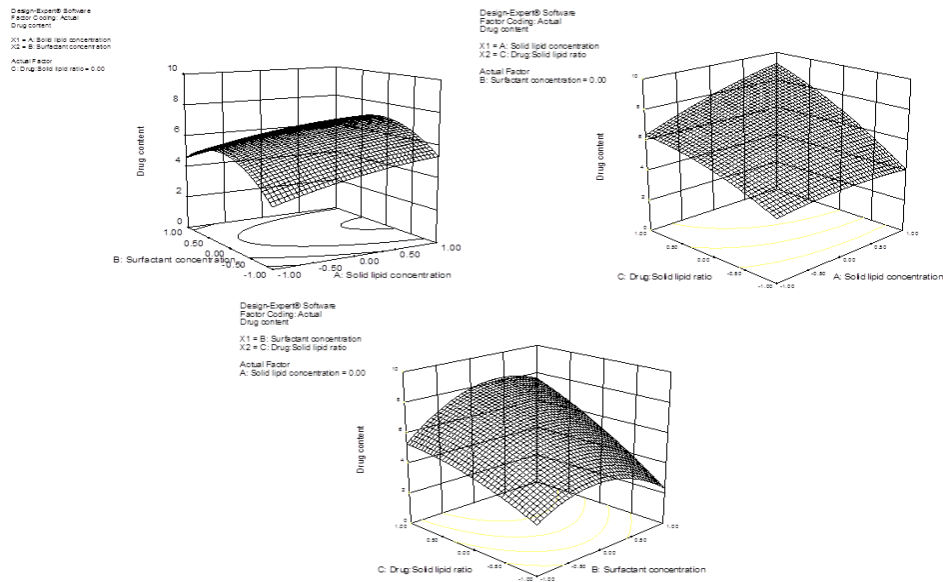


Figure 5.11: Response surface for drug content of ST NP: effect of solid lipid (A), surfactant concentration (B) and drug:lipid ratio (C)

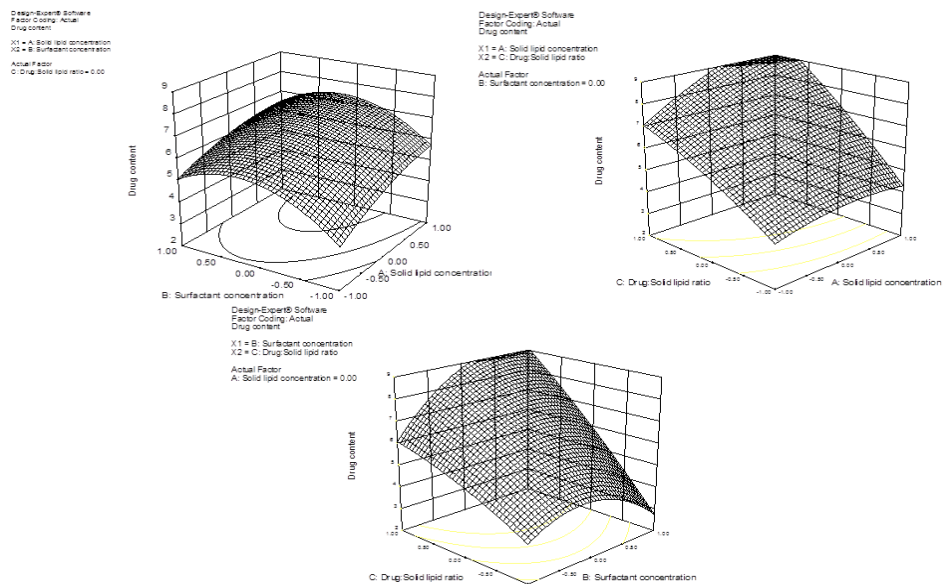


Figure 5.12: Response surface for drug content of GLY NP: effect of solid lipid (A), surfactant concentration (B) and drug:lipid ratio (C)

By studying the coefficients in the given second order polynomial equation and surface plots (Figures 5.11-5.12), it is apparent that drug content was influenced by the selected factors. However, the coefficient of C (drug: lipid ratio) for ST NP (1.87) and GLY NP (2.20) were found to be high as compared to all other factors either alone or in combination. An increase in drug amount resulted in an increased DC [25]. All other factors were affecting the DC with low coefficients, thereby affecting less as compared to factor C.

iv. Other findings

The effect of homogenization time (HT) on particle size was studied during the initial development phase. It was found that HT did not cause any significant effect on particle size. This might be due to the fact that rather than decreasing the size, homogenization mainly causes emulsification of lipid in aqueous external phase [26]. A very minimum time (<1min) was also not preferred since this might not produce uniform emulsions. A high HT can generate high heat energy, which might affect the stability of the drug and nano systems. Therefore, for optimum batches a HT of 3 min was selected, since these have produced good emulsions, which have distributed uniformly.

Unlike HT, sonication time had large influence on particle size and polydispersibility index (PI) of formulations. It was found that particle size and decreased with an increased sonication time. Therefore, sonication time has great significance in deciding the size of final NP obtained. Sonication breaks down the coarse emulsion droplets into nanoemulsion droplets. Longer the sonication time, more the application of sonication energy to dispersions, which would decrease the size of the emulsion droplets obtained [26, 27]. In nanoprecipitation method, a bath sonicator was used and sonication times of 30 min for polymeric NP and 60 min for SLN were optimized for the preparation. A high sonication time resulted in increase in the temperature of formulations and hence a good care was taken by keeping the formulations in ice bath during the sonication period in order to control the temperature. A probe sonicator was used for preparing SLN by emulsification-ultrasonication technique, with optimized sonication time of 10 min with sufficient control of temperature using ice bath.

The effect of freeze-drying and redispersibility of the developed formulations were also studied. In this study, it was found that an increase in stabilizer/surfactant

proportion resulted in increased redispersibility of the nanoparticle formulations. NP prepared with PF-68 as surfactant, demonstrated better average particle size, and better redispersibility (< 1 min) compared to formulations prepared with PVA. After some preliminary initial investigations with and without cryoprotectants, it was found that use of mannitol as cryoprotectants has a positive impact on the stability of nanoparticle formulations during freeze drying process. Mannitol as cryoprotectant decreased the effect of vacuum on NP, thereby augmenting its stability and thus no significant effect of freeze-drying was observed in final formulations [28]. It was also found that there was no significant change in particle size after freeze drying process.

Table 5.1: Composition and characterization of nanoparticles prepared with PCL by nanoprecipitation technique

Sr. No	Batch No.	^a Polymer (mg)	^b Surfactant (% w/w)	Drug (mg)	Particle size (nm)	Zeta potential (mV)	^c PDI \pm SD	^d D.C. \pm SD (%w/w)	^e E.E. \pm SD (%)
1	PCLNP/F68/01	-1	-1	5	52.19 \pm 2.12	-22.6 \pm 0.81	0.312 \pm 0.02	5.50 \pm 1.78	66.49 \pm 1.46
2	PCLNP/F68/02	-1	0	5	49.88 \pm 0.86	-26.8 \pm 0.63	0.172 \pm 0.05	5.18 \pm 1.18	62.66 \pm 0.97
3	PCLNP/F68/03	-1	1	5	47.78 \pm 1.76	-21.8 \pm 1.14	0.164 \pm 0.07	5.09 \pm 1.32	61.55 \pm 1.08
4	PCLNP/F68/04	0	-1	15	81.74 \pm 2.22	-23.8 \pm 1.31	0.568 \pm 0.14	6.72 \pm 1.52	81.28 \pm 1.25
5	PCLNP/F68/05	0	0	15	77.40 \pm 1.82	-31.41 \pm 1.92	0.134 \pm 0.06	6.83 \pm 1.72	82.64 \pm 1.41
6	PCLNP/F68/06	0	1	15	65.2 \pm 2.36	-27.5 \pm 0.43	0.111 \pm 0.08	6.53 \pm 0.55	78.96 \pm 0.45
7	PCLNP/F68/07	1	-1	30	90.24 \pm 1.63	-23.2 \pm 0.84	0.775 \pm 0.13	6.77 \pm 1.40	81.95 \pm 1.15
8	PCLNP/F68/08	1	0	30	99.15 \pm 2.82	-30.3 \pm 1.11	0.211 \pm 0.09	6.41 \pm 1.47	77.61 \pm 1.2
9	PCLNP/F68/09	1	1	30	101.2 \pm 1.38	-35.6 \pm 0.89	0.189 \pm 0.03	6.21 \pm 0.85	75.19 \pm 0.70
10	PCLNP/PVA/05	0	0	15	112.21 \pm 2.02	-16.82 \pm 1.94	0.573 \pm 0.05	5.85 \pm 2.55	74.26 \pm 2.71
11	CPCLNP/F68/05	0	0	15	83.42.40 \pm 2.38	-28.4 \pm 0.64	0.324 \pm 0.08	6.47 \pm 2.78	78.25 \pm 2.78

^aPolymer: 50 mg (-1), 150 mg (0) & 300 mg (+1) (volume selected, 25 mL); ^bSurfactant: 0.2% (-1), 0.6% (0) & 1.5% (volume selected, 50 mL); ^cPDI: Polydispersity index; ^dDC: Drug content; ^eEE: Encapsulation efficiency

Table 5.2: Composition and characterization of nanoparticles prepared with stearic acid by nanoprecipitation technique

Sr. No.	Batch No.	^a Solid lipid (mg)	^b Surfactant (% w/w)	Drug (mg)	Particle size (nm)	Zeta potential (mV)	^c PDI ± SD	^d D.C. ± SD (%w/w)	^e E.E. ± SD (%)
1	STNP/F68/01	-1	-1	5	161.21±1.82	-38.4±0.84	0.232±0.03	4.66±0.15	56.43±1.55
2	STNP/F68/02	-1	0	5	136.22±3.21	-40.7±0.92	0.478±0.06	4.47±0.20	54.08±1.99
3	STNP/F68/03	-1	1	5	124.12±2.52	-36.6±1.03	0.658±0.09	3.82±0.11	46.17±1.13
4	STNP/F68/04	0	-1	15	182.34±1.84	-35.2±1.59	0.320±0.02	6.15±0.16	74.47±1.62
5	STNP/F68/05	0	0	15	163.12±2.64	-38.3±2.51	0.207±0.03	5.90±0.04	71.38±0.42
6	STNP/F68/06	0	1	15	154.45±1.36	-46.1±0.83	0.562±0.12	5.70±0.14	68.99±1.46
7	STNP/F68/07	1	-1	30	252.19±2.12	-32.8±0.74	0.423±0.09	6.87±0.11	83.09±1.13
8	STNP/F68/08	1	0	30	205.46±3.05	-55.7±1.27	0.367±0.08	6.61±0.18	79.97±1.85
9	STNP/F68/09	1	1	30	180.14±1.26	-38.3±2.43	0.378±0.05	6.80±0.12	82.27±1.23
10	STNP/PVA/09	1	1	30	245.41±2.63	-37.3±2.01	0.561±0.06	6.55±0.17	75.13±1.6
11	CSTNP/F68/09	1	1	30	188.23±3.65	-52.5±1.68	0.681±0.07	6.61±0.05	75.13±1.6

^aSolid lipid: 50 mg (-1), 150 mg (0) & 300 mg (+1) (volume selected, 25 mL); ^bSurfactant: 0.2% (-1), 0.6% (0) & 1.5% (volume selected, 50 mL); ^cPDI: Polydispersity index; ^dDC: Drug content; ^eEE: Encapsulation efficiency

Table 5.3: Composition and characterization of nanoparticles prepared with glyceryl monostearate by nanoprecipitation technique

Sr. No.	Batch No.	^a Solid lipid (mg)	^b Surfactant (% w/w)	Drug (mg)	Particle size (nm)	Zeta potential (mV)	^c PDI ± SD	^d D.C. ± SD (%w/w)	^e E.E. ± SD (%)
1	GLYNP/F68/01	-1	-1	5	163.12±2.35	-33.2±0.92	0.187±0.02	6.18±0.16	76.23±0.39
2	GLYNP/F68/02	-1	0	5	158.78±2.68	-35.6±1.13	0.307±0.05	6.00±0.15	74.61±1.78
3	GLYNP/F68/03	-1	1	5	154.69±1.96	-38.1±0.53	0.192±0.03	5.98±0.33	73.23±2.36
4	GLYNP/F68/04	0	-1	15	234.13±3.12	-36.4±0.74	0.379±0.07	7.21±0.31	88.76±1.73
5	GLYNP/F68/05	0	0	15	217.41±2.61	-35.8±1.45	0.266±0.05	7.04±0.26	86.05±1.58
6	GLYNP/F68/06	0	1	15	161.18±1.34	-41.9±2.12	0.158±0.03	6.98±0.16	85.83±0.36
7	GLYNP/F68/07	1	-1	30	356.14±3.54	-28.4±0.68	0.423±0.06	7.43±0.24	91.22±0.62
8	GLYNP/F68/08	1	0	30	289.31±3.18	-32.2±1.05	0.105±0.08	7.19±0.17	88.75±1.06
9	GLYNP/F68/09	1	1	30	272.68±2.98	-36.1±0.89	0.143±0.07	6.82±0.22	84.22±0.76
10	GLYNP/PVA/06	0	1	15	243.72±1.84	-26.54±0.74	0.362±0.08	7.64±0.15	78.82±1.61
11	CGLYNP/F68/06	0	1	15	194.18±1.34	-38.5±1.16	0.518±0.03	6.76±0.23	81.83±2.81

^aSolid lipid: 50 mg (-1), 150 mg (0) & 300 mg (+1) (volume selected, 25 mL); ^bSurfactant: 0.2% (-1), 0.6% (0) & 1.5% (volume selected, 50 mL); ^cPDI: Polydispersity index; ^dDC: Drug content; ^eEE: Encapsulation efficiency

Table 5.4: Composition and characterization of nanoparticles prepared with stearic acid by emulsification-ultrasonication technique

Sr. No.	Batch No.	^a Solid lipid (Stearic acid)	^b Surfactant (% w/w)	^c Drug : lipid ratio	Particle size (nm)	Zeta potential (mV)	^d PDI ± SD	^e D.C. ± SD (%w/w)	^f E.E. ± SD (%)
1	ST EU01	-1	-1	0	139±1.76	-36.4±2.55	0.462±0.22	3.97±0.21	48.04±2.65
2	STEU02	1	1	0	217±2.82	-44.0±1.86	0.426±0.19	5.44±0.30	65.88±3.64
3	STEU03	-1	1	0	101±1.59	-30.7±1.65	0.390±0.09	4.38±0.24	53.02±2.92
4	STEU04	-1	0	1	106±1.82	-53.3±3.28	0.573±0.07	7.07±0.39	46.64±2.57
5	STEU05	0	0	0	134±1.33	-51.8±2.65	0.431±0.08	6.65±0.41	80.47±4.97
6	STEU06	1	-1	0	304±3.42	-36.6±2.73	0.558±0.13	5.63±0.31	68.17±3.76
7	STEU07	0	0	0	136±1.76	-36.2±1.93	0.522±0.07	6.55±0.35	80.47±4.28
8	STEU08	0	0	0	134±1.98	-36.3±1.81	0.4385±0.11	6.66±0.41	80.47±5.04
9	STEU09	0	-1	-1	172±1.66	-38.5±1.96	0.343±0.09	3.56±0.19	82.12±4.53
10	STEU10	0	0	0	137±1.48	-39.6±1.63	0.362±0.07	6.79±0.16	80.47±1.98
11	STEU11	1	0	1	297±3.03	-32.5±2.55	0.412±0.04	10.01±0.55	66.08±3.65
12	STEU12	0	0	0	134±1.48	-36.2±2.56	0.369±0.09	6.67±0.29	80.47±3.60
13	STEU13	-1	0	-1	108±1.25	-42.4±2.83	0.418±0.08	3.21±0.17	74.25±4.10
14	STEU14	0	-1	1	167±1.79	-31.2±2.74	0.568±0.06	4.37±0.24	52.92±2.92
15	STEU15	1	0	-1	261±2.88	-53.9±2.27	0.451±0.04	3.56±0.19	82.12±4.53
16	STEU16	0	1	-1	109±1.34	-32.8±1.51	0.323±0.05	3.46±0.19	79.83±4.41
17	STEU17	0	1	1	118±1.84	-43.3±2.83	0.388±0.08	7.31±0.40	48.24±2.66
18	CSTEU10	0	0	0	143±2.11	-34.1±1.16	0.461±0.07	6.14±0.22	79.69±2.02

^aSolid lipid: 500 mg (-1), 1000 mg (0) & 2500 mg (+1); ^bSurfactant: 0.5 (-1), 1 (0) & 2% (volume selected, 50 mL); ^cDrug: lipid ratio: 1:20 (-1), 1:10 (0) & 1:5 (+1);

^dPDI: Polydispersity index; ^eDC: Drug content; ^fEE: Encapsulation efficiency

Table 5.5: Composition and characterization of nanoparticles prepared with glyceryl monostearate by emulsification-ultrasonication technique

Sr. No.	Batch No.	^a Solid lipid (GMS)	^b Surfactant (% w/w)	^c Drug : lipid ratio	Particle size (nm)	Zeta potential (mV)	^d PDI ± SD	^e D.C. ± SD (% w/w)	^f E.E. ± SD (%)
1	GLYEU01	-1	-1	0	184±2.04	-33.2±2.32	0.479±0.04	4.45±0.22	53.84±2.72
2	GLYEU02	1	1	0	272±3.14	-34.1±1.51	0.366±0.05	6.08±0.30	73.61±3.72
3	GLYEU03	-1	1	0	132±1.49	-33.1±1.42	0.458±0.07	4.70±0.23	56.92±2.88
4	GLYEU04	-1	0	1	134±1.52	-32.3±1.28	0.482±0.08	7.65±0.38	50.46±2.55
5	GLYEU05	0	0	0	173±2.08	-38.8±2.62	0.305±0.06	7.04±0.21	83.94±2.44
6	GLYEU06	1	-1	0	346±3.98	-31.4±0.38	0.446±0.07	6.27±0.31	75.89±3.84
7	GLYEU07	0	0	0	172±2.14	-33.2±1.18	0.368±0.08	6.94±0.34	83.85±4.22
8	GLYEU08	0	0	0	170±1.36	-34.1±0.92	0.568±0.05	6.83±0.51	83.94±6.27
9	GLYEU09	0	-1	-1	214±2.13	-35.1±0.73	0.438±0.08	3.78±0.19	87.21±4.41
10	GLYEU10	0	0	0	171±1.83	-34.1±1.74	0.588±0.15	6.98±0.28	83.94±3.48
11	GLYEU11	1	0	1	312±3.56	-32.1±1.75	0.422±0.06	10.55±0.53	69.63±3.52
12	GLYEU12	0	0	0	170±1.23	-35.5±1.36	0.428±0.14	6.90±0.41	83.81±5.06
13	GLYEU13	-1	0	-1	146±1.18	-28.4±1.68	0.441±0.09	3.37±0.17	77.88±3.94
14	GLYEU14	0	-1	1	201±2.32	-31.6±1.53	0.462±0.07	5.13±0.25	62.08±3.14
15	GLYEU15	1	0	-1	304±3.67	-33.2±1.54	0.425±0.06	3.85±0.20	88.90±4.50
16	GLYEU16	0	1	-1	152±1.88	-34.2±1.18	0.399±0.13	3.81±0.19	87.91±4.45
17	GLYEU17	0	1	1	156±1.79	-30.3±1.68	0.418±0.09	9.06±0.45	59.80±3.02
18	CGLYEU05	0	0	0	182±2.28	-34.2±1.19	0.581±0.18	6.53±0.41	81.41±6.41

^aSolid lipid: 500 mg (-1), 1000 mg (0) & 2500 mg (+1); ^bSurfactant: 0.5 (-1), 1 (0) & 2% (volume selected, 50 mL); ^cDrug: lipid ratio: 1:20 (-1), 1:10 (0) & 1:5 (+1);

^dPDI: Polydispersity index; ^eDC: Drug content; ^fEE: Encapsulation efficiency

5.3.2 Particle size distribution, zeta potential and morphology

Particle size distribution by intensity profile, SEM images and zeta potential graph of selected formulations are represented in Figures 5.13 and 5.14. SEM images have shown smooth surface morphology of the developed nanoparticulate systems. Both polymeric and solid lipid NP were spherical in shape. Images further revealed that the particles are uniformly distributed. Some batches also showed slight agglomeration of particles. Zeta potential graphs, as depicted in Figures 5.15 to 5.20, have shown high value (near to -30 mV), indicating the physical stability of the formulations [29]. The tween 80 coated NP demonstrated a slight decrease in zeta potential values, which might be due to the masking of surface charge by tween 80, a non-ionic surfactant, adsorbed on to the surface of NP [30].

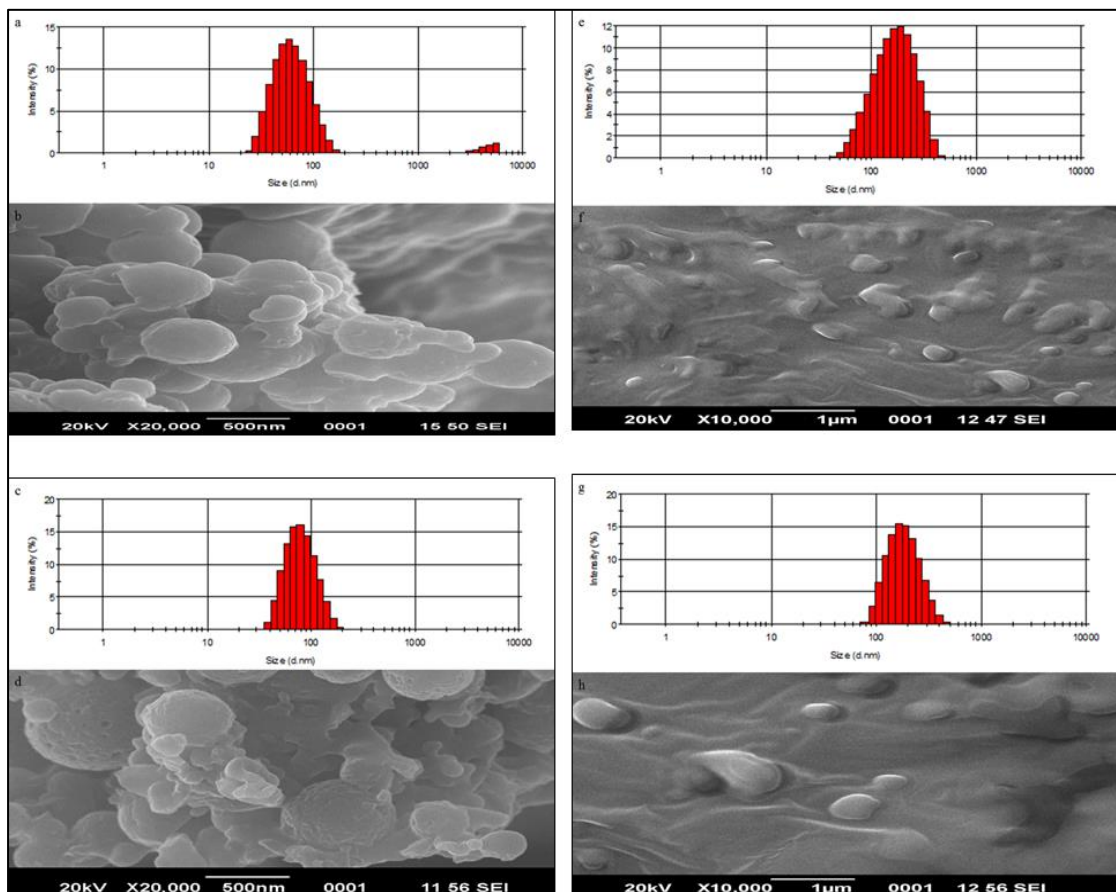


Figure 5.13: Representative size distribution by intensity profile and SEM image of PCL NP (a, b), C PCL NP (c, d), GLY NP (e, f) & C GLY NP (g, h)

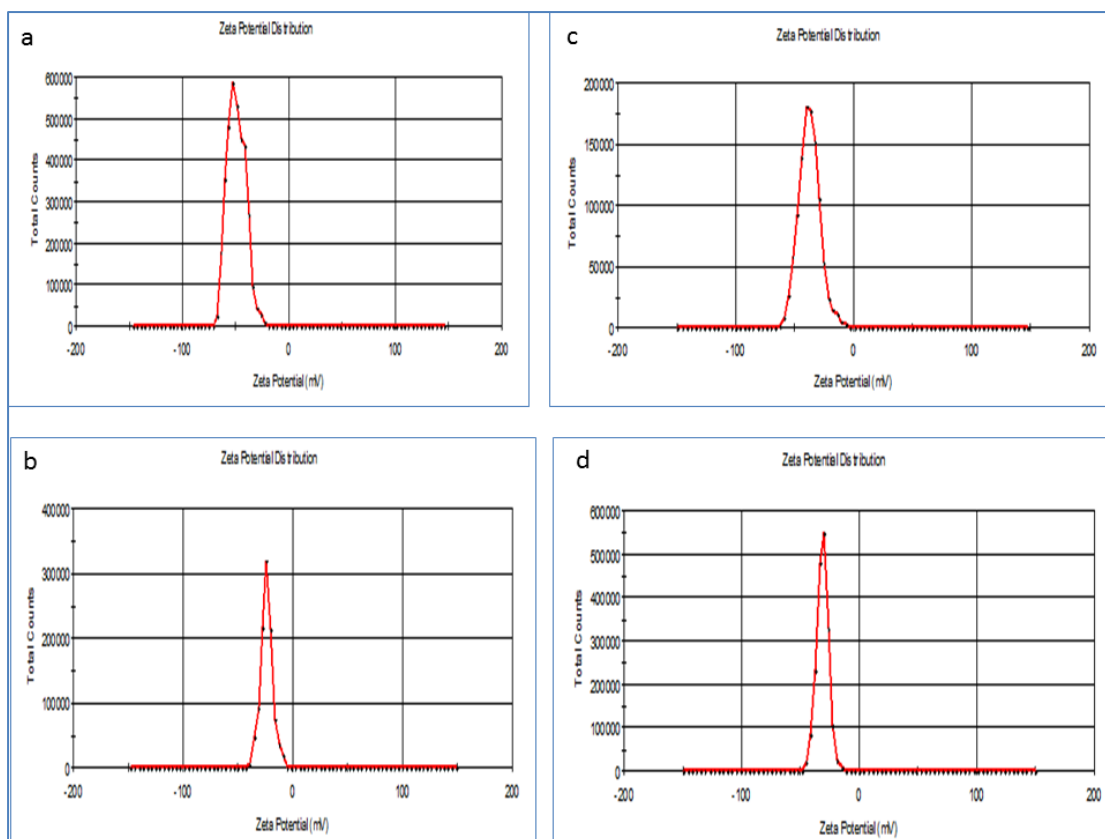


Figure 5.14: Representative zeta potential distribution profile of PCL NP (a), C PCL NP (b), GLY NP (c) & C GLY NP (d)

5.3.3 In-vitro drug release studies

a. Effect of various polymer/solid lipid on in-vitro drug release

Comparative in-vitro release profiles of PCL, ST and GLY NP with PF 68 and PVA as stabilizers have been depicted in Figures 5.15 and 5.16 respectively. During the study, it has been found that complete diffusion of OLN pure drug from dialysis bag to the medium occurred within 1 h. There was an initial burst release occurred in the first hour from all the formulations irrespective of the material and stabilizer used. This rapid initial release of the drug from the formulations might be mainly due to the presence of drug that was adsorbed on the surface of the formulations [31]. The release was extended for 24 h for ST NP and release extended for 48 h and 48-60 h for GLY and PCL NP respectively. It has been suggested that the hydrophobic character of polymer/solid lipid is responsible for the retarded release for a hydrophobic drug such as OLN. Polycaprolactone/glyceryl monostearate is more

hydrophobic as compared to stearic acid and therefore retarding the release of drug for a longer duration of time.

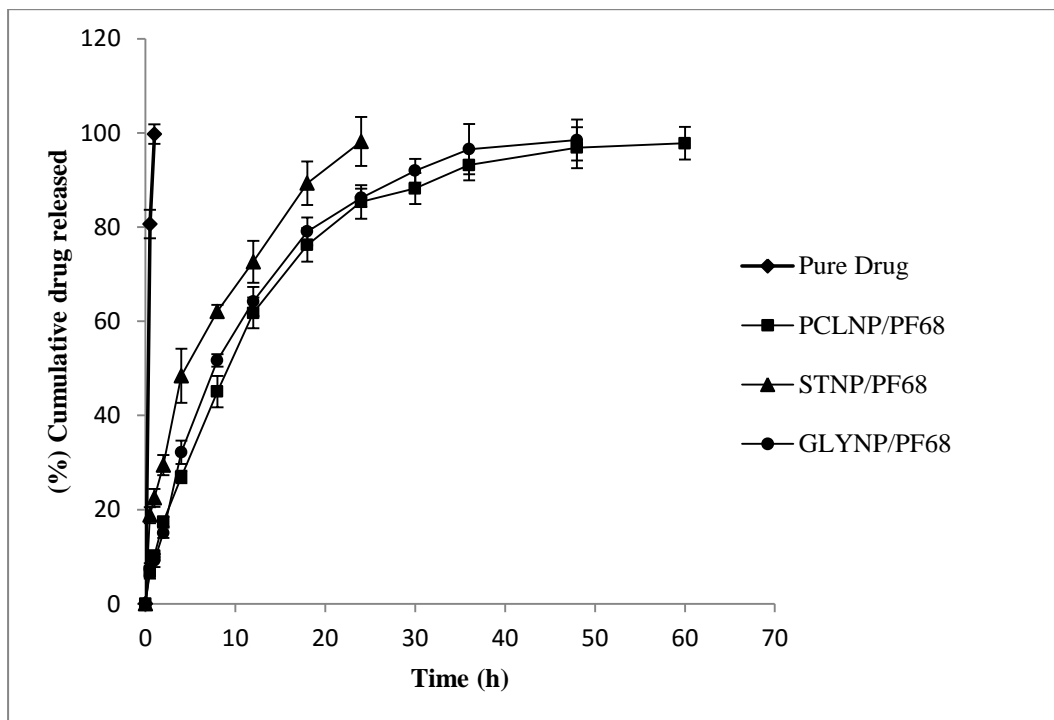


Figure 5.15: In-vitro release profiles of nanoparticulate systems prepared with various polymer/solid lipids with PF68 as stabilizer prepared using nanoprecipitation method

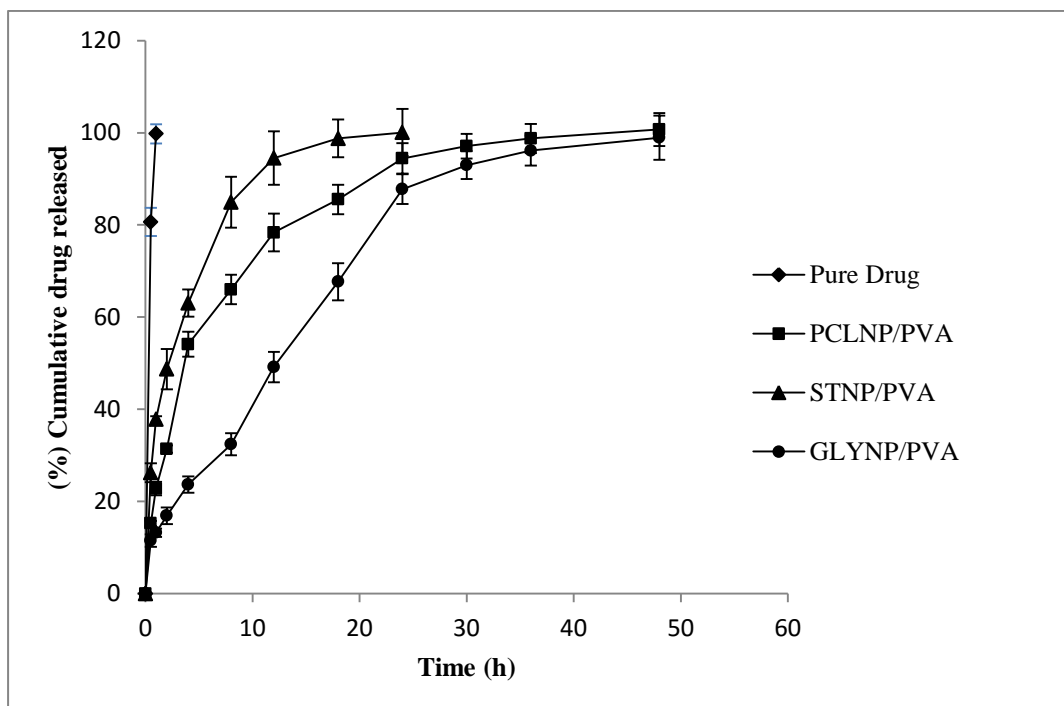


Figure 5.16: In-vitro release profiles of nanoparticulate systems prepared with various polymer/solid lipids with PVA as stabilizer prepared using nanoprecipitation method

b. Effect of polymer/solid lipid amount on in-vitro drug release

The in-vitro drug release profile of formulations with varying polymer/solid lipid amount showed a decreased rate of drug release with increase in total polymer/ solid lipid amount (Figure 5.17 – 5.21). The polymer/solid lipid amount played a major role in determining the burst release, as well as duration of drug release from the formulations. The duration of drug release was highly influenced by the amount of polymer/solid lipid in the formulations. As the polymer/solid lipid, quantity was increased, the drug release was found to be more sustained for a prolonged period. At higher proportions of polymer/solid lipid, the formation of compact matrix holds the drug more firmly on the matrix which might have resulted in the decreased burst release and slow release, thereby exhibiting a sustained release [32]. NP prepared from various polymer/solid lipid followed similar patterns, as can be seen in Figures 5.22-5.27, while studying the effect of polymer/solid lipid amount on in-vitro drug release.

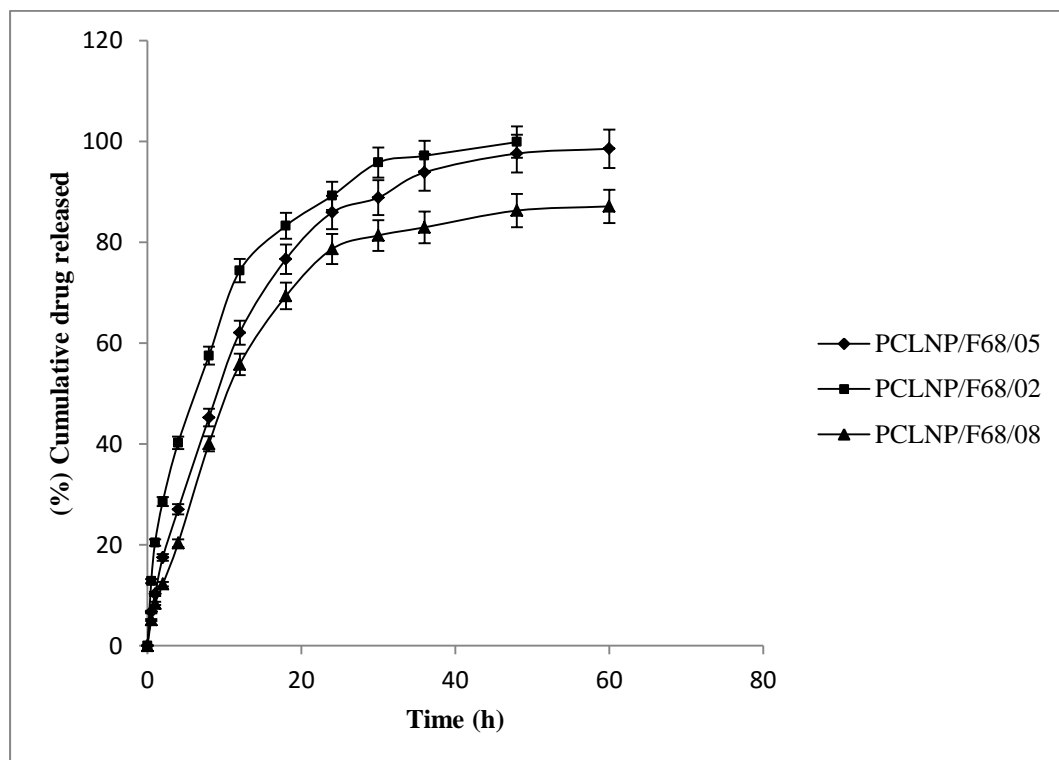


Figure 5.17: Effect of polymer amount on in-vitro release profiles of OLN loaded PCL NP prepared by nanoprecipitation method

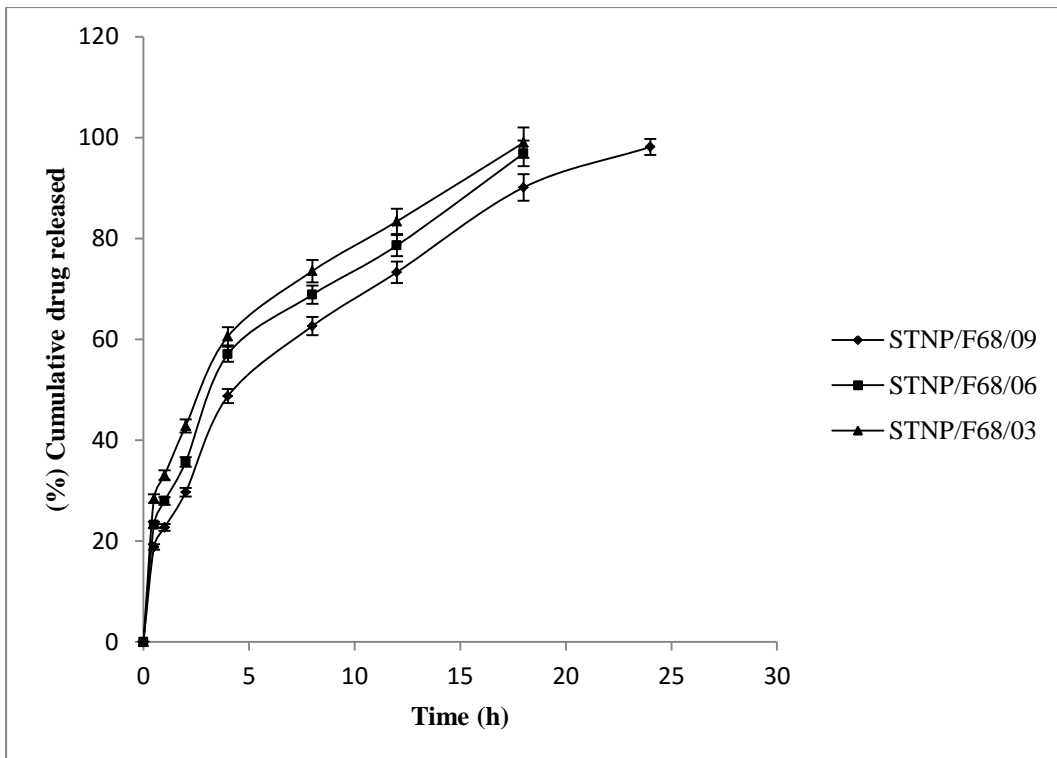


Figure 5.18: Effect of lipid amount on in-vitro release profiles of OLN loaded ST NP prepared by nanoprecipitation method

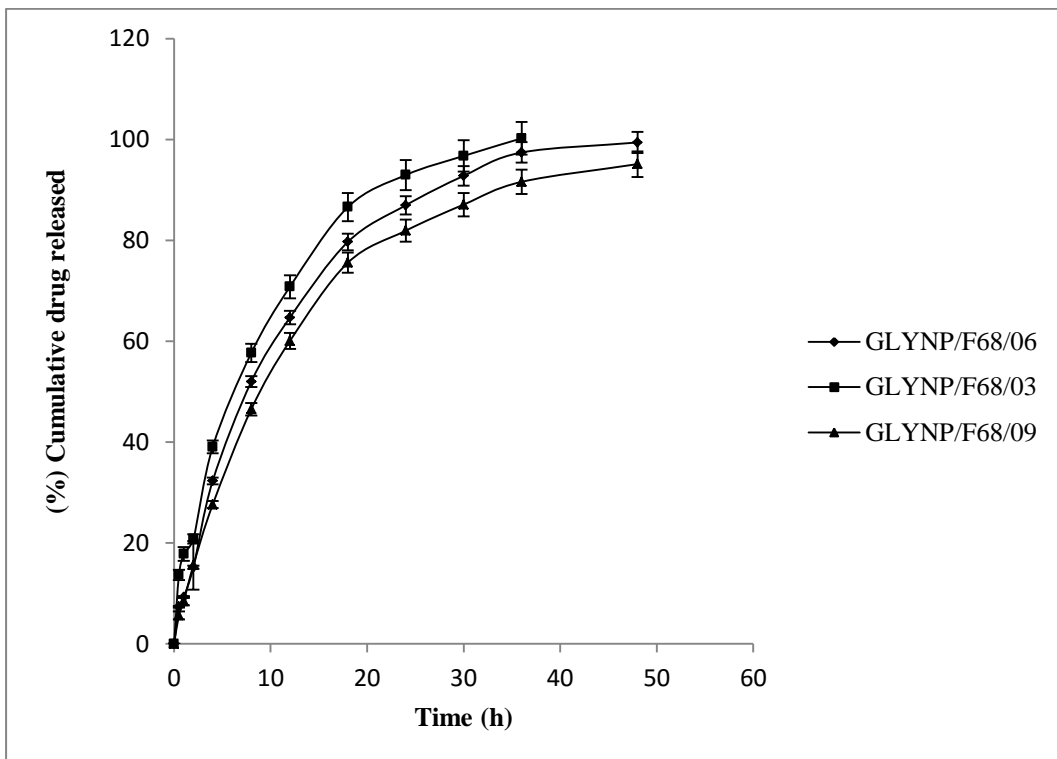


Figure 5.19: Effect of lipid amount on in-vitro release profiles of OLN loaded GLY NP prepared by nanoprecipitation method

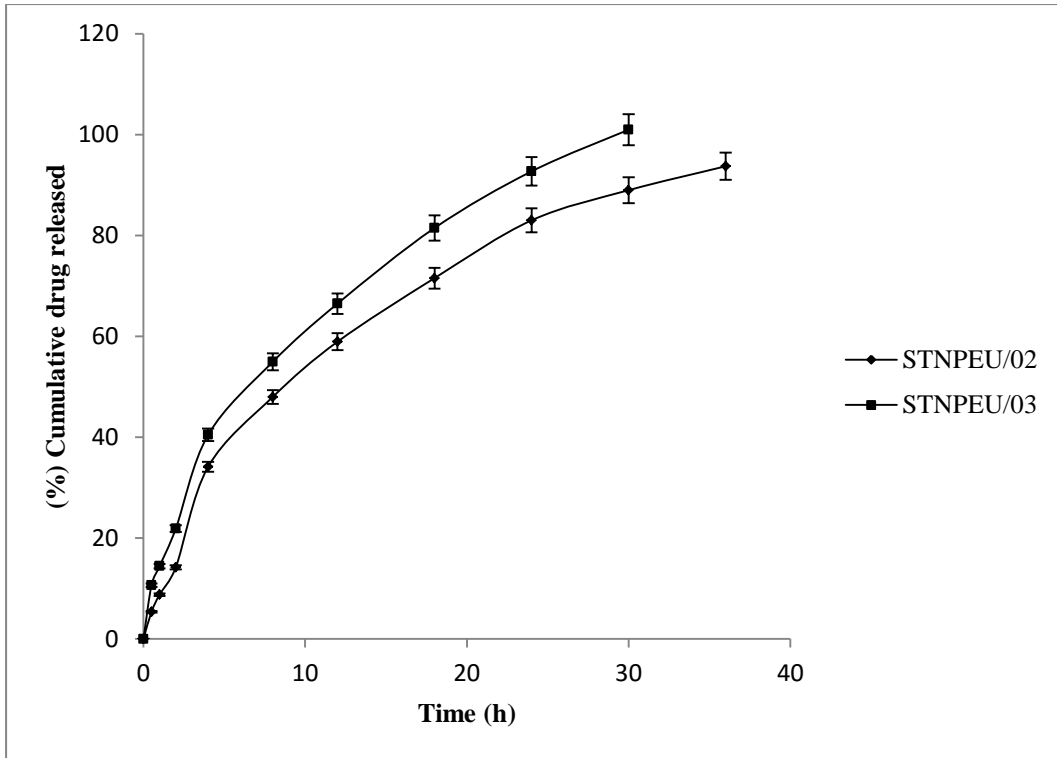


Figure 5.20: Effect of lipid amount on in-vitro release profiles of OLN loaded ST NP prepared by emulsification sonication technique.

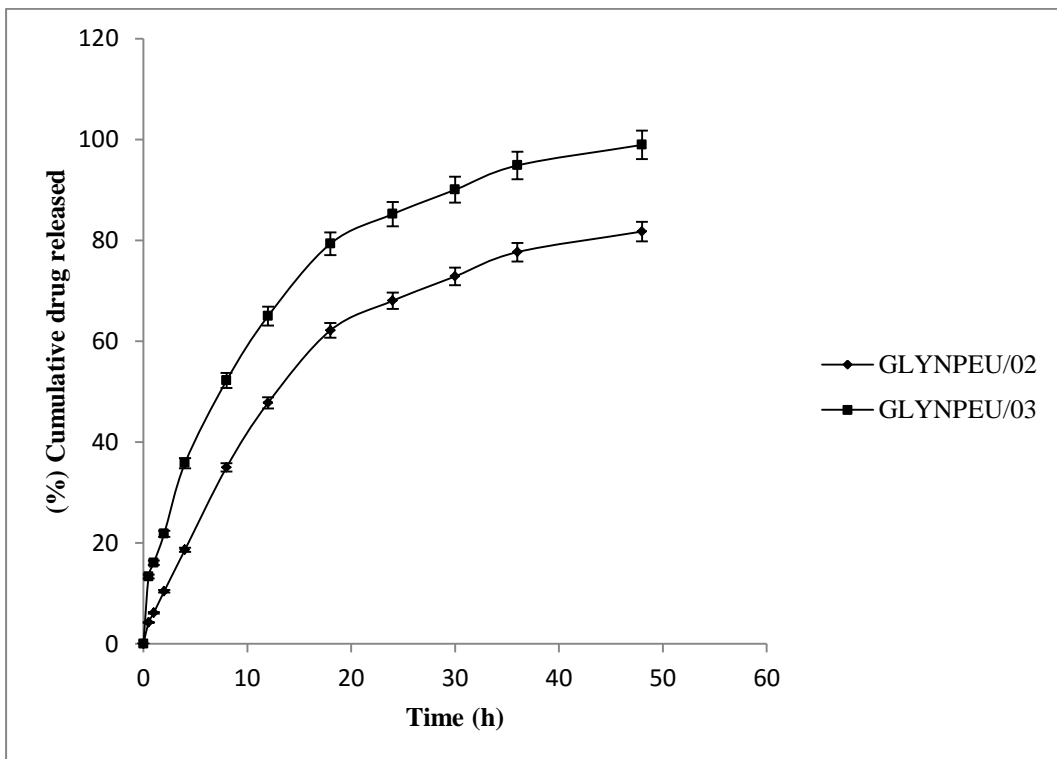


Figure 5.21: Effect of lipid amount on in-vitro release profiles of OLN loaded GLY NP prepared by emulsification sonication technique.

C. Effect of stabilizer/surfactant concentration on in-vitro drug release

It is evident from the Figures 5.22 to 5.29 that with an increase in surfactant concentration, the rate of drug release increased. This might be because higher concentration of surfactant present solubilizes the drug more, thereby augmenting the release of drug from the formulations. Besides, as discussed in the formulation development section, a high concentration of surfactant resulted in a decreased particle size and releases drug easily because of the increased surface area available [33, 34].

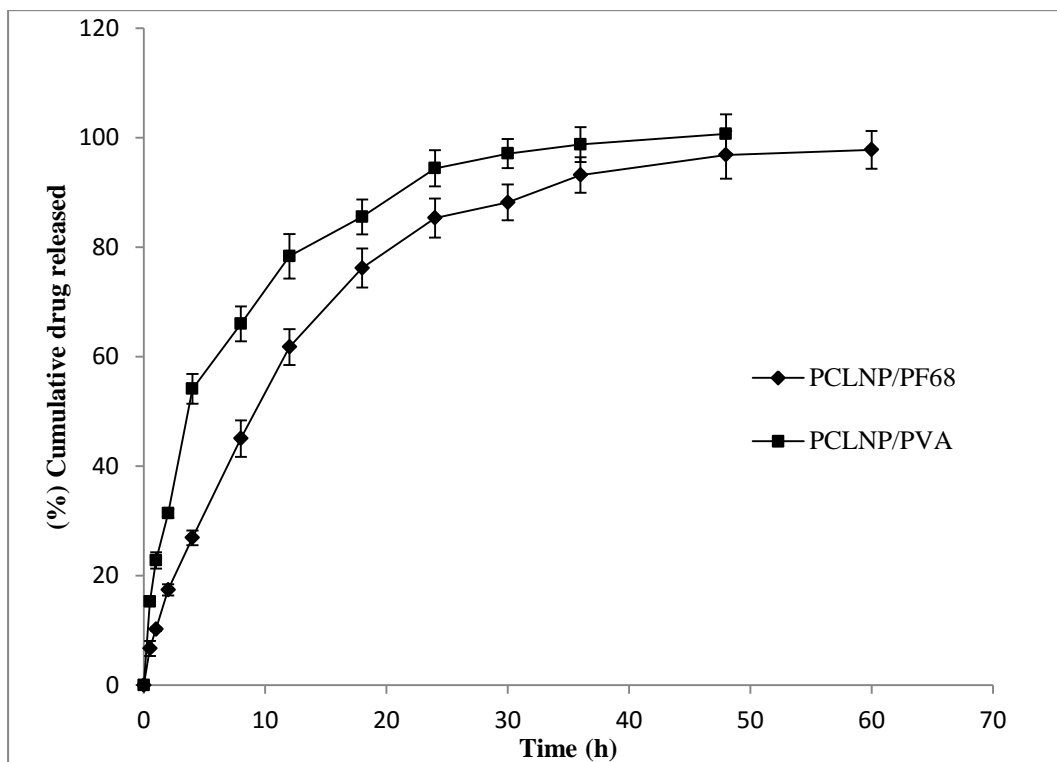


Figure 5.22: Effect of various stabilisers on in-vitro release profiles of nanoparticulate systems prepared with PCL prepared by nanoprecipitation method

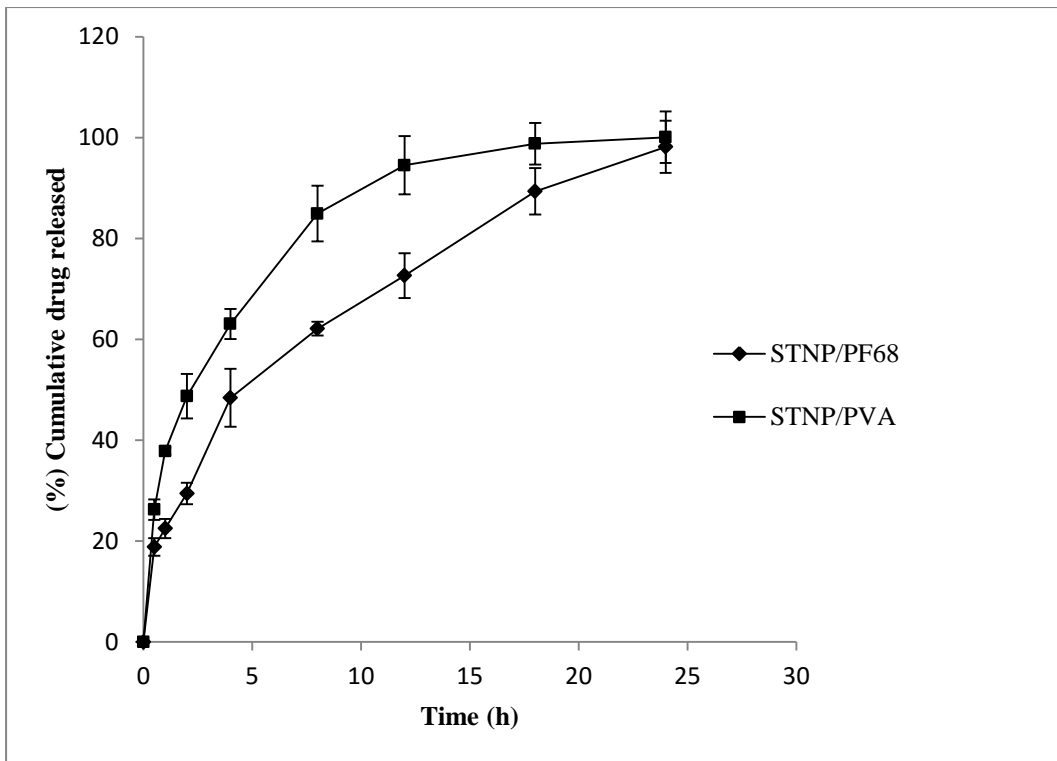


Figure 5.23: Effect of various stabilisers on in-vitro release profiles of nanoparticulate systems prepared with Stearic acid using nanoprecipitation method

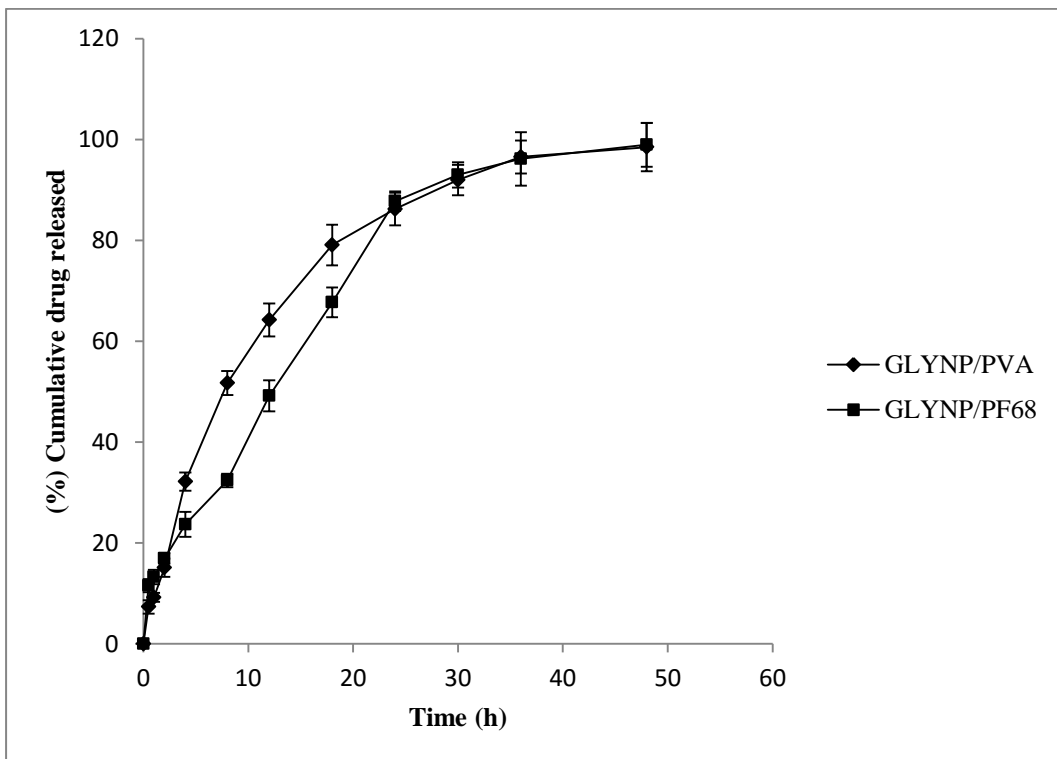


Figure 5.24: Effect of various stabilisers on in-vitro release profiles of nanoparticulate systems prepared with Glyceryl monostearate using nanoprecipitation method

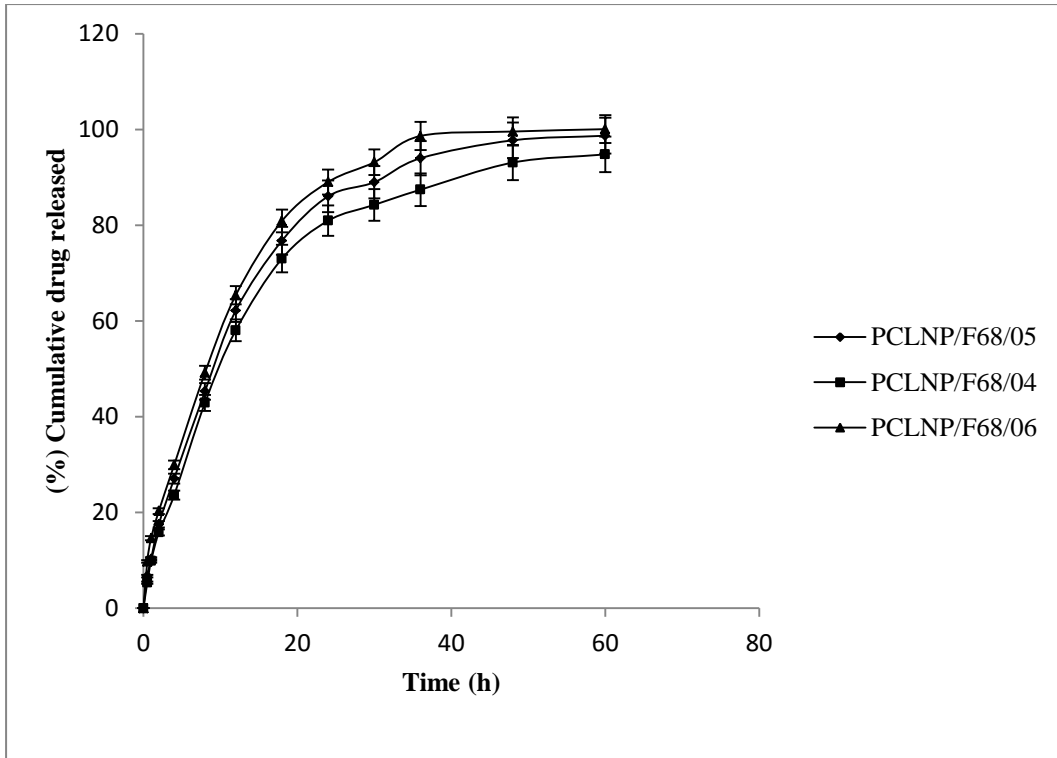


Figure 5.25: Effect of surfactant concentration on in-vitro release profiles of OLN loaded PCL NP prepared by nanoprecipitation method

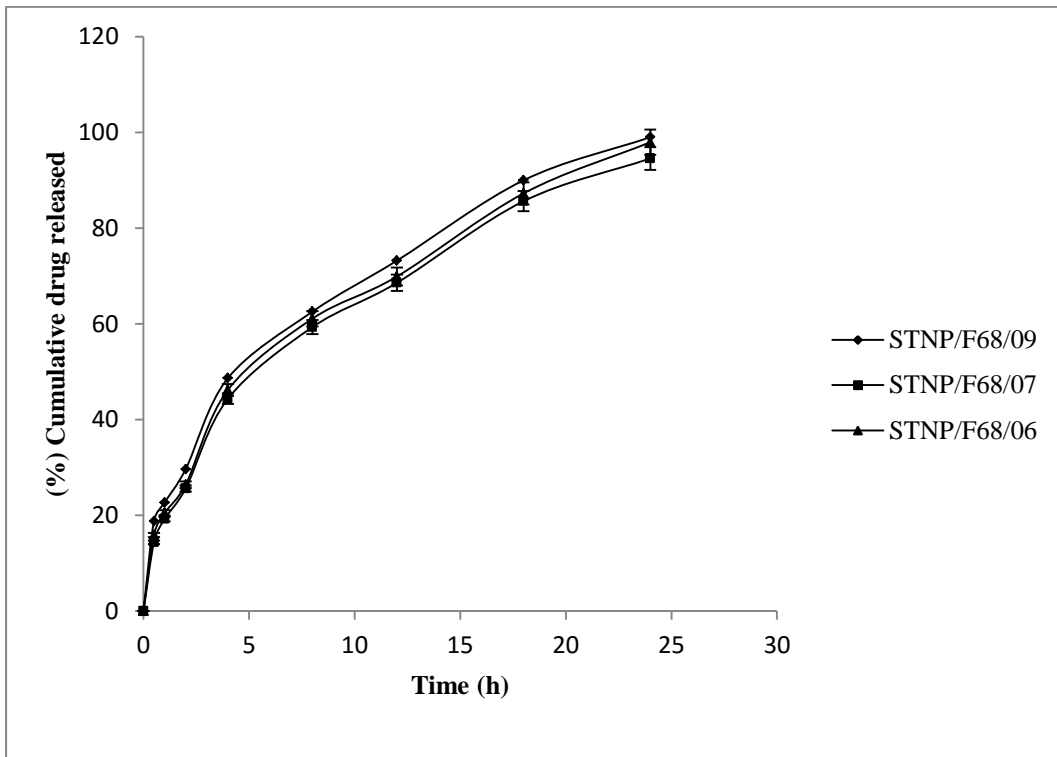


Figure 5.26: Effect of surfactant concentration on in-vitro release profiles of OLN loaded ST NP prepared by nanoprecipitation method

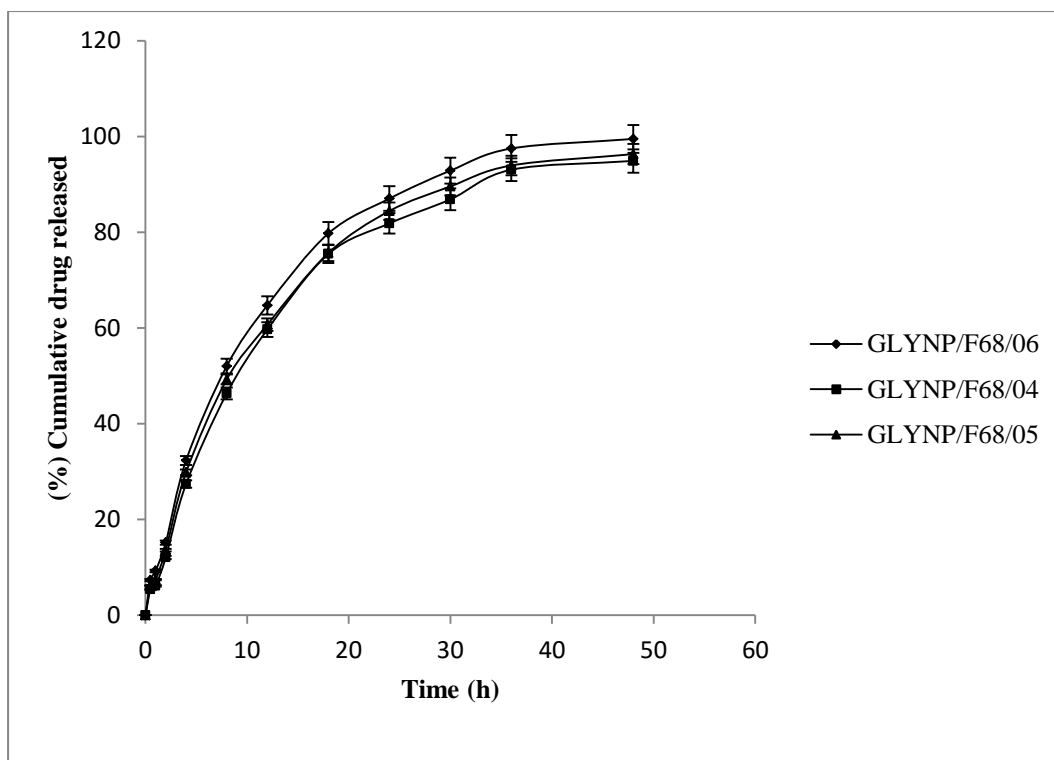


Figure 5.27: Effect of surfactant concentration on in-vitro release profiles of OLN loaded GLY NP prepared by nanoprecipitation method

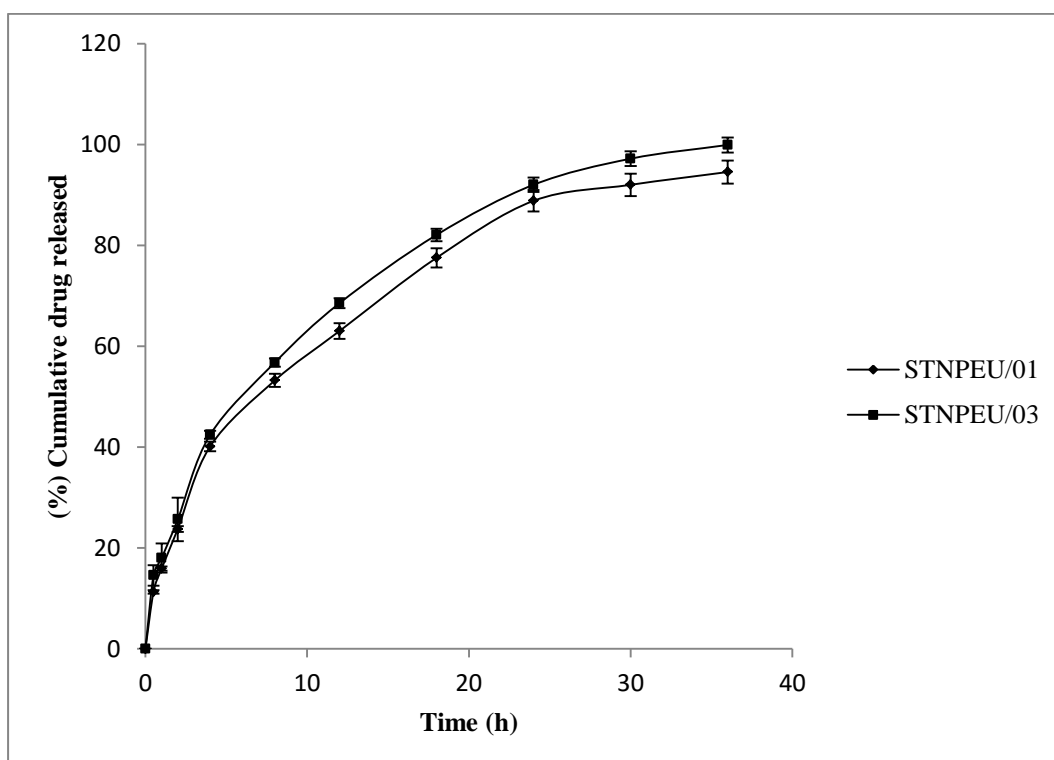


Figure 5.28: Effect of surfactant concentration on in-vitro release profiles of OLN loaded ST NP prepared by emulsification sonication technique.

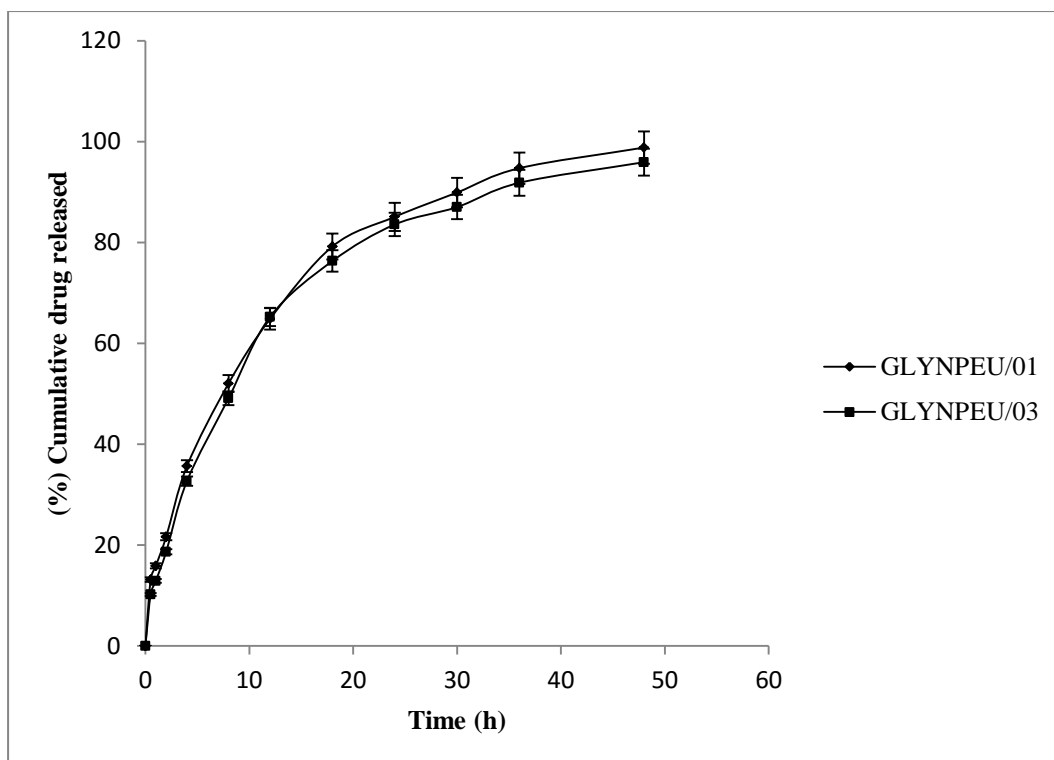


Figure 5.29: Effect of surfactant concentration on in-vitro release profiles of OLN loaded ST NP prepared by emulsification sonication technique.

d. Effect of Polysorbate coating on in-vitro release

As can be seen in Figures 5.30 to 5.34, both coated and uncoated systems demonstrated an extended release in a controlled manner. However, the burst release for coated systems were comparatively high which might mainly be due to the solubilization effects of surfactant (Tween 80) used for coating. This has not affected the overall sustained release and prolonged duration of release [35, 36].

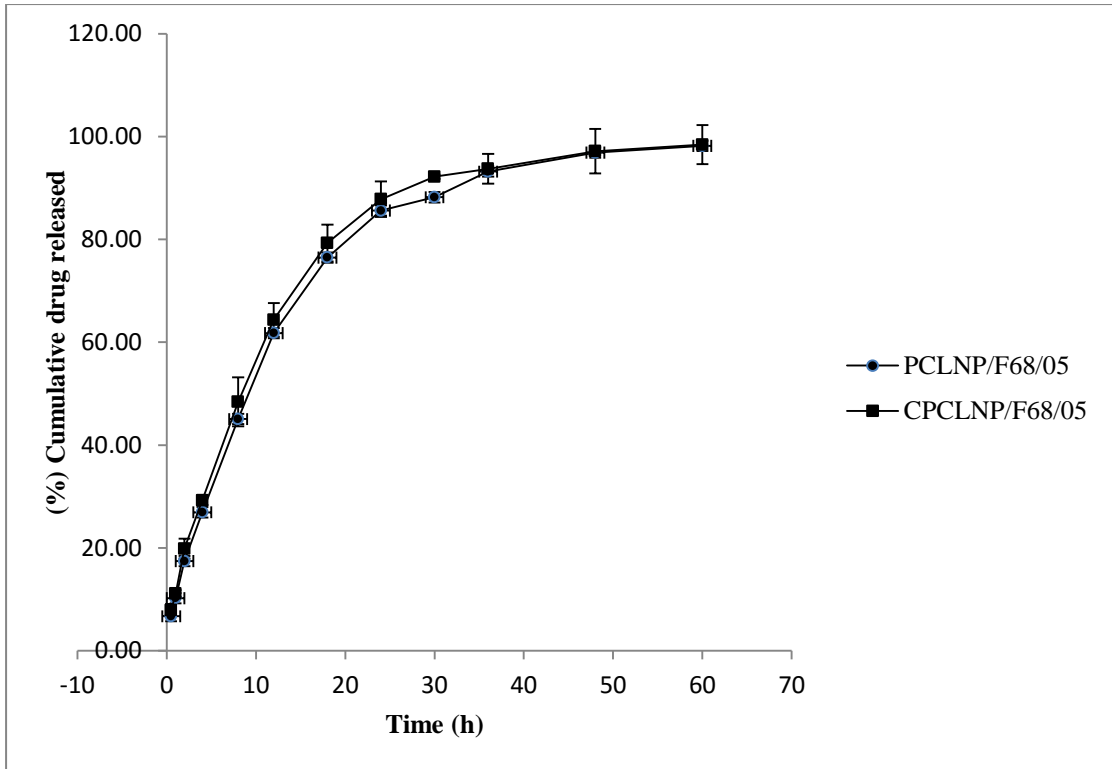


Figure 5.30: Comparative in-vitro release profiles of OLN from coated and un coated PCL NP prepared by nanoprecipitation method

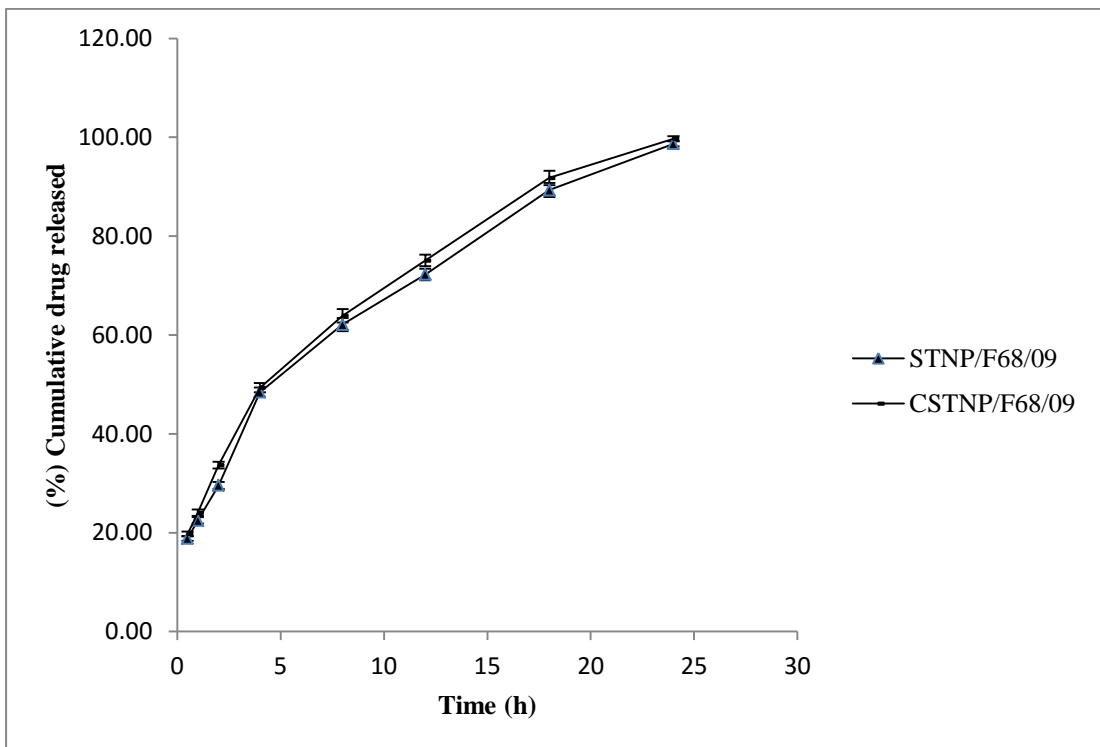


Figure 5.31: Comparative in-vitro release profiles of OLN from coated and un coated ST NP prepared by nanoprecipitation method

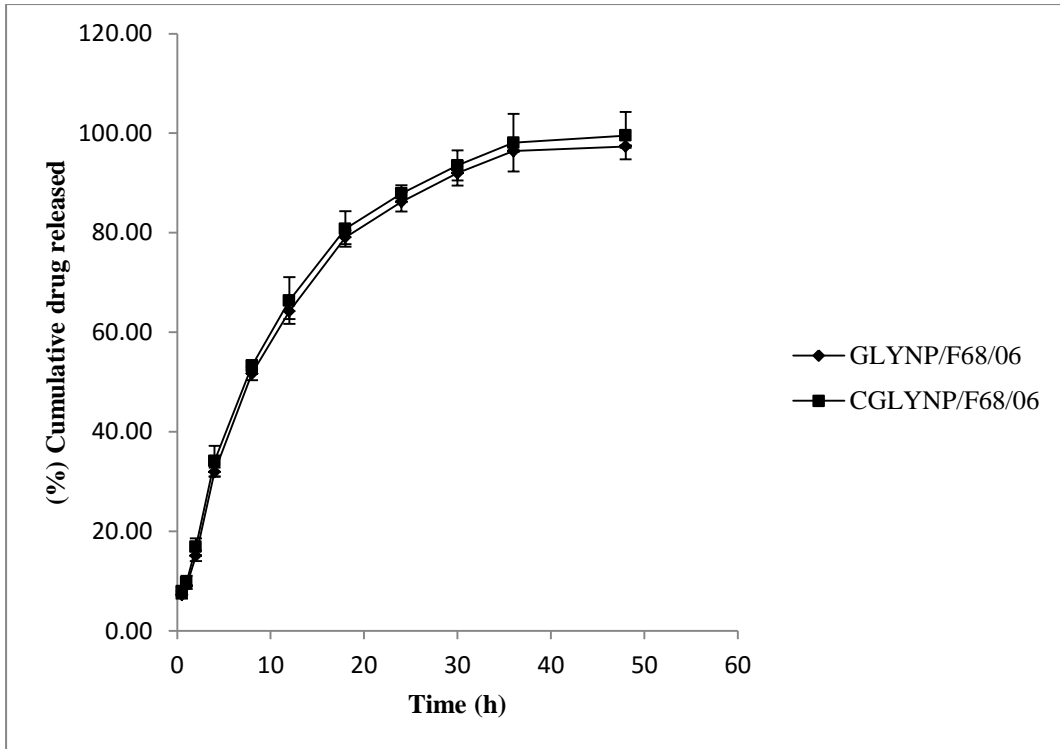


Figure 5.32: Comparative in-vitro release profiles of OLN from coated and un coated GLY NP prepared by nanoprecipitation method

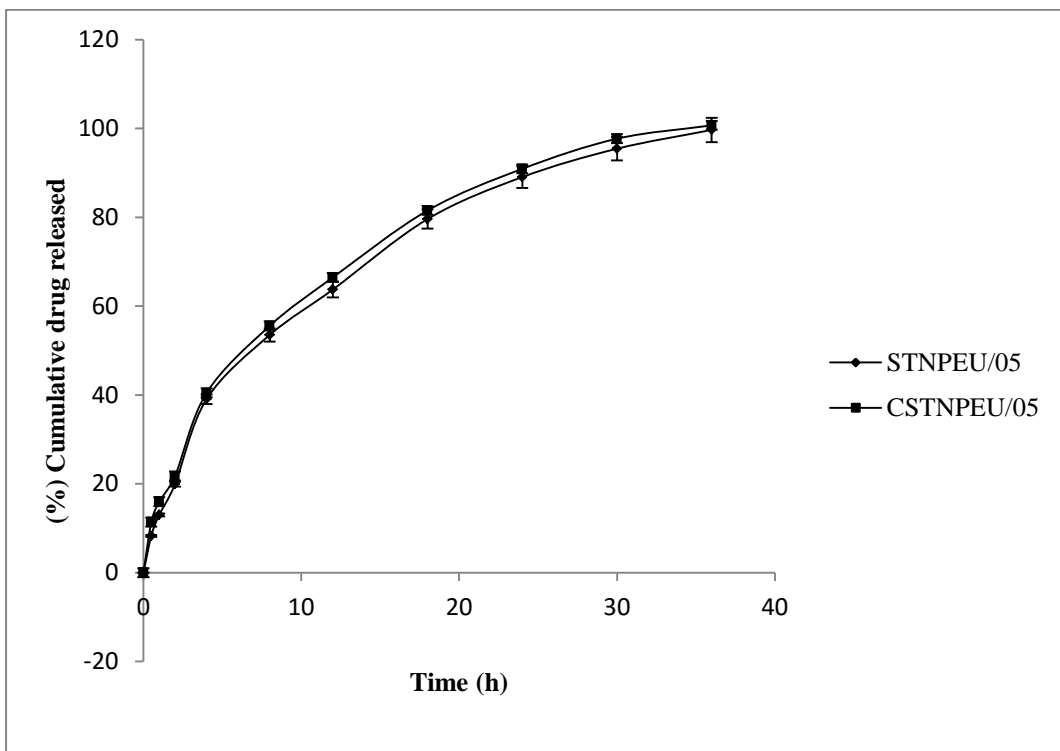


Figure 5.33: Comparative in-vitro release profiles of OLN from coated and un coated ST NP prepared by emulsification sonication technique

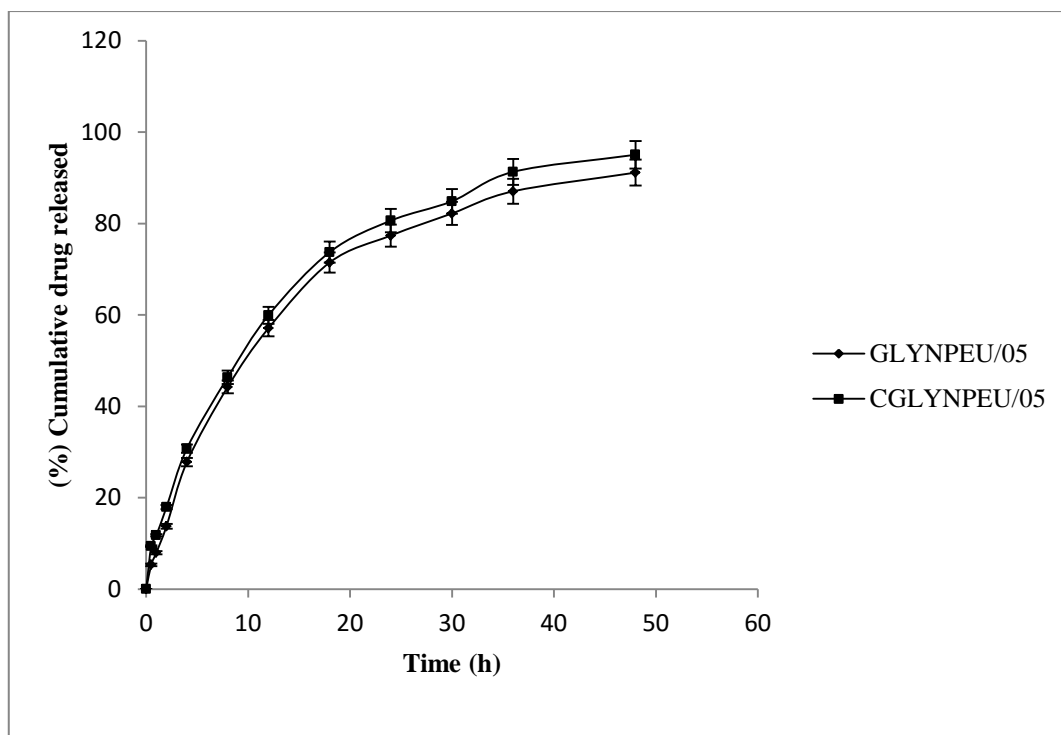


Figure 5.34: Comparative in-vitro release profiles of OLN from coated and un coated GLY NP prepared by emulsification sonication technique.

e. Effect of D: L ratio on in-vitro release profile

As seen in Figures 5.35 & 5.36, in-vitro release profiles of OLN from formulations were highly influenced by D: L ratio. Higher concentration of drug resulted in a faster rate of release and less duration of release. In the case of higher drug ratio, less lipid content would be available to hold the drug, thereby releasing the drug in a faster fashion.

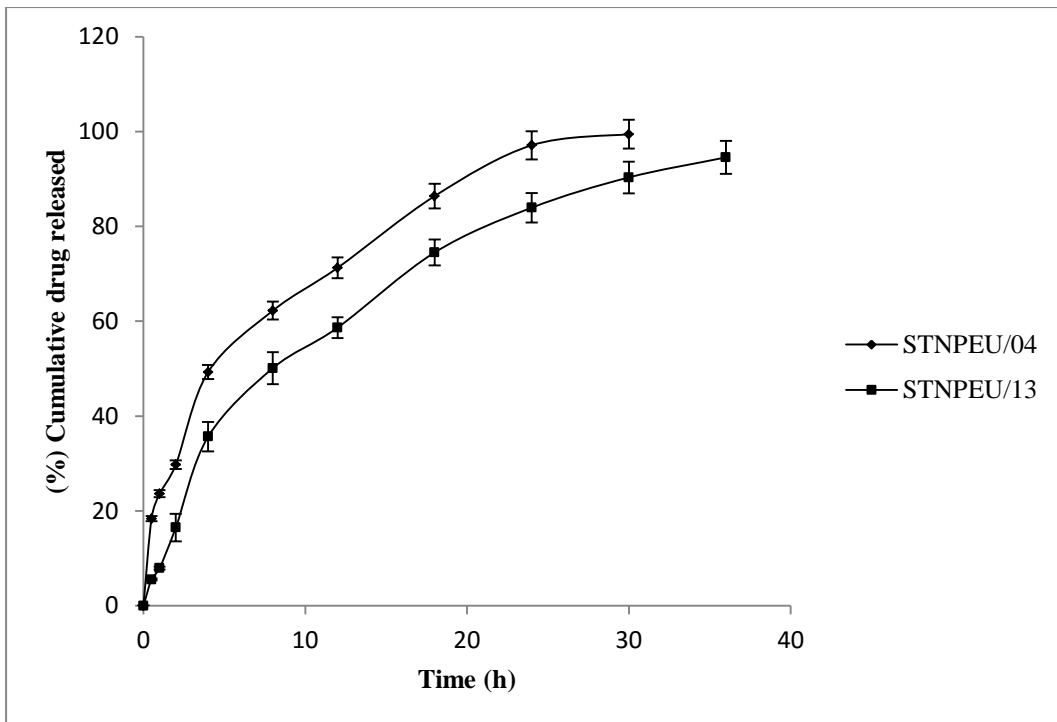


Figure 5.35: Effect of D: L ratio on in-vitro release profile of OLN loaded ST NP prepared by emulsification sonication method

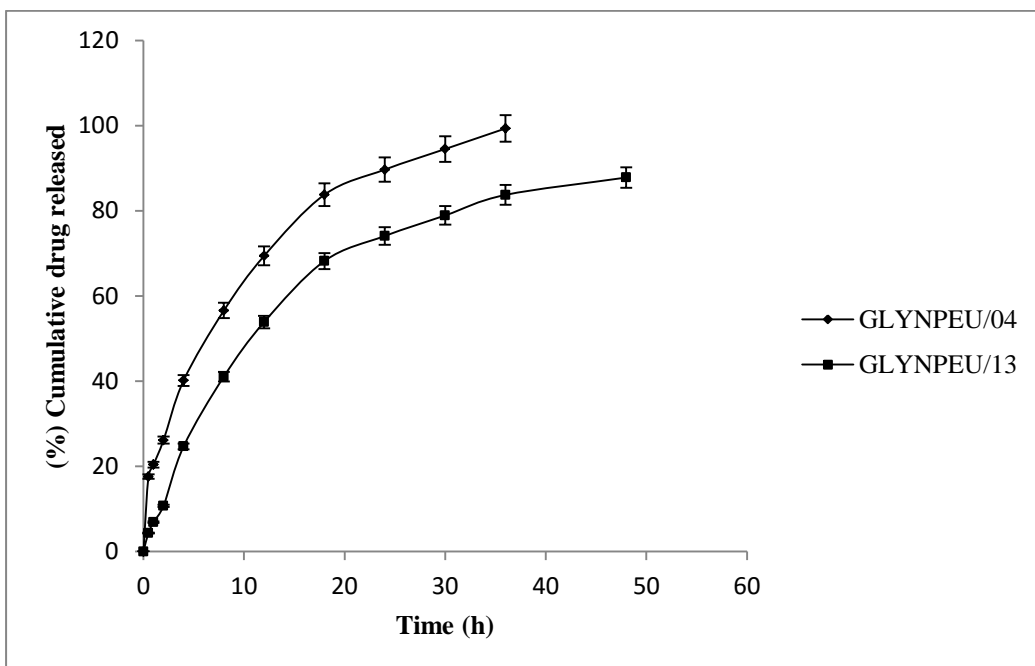


Figure 5.36: Effect of D: L ratio on in-vitro dissolution profile of OLN loaded GLY NP prepared by emulsification sonication method

Fitting of in-vitro release data of various formulations to different release models are represented in Table 5.6.

Table 5.6: Best fitting of in-vitro release data using mathematical modeling

Sr. No.	Batch	Suitable model	R2	AIC	MSC	n
1	PCL NP PF 68/05	Baker-Lonsdale	0.9617	77.41	3.09	-
2	PCLNPPVA/05	Baker-Lonsdale	0.9684	65.66	3.27	-
3	STNP PF68/09	Korsmeyer-Peppas	0.9946	32.45	4.71	0.446
4	STNPPVA/09	Baker-Lonsdale	0.96	43.78	3.22	-
5	GLYPF68/06	Korsmeyer-Peppas	0.9577	73.44	2.79	0.470
6	GLY PVA/06	Korsmeyer-Peppas	0.9633	71.74	2.94	0.550
7	CPCLNPPF68/05	Baker-Lonsdale	0.9653	76.21	3.19	-
8	CSTNP/09	Korsmeyer-Peppas	0.9971	27.34	5.35	0.429
9	CGLYNP/06	Baker-Lonsdale	0.9594	71.10	3.02	-
10	PCLNP/F68/02	Korsmeyer-Peppas	0.9740	75.27	3.05	0.380
11	PCLNP/F68/08	Baker-Lonsdale	0.9558	86.09	2.79	-
12	STF68/06	Korsmeyer-Peppas	0.9959	36.74	4.74	0.444
13	STF68/03	Korsmeyer-Peppas	0.9970	28.75	4.85	0.360
14	GLYNP/F68/03	Korsmeyer-Peppas	0.9816	65.08	3.39	0.453
15	GLYNP/F68/09	Korsmeyer-Peppas	0.9688	77.61	2.95	0.486
16	PCLNP/F68/04	Baker-Lonsdale	0.9558	83.12	3.10	-
17	PCLNP/F68/06	Baker-Lonsdale	0.9737	81.93	3.27	-
18	STNP/F68/07	Korsmeyer-Peppas	0.9953	37.55	4.64	0.481
19	STNP/F68/06	Korsmeyer-Peppas	0.9954	37.76	4.65	0.475
20	GLYNP/F68/04	Korsmeyer-Peppas	0.9636	79.89	2.80	0.501
21	GLYNP/F68/05	Korsmeyer-Peppas	0.9658	79.31	2.86	0.486
22	STNPEU/05	Korsmeyer-Peppas	0.9879	60.28	3.83	0.493
23	CSTNPEU/05	Korsmeyer-Peppas	0.9897	58.47	3.98	0.469
24	GLYNPEU/05	Korsmeyer-Peppas	0.9705	75.71	3.00	0.487
25	CGLYNPEU/05	Baker-Lonsdale	0.9802	69.09	3.55	-
26	STNPEU/02	Korsmeyer-Peppas	0.9846	61.95	3.62	0.535
27	STNPEU/03	Korsmeyer-Peppas	0.9945	45.72	4.59	0.515
28	GLYNPEU/02	Korsmeyer-Peppas	0.9712	73.04	3.05	0.534
29	GLYNPEU/03	Baker-Lonsdale	0.9883	63.22	4.04	-
30	STNPEU/01	Korsmeyer-Peppas	0.9890	57.84	3.90	0.451
31	GLYNPEU/01	Korsmeyer-Peppas	0.9806	71.33	3.37	0.422
32	STNPEU/04	Korsmeyer-Peppas	0.9934	46.92	4.31	0.412
33	STNPEU/13	Korsmeyer-Peppas	0.9832	63.16	3.53	0.524
34	GLYNPEU/04	Baker-Lonsdale	0.9915	53.26	4.31	-
35	GLYNPEU/13	Korsmeyer-Peppas	0.9683	75.96	2.94	0.507
36	PCL NP	Baker-Lonsdale	0.9682	82.94	3.11	-
37	C PCL NP	Baker-Lonsdale	0.9780	78.92	3.45	-
38	GLY NP	Korsmeyer-Peppas	0.9690	76.61	2.95	0.48
39	C GLY NP	Baker-Lonsdale	0.9807	69.07	3.57	-

The fitting of best model to the in-vitro release data was selected through three important parameters, R^2 , Akaike Information Criterion (AIC) and Model Selection Criterion (MSC). In general, a model with R^2 value close to one, low AIC value and MSC value more than 3 are considered to be the optimum model for the analyzed in-vitro release data. Korsmeyer-Peppas model describes drug release mainly from a polymeric system, where first 60% drug release data were fitted in the model [37, 38]. The diffusional exponent, n is indicative of mechanism of drug release: a value of $n = 0.45$ indicates fickian or case I release; $0.45 < n < 0.89$ indicates non-fickian or anomalous release; $n = 0.89$ indicates case II release; and $n > 0.89$ indicates super case II release. The “ n ” values for the formulations, as presented in Table 5.6, varies from 0.380 to 0.535, indicating that the type of release of the drug from these systems varies between Fickian and non Fickian behavior [39]. Many formulations, as demonstrated in the Table 5.6, follow Baker-Lonsdale model, which was originally developed by Baker and Lonsdale in 1974 from the Higuchi model [37, 40]. This model best describes the release of drug from spherical matrices, which is highly justified since the developed formulations were also supposed to be matrices with spherical shape.

5.3.4 Optimization and validation

The Design-Expert software was used in order to find the optimized conditions for optimized formulations. The desirability criteria set in design-expert for optimized formulations were minimum particle size, maximum entrapment efficiency and maximum drug content. New batches of NP with levels of factors predicted by software were prepared in order to study the validity of the optimization procedure under investigation. The predicted levels of factors and responses are given below, along with the practically obtained values in brackets.

Nanoprecipitation technique: a) PCL NP: Polymer amount - 138.75 mg; Surfactant amount- 0.32% w/v with predicted responses: Size - 69.50 nm (73.28 ± 2.14 nm); EE - 80.40% ($78.77 \pm 2.83\%$). b) ST NP: Solid lipid amount - 238.80 mg; Surfactant amount - 1.5% w/v with predicted responses: Size - 163.06 nm (166.43 ± 2.45 nm); EE - 75.31% ($73.27 \pm 1.24\%$). c) GLY NP: Solid lipid amount - 179.50 mg; Surfactant amount - 1.5% w/v with predicted responses: Size - 196.48 nm (198.28 ± 2.14 nm); EE - 84.75% ($82.68 \pm 1.78\%$)

Emulsification ultrasonication: a) ST NP: Solid lipid amount - 1510.00 mg; Surfactant amount - 1.38% w/v; D: Solid lipid ratio - 1:14 with predicted responses: Size - 131.55 nm (136.13 ± 3.12 nm); EE - 78.00% (76.76 ± 2.79 %); DC - 5.21% w/w (4.65 ± 0.16 % w/w). b) GLY NP: Solid lipid amount- 1292.00 mg; Surfactant amount - 1.53% w/v; D: Solid lipid ratio - 1:15 with predicted responses: Size - 147.02 nm (151.29 ± 3.36 nm); EE - 76.05% (74.51 ± 1.75 %); DC - 4.55% w/w (4.23 ± 0.09 % w/w).

The practical values (in brackets) found were in good agreement with the predicted responses, confirming the validity of the methods. Based on the desired criteria of low particle size, high EE/DC and better controlled release, PCL nanoparticles prepared from precipitation technique and GLY nanoparticles prepared from emulsification-ultrasonication technique were selected for the further studies. These formulations were further coated with Tween 80 and characterized as discussed earlier. The characteristics of selected final formulations are given below:

PCL NP: Size - 73.28 ± 2.14 nm; PDI - 0.231 ± 0.04 , ZP - -32.46 ± 1.15 mV; EE - 78.77 ± 2.83 %, DC - 6.51 ± 0.23 % w/w

GLY NP: Size - 151.29 ± 3.36 nm; PDI - 0.346 ± 0.08 , ZP - -37.25 ± 2.32 mV; EE - 74.51 ± 1.75 % ; DC - 4.23 ± 0.09 % w/w

C PCL NP: Size - 81.41 ± 2.14 nm; PDI - 0.312 ± 0.05 , ZP - -27.81 ± 1.26 mV; EE - 76.92 ± 2.05 %; DC - 6.36 ± 0.16 % w/w

C GLY NP: Size - 157.42 ± 4.16 nm); PDI - 0.411 ± 0.11 , ZP - -33.67 ± 1.84 mV; EE - 72.96 ± 1.95 %; DC - 4.15 ± 0.11 % w/w

The in-vitro release studies of these optimized formulations also demonstrated in Figures 5.37 to 5.40 and mechanisms of release have been presented in Table 5.6.

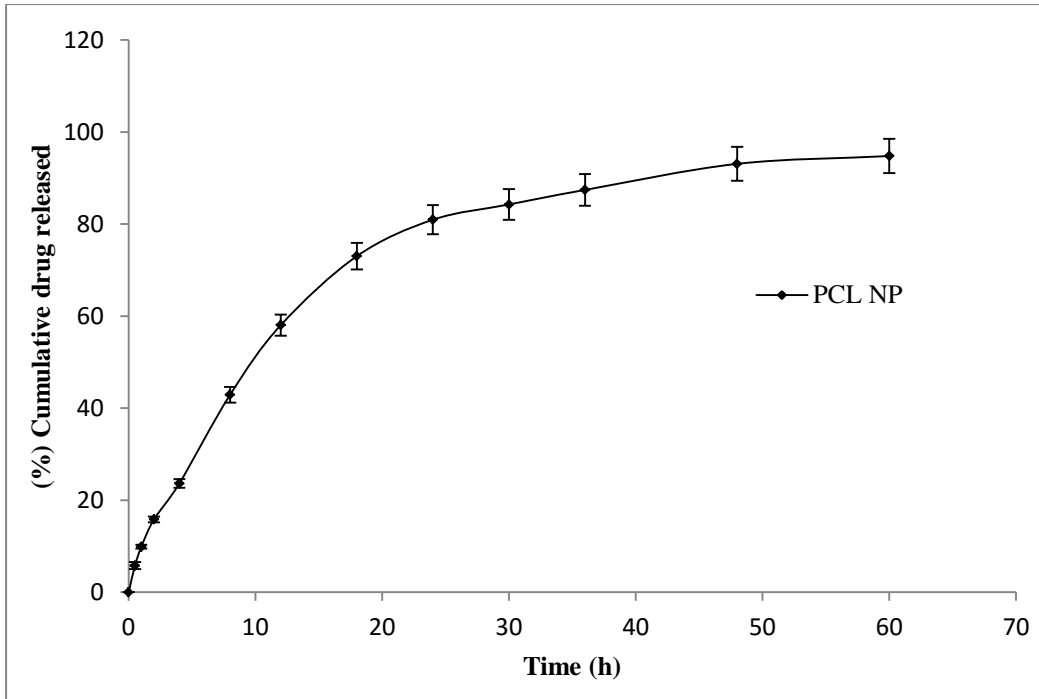


Figure 5.37: In-vitro release profiles of OLN from optimized nanoparticulate formulations of PCL NP

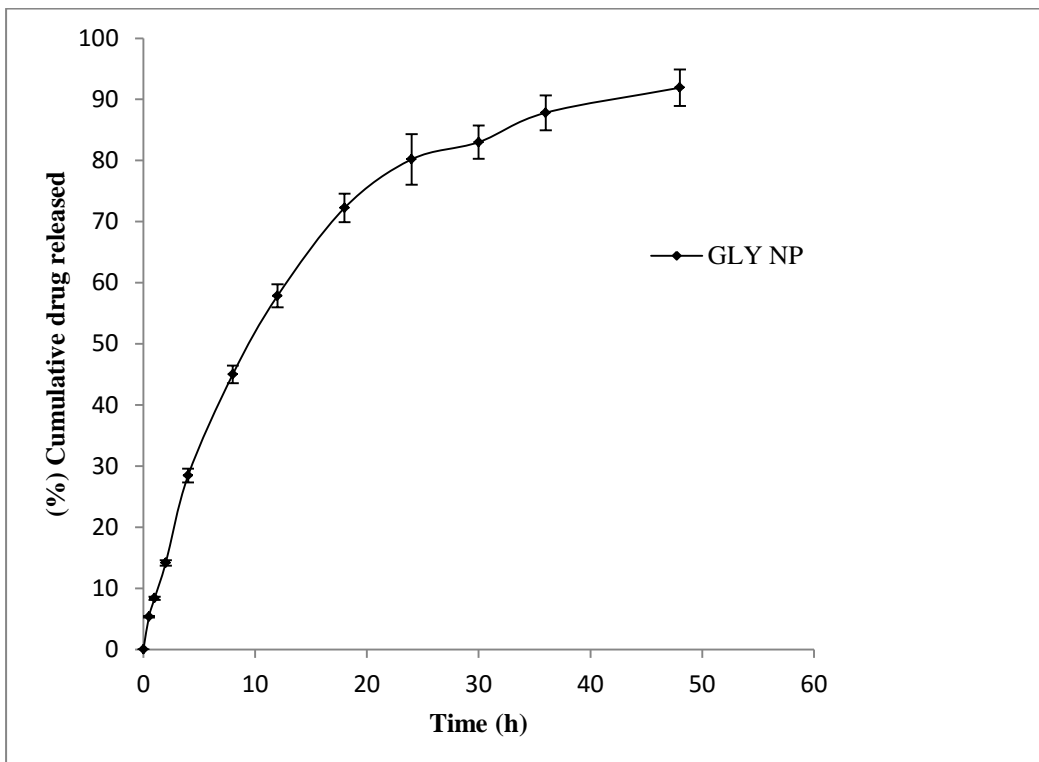


Figure 5.38: In-vitro release profiles of OLN from optimized nanoparticulate formulations of GLY NP

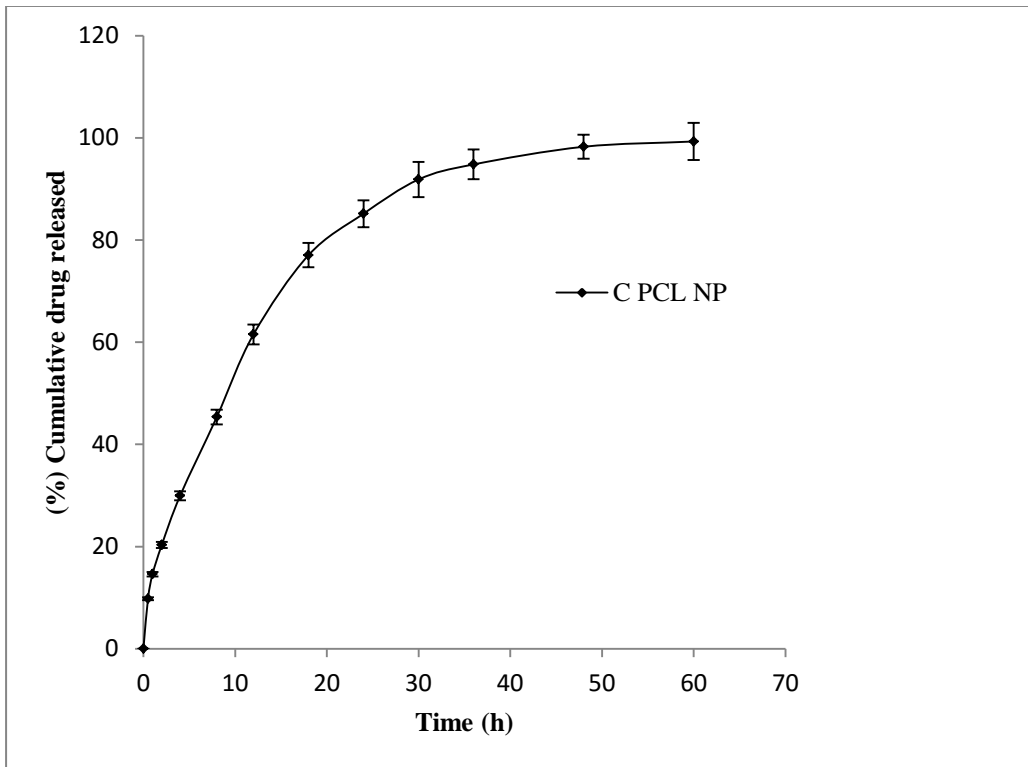


Figure 5.39: In-vitro release profiles of OLN from optimized nanoparticulate formulations of C PCL NP

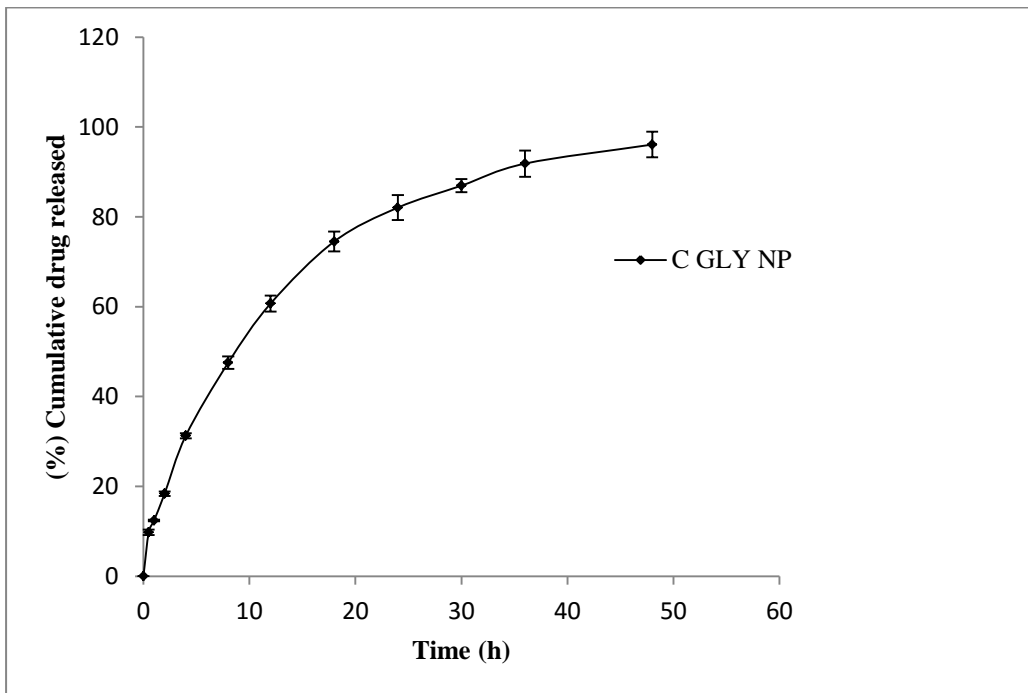


Figure 5.40: In-vitro release profiles of OLN from optimized nanoparticulate formulations of C GLY NP

5.3.5 Thermal study

The DSC curve of OLN (Figure 5.41, 5.42) showed a melting endotherm at 192 °C corresponding to the MP of OLN. However, no melting peak of OLN was detected for both nanoparticulate formulations. Therefore, it can be concluded that OLN present in the nanoparticle formulation might be in an amorphous form or dispersed in molecular level. Numerous authors also have reported similar results for both polymeric and solid lipid nanoparticulate systems for the molecular dispersion of drug encapsulated [41, 42].

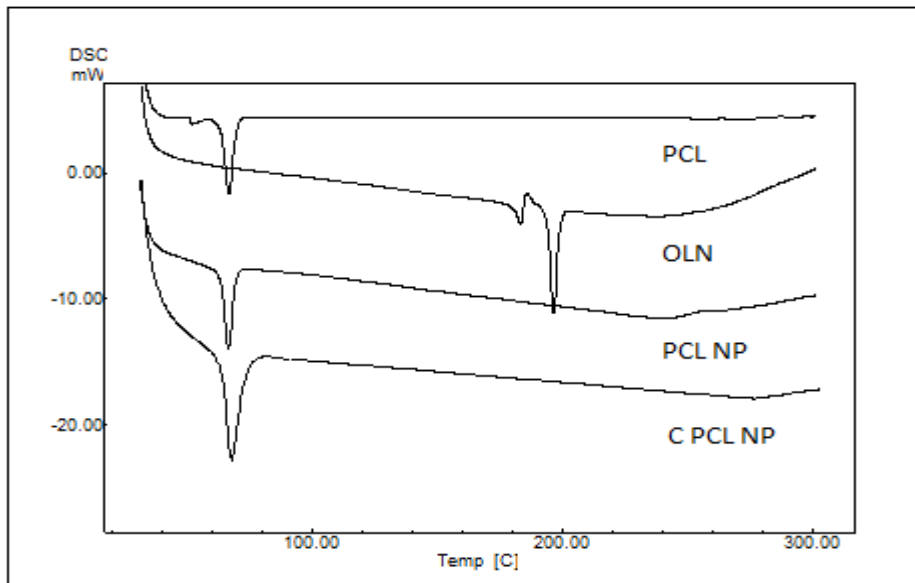


Figure 5.41: DSC thermograms of pure OLN and OLN loaded PCL nanoparticles

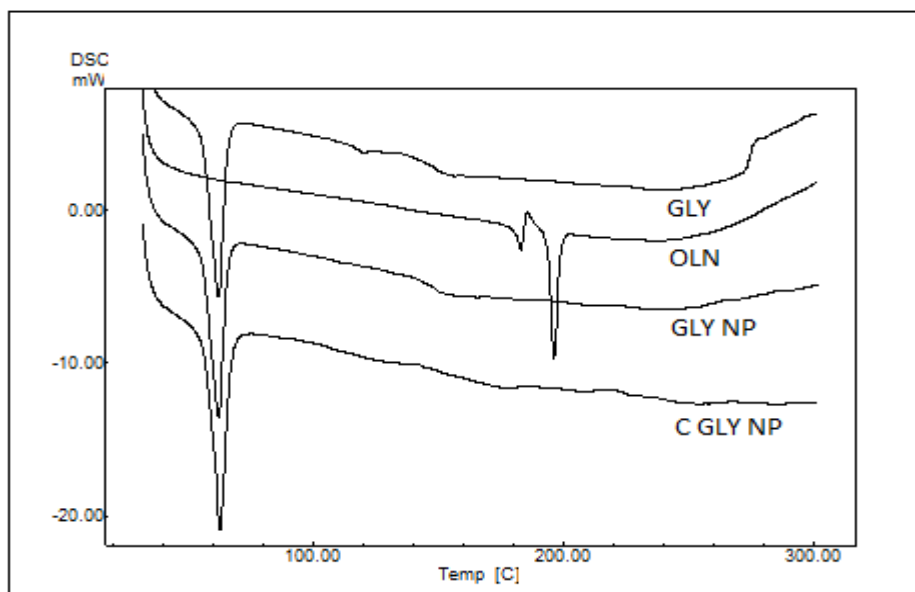


Figure 5.42: DSC thermograms of pure OLN and OLN loaded GLY nanoparticles

5.3.6 Stability studies

The results of 3 and 6 months stability studies are shown in Table 5.7. It has been found that nanoparticle batches showed detectable aggregation at ambient storage conditions while at refrigerated ($5^{\circ}\text{C} \pm 3^{\circ}\text{C}$) and frozen ($-20^{\circ}\text{C} \pm 5^{\circ}\text{C}$) conditions, negligible or very low aggregation was observed. It has also been found that the formulations stored at frozen conditions ($-20^{\circ}\text{C} \pm 5^{\circ}\text{C}$) showed no significant change in the drug content, average particle size and release profiles after 3 and 6 months of storage.

Conclusions

OLN-loaded nanoparticulate systems were prepared successfully using both nanoprecipitation and emulsification-ultrasonication techniques. These methods were found to be reproducible and they produced NP with narrow size distribution and good encapsulation efficiency with extended release. The influence of different formulation variables such as polymer/solid lipid concentration, surfactant concentration and drug proportions on studied responses such as size, encapsulation efficiency and drug content were studied in detail. OLN-loaded NP prepared from selected biodegradable polymer/solid lipid sustained the release of drug for 48 – 60 h, as found by the in-vitro release studies. Morphological studies by SEM have shown that both polymeric and solid lipid NP were spherical in shape with smooth surface. The formulations also exhibited high redispersibility after freeze-drying and stability study results demonstrated good stability, with no significant change in the drug content, average particle size and drug release for the formulations stored at frozen conditions for a period of 6 months.

Table 5.7: Stability study results for the selected OLN nanoparticle formulations stored at various conditions (3 & 6 months)

3 MONTHS STABILITY STUDY								
Formulation	Initial		Ambient (25°C ± 2°C / 60 ± 5 %RH)		Refrigerated (5°C ± 3°C)		Frozen (-20° C ± 5°C)	
	D.C. ± SD (%w/w)	Size ± SD (nm)	D.C. ± SD (%w/w)	Size ± SD (nm)	D.C. ± SD (%w/w)	Size ± SD (nm)	D.C. ± SD (%w/w)	Size ± SD (nm)
PCL NP	6.51±0.23	73.28±2.14	6.03±0.28	82.43±2.74	6.24±0.27	78.31±2.47	6.49±0.28	75.46±1.38
GLY NP	4.23±0.09	151.29±3.56	3.80±0.39	164.21±2.65	3.94±0.31	159.34±2.62	4.22±0.34	155.14±2.41
C PCL NP	6.36±0.16	81.41±2.46	5.93±0.32	91.41±2.41	6.02±0.29	88.32±1.91	6.33±0.28	83.14±1.62
C GLY NP	4.15±0.11	157.42±4.16	3.64±0.22	168.14±3.22	3.81±0.41	165.13.45±3.08	4.11±0.18	161.35±2.74
6 MONTHS STABILITY STUDY								
PCL NP	6.51±0.23	73.28±2.14	5.81±0.32	84.35±2.58	6.01±0.16	81.44±2.15	6.48±0.24	77.68±1.92
GLY NP	4.23±0.09	151.29±3.36	3.61±0.23	168.93±3.82	3.76±0.18	162.45±3.44	4.18±0.14	159.43±2.66
C PCL NP	6.36±0.16	81.41±2.40	5.84±0.34	96.14±2.86	5.96±0.39	93.74±2.62	6.29±0.28	86.44±1.49
C GLY NP	4.15±0.11	157.42±4.16	3.55±0.46	172.35±3.81	3.73±0.24	168.17±3.74	4.08±0.26	163.41±3.24

References

- [1] R.N. Saha, S. Vasanthakumar, G. Bende, M. Snehalatha, Nanoparticulate drug delivery systems for cancer chemotherapy, *Mol Membr Biol*, 27 (2010) 215-231.
- [2] N. Teekamp, L.F. Duque, H.W. Frijlink, W.L. Hinrichs, P. Olinga, Production methods and stabilization strategies for polymer-based nanoparticles and microparticles for parenteral delivery of peptides and proteins, *Expert opinion on drug delivery*, (2015) 1-21.
- [3] D.T. Birnbaum, J.D. Kosmala, L.B. Peppas, Optimization of preparation techniques for poly (lactic acid-co-glycolic acid) nanoparticles, *J Nanopart Res*, 2 (2000) 173-181.
- [4] H.S. Ribeiro, B.S. Chu, S. Ichikawa, M. Nakajima, Preparation of nanodispersions containing β -carotene by solvent displacement method, *Food Hydrocoll*, 22 (2008) 12-17.
- [5] W. Mehnert, K. Mäder, Solid lipid nanoparticles: Production, characterization and applications, *Adv Drug Deliv Rev*, 47 (2001) 165-196.
- [6] J.M. Barichello, M. Morishita, K. Takayama, T. Nagai, Encapsulation of hydrophilic and lipophilic drugs in PLGA nanoparticles by the nanoprecipitation method, *Drug Dev Ind pharm*, 25 (1999) 471-476.
- [7] S. Martins, I. Tho, I. Reimold, G. Fricker, E. Souto, D. Ferreira, M. Brandl, Brain delivery of camptothecin by means of solid lipid nanoparticles: formulation design, in vitro and in vivo studies, *Int J Pharm*, 439 (2012) 49-62.
- [8] A. Silva, E.G Mira, M. García, M. Egea, J. Fonseca, R. Silva, D. Santos, E. Souto, D. Ferreira, Preparation, characterization and biocompatibility studies on risperidone-loaded solid lipid nanoparticles (SLN): high pressure homogenization versus ultrasound, *Colloids Surf B Biointerfaces*, 86 (2011) 158-165.
- [9] S. Das, W.K. Ng, P. Kanaujia, S. Kim, R.B. Tan, Formulation design, preparation and physicochemical characterizations of solid lipid nanoparticles containing a hydrophobic drug: effects of process variables, *Colloids Surf B Biointerfaces*, 88 (2011) 483-489.
- [10] J. Kreuter, Influence of the surface properties on nanoparticle-mediated transport of drugs to the brain, *J Nanosci Nanotechnol*, 4 (2004) 484-488.
- [11] J. Kreuter, Nanoparticulate systems for brain delivery of drugs, *Adva Drug Deliv Rev*, 64, Supplement (2012) 213-222.

- [12] B. Wilson, M.K. Samanta, K. Santhi, K.P.S. Kumar, N. Paramakrishnan, B. Suresh, Targeted delivery of tacrine into the brain with polysorbate 80-coated poly(n-butylcyanoacrylate) nanoparticles, *Eur J Pharm Biopharm*, 70 (2008) 75-84
- [13] M. Snehalatha, K. Venugopal, R.N. Saha, Etoposide-loaded PLGA and PCL nanoparticles I: preparation and effect of formulation variables, *Drug Deliv*, 15 (2008) 267-275.
- [14] M. Schubert, C. Müller-Goymann, Solvent injection as a new approach for manufacturing lipid nanoparticles—evaluation of the method and process parameters, *Eur J Pharm Biopharm*, 55 (2003) 125-131.
- [15] J.C. Leroux, E. Allémann, E. Doelker, R. Gurny, New approach for the preparation of nanoparticles by an emulsification-diffusion method, *Eur J Pharm Biopharm*, 41 (1995) 14-18.
- [16] J. Hao, X. Fang, Y. Zhou, J. Wang, F. Guo, F. Li, X. Peng, Development and optimization of solid lipid nanoparticle formulation for ophthalmic delivery of chloramphenicol using a Box-Behnken design, *Int J Nanomed*, 6 (2011) 683-692.
- [17] L.M. Banderas, J.A. Fuentes, M.D. Lobato, J. Prados, C. Melguizo, M.F. Arevalo, M.A. Holgado, Cannabinoid derivate-loaded PLGA nanocarriers for oral administration: formulation, characterization, and cytotoxicity studies, *Int J Nanomed*, 7 (2012) 5793-5806.
- [18] P. Ebrahimnejad, R. Dinarvand, S.A. Sajadi, F. Atyabi, F. Ramezani, M.R. Jaafari, Preparation and characterization of poly lactide-co-glycolide nanoparticles of SN-38, *PDA J Pharm Sci Technol*, 63 (2009) 512-520.
- [19] S.Y. Tang, P. Shridharan, M. Sivakumar, Impact of process parameters in the generation of novel aspirin nanoemulsions--comparative studies between ultrasound cavitation and microfluidizer, *Ultrason Sonochem*, 20 (2013) 485-497.
- [20] J.Y. Fang, C.F. Hung, S.C. Hua, T.L. Hwang, Acoustically active perfluorocarbon nanoemulsions as drug delivery carriers for camptothecin: drug release and cytotoxicity against cancer cells, *Ultrason*, 49 (2009) 39-46.
- [21] J. Varshosaz, S. Ghaffari, M.R. Khoshayand, F. Atyabi, S. Azarmi, F. Kobarfard, Development and optimization of solid lipid nanoparticles of amikacin by central composite design, *J Liposome Res*, 20 (2010) 97-104.
- [22] C. Vitorino, F.A. Carvalho, A.J. Almeida, J.J. Sousa, A.A. Pais, The size of solid lipid nanoparticles: an interpretation from experimental design, *Colloids Surf B Biointerfaces*, 84 (2011) 117-130.

- [23] M.A. Schubert, C.C. Muller-Goymann, Solvent injection as a new approach for manufacturing lipid nanoparticles--evaluation of the method and process parameters, *Eur J Pharm Biopharm*, 55 (2003) 125-131.
- [24] V. Sanna, E. Gavini, M. Cossu, G. Rassu, P. Giunchedi, Solid lipid nanoparticles (SLN) as carriers for the topical delivery of econazole nitrate: in-vitro characterization, ex-vivo and in-vivo studies, *J Pharm Pharmacol*, 59 (2007) 1057-1064.
- [25] J. Liu, W. Hu, H. Chen, Q. Ni, H. Xu, X. Yang, Isotretinoin-loaded solid lipid nanoparticles with skin targeting for topical delivery, *Int J Pharm*, 328 (2007) 191-195.
- [26] V.V. Kumar, D. Chandrasekar, S. Ramakrishna, V. Kishan, Y.M. Rao, P.V. Diwan, Development and evaluation of nitrendipine loaded solid lipid nanoparticles: influence of wax and glyceride lipids on plasma pharmacokinetics, *Int J Pharm*, 335 (2007) 167-175.
- [27] Y. Wang, Y. Deng, S. Mao, S. Jin, J. Wang, D. Bi, Characterization and body distribution of beta-elemene solid lipid nanoparticles (SLN), *Drug Dev Ind Pharm*, 31 (2005) 769-778.
- [28] W. Abdelwahed, G. Degobert, S. Stainmesse, H. Fessi, Freeze-drying of nanoparticles: formulation, process and storage considerations, *Adv Drug Deliv Rev*, 58 (2006) 1688-1713.
- [29] A.B. Kovacevic, R.H. Müller, S.D. Savic, G.M. Vuleta, C.M. Keck, Solid lipid nanoparticles (SLN) stabilized with polyhydroxy surfactants: Preparation, characterization and physical stability investigation, *Colloids Surf A Physicochem Eng Asp*, 444 (2014) 15-25.
- [30] L.H. Reddy, R.S. Murthy, Pharmacokinetics and biodistribution studies of Doxorubicin loaded poly(butyl cyanoacrylate) nanoparticles synthesized by two different techniques, *Biomed Pap*, 148 (2004) 161-166.
- [31] H.M. Redhead, S.S. Davis, L. Illum, Drug delivery in poly(lactide-co-glycolide) nanoparticles surface modified with poloxamer 407 and poloxamine 908: in vitro characterisation and in vivo evaluation, *J Control Release*, 70 (2001) 353-363.
- [32] V. Jennings, M. Schafer-Korting, S. Gohla, Vitamin A-loaded solid lipid nanoparticles for topical use: drug release properties, *J Control Release*, 66 (2000) 115-126.

- [33] A. zur Muhlen, C. Schwarz, W. Mehnert, Solid lipid nanoparticles (SLN) for controlled drug delivery--drug release and release mechanism, *Eur J Pharm Biopharm*, 45 (1998) 149-155.
- [34] M. Chorny, I. Fishbein, H.D. Danenberg, G. Golomb, Lipophilic drug loaded nanospheres prepared by nanoprecipitation: effect of formulation variables on size, drug recovery and release kinetics, *J Control Release*, 83 (2002) 389-400.
- [35] B. Wilson, M.K. Samanta, K. Santhi, K.P. Kumar, N. Paramakrishnan, B. Suresh, Poly(n-butylcyanoacrylate) nanoparticles coated with polysorbate 80 for the targeted delivery of rivastigmine into the brain to treat Alzheimer's disease, *Brain Res*, 20 (2008) 159-168.
- [36] X.H. Tian, X.N. Lin, F. Wei, W. Feng, Z.C. Huang, P. Wang, L. Ren, Y. Diao, Enhanced brain targeting of temozolomide in polysorbate-80 coated polybutylcyanoacrylate nanoparticles, *Int J Nanomedicine*, 6 (2011) 445-452.
- [37] P. Costa, J.M.S. Lobo, Modeling and comparison of dissolution profiles, *Eur J Pharm Sci*, 13 (2001) 123-133.
- [38] S. Dash, P.N. Murthy, L. Nath, P. Chowdhury, Kinetic modeling on drug release from controlled drug delivery systems, *Acta Pol Pharm*, 67 (2010) 217-223.
- [39] S. Dhawan, R. Kapil, B. Singh, Formulation development and systematic optimization of solid lipid nanoparticles of quercetin for improved brain delivery, *J Pharm Pharmacol*, 63 (2011) 342-351.
- [40] J. Varshosaz, M. Soheili, Production and in vitro characterization of lisinopril-loaded nanoparticles for the treatment of restenosis in stented coronary arteries, *J Microencapsul*, 25 (2008) 478-486.
- [41] Y. Zhang, L. Tang, L. Sun, J. Bao, C. Song, L. Huang, K. Liu, Y. Tian, G. Tian, Z. Li, H. Sun, L. Mei, A novel paclitaxel-loaded poly(epsilon caprolactone)/Ploxamer 188 blend nanoparticle overcoming multidrug resistance for cancer treatment, *Acta Biomater*, 6 (2010) 2045-2052.
- [42] R. Tiwari, K. Pathak, Nanostructured lipid carrier versus solid lipid nanoparticles of simvastatin: comparative analysis of characteristics, pharmacokinetics and tissue uptake, *Int J Pharm*, 415 (2011) 232-243.

Chapter 6
Pharmacokinetic and
biodistribution
studies

6.1 Introduction

The effectiveness of a drug delivery system is highly dependent on its ability to deliver the therapeutic agent selectively/preferentially to the target site [1, 2]. Among the various strategies used for this purpose by pharmaceutical scientists, nanoparticulate drug delivery systems are considered to be a highly useful tool with their diverse physiochemical and biological properties. These kinds of carrier mediated drug delivery systems alter the pharmacokinetic and distribution characteristics of the drug encapsulated [3]. These systems overcome the major disadvantages of conventional dosage forms which exhibit non selective distribution in the body, resulting in the wastage of major portion of the administered dose by reaching the organs or tissues other than site of action producing undesired side effects [4]. Besides, nanoparticulate drug delivery systems are reported to cross biological barriers such as BBB [5]. Therefore in the case of nanoparticulate drug delivery systems, preferential distribution of drugs is possible, which minimizes the side effects and therefore offer huge potential for the delivery of highly distributed drugs, with possibility of decreasing the dose. The entry of drugs to many organs is also restricted by incorporating in nanoparticulate systems due to higher size of carriers compared to pure drug. In addition, controlled release of drug from nanoparticulate delivery systems can alter many pharmacokinetics parameters such as half life and clearance [6]. Therefore, increased delivery of drug to the site of action with altered distribution characteristics and controlled release would eventually result in huge improvement of efficiency in drug delivery with low dose leading to better therapeutic action with maximum patient compliance.

It is expected that in-vivo fate of drug in nanoparticulate drug delivery systems are very different from conventional dosage forms/pure drug. Therefore, it is highly essential to investigate in house prepared novel nanoparticulate drug delivery systems in animal model for its pharmacokinetics and biodistribution properties. These preclinical studies should be well understood before taking up the new dosage form to clinical stage. Moreover, there are regulatory requirements for NDDS, which are mentioned in federal register of FDA 21 CFR part 314, 1998. Nanoparticulate drug delivery systems are considered to be under this section and therefore should follow the regulatory guidelines accordingly. The investigation of the nanoparticulate drug delivery systems in animal model for its pharmacokinetics and biodistribution

properties would result in thorough understanding of various related parameters and thereby help in better design and delivery of drug and better therapeutic efficiency.

6.2 Experimental

6.2.1 Materials and Equipment

Drug and chemicals were obtained from same sources as mentioned in Chapter 5. Additionally, Urethane, procured from Sigma Aldrich Chemicals, USA was used as an anaesthetic agent. A high speed homogeniser (Kinematica®, USA) was used for tissue homogenization. All surgical instruments used in the study, such as scissors, glass syringes, forceps, silk suture etc. were sterilized before usage.

a) Animals

Healthy male Wistar rats were selected for pharmacokinetics and biodistribution studies of pure drug OLN and four specific OLN loaded nanoparticulate formulations. Rats with average weight of 225 ± 25 g (12 - 15 weeks old) were obtained from Central Animal Facility (CAF), BITS, Pilani which were procured from Choudhary Charan Singh Haryana Agricultural University Hissar, India (Reg. No. 417/01/a/CPCSEA). Animals were properly housed and maintained under standard laboratory conditions (temperature 22 ± 2 °C and room humidity $60 \pm 10\%$), 12:12 h of light/dark cycle and provided with food and water *ad libitum*. Rats were acclimatized to the study environment for at least five days before commencing the study. All experimental protocols were approved by the Institutional Animal Ethics Committee (IAEC) prior to the commencement of work (Protocol No. IAEC/RES/13/14/REV-2/17/16). All experimental procedures including euthanasia and disposal of carcass were in accordance with the guidelines set by the Institute, IAEC and the Committee for the Purpose of Control and Supervision of Experiments on Animals (CPCSEA), India. All animals were kept under observation during the entire study for any unusual signs, general conditions, potential clinical signs, toxicity or mortality.

6.2.2 In-vivo pharmacokinetic and biodistribution studies

Single dose i.v. pharmacokinetic studies were carried out for pure drug OLN and selected four nanoparticulate formulations (PCL NP, GLY NP, C PCL NP & C GLY NP). The drug concentration or amount levels in plasma, brain, liver, lungs, kidney, spleen and heart were determined in healthy rat model for determining pharmacokinetic parameters, biodistribution profile and expected therapeutic efficacy. The main objective of the study was to understand any change in the in-vivo

pharmacokinetic and biodistribution behaviour of drug loaded NP from pure drug after i.v. administration.

a) Formulation and sample preparation

OLN solution for i.v. injection was prepared using pure OLN in sterile PBS, pH 7.4 with the help of poloxomer 188 to obtain a concentration of 4 mg.mL⁻¹. The selected nanoparticulate systems were also administered as uniform aqueous dispersion with the help of vortex mixing. The dose selected for the study for both pure drug and formulations were equivalent to 4 mg.kg⁻¹ [7]. All the solutions and dispersions were prepared fresh and used immediately without any additional treatments.

b) Administration of free drug and nanoparticles

For each study, the selected animals were divided randomly in a group of five (n=3) and all studies were carried out in triplicate. Rats were fasted overnight (15 - 18 h) before commencing the study. Only adequate water was provided. All rats were marked according to the standard labelling scheme and animal weights were recorded. The in-vivo pharmacokinetic and biodistribution studies were performed for i.v. administration of pure drug and drug loaded formulations as per standard protocol. For i.v. administration, the dose equivalent to 4 mg of OLN per kg of the body weight was administered through the tail vein using a 1 mL syringe (25 G × 1/2" needle) under anaesthesia, after dilating the vein with hot water. In some animals when veins were not clearly visible with hot water, xylene was used for the vein dilatation and easy administration.

c) Plasma and tissue sample collection and processing

Blood samples were collected from rats using glass capillaries through retro-orbital route at predetermined time intervals such as 0.25, 0.5, 1, 1.5, 3, 6, 9, 12, 18, 24, 36, & 48 h of the post-dosing. At each time point, approximately 0.5 mL of blood sample was withdrawn under anaesthesia. Samples were collected in microcentrifuge tubes containing anticoagulant, EDTA. These samples were then kept for centrifugation at 3000 rpm and 4 °C for 15 min. Supernatant was then separated, labelled and stored at -80 °C in sealed cryo-vials, until further analysis.

Once the blood sampling was completed, the whole blood was drained from the inferior venacava using a 10 mL syringe (21 G × 1" needle) and various organs such as liver, lungs, kidney, spleen and heart were collected by surgical process. For this

purpose, under anaesthesia, the abdominal incision was made with a sterilized scissor to expose all organs and whole blood was drained. Organs were perfused with phosphate buffer saline to remove residual blood inside and were carefully excised. Excised organ samples were transferred to ice-cold petridish containing phosphate buffer saline with maintained temperature. All tissues were cleaned with sufficient volume of phosphate buffer saline and blotted dried with Whatman filter paper. In order to collect brain, rat was laid on its ventral aspect in the dissection tray and the skin over the head was removed in order to completely expose the surface of skull. One or two midline incisions were made over the skull with a surgical knife/scissors and the entire brain was dissected out.

Each tissue sample collected was weighed accurately and chopped using a tissue tearor and added equal volume of phosphate buffer saline. Individual tissues were homogenized (15,000 rpm) to get fine suspension using a tissue homogenizer in an ice-cold bath. Fine tissue homogenates were properly labelled and stored in a clean sealed glass vial at -80° C, until analysis. Extraction procedure followed is discussed in detail in chapter 3. All samples were processed and analyzed by the validated chromatographic method, within 10 days time period from the sample collection.

d) Analysis of biological samples

The plasma and tissue samples obtained from each animal at respective time point were processed independently. Concentration of the drug in biological plasma in terms of ng.mL^{-1} was determined by the bioanalytical method described in Chapter 3. The concentration of the drug in other biological matrices such as brain, lungs, liver, kidney, spleen and heart were determined in terms of ng.g^{-1} by analytical methods developed separately with same extraction procedure as that of plasma, with calibration equations; Brain: $Y = 0.0039x - 0.0017$ (10-1600 ng.mL^{-1}), Lungs: $Y = 0.0039x + 0.0196$ (10-2000 ng.mL^{-1}), Liver: $Y = 0.004x + 0.0177$ (10-1600 ng.mL^{-1}), Kidney: $Y = 0.0039x + 0.0387$ (10-2400 ng.mL^{-1}), Spleen: $Y = 0.004x + 0.0146$ (10-2000 ng.mL^{-1}) and Heart: $Y = 0.0041x - 0.0206$ (10-1600 ng.mL^{-1}).

Dilution integrity was assured up to 15 fold dilution for plasma/tissue samples. To study the dilution integrity, three dilution integrity (DI) standards were prepared in plasma/tissue homogenates at higher concentrations. Before extraction, these standards were diluted in rat plasma/organ homogenate to bring the concentrations within the calibration range. Five series of DI standards were prepared in rat

plasma/tissue homogenates at 8, 16 and 24 $\mu\text{g}\cdot\text{mL}^{-1}$ concentrations and they were diluted 5, 10 and 15 times, respectively. The DI standards were vortex mixed for 5 min and processed as mentioned previously. The dilution integrity of the methods were found to be acceptable with accuracy (% Bias) of maximum -3.36 , -5.42 and 2.72 for respectively for 8, 16 and 24 $\mu\text{g}\cdot\text{mL}^{-1}$ concentration levels. Precision values for 5, 10 and 15 times dilution were within acceptable limits with % RSD ≤ 6.05 , 5.80 and 3.63 , respectively. Thus, the results demonstrated that the methods were suitable for over-curve dilution up to 15 times in the rat plasma/organ homogenates.

e) Pharmacokinetic and biodistribution data analysis

The drug concentration in plasma and various tissues such as brain, liver, lungs, kidney, spleen and heart at different time intervals were analyzed by the non-compartmental analysis method using WinNonlin® ver. 2.1 (Pharsight Corporation, USA) software. The maximum drug concentration (C_{max}) and time to reach maximum concentration (T_{max}) were determined by model independent method. While, various pharmacokinetic parameters such as the area under the curve (AUC), the area under the moment curve (AUMC), the mean residence time (MRT) etc. were obtained from WinNonlin.

6.3 Results and discussion

a. Plasma pharmacokinetic study

The OLN plasma concentration–time curves after single i.v. administration of pure OLN and four formulations (PCL NP, GLY NP, C PCL NP & C GLY NP) in rats are shown in Figure.6.1. The various pharmacokinetic parameters calculated using a data modelling software are listed in Table 6.1. Pharmacokinetic profile of i.v. administration of pure OLN showed a rapid distribution of OLN into tissues with fall in the concentration of drug in the systemic circulation with detectable amount of the drug in plasma only up to 18 h. The non-compartmental data analysis of pure OLN solution indicated AUC^{∞} of $7987.27 \pm 487.28 \text{ ng}\cdot\text{h}\cdot\text{mL}^{-1}$ and AUMC^{∞} of $29345.10 \pm 1941.99 \text{ ng}\cdot\text{h}^2\cdot\text{mL}^{-1}$. MRT was found to be $3.66 \pm 0.43 \text{ h}$. The total systemic clearance (Cl) was found to be $0.5021 \pm 0.03 \text{ L}\cdot\text{kg}^{-1}\cdot\text{h}^{-1}$ and the elimination half-life in plasma was $2.85 \pm 0.37 \text{ h}$. As compared to OLN solution, administration of PCL and GLY nanoparticles resulted in a significant increase in AUC^{∞} of $9704.43 \pm 987.30 \text{ ng}\cdot\text{h}\cdot\text{mL}^{-1}$ and $11436.59 \pm 979.77 \text{ ng}\cdot\text{h}\cdot\text{mL}^{-1}$ respectively. MRT of these formulations

were also found to increase, with 8.15 ± 0.38 h for PCL NP and 9.06 ± 0.38 h for GLY NP. The systemic clearance (Cl) of these formulations have decreased significantly with values, 0.4151 ± 0.04 L.kg⁻¹.h⁻¹ for PCL NP and 0.3514 ± 0.02 L.kg⁻¹.h⁻¹ for GLY NP, with increase in elimination half-life in the plasma 6.42 ± 0.28 h for PCL NP and 6.77 ± 0.29 h for GLY NP, indicating extended circulation in body. Intra-venous administration of coated PCL (C PCL) and coated GLY (C GLY) nanoparticles resulted in further increased retention of the drug in the body with increased AUC[∞] to 13891.58 ± 970.71 ng.h.mL⁻¹ and 15611.60 ± 1383.45 ng.h.mL⁻¹. The MRT were found to increase to 9.47 ± 0.23 h and 10.17 ± 0.52 h respectively with reduced total systemic clearance (Cl) to 0.288 ± 0.03 L.kg⁻¹.h⁻¹ and 0.257 ± 0.02 L.kg⁻¹.h⁻¹. The results suggested that the initial drug concentration in plasma for pure OLN was higher than that of OLN loaded nanoparticles, but the pure drug was rapidly removed from the circulation system. In contrast, the i.v. administration of OLN loaded nanoparticles resulted in prolonged residence of OLN in systemic circulation of the animal with maximum residence for C GLY NP followed by C PCL NP.

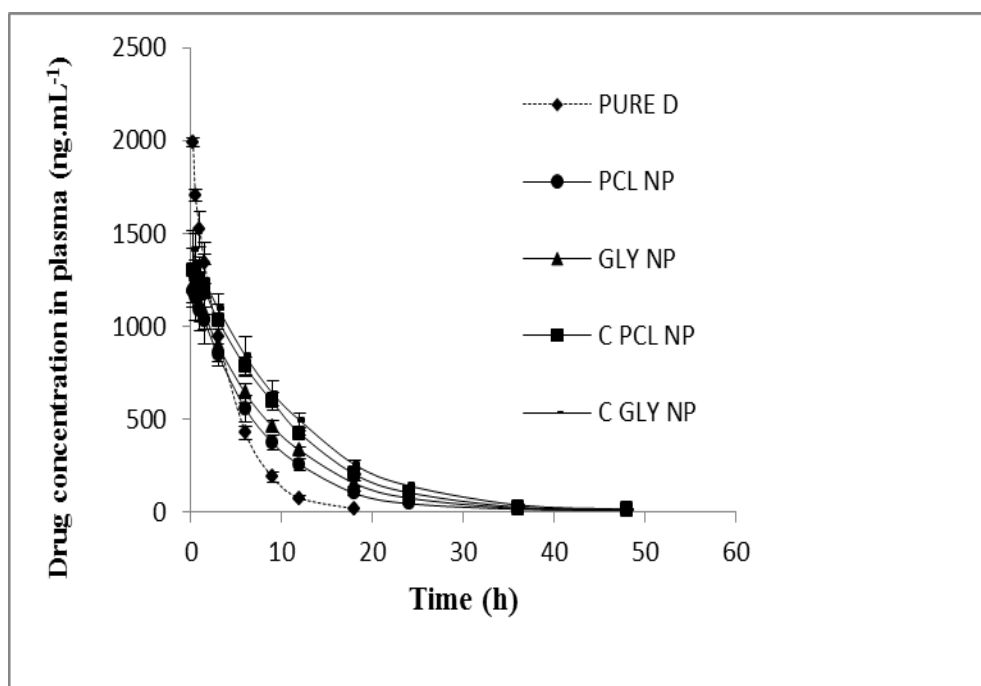


Figure 6.1: OLN concentration in plasma versus time profile following i.v. administration of the pure OLN and OLN loaded nanoparticles in rats

Table 6.1: Pharmacokinetic parameters of OLN and OLN loaded NP in plasma after i.v administration (n=3)

S.No	Parameters	OLN solution	PCL NP	GLY NP	C PCL NP	C GLY NP
1	AUC _{0-inf} (ng.h.mL ⁻¹)	7987.27 ± 487.28	9704.43 ± 987.30	11436.59 ± 979.77	13891.58 ± 970.71	15611.60 ± 1383.45
2	AUMC _{0-inf} (ng h ² mL ⁻¹)	29345.10 ± 1941.99	79499.96 ± 8475.16	104066.10 ± 9142.21	131646.50 ± 8767.49	159198.70 ± 12725.82
3	C _{max} (ng.mL ⁻¹)	2290.77 ± 169.48	1245.56 ± 102.04	1276.24 ± 104.72	1352.01 ± 118.83	1479.07 ± 84.15
4	t _{1/2} (h)	2.85 ± 0.37	6.42 ± 0.28	6.77 ± 0.29	6.86 ± 0.25	7.23 ± 0.41
5	MRT (h)	3.66 ± 0.43	8.15 ± 0.38	9.06 ± 0.38	9.47 ± 0.23	10.17 ± 0.52
6	Cl (L.h ⁻¹ kg ⁻¹)	0.5021 ± 0.03	0.4151 ± 0.04	0.3514 ± 0.02	0.288 ± 0.02	0.257 ± 0.02

The increased AUC of OLN in plasma for nanoparticulate formulations might be due to the change in overall distribution profile of these formulations as compared with the OLN solution. This might also be because of the reduced elimination of OLN from the systemic circulation, since there is a sustained release of OLN from these formulations. Similar results have been reported in the literature for particulate systems having sustained release properties, where the AUC and MRT were increased for the formulations as compared with drug solution [8-9]. The Tween 80 coated formulations have shown increased MRT and decreased clearance as compared to the un-coated formulations, which might be due to the different distribution profiles of these systems. Besides, low uptake of coated formulations by macrophage systems in the blood stream also might have contributed to the increased residence and higher plasma concentration [10].

b) Brain biodistribution studies

The concentrations of OLN in the rat brain, after the administration of single i.v. dose of the pure drug, PCL NP, GLY NP, C PCL NP & C GLY NP at different time points were determined and presented as a function of time in Figure 6.2. Different pharmacokinetic parameters were calculated using WinNonlin® software (Table 6.2). From these studies, it was found that i.v. administration of the pure drug resulted in a relatively slow and poor permeation of OLN to the rat brain. The maximum drug

concentration (C_{\max}) found for pure OLN in brain was $2951.08 \pm 170.43 \text{ ng.g}^{-1}$ at 0.5 h (T_{\max}) of the post dosing.

Intra-venous administration of PCL NP and GLY NP resulted in C_{\max} of $4143.03 \pm 328.85 \text{ ng.g}^{-1}$ and $5210.06 \pm 413.54 \text{ ng.g}^{-1}$ respectively in brain, at 1 h (T_{\max}) of the post dosing, which was much higher as compared to pure OLN administration. Moreover, these formulations demonstrated approximately two fold increase in MRT against the OLN solution ($13.01 \pm 0.36 \text{ h}$ for PCL NP & $10.46 \pm 0.67 \text{ h}$ for GLY NP as compared to MRT of $6.25 \pm 0.40 \text{ h}$ for OLN solution).

In case of coated nanoparticles, it was found that, i.v. administration resulted in very high increase in uptake and retention of the OLN, with increased AUC^{∞} of $160629.8 \pm 17131.38 \text{ ng.h.mL}^{-1}$ for C PCL NP & $189931.22 \pm 19356.08 \text{ ng.h.mL}^{-1}$ for C GLY NP. These coated formulations showed a very high MRT of $19.37 \pm 0.84 \text{ h}$ and $17.94 \pm 0.89 \text{ h}$ for C PCL NP and C GLY NP respectively.

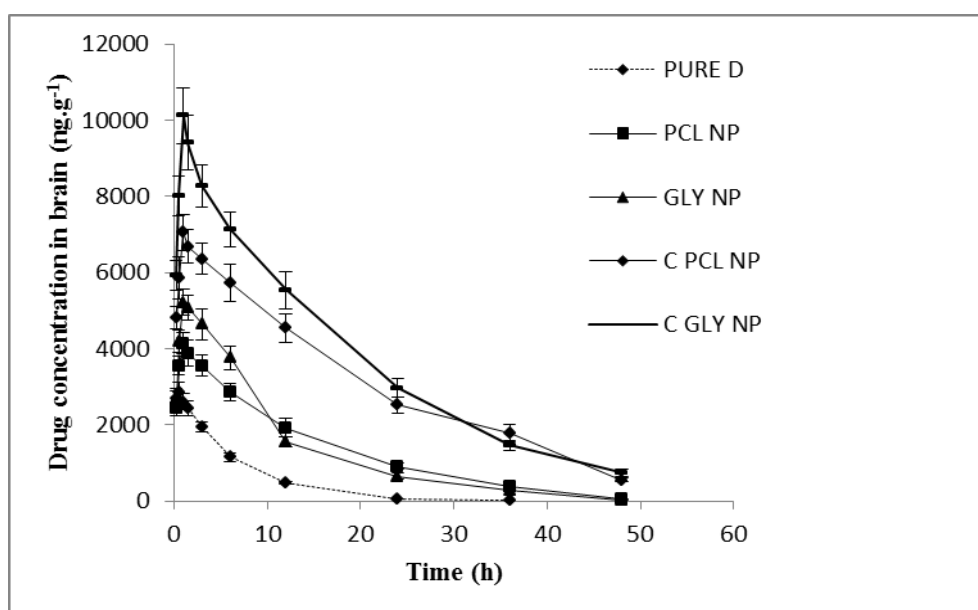


Figure 6.2: OLN concentration in brain versus time profile following i.v. administration of the pure OLN and OLN loaded nanoparticles in rats

The increase in AUC along with high MRT demonstrated higher permeation of the drug to brain in un-coated and coated nanoparticulate formulations with extended release properties. Similar results have been found in the literature for the better delivery of therapeutic molecule through nanocarriers, especially coated ones [11-14]. The higher concentration of OLN observed in the brain for these systems would be the result of transport of intact OLN loaded nanoparticulate systems through the BBB

by various mechanisms and subsequent simple diffusion of OLN from OLN loaded nanoparticulate systems.

Table 6.2: Pharmacokinetic parameters of OLN and OLN loaded NP in brain after i.v administration (n=3)

S.No	Parameters	OLN solution	PCL NP	GLY NP	C PCL NP	C GLY NP
1	AUC _{0-inf} (ng.h.g ⁻¹)	20240.87 ± 1823.09	62348.14 ± 7084.53	62595.86 ± 6527.18	160629.82 ± 17131.38	189931.31 ± 19356.08
2	C _{max} (ng.g ⁻¹)	2951.08 ± 170.43	4143.03 ± 328.85	5210.06 ± 413.54	7054.02 ± 583.99	10114.05 ± 884.88
3	MRT (h)	6.25 ± 0.40	13.01 ± 0.36	10.46 ± 0.67	19.37 ± 0.84	17.94 ± 0.89
4	Cl (L.h ⁻¹ .kg ⁻¹)	0.198 ± 0.017	0.0647 ± 0.007	0.0643 ± 0.006	0.025 ± 0.002	0.021 ± 0.002

As discussed in chapter 1, Kreuter J et al described number of possibilities that could explain the mechanism of the delivery of nanoformulations across the BBB, which include, increased retention of the nanoformulations in the brain blood capillaries, opening of the tight junctions between the brain endothelial cells, general surfactant effect of nanoformulations, inhibition of the efflux system, especially P-glycoprotein (Pgp) etc. [15, 16]. In the case of Tween 80 coated systems, additional to above mechanisms, endocytosis via the low density lipoprotein (LDL) receptor, mediated by the adsorption of apolipoprotein B and/or E from the blood is also a suggested mechanism for higher brain permeation. Probable low uptake of coated NP by macrophage system (discussed in next sections), further might have enhanced distribution of OLN to brain. These results indicated that the investigated nanoparticulate systems have been successfully targeted OLN to brain and could enhance greatly the efficacy of OLN to treat schizophrenia with decreased dose.

c. Liver biodistribution studies

Similar to brain distribution studies, OLN concentration in the rat liver following single i.v. dose administration of the pure drug, PCL NP, GLY NP, C PCL NP & C GLY NP was also determined. The results obtained are depicted in Figure 6.3. Furthermore, various pharmacokinetic parameters were calculated and are shown in Table 6.3. The administration of pure OLN resulted in a maximum drug concentration (C_{max}) of 12921.52 ± 597.76 ng.g⁻¹ in liver at a T_{max} of 0.5 h. Intra-venous administration of PCL NP and GLY NP indicated an increase in C_{max} of 24763.89 ± 2169.91 ng.g⁻¹ and 36210.41 ± 2022.62 ng.g⁻¹ respectively at a T_{max} of 1 h. Besides,

there was an increase in MRT of these formulations with values, 10.61 ± 0.35 h for PCL NP and 9.10 ± 0.90 h for GLY NP, as compared to an MRT of 6.31 ± 0.43 h for OLN solution.

In the case of i.v. administration of coated nanoparticles, comparatively less retention and AUC was observed than un-coated counterparts. However, AUC and MRT in liver of coated NP were found to be higher than pure OLN. AUC were found to be 113081.05 ± 10018.96 ng.h.g⁻¹ for C PCL NP and 92260.64 ± 4551.37 ng.h.g⁻¹ for C GLY NP whereas, MRT was found to be 8.61 ± 0.74 h for C PCL NP & 8.01 ± 0.30 h for C GLY NP.

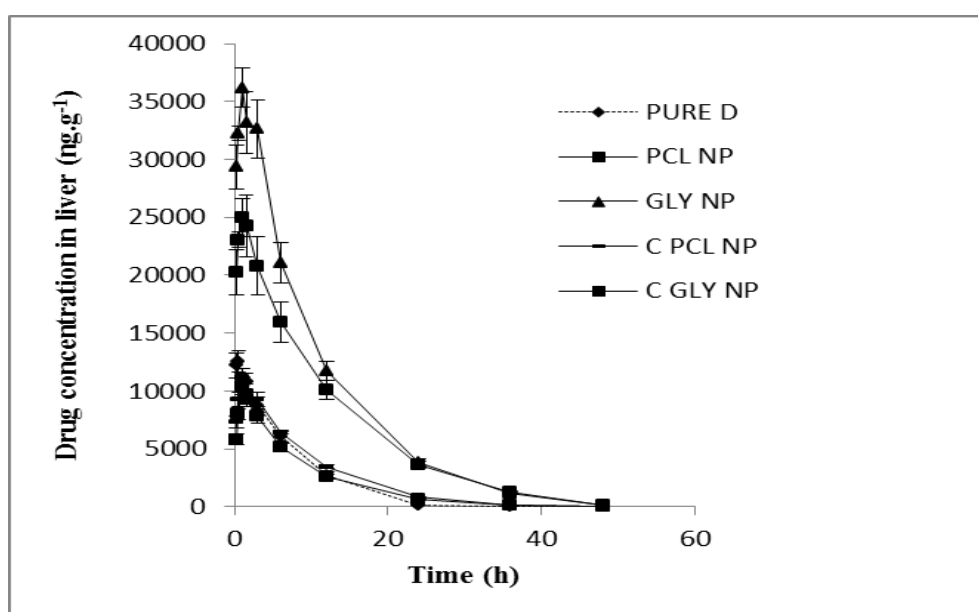


Figure 6.3: OLN concentration in liver versus time profile following i.v. administration of the pure OLN and OLN loaded nanoparticles in rats

Table 6.3: Pharmacokinetic parameters of OLN and OLN loaded NP in liver after i.v. administration (n=3)

S. No	Parameters	OLN solution	PCL NP	GLY NP	C PCL NP	C GLY NP
1	AUC _{0-inf} (ng.h.g ⁻¹)	98696.11 ± 8665.65	322152.83 ± 28155.30	404281.29 ± 21192.62	113081.05 ± 10018.96	92260.64 ± 4551.37
2	C _{max} (ng.g ⁻¹)	12921.52 ± 597.76	24763.89 ± 2169.91	36210.41 ± 2022.62	11733.77 ± 839.50	10574.09 ± 848.09
3	MRT (h)	6.31 ± 0.43	10.61 ± 0.35	9.10 ± 0.90	8.61 ± 0.74	8.01 ± 0.30
4	Cl (L.h ⁻¹ .kg ⁻¹)	0.041 ± 0.003	0.012 ± 0.001	0.009 ± 0.001	0.035 ± 0.002	0.043 ± 0.003

It is a very well known fact that i.v. administered nano/micro particulate systems of drug carriers with size less than 7 μm are considered as foreign and a major portion is immediately taken up by the circulating macrophages of the reticuloendothelial system [17, 18]. The high concentrations of OLN loaded nanoparticulate systems in liver indicated that OLN loaded NP are mainly accumulated in reticuloendothelial system (RES) organs. Several groups have reported similarly [19-21]. The RES system is considered to be a highly equipped defense mechanism with a major role in removing small foreign particles from blood circulation. This is done by coating those particles with serum components, the opsonins, which aids to target the nanoparticles/foreign bodies by phagocytic cells. The accumulation of OLN in the liver was reduced, when coated nanoparticles were investigated. This might be because of the hydrophilicity gained by the nanoparticulate systems by surfactant coating, which would resist/hinder the opsonin binding, thereby decreasing the macrophage uptake. This result supports the findings reported earlier by various groups for coated nanoparticulate systems [22, 23]. It is also possible that uncoated/coated OLN loaded nanoparticles might captured by the RES, and from there, the nanoparticles continuously released OLN into the blood stream, thereby resulting in elevated plasma and brain concentration of OLN.

d. Lungs biodistribution studies

The drug concentration-time profiles in lungs obtained after single i.v. dose of the pure drug and from nanoparticle formulations in rats are represented in Figure 6.4 and respective pharmacokinetics parameters are listed in Table 6.4. It has been found that i.v. administration of the pure OLN resulted in the maximum drug concentration (C_{max}) of $14476.35 \pm 434.76 \text{ ng.g}^{-1}$ in lungs, with AUC^{∞} of $53233.61 \pm 3659.11 \text{ ng.h.g}^{-1}$, and MRT of $4.18 \pm 0.44 \text{ h}$. The i.v. administration of PCL NP and GLY NP resulted in a maximum drug concentration (C_{max}) of $15239.22 \pm 999.31 \text{ ng.g}^{-1}$ and $14799.97 \pm 837.61 \text{ ng.g}^{-1}$ in lungs respectively. As compared to pure OLN, AUC^{∞} of PCL NP and GLY NP was increased to $132058.71 \pm 8077.68 \text{ ng.h.g}^{-1}$ and $125246.50 \pm 5934.61 \text{ ng.h.g}^{-1}$ respectively. Moreover, MRT was also found to increase to $7.11 \pm 0.38 \text{ h}$ and $7.03 \pm 0.22 \text{ h}$ respectively for PCL NP & GLY NP.

Intra-venous administration of coated formulations also resulted in increased distribution of the OLN to the lungs with increased AUC^{∞} of $145354.51 \pm 9140.79 \text{ ng.h.g}^{-1}$ and $148475.70 \pm 10788.77 \text{ ng.h.g}^{-1}$ for C PCL NP and C GLY NP respectively. Furthermore, administration of C PCL NP and C GLY NP resulted in

the C_{max} of $16788.39 \pm 1467.79 \text{ ng.g}^{-1}$ and $16367.18 \pm 1191.03 \text{ ng.g}^{-1}$ respectively in the lungs at a T_{max} of 1 h of the post dosing. The MRT was also found to be increased with values, $7.40 \pm 0.11 \text{ h}$ and $7.39 \pm 0.15 \text{ h}$ for C PCL NP and C GLY NP respectively.

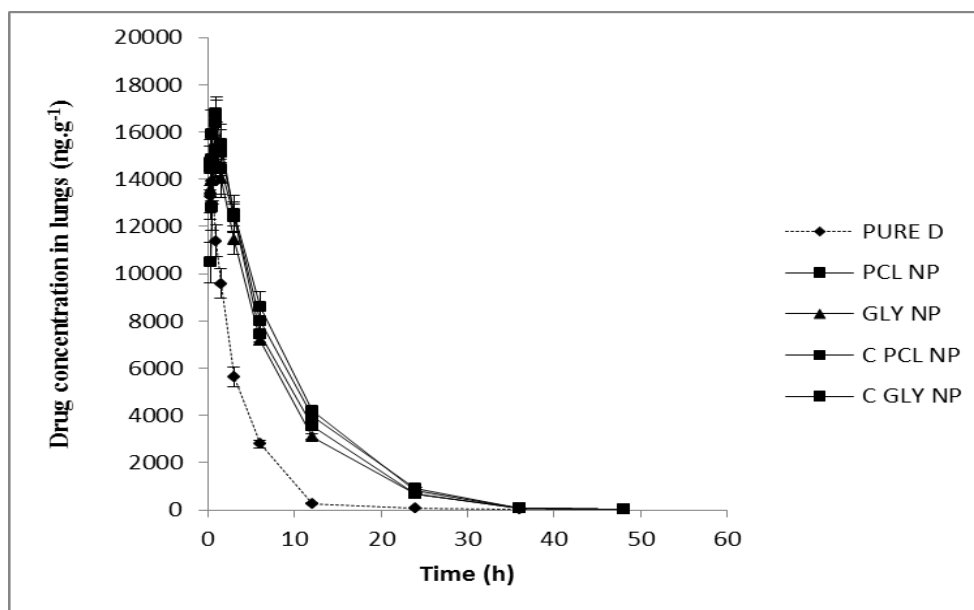


Figure 6.4: OLN concentration in lungs versus time profile following i.v. administration of the pure OLN and OLN loaded nanoparticles in rats

Table 6.4: Pharmacokinetic parameters of OLN and OLN loaded NP in lungs after i.v administration (n=3)

S.No	Parameters	OLN solution	PCL NP	GLY NP	C PCL NP	C GLY NP
1	AUC_{0-inf} (ng.h.g ⁻¹)	53233.61 ± 3659.11	132058.71 ± 8077.68	125246.50 ± 5934.61	145354.51 ± 9140.79	148475.70 ± 10788.77
2	C_{max} (ng.g ⁻¹)	14476.35 ± 434.76	15239.22 ± 999.31	14799.97 ± 837.61	16788.39 ± 1467.79	16367.18 ± 1191.03
3	MRT (h)	4.18 ± 0.44	7.11 ± 0.38	7.03 ± 0.22	7.40 ± 0.11	7.39 ± 0.15
4	Cl (L.h ⁻¹ .kg ⁻¹)	0.072 ± 0.003	0.030 ± 0.002	0.031 ± 0.002	0.027 ± 0.001	0.026 ± 0.002

e. Kidney biodistribution studies

The drug concentration-time profiles in kidney obtained after single i.v. dose of the pure drug, PCL NP, GLY NP, C PCL NP & C GLY NP in rats are represented in Figure 6.5 and respective pharmacokinetics parameters are listed in Table 6.5. Kidney

biodistribution studies of the pure OLN resulted in the maximum drug concentration (C_{max}) of $11523.92 \pm 581.32 \text{ ng.g}^{-1}$ at 1h (T_{max}) of the post dosing and AUC^{∞} of $65795.40 \pm 2929.72 \text{ ng.h.g}^{-1}$. MRT of the pure OLN in kidney was calculated to be $4.68 \pm 0.26 \text{ h}$.

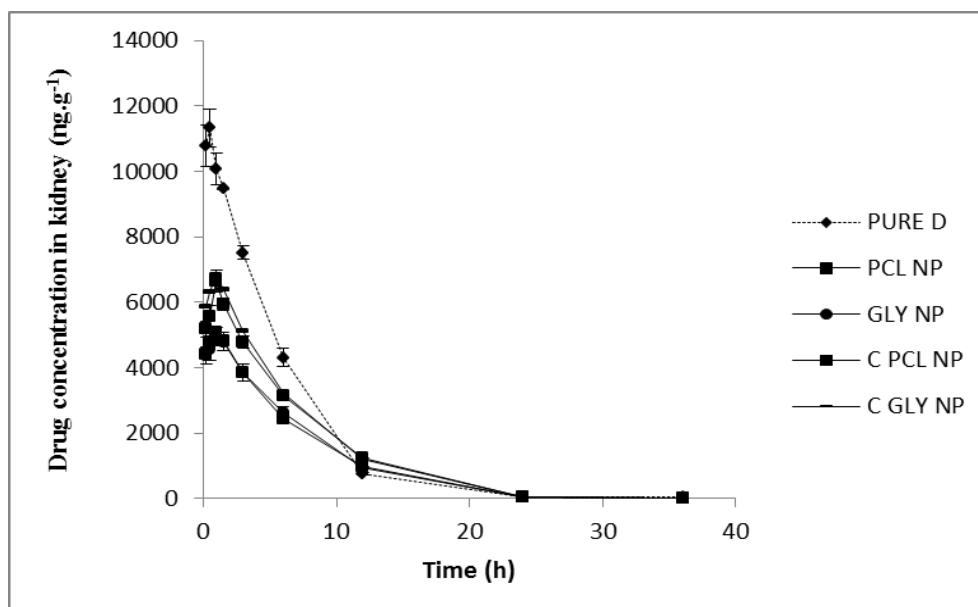


Figure 6.5: OLN concentration in kidney versus time profile following i.v. administration of the pure OLN and OLN loaded nanoparticles in rats

Table 6.5: Pharmacokinetic parameters of OLN and OLN loaded NP in kidney after i.v administration (n=3)

S.No.	Parameters	OLN solution	PCL NP	GLY NP	C PCL NP	C GLY NP
1	AUC_{0-inf} (ng.h.g ⁻¹)	65795.40 ± 2929.72	39510.91 ± 1840.80	39907.31 ± 2715.85	49688.74 ± 2557.19	51108.19 ± 2513.46
2	C_{max} (ng.g ⁻¹)	11523.92 ± 581.32	5095.45 ± 406.76	4986.65 ± 287.79	6642.82 ± 385.30	6831.77 ± 396.26
3	MRT (h)	4.68 ± 0.26	5.83 ± 0.11	5.84 ± 0.23	5.82 ± 0.24	5.58 ± 0.29
4	Cl (L.h ⁻¹ .kg ⁻¹)	0.06 ± 0.002	0.10 ± 0.003	0.11 ± 0.002	0.08 ± 0.002	0.07 ± 0.002

The biodistribution studies of PCL NP and GLY NP in kidney resulted in the maximum drug concentration (C_{max}) of $5095.45 \pm 406.76 \text{ ng.g}^{-1}$ and $4986.65 \pm 287.79 \text{ ng.g}^{-1}$ respectively, which were much less as compared to the values observed for pure OLN. Besides, AUC^{∞} of PCL NP and GLY NP were calculated to be $39510.91 \pm 1840.80 \text{ ng.h.g}^{-1}$ and $39907.31 \pm 2715.85 \text{ ng.h.g}^{-1}$ respectively. MRT of PCL NP and GLY NP were found to be $5.83 \pm 0.11 \text{ h}$ and $5.84 \pm 0.23 \text{ h}$ respectively.

In case of coated formulations: C PCL NP & for C GLY NP, distribution studies in kidney resulted in AUC^∞ of $49688.74 \pm 2557.19 \text{ ng.h.g}^{-1}$ and $51108.19 \pm 2513.46 \text{ ng.h.g}^{-1}$ respectively. Also, administration of C PCL NP & for C GLY NP resulted in the maximum drug concentration (C_{\max}) of $6642.82 \pm 385.30 \text{ ng.g}^{-1}$ and $6831.77 \pm 396.26 \text{ ng.g}^{-1}$ respectively. The MRT in kidneys were found to be $5.82 \pm 0.24 \text{ h}$ and $5.58 \pm 0.29 \text{ h}$ for C PCL NP & C GLY NP respectively.

The lower concentrations of OLN for both coated and un-coated nanoparticles in kidney as compared with OLN solution showed that kidney was not an effective targeting organ for these nanoparticulate systems. There have been recent reports that OLN is toxic to rat kidney cells in a dose dependent manner [24]. Therefore, administration of these developed formulations would decrease renal accumulation of the OLN, thereby decreasing the associated nephrotoxicity.

f. Spleen biodistribution studies

The OLN concentration in the rat spleen following single i.v. administration of the OLN solution, PCL NP, GLY NP, CPCL NP and CGLY NP was also estimated, which was plotted as a function of time and represented in Figure 6.6. The various pharmacokinetic parameters are calculated and listed in Table 6.6. Spleen biodistribution studies of OLN solution resulted in maximum drug concentration (C_{\max}) of $9291.92 \pm 761.24 \text{ ng.g}^{-1}$ at 0.5 h (T_{\max}) of the post dosing. Administration of the pure OLN resulted in AUC^∞ of $48979.76 \pm 3365.11 \text{ ng.h.g}^{-1}$. MRT of the pure drug in spleen was calculated to be $4.71 \pm 0.24 \text{ h}$.

Intra-venous administration of PCL NP and GLY NP resulted in the maximum drug concentration (C_{\max}) of $19097.43 \pm 763.69 \text{ ng.g}^{-1}$ and $20746.45 \pm 163.94 \text{ ng.g}^{-1}$ respectively in spleen which was higher than that of pure OLN. Also, AUC^∞ were found to be higher with values, $197167.30 \pm 13906.26 \text{ ng.h.g}^{-1}$ and $184358.61 \pm 7483.66 \text{ ng.h.g}^{-1}$ respectively for PCL NP and GLY NP. Moreover, MRT were also found to be increased to $8.51 \pm 0.16 \text{ h}$ and $7.41 \pm 0.31 \text{ h}$ for PCL NP and GLY NP respectively. In case of administration of C PCL NP and C GLY NP, maximum drug concentrations (C_{\max}) were found to be $7644.96 \pm 410.02 \text{ ng.g}^{-1}$ and $6441.44 \pm 500.74 \text{ ng.g}^{-1}$ respectively in the spleen, which were much lesser than that of un-coated formulations. AUC^∞ also were less for coated formulations as compared to un-coated counterparts and were found to be $48129.95 \pm 2254.05 \text{ ng.h.g}^{-1}$ and $40716.11 \pm 2411.38 \text{ ng.h.g}^{-1}$ respectively for C PCL NP and C GLY NP. The MRT was also determined and were found to be $5.38 \pm 0.17 \text{ h}$ and $5.56 \pm 0.22 \text{ h}$ for C PCL NP & C

GLY NP respectively, which were lesser than coated ones, but higher than pure OLN. Spleen, a major component of RES system along with liver would consider administered nanoparticles as foreign bodies and would be taken up immediately, thereby increasing the drug concentration in spleen. However, coated nanoparticles could avoid macrophage systems more than that of un-coated nanoparticles.

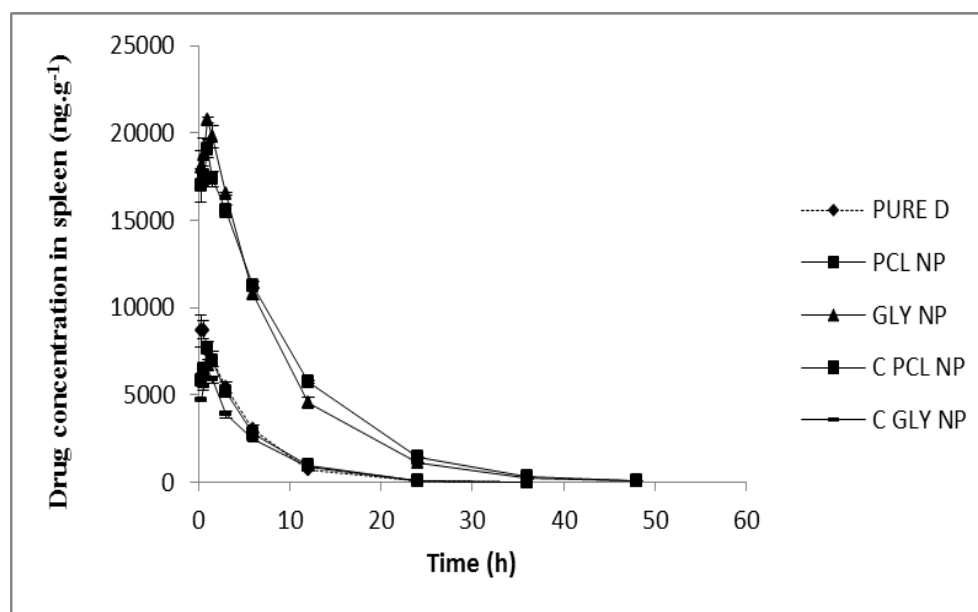


Figure 6.6: OLN concentration in spleen versus time profile following i.v. administration of the pure OLN and OLN loaded nanoparticles in rats

Table 6.6: Pharmacokinetic parameters of OLN and OLN loaded NP in spleen after i.v administration (n=3)

S.No	Parameters	OLN solution	PCL NP	GLY NP	C PCL NP	C GLY NP
1	AUC _{0-inf}	48979.76	197167.30	184358.61	48129.95	40716.11
	(ng.h.g ⁻¹)	± 3365.11	± 13906.26	± 7483.66	± 2254.05	± 2411.38
2	C _{max} (ng.g ⁻¹)	9291.92	19097.43	20746.45	7644.96	6441.44
		± 761.24	± 763.69	± 163.94	± 410.02	± 500.74
3	MRT (h)	4.71	8.51	7.41	5.38	5.56
		± 0.24	± 0.16	± 0.31	± 0.17	± 0.22
4	Cl (L.h ⁻¹ .kg ⁻¹)	0.08	0.020	0.021	0.08	0.09
		± 0.002	± 0.001	± 0.001	± 0.002	± 0.003

Similar results have been published, which have shown to take up the administered nanoparticulate systems by spleen through RES, thereby increasing the concentration

of the drug loaded in these systems in it [25]. The decreased accumulation of OLN in the spleen for tween coated nanoparticles was observed due to the hydrophilicity of these nanoparticulate systems by surfactant coating, which avoided macrophage systems. It has been reported that hydrophobic particulate systems are more prone towards macrophage uptake and hydrophilicity would decrease the possibility of phagocytosis process [26-28].

g. Heart biodistribution studies

The OLN concentration in the rat heart following single i.v. administration of the OLN solution, PCL NP, GLY NP, CPCL NP and CGLY NP was also determined. The concentration found was plotted as a function of time and represented in Figure 6.7 and various pharmacokinetic parameters calculated are listed in Table 6.7. Biodistribution studies in heart of the pure drug resulted in the maximum drug concentration (C_{max}) of $27298.15 \pm 1478.78 \text{ ng.g}^{-1}$ at 0.5 h (T_{max}) of the post dosing. AUC^{∞} and MRT were found to be $168641.3 \pm 2420.24 \text{ ng.h.g}^{-1}$ and $7.17 \pm 0.17 \text{ h}$ respectively.

For PCL NP and GLY NP, the maximum drug concentrations (C_{max}) observed in heart were $13095.85 \pm 853.15 \text{ ng.g}^{-1}$ and $14117.2 \pm 996.75 \text{ ng.g}^{-1}$ respectively. AUC^{∞} found for PCL NP and GLY NP were $112363.1 \pm 6970.09 \text{ ng.h.g}^{-1}$ and $118420.6 \pm 118420.6 \text{ ng.h.g}^{-1}$ respectively. The MRT were found to be $6.96 \pm 0.29 \text{ h}$ and $7.13 \pm 0.24 \text{ h}$ respectively for PCL NP and GLY NP.

Administration of coated nanoparticles resulted in maximum drug concentration (C_{max}) of $15181.44 \pm 611.91 \text{ ng.g}^{-1}$ in case of C PCL NP and $14703.94 \pm 1280.28 \text{ ng.g}^{-1}$ for C GLY NP respectively in the heart. Furthermore, administration of C PCL NP and C GLY NP resulted in AUC^{∞} of $130333.40 \pm 9052.32 \text{ ng.h.g}^{-1}$ and $133955.9 \pm 7304.18 \text{ ng.h.g}^{-1}$ respectively in the heart. The MRT were found to be $7.32 \pm 0.21 \text{ h}$ and $7.38 \pm 0.10 \text{ h}$ for C PCL NP and C GLY NP respectively. Unlike observed in other organs, lower concentrations of OLN in heart for both coated and un-coated nanoparticles showed that distribution of NP to heart was found to be lesser indicating higher distribution of pure drug. Therefore, administration of these formulations would decrease accumulation of the OLN in heart, which might help to decrease the toxicity associated with heart.

Several authors have observed similar results with other drugs, with less distribution of loaded drug to the heart, when administered in nanoparticulate systems [23, 29]. This is very significant since OLN produces high level of adverse cardiovascular

effects resulting in hypotension, prolonging ECG QT-corrected interval, chest pain, tachycardia, peripheral edema, ventricular tachycardia/fibrillation, ventricular arrhythmias and even sudden death [30-32]. By minimizing the distribution of OLN to the heart by incorporating in nanoparticulate systems, these adverse cardiovascular effects could be minimised to a great extent.

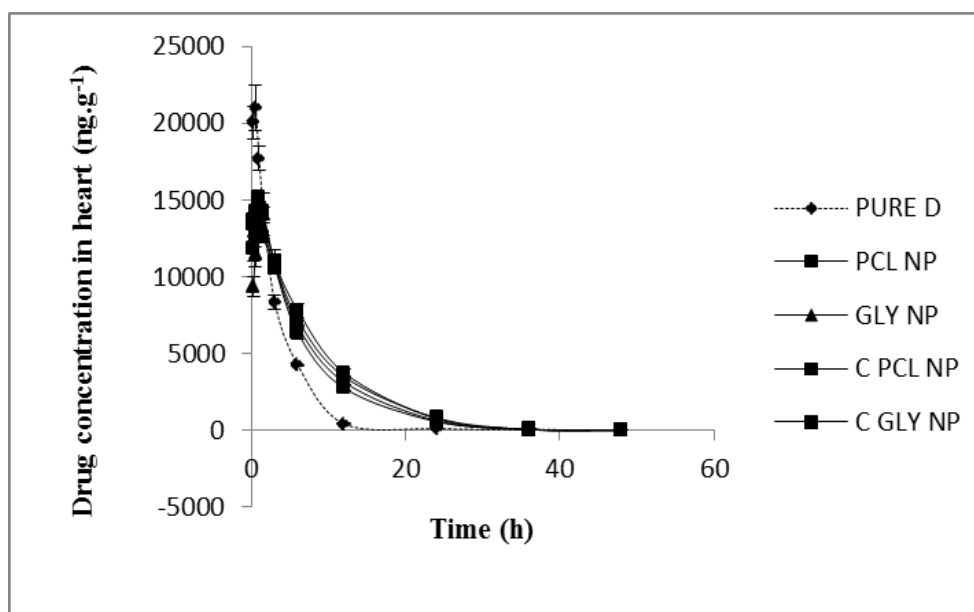


Figure 6.7: OLN concentration in heart versus time profile following i.v. administration of the pure OLN and OLN loaded nanoparticles in rats

Table 6.7: Pharmacokinetic parameters of OLN and OLN loaded NP in heart after i.v administration (n=3)

S.No	Parameters	OLN solution	PCL NP	GLY NP	C PCL NP	C GLY NP
1	AUC _{0-inf} (ng.h.g ⁻¹)	168641.3 ± 2420.24	112363.1 ± 6970.09	118420.6 ± 6767.78	130333.4 ± 9052.32	133955.9 ± 7304.18
2	C _{max} (ng.g ⁻¹)	27298.15 ± 1478.78	13095.85 ± 853.15	14117.2 ± 996.75	15181.44 ± 611.91	14703.94 ± 1280.28
3	MRT (h)	7.17 ± 0.17	6.96 ± 0.29	7.13 ± 0.24	7.32 ± 0.21	7.38 ± 0.10
4	Cl (L.h ⁻¹ .kg ⁻¹)	0.023 ± 0.001	0.035 ± 0.002	0.033 ± 0.002	0.031 ± 0.001	0.029 ± 0.001

Conclusions

The pharmacokinetic and biodistribution studies of OLN indicated that modified and selective distribution can be achieved by administering NP as found from results. It has been found that as compared to OLN solution, PCL NP, GLY NP, C PCL NP and CGLY NP have demonstrated higher AUC values along with prolonged residence time of OLN in the rat blood circulation. Increased plasma concentration levels of OLN for nanoparticulate systems indicated change in distribution profile of OLN. More importantly, the distribution of OLN to the brain was significantly enhanced with coated nanoparticulate systems (C PCL NP & C GLY NP), followed by uncoated nanoparticulate formulations (PCL NP, GLY NP) as compared with OLN solution. Biodistribution study showed low uptake of studied nanoparticulate systems by kidney and heart, thereby decreasing the nephrotoxicity and adverse cardiovascular effects. Therefore, pharmacokinetic and biodistribution studies confirmed that the biodistribution of the OLN could be modified effectively by incorporating in nanoparticulate drug delivery systems. By coating the NP with surfactant, uptake of macrophage can be reduced as found with liver and spleen distribution, where drug concentration and AUC were found to be much lower in coated NP than un-coated NP. The results of pharmacokinetic and biodistribution study indicate that OLN-loaded nanoparticulate systems may be highly promising for targeting of OLN with effective OLN concentrations in brain for prolonged period of time.

References

- [1] J. Panyam, V. Labhasetwar, Biodegradable nanoparticles for drug and gene delivery to cells and tissue, *Adv Drug Deliv Rev*, 55 (2003) 329-347.
- [2] R. Singh, J.W. Lillard, Nanoparticle-based targeted drug delivery, *Exp Mol Path*, 86 (2009) 215-223.
- [3] Y. Takakura, M. Hashida, Macromolecular carrier systems for targeted drug delivery: pharmacokinetic considerations on biodistribution, *Pharm Res*, 13 (1996) 820-831.
- [4] L.Z. Benet, D. Kroetz, L. Sheiner, J. Hardman, L. Limbird, Pharmacokinetics: the dynamics of drug absorption, distribution, metabolism, and elimination, *Goodman and Gilman's the pharmacological basis of therapeutics*, (1996) 3-27.
- [5] S. Wohlfart, S. Gelperina, J. Kreuter, Transport of drugs across the blood–brain barrier by nanoparticles, *J Control Rel*, 161 (2012) 264-273.
- [6] M. Snehalatha, V. Kolachina, R.N. Saha, A.K. Babbar, N. Sharma, R.K. Sharma, Enhanced tumor uptake, biodistribution and pharmacokinetics of etoposide loaded nanoparticles in Dalton's lymphoma tumor bearing mice, *J Pharm Bioal Sci*, 5 (2013) 290-297.
- [7] F.A. Dimer, M.C. Pigatto, A.R. Pohlmann, T.D. Costa, S.S. Guterres, LC-MS/MS method applied to preclinical pharmacokinetic investigation of olanzapine-loaded lipid-core nanocapsules, *Química Nova*, 37 (2014) 1371-1376.
- [8] J.K. Kim, J.S. Park, C.K. Kim, Development of a binary lipid nanoparticles formulation of itraconazole for parenteral administration and controlled release, *Int J Pharm*, 383 (2010) 209-215.
- [9] S.S. Dodiya, S.S. Chavhan, K.K. Sawant, A.G. Korde, Solid lipid nanoparticles and nanosuspension formulation of Saquinavir: preparation, characterization, pharmacokinetics and biodistribution studies, *J Microencapsul*, 28 (2011) 515-527.
- [10] A. Ambruosi, H. Yamamoto, J. Kreuter, Body distribution of polysorbate-80 and doxorubicin-loaded [14C] poly (butyl cyanoacrylate) nanoparticles after iv administration in rats, *J Drug Target*, 13 (2005) 535-542.
- [11] A.E. Gulyaev, S.E. Gelperina, I.N. Skidan, A.S. Antropov, G.Y. Kivman, J. Kreuter, Significant transport of doxorubicin into the brain with polysorbate 80-coated nanoparticles, *Pharm Res*, 16 (1999) 1564-1569.
- [12] B. Wilson, M.K. Samanta, K. Santhi, K.P.S. Kumar, N. Paramakrishnan, B. Suresh, Poly (n-butylcyanoacrylate) nanoparticles coated with polysorbate 80 for the

targeted delivery of rivastigmine into the brain to treat Alzheimer's disease, *Brain Res*, 1200 (2008) 159-168.

[13] S. Gelperina, O. Maksimenko, A. Khalansky, L. Vanchugova, E. Shipulo, K. Abbasova, R. Berdiev, S. Wohlfart, N. Chepurnova, J. Kreuter, Drug delivery to the brain using surfactant-coated poly (lactide-co-glycolide) nanoparticles: influence of the formulation parameters, *Eur J Pharm Biopharm*, 74 (2010) 157-163.

[14] R. Alyautdin, E. Tezikov, P. Range, D. Kharkevich, D. Begley, J. Kreuter, Significant entry of tubocurarine into the brain of rats by adsorption to polysorbate 80-coated polybutylcyanoacrylate nanoparticles: an in situ brain perfusion study, *J Microencapsul*, 15 (1998) 67-74.

[15] J. Kreuter, Influence of the surface properties on nanoparticle-mediated transport of drugs to the brain, *J Nanosci Nanotechnol*, 4 (2004) 484-488.

[16] J. Kreuter, Nanoparticulate systems for brain delivery of drugs, *Adv Drug Deliv Rev*, 64, Supplement (2012) 213-222.

[17] R.A. Petros, J.M. DeSimone, Strategies in the design of nanoparticles for therapeutic applications, *Nat Rev Drug Discov*, 9 (2010) 615-627.

[18] R. Löbenberg, L. Araujo, H. von Briesen, E. Rodgers, J. Kreuter, Body distribution of azidothymidine bound to hexyl-cyanoacrylate nanoparticles after iv injection to rats, *J Control Rel*, 50 (1998) 21-30.

[19] N. Chiannikulchai, N. Ammouy, B. Caillou, J.P. Devissaguet, P. Couvreur, Hepatic tissue distribution of doxorubicin-loaded nanoparticles after iv administration in reticulosarcoma M 5076 metastasis-bearing mice, *Cancer Chemother Pharmacol*, 26 (1990) 122-126.

[20] F. Ahsan, I.P. Rivas, M.A. Khan, A.I.T. Suarez, Targeting to macrophages: role of physicochemical properties of particulate carriers—liposomes and microspheres—on the phagocytosis by macrophages, *J Control Rel*, 79 (2002) 29-40.

[21] Z. Xu, L. Chen, W. Gu, Y. Gao, L. Lin, Z. Zhang, Y. Xi, Y. Li, The performance of docetaxel-loaded solid lipid nanoparticles targeted to hepatocellular carcinoma, *Biomater*, 30 (2009) 226-232.

[22] L. Araujo, R. Löbenberg, J. Kreuter, Influence of the surfactant concentration on the body distribution of nanoparticles, *J Drug Target*, 6 (1999) 373-385.

[23] M. Liu, H. Li, G. Luo, Q. Liu, Y. Wang, Pharmacokinetics and biodistribution of surface modification polymeric nanoparticles, *Archiv Pharm Res*, 31 (2008) 547-554.

- [24] M. Gulec, H. Ozcan, E. Oral, O.B. Dursun, D. Unal, S. Aksak, J. Selli, O.N. Keles, B. Unal, A. Albayrak, Nephrotoxic effects of chronically administered olanzapine and risperidone in male rats, *Bull Clinic Psychopharm*, 22 (2012) 139-147.
- [25] V. Saxena, M. Sadoqi, J. Shao, Polymeric nanoparticulate delivery system for Indocyanine green: biodistribution in healthy mice, *Int J Pharm*, 308 (2006) 200-204.
- [26] S.D. Li, L. Huang, Nanoparticles evading the reticuloendothelial system: role of the supported bilayer, *Biochim Biophys Acta*, 1788 (2009) 2259-2266.
- [27] U. Gaur, S.K. Sahoo, K. De Tapas, P.C. Ghosh, A. Maitra, P. Ghosh, Biodistribution of fluoresceinated dextran using novel nanoparticles evading reticuloendothelial system, *Int J Pharm*, 202 (2000) 1-10.
- [28] M. Hans, A. Lowman, Biodegradable nanoparticles for drug delivery and targeting, *Curr Opin Solid State Mater Sci*, 6 (2002) 319-327.
- [29] Y.M. Tsai, C.F. Chien, L.C. Lin, T.H. Tsai, Curcumin and its nano-formulation: the kinetics of tissue distribution and blood–brain barrier penetration, *Int J Pharm*, 416 (2011) 331-338.
- [30] P. Pacher, V. Kecskemeti, Cardiovascular side effects of new antidepressants and antipsychotics: new drugs, old concerns?, *Curr Pharm Des*, 10 (2004) 2463-2475.
- [31] W.A. Ray, S. Meredith, P.B. Thapa, K.G. Meador, K. Hall, K.T. Murray, Antipsychotics and the risk of sudden cardiac death, *Archiv Gen Psychiatry*, 58 (2001) 1161-1167.
- [32] A.H. Glassman, J.T. Bigger, Antipsychotic drugs: prolonged QTc interval, torsade de pointes, and sudden death, *Am J Psychiatry*, (2014) 774-1782.

Chapter 7

In-vivo evaluation and adverse effects studies

7.1 Introduction

Novel delivery systems are essential for better therapeutic efficacy and patient compliance. Apart from pharmacokinetic and biodistribution studies, it is necessary to study the therapeutic efficacy of developed delivery systems [1-3]. Thus, efficacy of the developed formulations should be investigated and well understood in appropriate animal models before performing the clinical studies. Moreover, adverse effects exhibited by many drugs and their conventional dosage forms could be minimized/modified by designing suitable novel drug delivery systems [4, 5]. The investigated drug, OLN is reported to produce dose dependent extrapyramidal adverse effects and weight gain, because of which there were reports that patients discontinued the OLN antipsychotic therapy [6-9]. Therefore, it is highly essential to investigate in-house prepared novel nanoparticulate drug delivery systems in animal model for its efficacy and adverse effects. Suitable animal models were adapted from the literature for the purpose.

7.2 Experimental

7.2.1 Animals

Wistar rats were selected for the study and the detailed process were same as that discussed in chapter 6. All experimental protocols were approved by the Institutional Animal Ethics Committee (IAEC) prior to the commencement of work (Protocol No. IAEC/RES/13/14/REV-2/17/16).

7.2.2 In-vivo evaluation of efficacy of OLN formulations

Apomorphine induced sniffing and climbing behavior

For the behavioral observation, suitable procedure was identified and adopted from the literature and slightly modified as per the lab requirements [10-12]. Animals (Wistar rats) were individually habituated for 60 min by placing them into cage. Animals were randomly divided into six groups (n=6/group). Group-I consisted of vehicle control, Group-II Pure OLN, Group-III PCL NP, Group-IV C PCL NP, Group-V GLY NP and Group-VI C GLY NP. Each group was administered with their respective drug/formulations at a daily dose equivalent to OLN 3 mg kg⁻¹. Phosphate buffer saline with pH 7.4 was selected as the vehicle control. Administration of pure OLN/Formulations/vehicle control was followed by immediate subcutaneous injection of apomorphine (2.5 mg/kg) at several time points (30 min, 1, 4, 8, 12, 24 and 48 h) in order to induce the psychotic symptoms. Sniffing and climbing

behavioral were observed from 11 to 20 min after every single apomorphine injection. Animals were observed for sniffing and climbing behavior for first 10 s of every minute (from 11-20 min). Sniffing was considered when rat showed continuous sniffing behavior for 3 s and the score was given as 0 for disturbed sniffing and 1 for continuous sniffing. Climbing score was considered 0 for four paws on the floor and 1 when all four paws were above the floor on the cage. The score of sniffing/climbing could vary in a range of 0 to 10 for the observation period.

7.2.3 Extrapyramidal side effects/ catalepsy (EPS) Study

Method of Kalkman et al., was adopted for catalepsy study [13]. Catalepsy was measured after i.v. administration of vehicle/PURE OLN/PCL NP/C PCL NP/GLY NP/C GLY NP at 0, 30, 60,120, 180, and 240 min, in a noise free and dimly lit laboratory room. A dose equivalent to 10 mg kg⁻¹ of drug was selected for pure drug as well as all the formulations under study. Forepaws of each animal was individually placed on a wooden block at a height of 7 cm, and the time taken by the animal to withdraw both the paws from the wooden block was measured as catalepsy score in seconds (s). The cut off time was 45 s. Graph Pad PRISM software version 2.01 (Graph Pad Software, La Jolla, USA) was used for data analysis. Values were expressed as mean ± standard error of the mean (S.E.M.). One way analysis of variance (ANOVA) followed by Dunnett's post test for multiple comparison was used for analysis of differences between various groups for catalepsy score and body weight measurement, where P<0.05 was considered statistically significant.

7.2.4 Weight gain Study

The procedure for weight gain study of OLN and OLN loaded nanoparticulate systems were as follows [14-16]. Animals (female rats) were randomly divided into six groups (n=6/group). Group-I consisted of Vehicle control, Group-II Pure OLN, Group-III PCL NP, Group-IV C PCL NP, Group-V GLY NP, Group-VI C GLY NP. Each group was administered with their respective drug/formulations at a daily dose equivalent to 3 mg/kg of drug for 28 days and body weight was measured every alternative day.

7.3 Results and discussion

7.3.1 In-vivo evaluation of efficacy of OLN formulations

This experiment was done to study the efficacy of pure and nanoparticulate formulations of olanzapine on apomorphine induced sniffing and climbing behavior in rats. The results are represented in Figure 7.1 to 7.14. Pure olanzapine at 3 mg kg⁻¹,

i.v. inhibited ($P < 0.01$) the apomorphine induced sniffing and climbing behavior in rats at 30 min, 1, 4, 8 h respectively after apomorphine injection (2.5 mg kg^{-1} , s.c.). Nanoparticulate formulations of olanzapine PCL NP, C PCL NP, GLY NP, C GLY NP at 3 mg/kg , i.v., significantly ($P < 0.01$) inhibited the apomorphine induced sniffing and climbing behavior in rats at 30 min, 1, 4, 8, 24 and 48 h after apomorphine injection (2.5 mg kg^{-1} , s.c). Degree of inhibition was found to be more in nanoparticles and all were found to produce efficacy for longer time (upto 48 h) indicating extended efficacy. These results have demonstrated an improved therapeutic efficacy of OLN-loaded nanoparticulate systems than pure OLN. The antipsychotic effect of OLN-loaded NP was maintained for a prolonged period of time. The sustained release of OLN from the nanoformulations would have resulted in the prolonged period of activity.

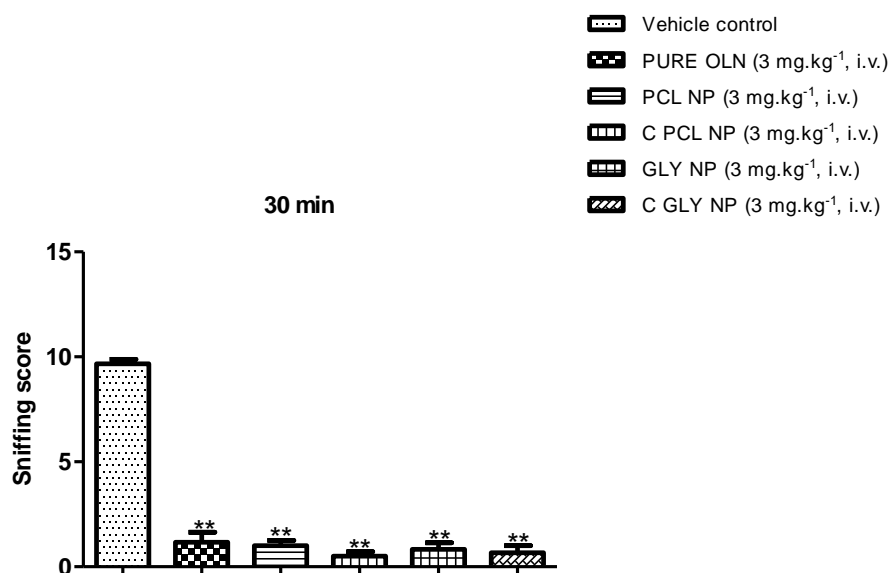


Figure 7.1: Effect of pure olanzapine and nanoparticulate formulations of olanzapine on apomorphine induced sniffing behavior at 30 min. Values represents mean \pm S.E.M., ** $P < 0.01$ vs vehicle control, $n = 6/\text{group}$.

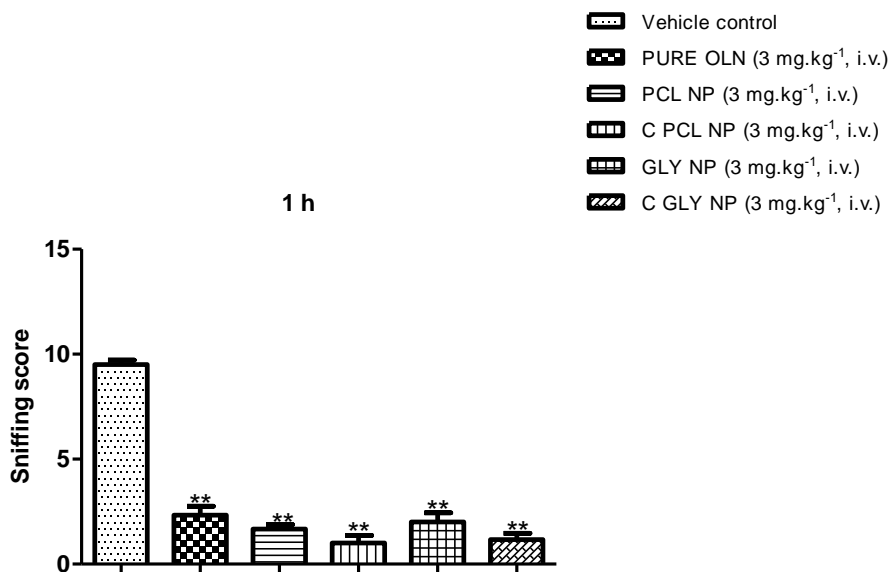


Figure 7.2: Effect of pure olanzapine and nanoparticulate formulations of olanzapine on apomorphine induced sniffing behavior at 1 h. Values represents mean \pm S.E.M., **P<0.01 vs vehicle control, n = 6/group.

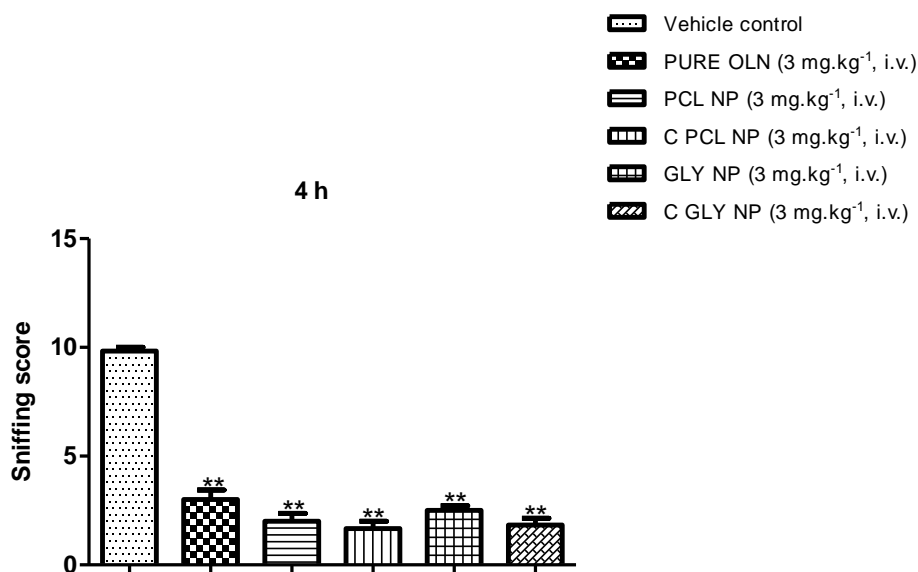


Figure 7.3: Effect of pure olanzapine and nanoparticulate formulations of olanzapine on apomorphine induced sniffing behavior at 4 h. Values represents mean \pm S.E.M., **P<0.01 vs vehicle control, n = 6/group.

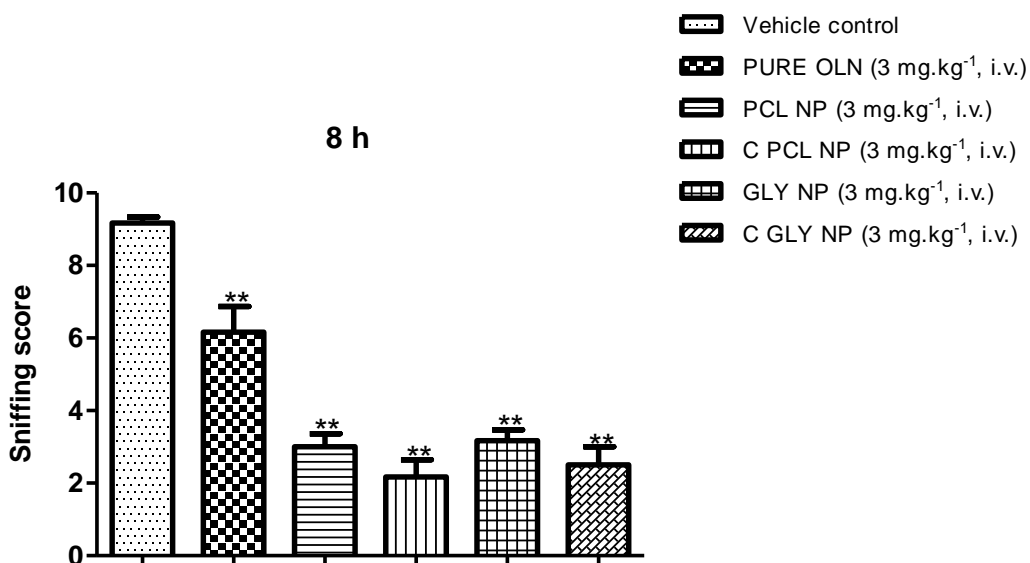


Figure 7.4: Effect of pure olanzapine and nanoparticulate formulations of olanzapine on apomorphine induced sniffing behavior at 8 h. Values represents mean ± S.E.M., **P<0.01 vs vehicle control, n = 6/group.

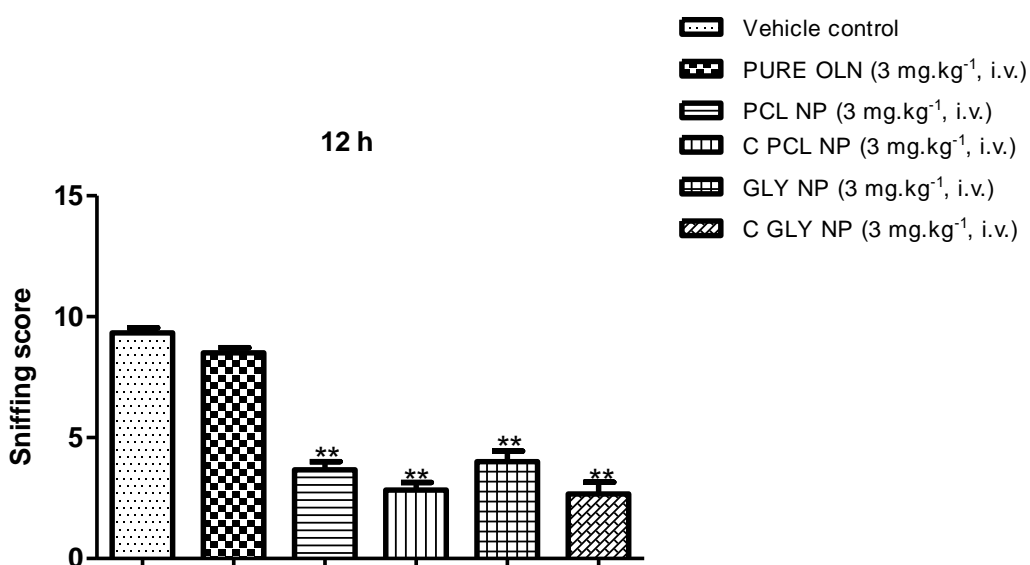


Figure 7.5: Effect of pure olanzapine and nanoparticulate formulations of olanzapine on apomorphine induced sniffing behavior at 12 h. Values represents mean ± S.E.M., **P<0.01 vs vehicle control, n = 6/group.

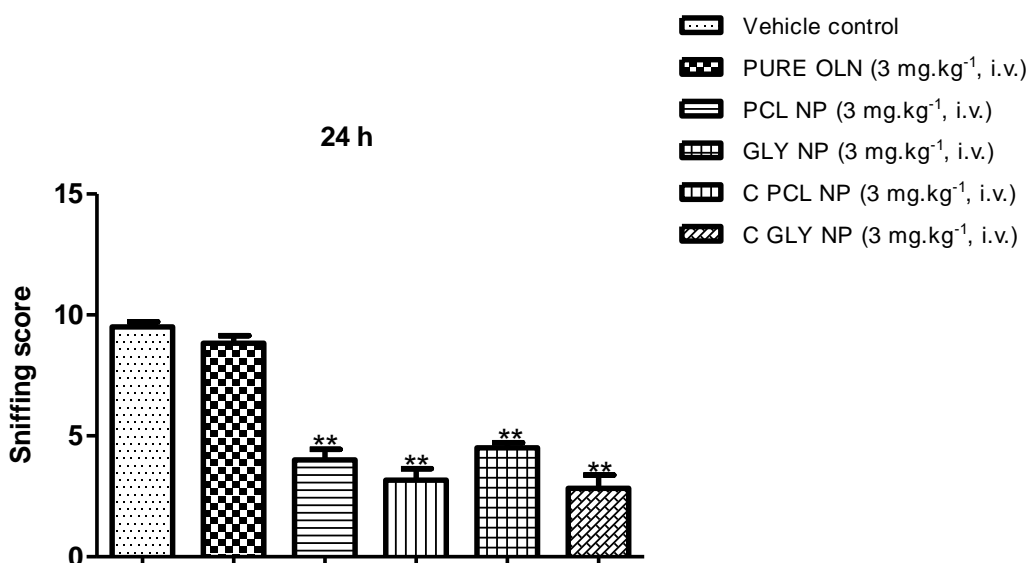


Figure 7.6: Effect of pure olanzapine and nanoparticulate formulations of olanzapine on apomorphine induced sniffing behavior at 24 h. Values represents mean \pm S.E.M., **P<0.01 vs vehicle control, n = 6/group.

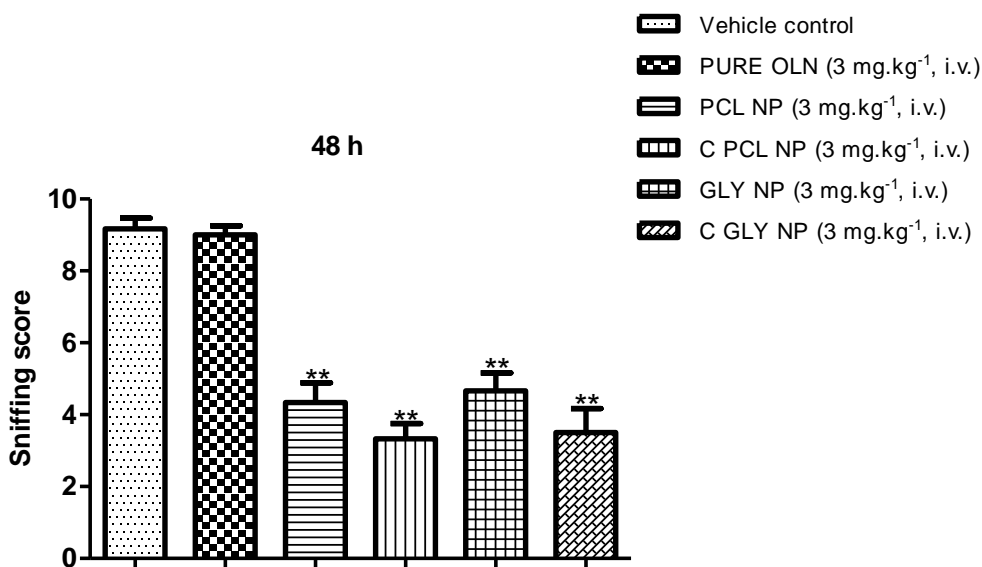


Figure 7.7: Effect of pure olanzapine and nanoparticulate formulations of olanzapine on apomorphine induced sniffing behavior at 48 h. Values represents mean \pm S.E.M., **P<0.01 vs vehicle control, n = 6/group.

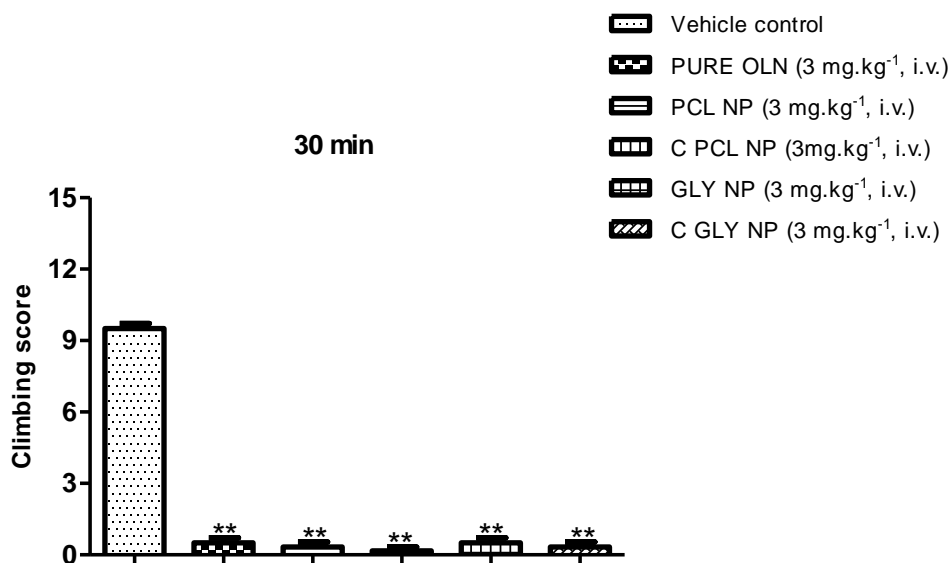


Figure 7.8: Effect of pure olanzapine and nanoparticulate formulations of olanzapine on apomorphine induced climbing behavior at 30 min. Values represents mean \pm S.E.M., **P<0.01 vs vehicle control, n = 6/group.

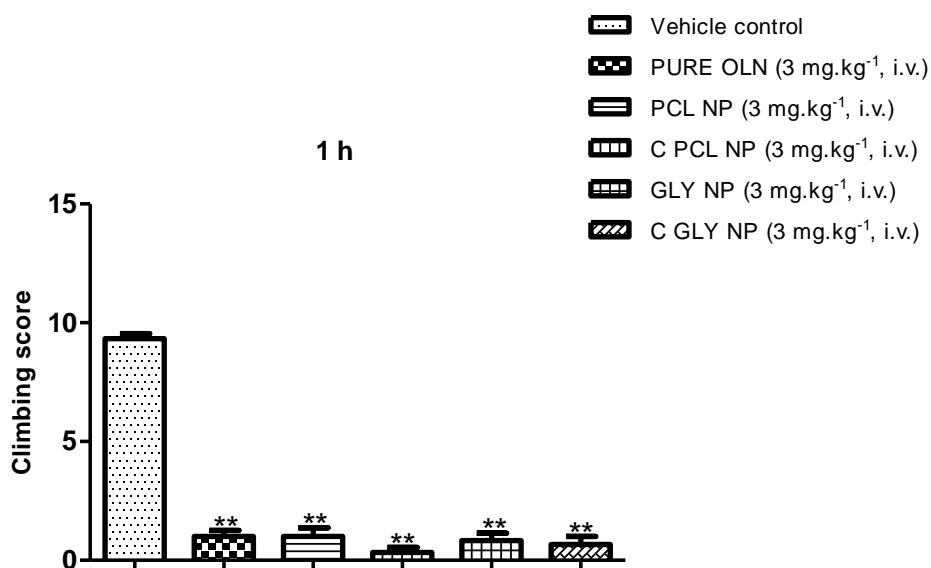


Figure 7.9: Effect of pure olanzapine and nanoparticulate formulations of olanzapine on apomorphine induced climbing behavior at 1 h. Values represents mean \pm S.E.M., **P<0.01 vs vehicle control, n = 6/group.

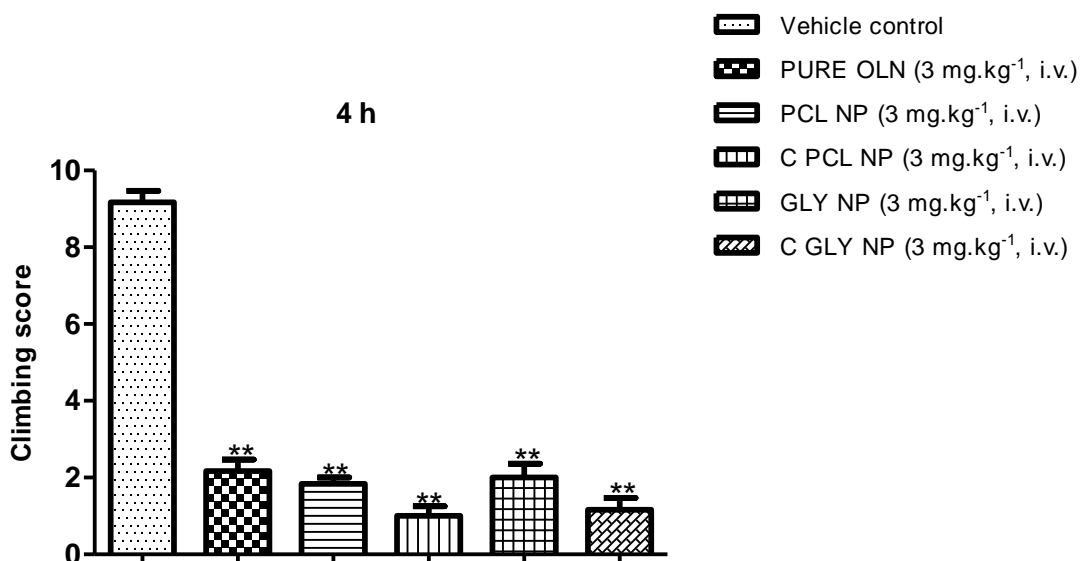


Figure 7.10: Effect of pure olanzapine and nanoparticulate formulations of olanzapine on apomorphine induced climbing behavior at 4 h. Values represents mean \pm S.E.M., **P<0.01 vs vehicle control, n = 6/group.

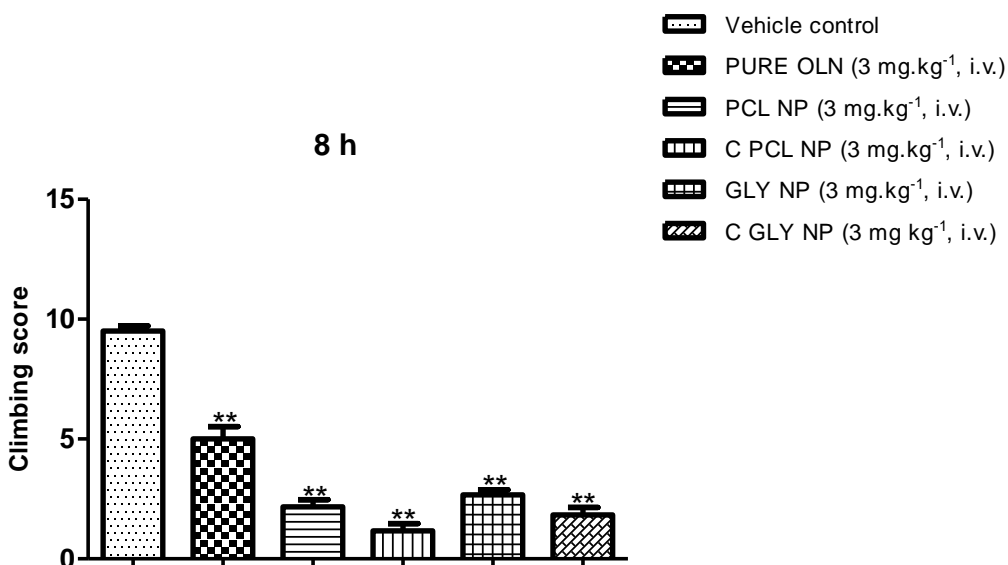


Figure 7.11: Effect of pure olanzapine and nanoparticulate formulations of olanzapine on apomorphine induced climbing behavior at 8 h. Values represents mean \pm S.E.M., **P<0.01 vs vehicle control, n = 6/group.

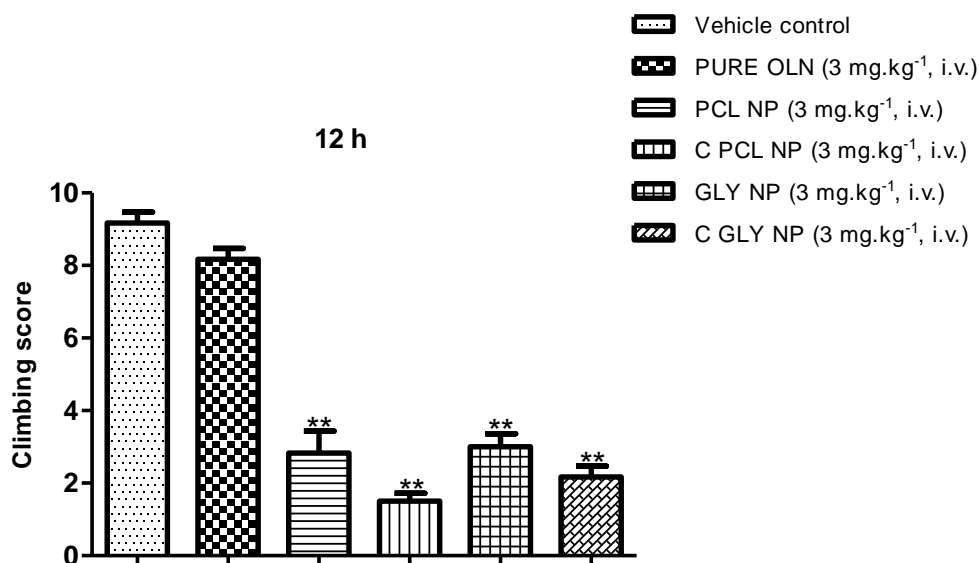


Figure 7.12: Effect of pure olanzapine and nanoparticulate formulations of olanzapine on apomorphine induced climbing behavior at 12 h. Values represents mean \pm S.E.M., **P<0.01 vs vehicle control, n = 6/group.

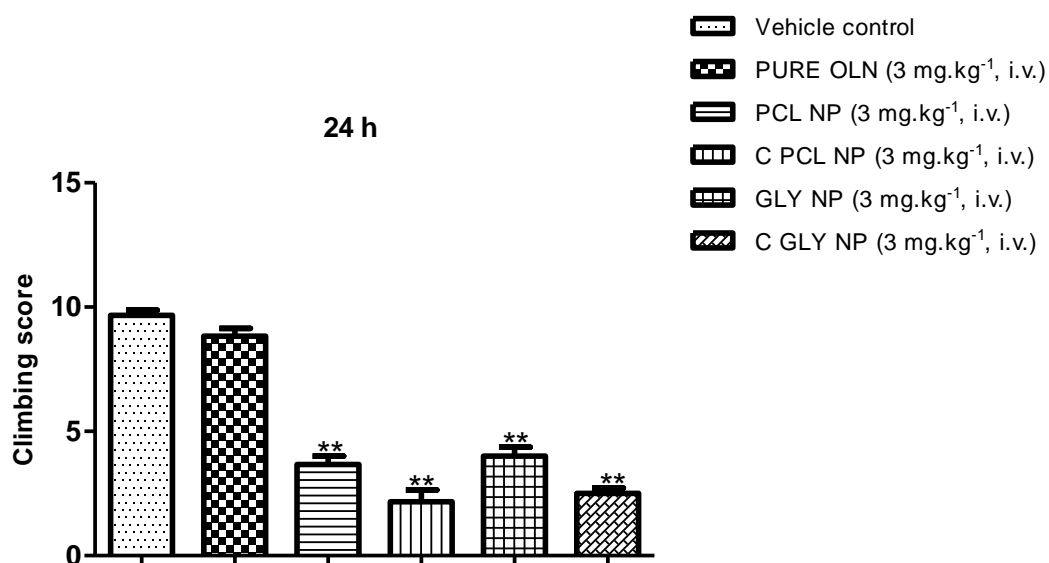


Figure 7.13: Effect of pure olanzapine and nanoparticulate formulations of olanzapine on apomorphine induced climbing behavior at 24 h. Values represents mean \pm S.E.M., **P<0.01 vs vehicle control, n = 6/group.

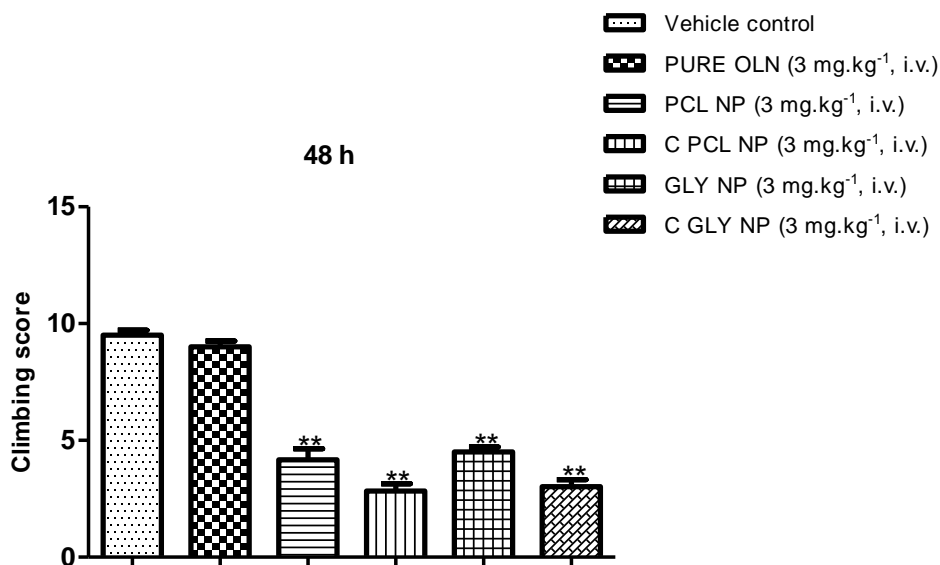


Figure 7.14: Effect of pure olanzapine and nanoparticulate formulations of olanzapine on apomorphine induced climbing behavior at 48 h. Values represents mean \pm S.E.M., ** $P < 0.01$ vs vehicle control, $n = 6$ /group.

7.3.2 Catalepsy studies:

The results obtained for catalepsy study are demonstrated in Figures 7.15 to 7.20. Animals administered with OLN pure drug displayed significantly ($P < 0.01$) higher catalepsy score at 30, 60, 120, 180 and 240 min compared to vehicle control group. PCL NP showed significant ($P < 0.05$) inhibition of catalepsy score at 60 and 120 min, whereas, GLY NP significantly ($P < 0.05$) inhibited catalepsy score at 60 min as compared to pure OLN group. The administration of C PCL NP and C GLY NP showed significant ($P < 0.05$) inhibition of catalepsy score at 30, 60, 120, 180 and 240 min respectively compared to pure OLN group.

Results indicate that coated nanoformulations C PCL NP and C GLY NP showed better inhibition of catalepsy behavior in rats. However, PCL NP and GLY NP also demonstrated inhibition of catalepsy score as compared to pure OLN. Hence, from these preliminary data it can be concluded that the nanoformulations could be effective in the treatment of psychotic disorders with minimum extra pyramidal symptoms. Since it was evident from the biodistribution study that, OLN loaded nanoparticulate systems permeate the brain preferentially than the pure drug, the assumption of lower delivery of OLN to the brain could not be considered as reason for the less occurrence of EPS. Similar results have been observed by scientific groups

recently and have suggested two major hypotheses for the efficiency of nanoparticulate systems in lowering the EPS: a) Most importantly, with OLN loaded NP, there could be an alteration in the distribution of OLN in the different areas of the brain itself. It is a well-known fact that EPS are commonly related to the blockade of dopamine receptors at the nigro-striatal system. Therefore, it has been suggested that OLN-loaded NP, especially the coated ones, target the drug preferentially to the mesocortico-limbic region of the brain (related to psychotic symptoms), reaching the nigro-striatal system in very low concentrations and thereby, minimizing the extrapyramidal adverse effects. b) OLN-loaded NP produces a sustained delivery of drug, without resulting in an excessive bioaccumulation in brain extrapyramidal area, as compared to pure OLN, thereby evoking less motor side effects [17-19].

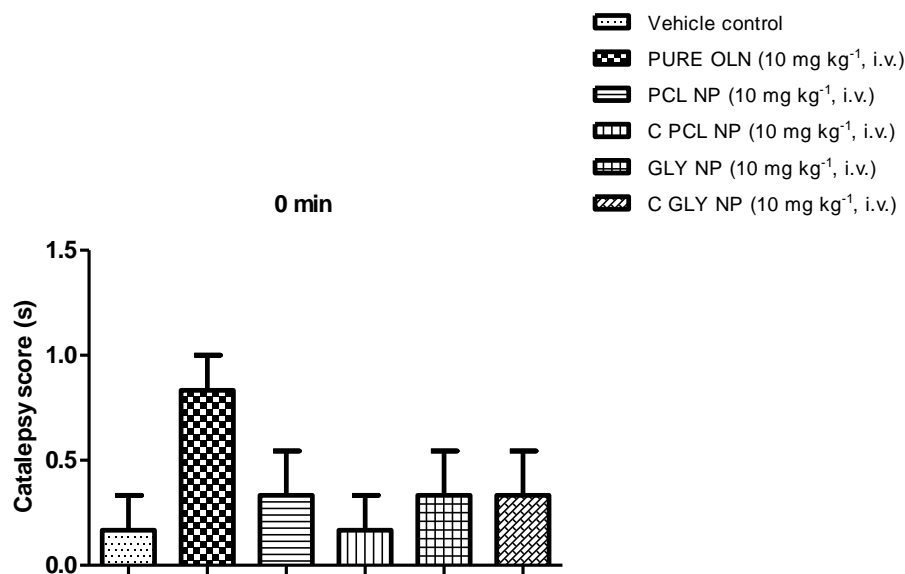


Figure 7.15: Effect of OLN and nanoformulations of OLN on catalepsy score (s) at 0 min. Values represents mean \pm S.E.M., n = 6/group.

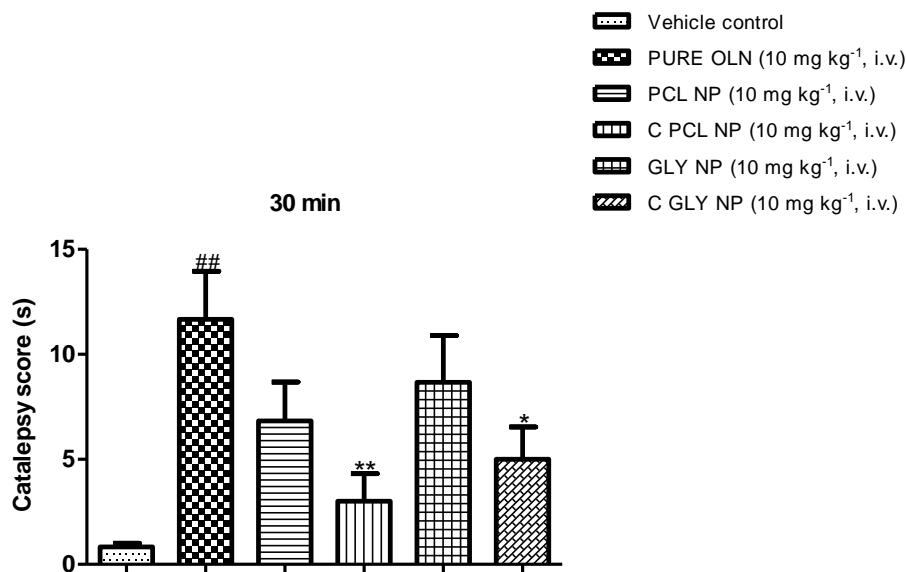


Figure 7.16: Effect of OLN and nanoformulations of OLN on catalepsy score (s) at 30 min. Values represents mean \pm S.E.M., ##P<0.01 vs vehicle control, *P<0.05; **P<0.01 vs pure OLN, n = 6/group.

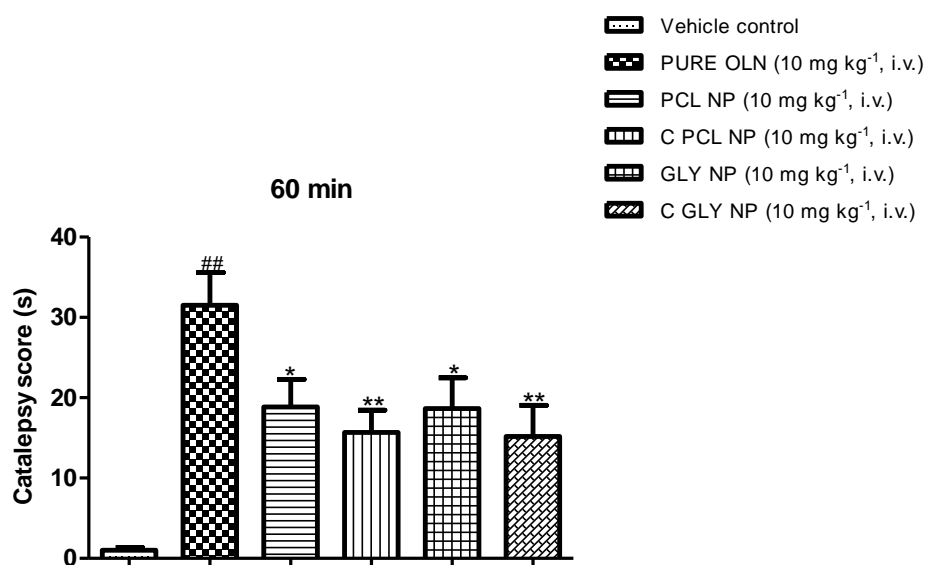


Figure 7.17: Effect of OLN and nanoformulations of OLN on catalepsy score (s) at 60 min. Values represents mean \pm S.E.M., ##P<0.01 vs vehicle control, *P<0.05; **P<0.01 vs pure OLN, n = 6/group.

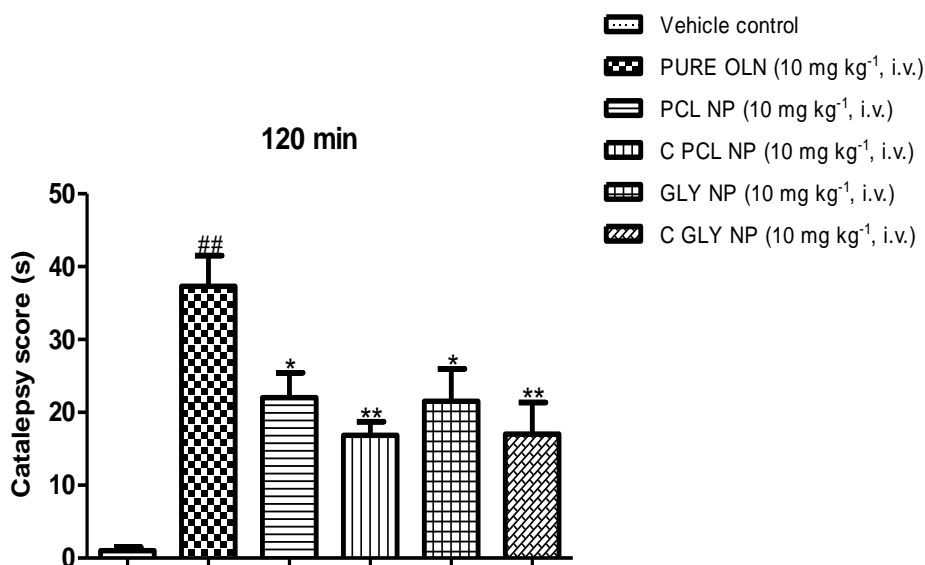


Figure 7.18: Effect of OLN and nanoformulations of OLN on catalepsy score (s) at 120 min. Values represents mean \pm S.E.M., ##P<0.01 vs vehicle control, *P<0.05; **P<0.01 vs pure OLN, n = 6/group.

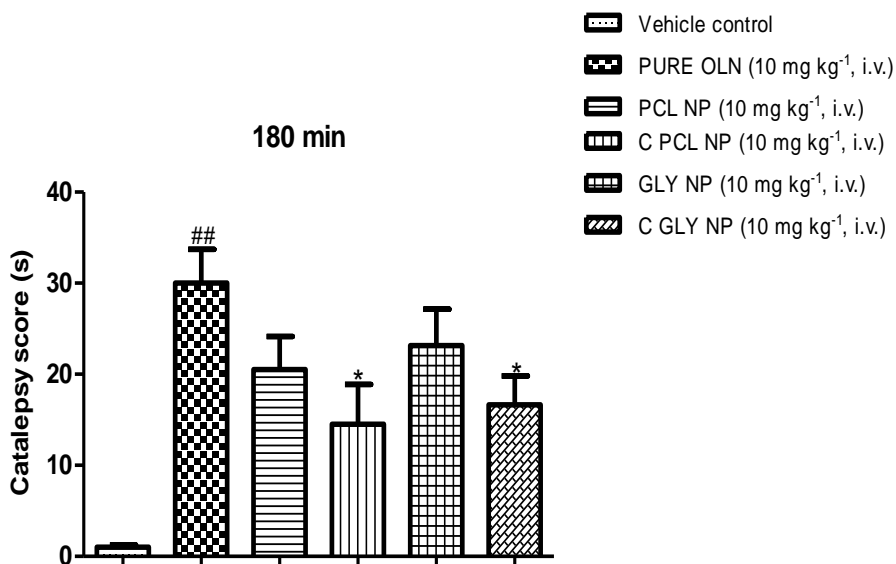


Figure 7.19: Effect of OLN and nanoformulations of OLN on catalepsy score (s) at 180 min. Values represents mean \pm S.E.M., ##P<0.01 vs vehicle control, *P<0.05 vs pure OLN, n = 6/group.

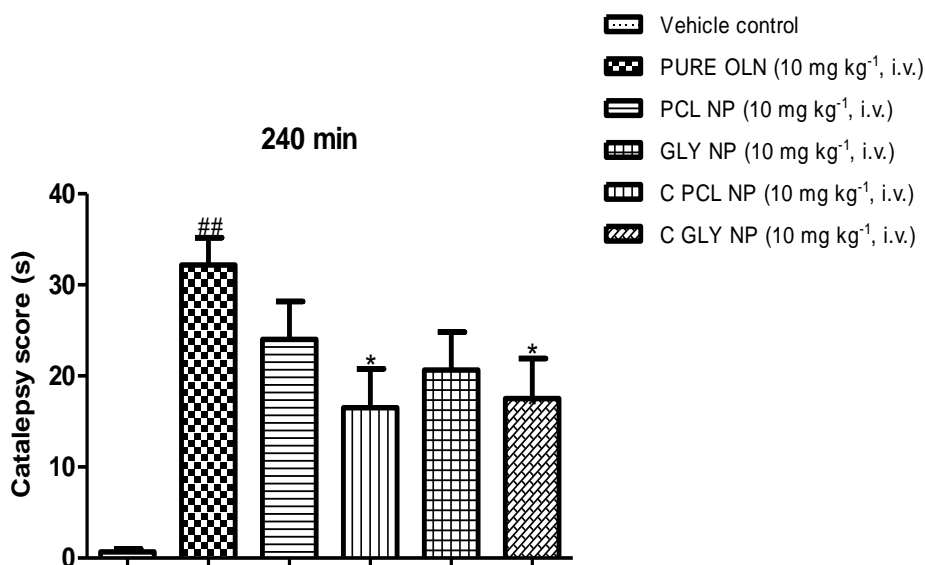


Figure 7.20: Effect of OLN and nanoformulations of OLN on catalepsy score (s) at 240 min. Values represents mean \pm S.E.M., ## $P < 0.01$ vs vehicle control, * $P < 0.05$ vs pure OLN, n = 6/group.

7.3.3 Weight gain studies:

Body weight of animals treated with pure OLN was significantly ($P < 0.05$) higher as compared to vehicle control group. The results are represented in Figure 7.21. Coated nanoformulations C PCL NP and C GLY NP showed significantly ($P < 0.05$) lesser weight gain as compared to pure OLN group.

Animals in PCL NP and GLY NP groups also demonstrated inhibition of weight gain as compared to pure OLN group, but to a lesser extent than that of coated formulations. A similar results of inhibition of weight gain using lipid-core nanocapsules have been reported recently [20].

Even though numerous authors have suggested various mechanisms for the increased body weight by OLN (H_1 receptor blockade, insulin/leptin dysregulation etc), the complete mechanism is not much understood yet [21-24]. Hence, a single mechanism of inhibition in the body weight by OLN-loaded nanoparticulate formulations could not be postulated. Therefore it has been suggested that the different distribution profiles of OLN-loaded nanoparticles inside the brain/peripheral tissues and controlled release would result in different levels of interactions with various receptors inside the brain and in peripheral tissues, thereby affecting the hormones and systems regulating body weight. A much detailed molecular level study with

sophisticated instruments should be performed in future for the complete understanding of the mechanism involved in inhibition of weight gain by the developed systems.

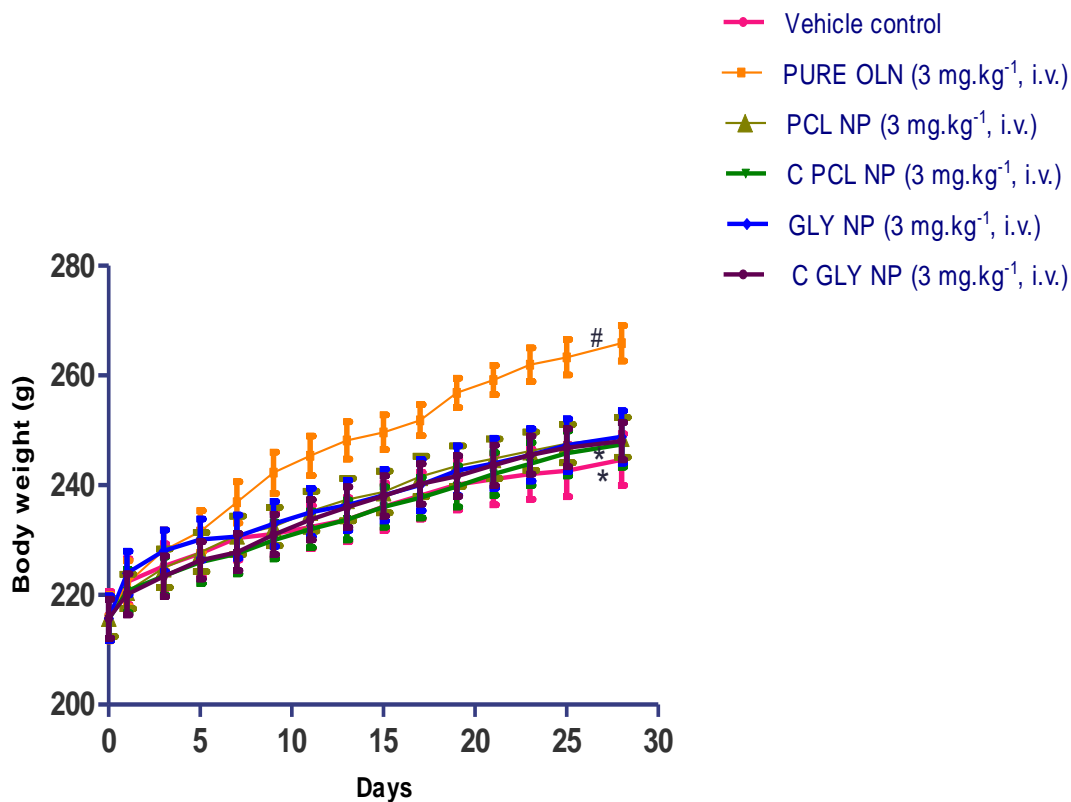


Figure 7.21: Effect of OLN and nanoformulations of OLN on body weight (g). Values represents mean \pm S.E.M., ###P<0.05 vs vehicle control, *P<0.05; vs OLN pure, n = 6/group.

Conclusions


In-vivo efficacy evaluation and adverse effects studies of OLN-loaded nanoparticulate systems in animal model have demonstrated an improved therapeutic efficacy, both in degree and duration with lesser side effects than pure OLN. The antipsychotic effect of OLN-loaded NP was maintained for a prolonged period of time, suggesting controlled or extended release of OLN from nanoparticles. The adverse effects studies demonstrated a decreased EPS and inhibition in weight gain as compared to the pure OLN. From these preliminary data it can be concluded that the OLN-loaded nanoformulations could be effective in the better treatment of psychotic disorders with minimum adverse effects. Further studies are necessary to investigate the exact mechanisms related to the findings of the study.

References

- [1] D. Peer, J.M. Karp, S. Hong, O.C. Farokhzad, R. Margalit, R. Langer, Nanocarriers as an emerging platform for cancer therapy, *Nat Nanotechnol*, 2 (2007) 751-760.
- [2] R. Zhou, R.V. Mazurchuk, J.H. Tamburlin, J.M. Harrold, D.E. Mager, R.M. Straubinger, Differential pharmacodynamic effects of paclitaxel formulations in an intracranial rat brain tumor model, *J Pharmacol Exp Ther*, 332 (2010) 479-488.
- [3] A. Hoffman, Pharmacodynamic aspects of sustained release preparations, *Adv Drug Deliv Rev*, 33 (1998) 185-199.
- [4] L. Zhang, F. Gu, J. Chan, A. Wang, R. Langer, O. Farokhzad, Nanoparticles in medicine: therapeutic applications and developments, *Clinic Pharmacol Ther*, 83 (2008) 761-769.
- [5] L. B. Peppas, J.O. Blanchette, Nanoparticle and targeted systems for cancer therapy, *Adv Drug Deliv Rev*, 64 (2012) 206-212.
- [6] H. Nasrallah, A review of the effect of atypical antipsychotics on weight, *Psychoneuroendocrinology*, 28 (2003) 83-96.
- [7] P.M. Haddad, S.G. Sharma, Adverse effects of atypical antipsychotics, *CNS drugs*, 21 (2007) 911-936.
- [8] M. De Hert, J. Detraux, R. V Winkel, W. Yu, C.U. Correll, Metabolic and cardiovascular adverse effects associated with antipsychotic drugs, *Nat Rev Endocrinol*, 8 (2012) 114-126.
- [9] A.A. Shirzadi, S.N. Ghaemi, Side effects of atypical antipsychotics: extrapyramidal symptoms and the metabolic syndrome, *Harv Rev Psychiatry*, 14 (2006) 152-164.
- [10] P. Fray, B. Sahakian, T. Robbins, G. Koob, S. Iversen, An observational method for quantifying the behavioural effects of dopamine agonists: contrasting effects of d-amphetamine and apomorphine, *Psychopharmacol*, 69 (1980) 253-259.
- [11] J. Waddington, Psychopharmacological studies in rodents: stereotaxic intracerebral injections and behavioural assessment, in, Manchester University Press, Manchester, UK, 1986.
- [12] M.S. Muthu, M.K. Rawat, A. Mishra, S. Singh, PLGA nanoparticle formulations of risperidone: preparation and neuropharmacological evaluation, *Nanomedicine*, 5 (2009) 323-333.

- [13] H. Kalkman, V. Neumann, M. Tricklebank, Clozapine inhibits catalepsy induced by olanzapine and loxapine, but prolongs catalepsy induced by SCH 23390 in rats, *Naunyn-Schmiedeberg's Archiv Pharmacol*, 355 (1997) 361-364.
- [14] J. M. Ringuet, P.C. Even, M. Lacroix, D. Tome, R. D Beaurepaire, A model for antipsychotic-induced obesity in the male rat, *Psychopharmacology*, 187 (2006) 447-454.
- [15] A.A. Arjona, S.X. Zhang, B. Adamson, R.J. Wurtman, An animal model of antipsychotic-induced weight gain, *Behav Brain Res*, 152 (2004) 121-127.
- [16] B. Pouzet, T. Mow, M. Kreilgaard, S. Velschow, Chronic treatment with antipsychotics in rats as a model for antipsychotic-induced weight gain in human, *Pharmacol Biochem Behav*, 75 (2003) 133-140.
- [17] D.M. Benvegna, R.C. Barcelos, N. Bouffleur, C.S. Pase, P. Reckziegel, F.C. Flores, A.F. Ourique, M.D. Nora, B.D Silva, R.C. Beck, M.E. Burger, Haloperidol-loaded polysorbate-coated polymeric nanocapsules decrease its adverse motor side effects and oxidative stress markers in rats, *Neurochem Int*, 61 (2012) 623-631.
- [18] D.M. Benvegna, R.C. Barcelos, N. Bouffleur, P. Reckziegel, C.S. Pase, A.F. Ourique, R.C. Beck, M.E. Burger, Haloperidol-loaded polysorbate-coated polymeric nanocapsules increase its efficacy in the antipsychotic treatment in rats, *Eur J Pharm Biopharm*, 77 (2011) 332-336.
- [19] M.S. Muthu, M.K. Rawat, A. Mishra, S. Singh, PLGA nanoparticle formulations of risperidone: preparation and neuropharmacological evaluation, *Nanomedicine*, 5 (2009) 323-333.
- [20] F.A. Dimer, M. Ortiz, C.S. Pase, K. Roversi, R.B. Friedrich, A.R. Pohlmann, M.E. Burger, S.S. Guterres, Nanoencapsulation of olanzapine increases its efficacy in antipsychotic treatment and reduces adverse effects, *J Biomed Nanotechnol*, 10 (2014) 1137-1145.
- [21] W.K. Kroeze, S.J. Hufeisen, B.A. Popadak, S.M. Renock, S. Steinberg, P. Ernsberger, K. Jayathilake, H.Y. Meltzer, B.L. Roth, H1-histamine receptor affinity predicts short-term weight gain for typical and atypical antipsychotic drugs, *Neuropsychopharmacol*, 28 (2003) 519-526.
- [22] R.P Iglesias, B.C. Facorro, O.M. Garcia, M.L.R. Bonilla, M.A. Jimenez, J.M.P Teran, M.T.G. Unzueta, J.A. Amado, J.L.V. Barquero, Weight gain induced by haloperidol, risperidone and olanzapine after 1 year: findings of a randomized clinical trial in a drug-naive population, *Schizophr Res*, 99 (2008) 13-22.

- [23] F. Brambilla, P. Monteleone, M. Maj, Olanzapine-induced weight gain in anorexia nervosa: Involvement of leptin and ghrelin secretion?, *Psychoneuroendocrinol*, 32 (2007) 402-406.
- [24] F. Theisen, M. Haberhausen, M. Firnges, P. Gregory, J. Reinders, H. Renschmidt, J. Hebebrand, J. Antel, No evidence for binding of clozapine, olanzapine and/or haloperidol to selected receptors involved in body weight regulation, *Pharmacogenomics J*, 7 (2007) 275-281.



Chapter 8

Summary and conclusions

8.1 Summary and conclusions

The effectiveness of a drug delivery system is highly dependent on its ability to deliver the therapeutic agent selectively/preferentially to the target site. Targeting the therapeutic agent to the brain is always a challenging task for the formulation scientists because of the presence of blood brain barrier, with tight junctions in the brain endothelial cells. The application of nanotechnology for the drug delivery to the brain opens the doors of new opportunities for the formulation scientists for the better delivery to brain. In the current research, studies were carried out to design and characterize polymeric/solid lipid nanoparticulate delivery systems for better delivery and to enhance the therapeutic efficacy of Olanzapine with controlled release and preferential brain distribution.

As analytical methods are highly essential for the successful development of any kind of drug delivery systems, new UV-spectrophotometric and liquid chromatographic (analytical and bio analytical) methods, suitable for the current project, were developed in-house and successfully validated. The developed UV-spectrophotometric and liquid chromatographic methods were found to be highly selective, sensitive, accurate, precise and robust, for the estimation of OLN in bulk and formulations. These validated analytical methods were applied successfully for the analysis of drug during various preformulation and formulation studies. The bioanalytical methods developed were found to be highly sensitive and selective for the estimation of OLN in biological samples such as rat plasma and various organs. These bioanalytical methods were successfully applied for the estimation of OLN during in-vivo pharmacokinetic and biodistribution studies of the pure drug and nanoparticulate formulations in rats.

Preformulation studies demonstrated that OLN exhibited a pH dependent solubility in different buffers with high solubility in acidic pH buffers and low solubility in basic pH buffers. Distribution coefficients in various buffers and dissociation constant were determined successfully. Solution state stability studies suggested that OLN was found to be more stable in acidic pH as compared to alkaline pH, and degradation process was found to be of first order. The solid admixtures of OLN with various excipients showed good stability with high drug content values during solid state stability studies. Results obtained for the drug-excipient compatibility studies by

DSC, demonstrated no significant interaction with various excipients selected for the formulation development.

OLN-loaded nanoparticles were prepared successfully using nanoprecipitation and emulsification-ultrasonication techniques. These methods were easy, reproducible, and found to produce nanoparticles with narrow size distribution and good entrapment efficiency. The influence of different formulation variables such as polymer/solid lipid concentration, surfactant concentration and drug proportions on studied responses such as size, encapsulation efficiency and drug content were studied in detail. OLN-loaded nanoparticles prepared from selected biodegradable polymer/solid lipids sustained the release of drug for prolonged period of time as found by the in-vitro release studies. Morphological studies by SEM have shown that both polymeric and solid lipid nanoparticles were spherical in shape with smooth surface. The formulations also exhibited high redispersibility after freeze drying and stability study results demonstrated good stability, with no significant change in the drug content, average particle size and release characters for the formulations stored at frozen conditions for a period of 6 months.

The pharmacokinetic and biodistribution studies of OLN formulations indicated that modified and selective distribution can be achieved by administering designed nanoparticulate systems. It has been found that as compared to OLN solution, PCL NP, GLY NP, C PCL NP and CGLY NP have demonstrated higher AUC values along with prolonged residence time of OLN in the rat blood circulation. Increased plasma concentration levels of OLN for nanoparticulate systems indicated change in distribution profile of OLN. More importantly, the distribution of OLN to the brain was significantly enhanced with surfactant coated nanoparticulate systems (C PCL NP & C GLY NP), followed by un-coated nanoparticulate formulations (PCL NP, GLY NP) as compared with OLN solution. Biodistribution study showed low uptake of studied nanoparticulate systems by kidney and heart, thereby decreasing possibility of nephrotoxicity and adverse cardiovascular effects. Therefore, pharmacokinetic and biodistribution studies confirmed that the biodistribution of the OLN could be modified effectively by incorporating in nanoparticulate drug delivery systems. By coating the NP with surfactant, uptake of macrophage can be reduced as found with liver and spleen distribution, where drug concentration and AUC were found to be much lower in coated NP than un-coated NP. The results of pharmacokinetic and

biodistribution study indicate that OLN-loaded nanoparticulate systems may be highly promising for targeting of OLN with effective OLN concentrations in brain for prolonged period of time.

In-vivo evaluation and adverse effects studies of OLN-loaded nanoparticulate systems in animal model have demonstrated an improved therapeutic efficacy than pure OLN. The antipsychotic effect of OLN-loaded NP was maintained for a prolonged period of time. The adverse effects studies demonstrated a decreased EPS and inhibition in weight gain as compared to the pure OLN. From these preliminary data it can be concluded that the OLN-loaded nanoformulations could be effective in the treatment of psychotic disorders with minimum adverse effects.

8.2 Future perspectives

Scale-up studies of the manufacturing process from lab scale to industrial scale have to be performed and optimized. More studies could be performed in order to find out the exact mechanism of preferential permeation of drug loaded nanoparticulate systems to brain. Further studies are necessary to investigate the exact mechanisms related to the findings of decreased adverse effects. Additionally, studies need to be carried out for the optimized formulations in the diseased human subjects. This research work may be further extended by using several other CNS active drugs and polymers/solid lipids which are not yet investigated.

Appendix

LIST OF PUBLICATIONS FROM THESIS

1. Emil Joseph., Vibhu Nagpal., Garima Balwani., Ranendra Narayan Saha., A Validated RP-HPLC Method for the Estimation of Olanzapine in Polymeric and Solid Lipid Nanoparticles. 2012, AAPS Annual Meeting and Exposition, Chicago, USA. M 1199. http://app.imsswift.com/aaps2012/sessions/aaps12_M1199.
2. Emil Joseph., Garima Balwani., Vibhu Nagpal., Satish Reddi., R N Saha., QbD based design and development of surface modified polymeric nanoparticulate systems of antipsychotic drug for brain targeting. *Pharmaceutica Analytica Acta*, 2015 6 (1): 96.
3. Emil Joseph., Vibhu Nagpal., Garima Balwani., Satish Reddi., R N Saha., Preformulation solubility and distribution coefficient studies of Olanzapine in various buffers using in-house developed UV-spectrophotometric method., *Pharmaceutica Analytica Acta*, 2015, 6 (1): 89.
4. Emil Joseph., Ranendra Narayan Saha., *Advances in Brain Targeted Drug Delivery: Nanoparticulate Systems*. *Journal of Pharma SciTech*. 2013, 3: 1-8.
5. Emil Joseph., Garima Balwani., Vibhu Nagpal., Satish Reddi., R N Saha. Validated UV Spectrophotometric methods for the estimation of Olanzapine in bulk, pharmaceutical formulations and preformulation studies. *British Journal of Pharmaceutical Research*. 2015, 6 (3): 181-190.

PRESENTATIONS

1. Emil Joseph., Vibhu Nagpal., Garima Balwani., R. N Saha., A new, sensitive and validated RP-HPLC method for estimation of olanzapine, an antipsychotic drug, in bulk and pharmaceutical dosage form, presented in *Contemporary Trends in Biological and Pharmaceutical Research (CTBPR)*, 2011, at BITS Pilani.
2. Emil Joseph., Vibhu Nagpal., Garima Balwani., R. N Saha., New and validated UV-spectrophotometric methods for the estimation of olanzapine in bulk, formulations and dissolution studies presented in *Indian Pharmaceutical Congress (IPC)*, 2010, at Manipal College of Pharmaceutical Sciences, Manipal.

Biography of Prof. Ranendra N. Saha

Prof. Ranendra N. Saha is Shri B K Birla & Shrimati Sarala Birla Chair Professor (Senior Professor of Pharmacy) and Director of BITS Pilani, Dubai Campus. He has served BITS Pilani, Pilani campus as HOD, Dean and Deputy Director. He completed his Bachelor of Pharmacy and Master of Pharmacy from Jadavpur University, Kolkata and Ph.D. from BITS, Pilani. In 2011 he has been awarded *Shri B. K. Birla and Shrimati Sarala Birla Chair Professorship* at BITS Pilani for his excellence in teaching and research. He has vast experience in the field of Pharmacy especially in Pharmaceutics, novel drug delivery systems and Pharmacokinetics. He received “*Pharmacy Professional of the Year 2013*” Award given by Indian Association of Pharmaceutical Scientists and Technologists. He is also recipient of “*The Best Pharmacy Teacher Award*” for the year 2005, awarded by Association of Pharmaceuticals Teachers of India (APTI), in recognition of his contribution in teaching and research in the field of Pharmacy. He visited several countries on invitation and Visiting Professor to Kathmandu University, Nepal. Prof. R. N Saha has more than 33 years of teaching, research and administrative experience. He has supervised large number of doctoral, postgraduate and undergraduate students. He has published book, several book chapters, research articles in renowned journals and presented papers in conferences in India and abroad. He has successfully completed several government and industry sponsored projects. Dr. Saha has developed commercial products for industries, transferred technologies to industries and filed patents. He is member of advisory board and selection committee member of a number of Universities in India and abroad.

Biography of Emil Joseph

Emil Joseph is a senior research fellow at Industrial Research Lab, Department of Pharmacy, BITS Pilani, with UGC fellowship for pursuing doctoral research. He has qualified national level competitive exam, GATE twice and received awards including prestigious DST-Govt of India international travel award for young scientist. He has published articles in reputed journals and presented as well as reviewed posters in international conferences. He has completed his Bachelor of Pharmacy from Rajiv Gandhi University, Karnataka and Master of Pharmacy in Pharmaceutics from University campus, Mahatma Gandhi University, Kerala. He also has research experience in central labs such as Central Drug Research Institute (CDRI), Lucknow and Formulation & Development division of reputed pharmaceutical industry before joining BITS for doctoral research.